RNA interference, understanding the collateral effects of HIV-1 and ZIKV

Sergio Paulo Alpuche Lazcano

Department of Medicine

Division of Experimental Medicine

McGill University, Montréal, Québec, Canada

December, 2019

A thesis submitted to McGill University in partial fulfillment of the requirements of the degree of Doctor of Philosophy.

Table of Contents

LIST OF FIGURES

Chapter I

Chapter II

Chapter III

Chapter IV

Chapter VI

LIST OF TABLES

Chapter I

Chapter II

Chapter III

Chapter IV

Chapter VI

ABSTRACT

Eukaryotic cells possess different mechanisms of gene regulation at various stages from transcription to translation. RNA interference (RNAi) is a mechanism of post-transcriptional gene modulation based on short double-stranded RNA sequences called micro RNAs (miRNA). MiRNAs are partially complementary to a specific sequence in messenger RNAs (mRNA) and their binding to a targeted mRNA mediates its repression and/or degradation. In humans, RNAi controls over 50 % of protein-coding genes. The improper functioning of this process leads to the development of different pathologies. Internal or external factors influence the malfunctioning of RNAi. Among them, viral infections fine-tune RNAi, which can be beneficial or detrimental for viral replication.

Human immunodeficiency virus type-1 (HIV-1) and Zika virus (ZIKV) are two different viruses that have distinct mechanisms of infection. Nonetheless, both viruses change the miRNA landscape through modifications in the RNAi pathway. This thesis explores the interplay between RNAi and either HIV-1 or ZIKV. In the first project, we re-evaluated the relationship between RNAi and HIV-1. Our experiments demonstrated that RNAi is functional in HIV-1 replicating cells. Besides, proteins of the RNA induced silencing complex (RISC) are not relocalized in HIV-1 producing cells. In contrast, we showed that HIV-1 Gag interacts specifically with Dicer, an essential protein of the RISC. We found that Gag does not change the cleavage of precursor. miRNAs by Dicer but modifies their availability. Gag modifies the loading of specific miRNAs on Dicer, which leads to sequestration or higher loading of particular miRNAs. Among these miRNAs, we found miR-642a 3p that has been predicted to target the AFF4 protein. AFF4 is an essential component of the virus transcription and its absence profoundly impairs HIV-1 replication.

Our second goal was to examine mRNAs and miRNAs in an integrative analysis of infected cells with ZIKV. Because little information on the neurological consequences after ZIKV infection were available at the beginning of our study, we first compared two different viral strains. We determined that a Brazilian isolate was more cytopathic than an early Asian one in distinct cell types. Then, using the Brazilian virus, we studied the impact of ZIKV infection on the expression of host mRNAs and miRNAs in fetal mice neurons. Notably, we determined a downregulation of NPAS4 and NR4A transcripts, which have been linked to the neurogenesis process. Moreover, our integrative analysis showed a correlation between dysregulated mRNAs and miRNAs in the infected cells. Particularly, NR4A3 transcripts might be controlled by the dysregulated levels of miR-7116-5p and miR-7013-5p upon the infection.

The results presented in this thesis contribute to the understanding of 1) HIV-1-induced modification of miRNAs loaded on Dicer and their consequences on mRNAs expression and 2) ZIKV cytopathicity and its impact on miRNAs and mRNAs expression profile in murine fetal neurons.

RÉSUMÉ

Les cellules eucaryotes possèdent différents mécanismes de régulation génique à la fois au niveau transcriptionnel et traductionnel. L'interférence ARN (iARN) est un mécanisme de modulation de l'expression post-transcriptionnelle des gènes impliquant de petits ARN double brin, appelés micro-ARN (miARN). Les miARN ont une complémentarité imparfaite avec une séquence cible présente sur les ARN messagers (ARNm). La liaison des miARN à un ARNm induit la répression traductionnelle de ce dernier et/ou sa dégradation. Chez l'humain, l'iARN contrôle l'expression de plus de 50% des gènes codant pour des protéines. Le disfonctionnement de l'interférence ARN conduit au développement de différentes pathologies. En effet, des évènements d'origine cellulaire ou extracellulaire tels que les infections virales peuvent déréguler l'iARN, que ce soit bénéfique ou néfaste pour la réplication virale.

Le virus de l'immunodéficience humaine de type 1 (VIH-1) et le virus Zika (ZIKV) ont des mécanismes d'infection différents. Toutefois, ces deux virus modifient la composition des miARN cellulaires en perturbant la voie de l'iARN. Cette thèse a permis d'explorer l'interaction entre la voie de l'interférence ARN et le VIH-1 ou le ZIKV. Dans le premier projet, nous avons étudié la relation entre l'iARN et le VIH-1. Nos expériences ont démontré que la voie de l'iARN reste fonctionnelle dans les cellules produisant du VIH-1. De plus, la localisation cellulaire des protéines du complexe RISC ("RNA-Induced Silencing Complex") n'est pas modifiée dans les cellules productrices du VIH-1. En revanche, nous avons montré que la protéine Gag du VIH-1 interagit avec Dicer, une protéine essentielle du complexe RISC. Nous avons constaté que cette interaction protéique ne modifie pas le clivage des précurseurs de miARN mais modifie leur disponibilité. En effet, Gag modifie le chargement de miARN spécifiques sur Dicer. Ceci conduit soit à une séquestration soit à une quantité plus élevée de certains miARN chargés sur Dicer. Parmi ces

miARN, nous avons trouvé le miR-642a 3p qui ciblerait la protéine AFF4. AFF4 est une protéine essentielle à la transcription du virus et son absence altère profondément la réplication du VIH-1.

Notre deuxième objectif était d'examiner le profil d'expression des ARNm et des miARN de cellules infectées par le ZIKV. Très peu d'informations sur les conséquences neurologiques de l'infection par le ZIKV étaient disponibles au début de notre étude. Nous avons commencé par comparer deux souches virales distinctes. Ainsi, nous avons déterminé qu'un isolat brésilien était plus cytopathique qu'une souche de lignée asiatique précoce et ceci dans différents types cellulaires. Par la suite, en utilisant le virus brésilien, nous avons étudié l'impact de l'infection du ZIKV sur l'expression des ARNm et des miARN cellulaires dans des neurones fœtaux de souris. Nous avons déterminé une régulation négative des transcrits NPAS4 et NR4A, qui sont impliqués dans le processus de neurogenèse. De plus, notre analyse intégrative a montré une corrélation entre les ARNm et les miARN dérégulés dans les cellules infectées. En effet, lors de l'infection par le ZIKV, les transcrits de NR4A3 pourraient être contrôlés par les miARN miR-7116-5p et miR-7013-5p dont l'expression est dérégulée.

Les résultats présentés dans cette thèse contribuent à la compréhension:

1) des modifications induites par le VIH-1 dans le chargement de miARN sur la protéine Dicer et de l'impact de ceux-ci sur l'expression des ARNm cibles et

2) de l'effet cytopathique du ZIKV et de l'impact de ce dernier sur le profil d'expression des miARN et des ARNm cellulaires dans les neurones fœtaux murins.

ACKNOWLEDGMENTS

Undoubtedly, the first people to acknowledge are my supervisors Dr. Anne Gatignol and Dr. Andrew Mouland. Both welcomed me to come in Montreal to do my Ph.D. under their supervision. I am eternally grateful to them for this opportunity and for their mentorship. I also thank you for those hours of discussion and assistance that allowed me to enhance my scientific skills. To Anne, thanks for making me part of your projects, for all that you taught me to do and not to do in papers and presentations. Every correction, all the feedback, all your expertise and leadership nurtured my professional formation. To Andrew, for all those hours of discussion and rationale on experiments, for your guidance and concern in my professional career, for all the feedback on those papers and this thesis, I genuinely say thank you.

I also want to acknowledge my committee meeting members whose input was invaluable. Thanks to Dr. Eric Lecuyer and Dr. Selena Sagan for making me think of what was needed in that idea or experiment. I also thank my academic advisor Dr. Koren Mann whose opinion was always useful. Thanks to the Department of Experimental Medicine at McGill University that provided me the opportunity to be part of its community.

I also acknowledge Consejo Nacional de Ciencia y Tecnologia (CONACYT) and Secretaria de Educacion Publica (SEP) that granted me the scholarship to obtain this degree. I also acknowledge all the support provided by the Canadian Institutes of Health Research (CIHR) to my supervisors.

I also want to thank my former and current lab mates. Five years of being at the Lady Davis Institute made me meet quite a bit of people. I wouldn't have enough space to acknowledge every one of you but in a few words, thanks to you all for all those moments. However, I want especially to recognize some of my lab mates. To Robert Scarborough, I appreciate all your expertise and

friendship. You are a humble, smart and nice man; without all those talks, I wouldn't have achieved this goal. Aïcha Daher, our lab manager that always had a smile to share, thanks for sharing all your knowledge and techniques with me. To Elodie Rance, whose expertise and input in experiments was always appreciated. To my closest friends in this adventure, Ryan G and Roman R. You guys make my life easier, happier and give me the strength to continue. Thanks to Meijuan Niu and Anne Monette for their contributions to experiments. To past members Craig, Shringar, and Roman L, you are gone, but I hope this message will get you.

Last but not least, the closest people in my life, my family and God. Por ti mamá nada de esto hubiese sido posible. Sin la formación que me diste y tu apoyo incondicional en todo sentido, esto jamás hubiese pasado. A mi papá, que siempre estuvo ahi, siempre apoyándome, siempre cuidándome y alentandome, gracias. A mi hermano, aunque siempre pones cara, tu apoyo en muchos sentidos a sido determinante para alcanzar estas metas. Y finalmente, a todos mis amigos que han sido mi mejor apoyo.

LIST OF ABBREVIATIONS

Ab	Antibody
A/G	Adenines and guanines
AFF4	AF4/FMR2 family member 4
ADAM	A Disintegrin and metalloproteinase domain-containing protein
Ad	adenovirus-based vaccine
Aae	*Aedes aegypti*
AGO	Argonaute
AIDS	Acquired Immunodeficiency Syndrome
cART	Combination antiretroviral therapy
AZT	Zidovudine
BnAb	Broadly neutralizing antibodies
CA	Capsid (HIV-1)
C	Capsid (ZIKV)
CCR5	C-C chemokine receptor type 5
cART	Combination ART
CD4	Cluster of differentiation 4
$CD4^+$ T	Lymphocytes T $CD4^+$
CDC	Centers for Disease Control and Prevention
Cdk9	Cyclin-dependent kinase
cEM	Cryogenic electron microscopy
CLIMP-63	cytoskeleton-linking endoplasmic reticulum membrane protein of 63 kD
CMC	Carboxymethylcellulose
CPSF6	Cleavage and polyadenylation specific factor 6
CRISPR-Cas9	Clustered Regularly Interspaced Short Palindromic Repeats- Cas9
Ct	Threshold cycle
Cq	Quantitation cycle

CRM1	Chromosomal maintenance 1
CXCR4	C-X-C Chemokine Receptor Type 4
CycT1	Cyclin T1
CYPA	Cyclophilin A
CZVS	Congenital ZIKV syndrome
DDX6	DEAD-box helicase 6
DC	Dendritic cells
Dcp	Decapping mRNA
DIS	Dimerization initiation site
Dcr-1	Dicer-1
DDX	DEAD-box helicase
dNTPs	Deoxyribonucleotide triphosphate
DGCR8	DiGeorge syndrome critical region gene 8
DMEM	Dulbecco’s modified Eagle’s medium
Ds	Double-stranded
DSB	Double-strand breaks
DUF	Domain of unknown function
dsRNA	Double-stranded RNA
dsRBD	dsRNA-binding domain
dsmiRNA	Double-stranded miRNA
dsRBD	dsRNA binding domain
E2F3	E2F transcription factor 3
EC	Elite controllers
EM	Electron microscopy
EMEM	Eagle's Minimum Essential Medium
Env	Envelope
EPBHB2	EPH receptor B2
E	Envelope (ZIKV)
ESCRT	Endosomal sorting complexes required for transport
ER	Endoplasmic reticulum

eIF4F	Eukaryotic initiation factor 4F
eIF2α	Eukaryotic initiation factor 2α
FBS	Fetal bovine serum
Gag	Group Specific Antigen
GALT	Gut-associated lymphoid tissue
GBS	Guillain-Barré syndrome
GCH1	GTP cyclohydrolase 1
gRNA	Guide RNA
GPD2	Glycerol-3-phosphate dehydrogenase 2
GLIS2	GLIS family zinc finger 2
HEK	Human embryonic kidney
HSCT	Hematopoietic stem-cell transplantation
HCV	Hepatitis C virus
HAART	Highly active antiretroviral therapy
HIV	Human immunodeficiency virus
HBR	Highly basic region
HDF	Host dependency factors
HEXIM1	HEXamethylene-bis-acetamide-Inducible protein in vascular smooth Muscle cells
HLA	Human leukocyte antigens
HDR	Homology-direct repair
IF	Immunofluorescence
IFN	Interferon
Imp	Importin
IN	Integrase
INDELs	Insertions or deletions
INSTI	Integrase strand transfer inhibitors
IP	Immunoprecipitation

IRES	Internal ribosome entry site
IsomiRNAs	MiRNA isomers
KO	Knockout
LDGF	Lens epithelium-derived growth factor
LRA	Latency Reverse Agents
LPA	Latency Promoting Agents
LPS	Lipopolysaccharide
LaRP7	La-related protein 7
LAV	Lymphadenopathy associated virus
LPS	Lipopolysaccharide
lncRNA	Long non-coding RNA
LTR	Long Terminal Repeat
MA	Matrix
MAVS	Mitochondrial antiviral-signaling
MePCE	Methylphosphate capping enzyme
MID	Middle domain
MFN2	Mitofusin 2
MHR	Major homology region
mRNA	Messenger RNA
miRNA	Micro RNA
MOI	Multiplicity of infection
MVA	Modified vaccinia virus Ankara
MV	Measles virus-based vaccine
NC	Nucleocapsid
ND	Not detected
ncRNA	Non-coding RNAs
NHEJ	Non-homologous end joining
NMD	Nonsense-mediated mRNA decay
NNRTI	Non-nucleoside analog reverse transcriptase inhibitor
NRTI	Nucleoside analog reverse transcriptase inhibitor

NP-40	Nonidet P-40
nt	Nucleotide
NLS	Nuclear localization signal
NPC	Neuroprogenitor cells
NS	Non-structural
NPM1	Nucleophosmin 1
NCOR1	Nuclear receptor corepressor 1
NUP	Nucleoporin
ORF	Open reading frame
PACT	Protein activator of the interferon-induced protein kinase
PFA	Paraformaldehyde
PAHO	Pan American Health Organization
PAMs	Proto-spacer adjacent motifs
PAZ	Piwi, Argonaut, Zwille domain
PBMC	Peripheral blood mononuclear cells
PBS	Primer Binding Site
PBS	Phosphate-buffered saline
PEI	Polyethyleneimine
PFU	Plaque forming units
PIP2	Phosphatidylinositol-4,5 bisphosphate
PI	Protease inhibitor
Piwi	P element-induced wimpy testes
piRNA	Piwi RNAs
PIC	Pre-integration complex
PKR	Protein kinase R
PLA	Proximity ligation assay
P-bodies	Processing bodies

Pol	Polymerase
Ppt	polypurine tract
POU2AF1	POU class 2 associating factor 1
PABPN1	Poly(A) binding protein nuclear 1
PIP4P1	Phosphatidylinositol-4,5-bisphosphate 4-phosphatase 1
PPIA	Peptidylprolyl isomerase A
prM	Pre-membrane
pri-miRNA	Primary miRNA
PR	Protease
PPPIR10	Protein phosphatase 1 regulatory subunit 10
P-TEFb	Positive transcription elongation factor b
psnoRNA	Processed snoRNA
qRT-PCR	Quantitative reverse transcription polymerase chain reaction
RER	Rough Endoplasmic Reticulum
RISC	RNA induced silencing complex
RIP-seq	RNA Immunoprecipitation and sequencing
RIG-I	Retinoic acid inducible gene I
RNAi	RNA interference
RNAse	ribonuclease
RNA seq	RNA sequencing
RRE	Rev response element
rRNA	Ribosomal RNA
RT	Retrotranscriptase
SEM	Standard error of the mean
SIV	Simian immunodeficiency virus
shRNA	Short-hairpin RNA
snRNA	Small nuclear RNA
snoRNA	Small nucleolar RNA
sdRNA	snoRNA-derived RNA
SDS-PAGE	Sodium dodecyl sulfate polyacrylamide gel electrophoresis

sfRNA	Subgenomic flavivirus RNA
SIRT1	Sirtuin-1
SOD2	Superoxide dismutase 2
ssRNA-dsRNA	Single strand RNA -double strand RNA
SL1	Stem loop 1
TALEN	Transcription activator-like effector nuclease
TAR	Trans-activation response element
TASK	TWIK-related acid-sensitive K
TBK	Tank-binding kinase
TBS-T	Tris-buffered saline tween 20
TGF	Transforming growth factor
TNRC6	Trinucleotide Repeat-Containing gene 6
TLR	Toll like receptor
TNF	Tumor necrosis factor
TNPO	Transportin
TRBP	TAR RNA binding protein
tRNA	Transfer RNA
TBP	TATA-box binding protein
T reg	T regulatory
UPF1	Upframeshift protein 1
UTR	Untranslated region
vcDNA	Viral complementary DNA
VLP	Virus-like particles
vmiRNA	Viral miRNA
vsiRNA	Viral siRNA
WAGO	Worm-specific Argonaute
WHO	World Health Organization
xrRNAs	Xrn1-resistant RNAs
ZFN	Zinc finger nucleases

ZIKV	Zika virus
ZIPV	ZIKV purified inactivated
ZIKV-LAV	Live attenuated Zika virus vaccine

CONTRIBUTION TO ORIGINAL KNOWLEDGE

The work presented in this thesis highlights new findings in the field of RNAi and its interplay with HIV-1 and ZIKV. The elements of the thesis are considered original scholarship and distinct contributions to knowledge. Of note, this work shows that HIV-1 can modulate the availability of miRNAs. It is also shown that a cytopathic ZIKV strain can alter the miRNA landscape and transcriptome upon infection. The research here shows:

Chapter II

- The HIV-1 protein Gag interacts with the RNAi protein Dicer.
- The Dicer/Gag complex harbors different concentrations of non-coding RNA compared to Dicer alone.
- Among non-coding RNAs, thre miRNAs (miR642a 3p, miR766 5p and 3p) were bound to Dicer significantly more in the presence of Gag.

Chapter III and IV

- A Brazilian ZIKV strain is more cytopathic than an early Asian strain in different cell types.
- Infection of neurons with the Brazilian ZIKV strain resulted in a decrease in the expression of transcriptional factors NPAS4 and NR4As.
- An integrative analysis of the differentially expressed miRNAs indicates that transcriptional factors NPAS4 and NR4A3 could be modulated by the miRNA response.

CONTRIBUTION OF AUTHORS

In accordance with departmental guidelines, I disclose the author contribution for each Chapter

Chapter I is literature review on RNAi, HIV-1 and ZIKV.

Chapter II is an original paper on HIV-1 and RNAi: "*HIV-1 Gag interacts with Dicer and increases its binding to specific microRNAs"/submitted.* SPAL, AJM and AG conceived and designed the experiments; SPAL, RJS and SMD performed the experiments; SPAL and ER set-up the initial Dicer catalytic activity, SPAL designed and set-up the IP-Dicer and qRT-PCR for miRNAs technique. ER, RJS, AJM, and AG provided the expertise in various assays; SPAL, RJS, ER, AJM, and AG analyzed the data. AJM and AG provided the facilities and reagents for experiments and supervised the work; SPAL, RJS and AG wrote the manuscript. All authors read, corrected and approved the manuscript and its contents.

Chapter III is an original paper on ZIKV and its cytopathicity in different cell types which is linked to Chapter IV. *"Higher Cytopathic Effects of a Zika Virus Brazilian Isolate from Bahia Compared to a Canadian-Imported Thai Strain". This work was reproduced with permission of MDPI under the terms and conditions of the Creative Commons Attribution (CC BY) license.* SPAL and AG conceived and designed the experiments; SPAL CRM performed the experiments; SPAL, ODC, ER, RJS set-up the initial techniques and experiments; AG, MMT, SMS and AJM provided reagents and expertise in the various assays; SPAL, CRM and AG wrote the manuscript; All authors have contributed to data analysis and manuscript revision.

Chapter IV provides further information of one of the strains of ZIKV used in Chapter III and in the context of RNAi and the transcriptome. "*Downregulation of nuclear transcription factor*

NPAS4 and NR4A family correlates with the death of fetal mice neurons infected with ZIKV"/submitted. SPAL, MMT, and AG conceived and designed the experiments; SPAL, JS, VVC and LSR performed the experiments; SPAL and JS performed the bioinformatics analysis; SPAL and VVC set-up the initial techniques and experiments; AG, MMT and AJM provided reagents and expertise; SPAL and AG wrote the manuscript; AG, MMT and VB provided facilities and equipment. All authors have read and approved the manuscript.

CHAPTER I

INTRODUCTION

1.1 RNA interference (RNAi)

RNAi is a post-transcriptional gene regulation mechanism that represses mRNAs expression after its hybridization with small non-coding RNAs (ncRNAs). In humans, it is estimated that more than 60% of protein-coding genes are regulated through this pathway (1). The RNAi impact on human health goes from normal development and cell cycle to pathological conditions including cancer, viral infections, genetic diseases, aging and many others. This thesis is relevant to RNAi components and related pathways and how they are orchestrated in the context of viral infections.

1.1.1 RNAi discovery and general characteristics

The first observation that could retrospectively be attributed to RNAi occurred more than twenty years ago when Guo and Kemphues found that sense and antisense RNAs were effective to decrease gene expression (2). Three years later, Fire *et al.*, discovered that using sense and antisense RNAs as double-stranded RNAs (dsRNA) enhanced the silencing of genes by several fold (3). Subsequent experiments showed that the RNAi activity is functional through small RNA sequences of 21-22 nucleotides (nt) length called small interfering RNAs (siRNA) which induces specific posttranscriptional gene silencing (4). SiRNAs are generated from long dsRNA sequences within the nucleus and are edited in the cytoplasm by the RNA induced silencing complex (RISC) to produce the mature siRNA that can hybridize to a specific mRNA and induce its degradation (5-7).

There are three types of dsRNAs commonly recognized as functional for RNAi: siRNA, short-hairpin RNA (shRNA) and microRNA (miRNA) (Fig 1.1). SiRNAs are produced mostly in plants, nematodes and other small organisms to regulate genes involved in the development, reproduction, phenotypic plasticity, and immunity. SiRNAs can also be engineered as synthetic linear siRNAs

that bypasses the cytoplasmic edition of the RISC (Fig 1.1) (8). The DNAs coding for shRNAs are designed and cloned into a plasmid, which is transfected into competent cells to be transcribed. ShRNAs are similar to natural siRNAs regarding their processing by the RISC (Fig 1.1) (9). MiRNAs are mainly produced by mammalian cells and their most characteristic feature is that they do not have 100 % complementarity with their corresponding target mRNA. Consequently, unlike siRNAs, which induce mRNA cleavage, miRNAs trigger complex mechanisms of translational repression for gene silencing (Fig 1.1). To date, the total number of known miRNAs in humans is of 2300, controlling 60% of protein-coding genes (10).

1.1.2. The canonical miRNA biogenesis

The canonical pathway of miRNAs begins with the synthesis of a primary miRNA (pri-miRNA) in the nucleus by the RNA polymerase II (pol II) (11). Pri-miRNAs vary in length, but most are several kilobases in length and include a 5' cap as well as a 3' polyadenylation tail (12). Pri-miRNAs have features within their hairpin structure, such as optimal length, apical loop size, and sequence motifs that allow them to be processed correctly (13). The nascent pri-miRNA immediately associates with the nuclear RNase III Drosha and its co-factor DiGeorge syndrome critical region gene 8 (DGCR8) (14). DGCR8 binds pri-miRNAs at the single stranded RNA (ssRNA)-dsRNA junction and at the terminal loop of ~33 bp. Drosha then simultaneously recognizes DGCR8 and the pri-miRNA, cleaving the later one helical turn away from the ssRNA-dsRNA junction to produce a precursor miRNA (pre-miRNA) of 60-110 nt length (12). Once the pre-miRNA is synthesized, it will bind to Ran(GTP) to be shuttled to the cytoplasm by Exportin 5 where it will associate with the ribonuclease (RNAse) III Dicer and the TAR RNA binding protein (TRBP) to produce a double-stranded miRNA (dsmiRNA) (15-17). This dsmiRNA will be

unwound where the guide strand is eventually incorporated into the loading RISC created by the recruitment of Ago2 by the TRBP-Dicer complex, while the passenger strand will degrade. Thus, the guide strand of the miRNA that is loaded onto the RISC will direct the complex to the proper target mRNA (18). If there is perfect hybridization between the miRNA and the target mRNA, Ago2 will cleave the mRNA. However, hybridization between miRNAs and the target mRNAs often includes nucleotide (nt) mismatches. This will result instead in the inhibition of gene expression via processing bodies (P-bodies) where the mRNA within the miRNA-mRNA duplex is de-capped and de-adenylated, resulting in either translational arrest or degradation (Fig 1.1) (18).

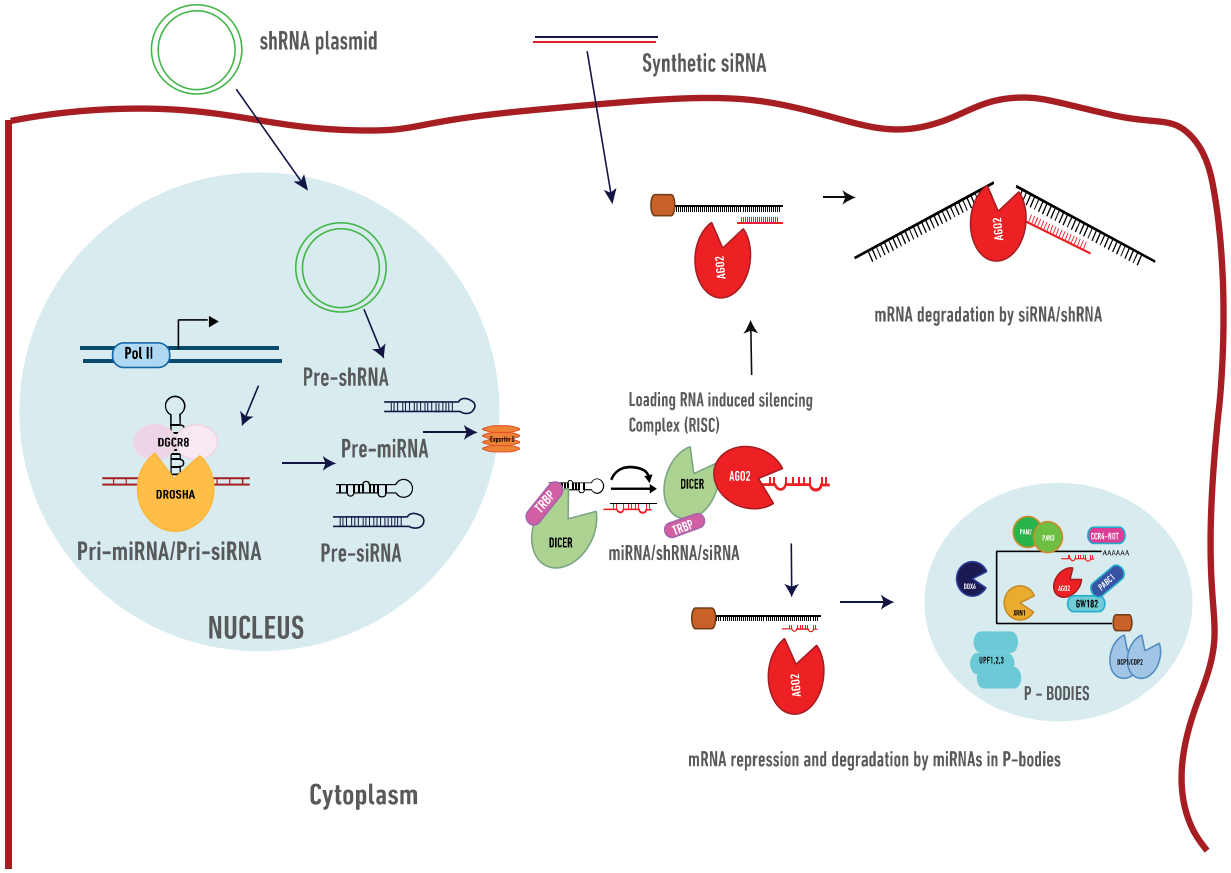

Figure 1. 1 The RNAi pathway in eukaryotic cells.

Endogenous RNAi begins with the transcription of a pri-miRNA/siRNA that is cleaved by Drosha and DGCR8. The edited product called pre-miRNA/pre-siRNA is exported to the cytoplasm where it associates with Dicer and TRBP. Dicer associated with TRBP cleaves the pre-miRNA/pre-siRNA and produces a ds-miRNA/ds-siRNA of 22 nt. Ago2 is then recruited to the complex and, after RNA strand separation, associates with the guide strand, which will then hybridize with the target mRNA. If there is a perfect complementarity during the hybridization between the siRNA and the mRNA, Ago2 will cleave the mRNA (top). MiRNAs do not generally have perfect complementarity and the complex will trigger the formation of P-bodies where the mRNA will either be translationally repressed or degraded after de-capping and de-adenylation (bottom). RNAi can also be induced by the transfection of plasmids containing shRNAs that transcribe a pre-shRNA. The pre-shRNA is exported to the cytoplasm, cleaved by Dicer and forms a complex with Ago2 and targets an mRNA with the same outcome as an endogenous siRNA. In addition, siRNAs can be engineered and artificially synthesized. These synthetic siRNAs bypass Dicer

processing, recruit Ago2 and hybridize with their target mRNA that will be cleaved directly by Ago2.

1.1.3 The loading RISC

1.1.3.1 The loading RISC: Dicer

Dicer belongs to the family of proteins called RNase type III and has a molecular weight of approximately 215 kDa. Dicer plays a key role in the maturation of miRNAs where it recognizes dsRNAs and cleaves them to generate products of ~22nt. Dicer is a multidomain protein with a DEXH-box ATPase helicase domain; a domain of unknown function (DUF) 283; a Piwi, Argonaut, Zwille (PAZ) domain that function as a platform-PAZ-connector pocket; the RNase III A and the RNase III B domains; and a dsRNA-binding domain (dsRBD) (19, 20) (Fig 1.2). Protein models and reconstruction through electron microscopy (EM) has generated an L shape of Dicer; this shape facilitates the end recognition of dsRNAs and other motifs through the PAZ domain (21, 22). Experiments where PAZ was replaced by another RNA-recognition domain, demonstrate not only the RNA recognition capacity but also a measuring function that generates the specific length of miRNAs (23). Next to PAZ, the platform domain carries a phosphate pocket that provides the efficiency in the miRNA processing and cleavage (20).

The helicase domain is subdivided into the globular domains, HEL1, HEL2, and HEL3, which form the base of the L shape of Dicer (24). The structure of the Dicer helicase domain is similar to one of the retinoic acid inducible gene I (RIG-I) protein, wherein the conformation causes Dicer to clamp dsRNAs (21). The RNase domain, the platform, and the PAZ domain are rigid structures that contain hinges by which Dicer can clamp and bend dsRNA substrates containing minor deviations in the duplex from non-canonical base-pairings. This allows Dicer to interact with

virtually any dsRNA (25, 26), being only limited in its cleavage potential with dsRNAs that lack open ends (27).

Dicer's cofactor, TRBP, acts as a molecular ruler to accurately establish the cleavage site within the pre-miRNA (Fig 1.2B) (7, 27). Beyond mediating the cleavage of pre-miRNAs, Dicer can bind and cleave other dsRNA (Fig 1.2C) molecules such as transfer RNAs (tRNAs) (28). Dicer's edition over a tRNA produces three fragments called tRF-1, tRF-5 and tRF-3 (29). Interestingly, tRNA (Gly) edition generates tRF-3 and tRF-5, which have characteristics similar to those of pre-miRNAs that can re-enter into Dicer's cleavage core for the production of miRNA-like molecules (30).

Small nucleolar RNAs (snoRNAs) are also edited by Dicer into snoRNA-derived RNAs (sdRNAs) and processed snoRNAs (psnoRNAs) (31, 32). Dicer generates fragments of 17-19 nt on H/ACA box snoRNAs and 22-27 nt on C/D box snoRNAs with a high resemblance to miRNAs (32). As examples, among eighteen C/D box snoRNAs and three H/ACA snoRNAs tested for miRNA production, eleven C/D box and the snoRNAs H/ACA behaved as miRNAs (33). In another study, snoRNA ACA45 processing needed Dicer but was independent of Drosha and DGCR8 (34). Furthermore, Dicer also targets transposable elements such as LINE-1, resulting in the production of repeat-associated siRNAs. These siRNAs then recruit Ago2 and the complex mediates an autoregulation of LINE-1 (35, 36). Dicer binding and cleavage are not compulsory in all ncRNAs. For instance, rncs-1 in *Caenorhabditis elegans* inhibits Dicer RNAse activity and makes it act in a passive manner (37).

Dicer can also process exogenous RNAs (Fig 1.2C). HIV-1 trans-activation response element (TAR) sequence has a structure similar to pre-miRNAs, and several studies point out that TAR generates viral miRNAs (vmiRNA) after Dicer cleavage (38-40). Herpesviruses utilize the RNAi

pathway inducing hundreds vmiRNAs; some calculations estimate over 200 hundred vmiRNAs (41, 42). Another example is the Simian Virus 40, which also spawns vmiRNAs using Dicer cleaving activities (43). Flaviviruses do not produce miRNAs, but the excessive synthesis of genomic RNAs activates exonucleases like XRN1, which degrades the viral RNA and leaves small fragments in the 3'untranslated region (UTR) that antagonize pre-miRNA and sequester Dicer (44).

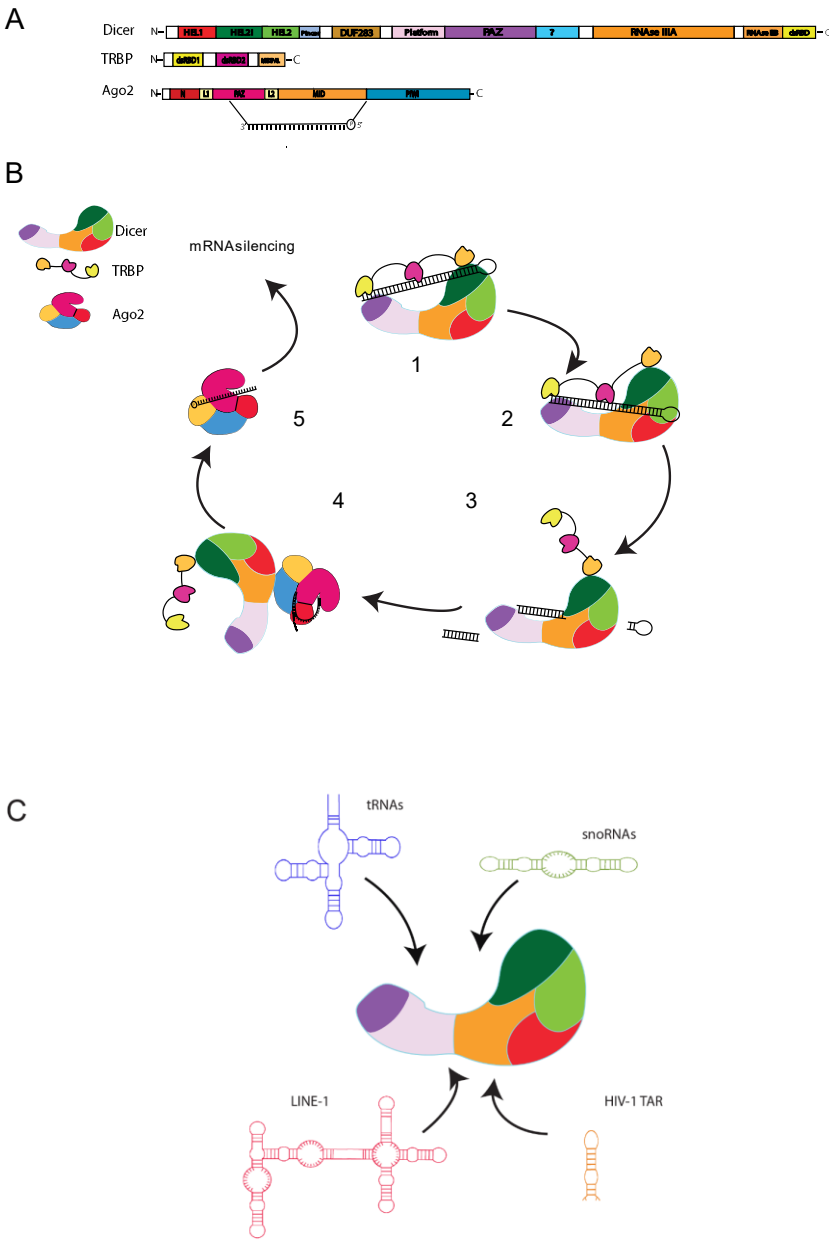

Figure 1. 2 Loading RISC components and interactions.

A) Protein components of the loading RISC. Dicer (top) domains are: HEL1/2i/2- helicase domain, DUF283 domain, platform-PAZ-connector domain, RNAse III A and B and a dsRBD (20-22, 45). Dicer can interact with TRBP (middle) through HEL2i domain and TRBP by Merlin-Dicer-PACT liaison (Medipal) domain (19). Ago2 (bottom) contains five domains and interacts through the P element-induced wimpy testes (Piwi) domain with the Dicer RNAse IIIA domain. (46). B) The loading RISC interaction and dynamics. 1) Dicer recognizes the pre-miRNA alongside TRBP. 2) Dicer and TRBP load the pre-miRNA into the Dicer's processing center for a precise cleavage. 3) After the cut, TRBP releases its dsRBDs from the miRNA that remains bound to the Dicer RNase domain. 4) Ago2 binds to Dicer and the miRNA strand selection occurs. Ago2-Piwi and Middle domain (MID) interact with the miRNA 5' end while PAZ interacts with the 3'end (47). 5) The Ago2-miRNA association triggers a conformational change that facilitates the exposure and hybridization of the single strand miRNA to a specific target mRNA. C) Dicer binding and cleavage capacity to other dsRNAs such as snoRNAs, tRNAs, LINE-1 and exogenous RNAs like HIV-1 TAR.

1.1.3.2 The loading RISC: TRBP

TRBP plays a significant role in RNAi, along with Dicer. TRBP was identified using an expression library coding for proteins that bind the radiolabelled HIV-1 TAR. Various assays showed that TRBP is a translational enhancer of HIV-1 (15, 48, 49). TRBP has two isoforms, TRBP1, and TRBP2. TRBP2 is 21 amino acids longer than TRBP1 in its N-terminal end (50). TRBP is a dsRNA binding protein with two highly conserved dsRNA binding domains (dsRBD1 and dsRBD2) and the Dicer, Merlin and protein activator of the interferon-induced protein kinase R (PACT) liaison (Medipal) domain (Fig 1.2) (51, 52).

Dicer-TRBP interaction occurs through the C4 domain in the Medipal domain of TRBP and the DEXDH domain in Dicer (19, 53). The loading activity of pre-miRNAs by Dicer and TRBP occurs

predominantly in the endoplasmic reticulum (ER) (54-56). TRBP can be redistributed from the ER to the cytoplasm while Dicer remains in the ER. The dissociation consequently reduces Dicer activity on specific miRNAs (57, 58). In the context of RNAi, TRBP enhances the cleavage rate and processing kinetics of Dicer (59, 60). The accuracy of Dicer is compromised in the absence of TRBP, which leads to the production of miRNA isomers (isomiRNAs) (16, 61). Cryogenic electron microscopy (cEM) analysis showed a reconstruction of TRBP and how it stabilizes the stem duplex of pre-miRNAs during Dicer loading (45). TRBP begins the recognition of pre-miRNAs through the dsRBD1 and dsRBD2 in a sequence-independent manner. When the precursor is unstable, the Dicer-TRBP complex finds the equilibrium in a pre-dicing state to load it into the Dicer processing center for a precise cleavage (Fig 1.2B) (45, 62).

TRBP has other functions different than the RNAi pathway, such as inhibiting the interferon-induced dsRNA-dependent protein kinase R (PKR) (63, 64). PKR regulates RNA translation by the phosphorylation of the alpha subunit of the eukaryotic translation initiation factor 2α (eIF2α). Indeed, PKR monomers remain inactive within cells until they bind dsRNA typically found in viruses (65). The recognition induces dimerization, followed by autophosphorylation at residues Thr 446 and Thr 451 (65-67). The activated PKR phosphorylates eIF2α, which arrests the formation of the translation initiation complex eIF2-GTP-Met-tRNA (68-70). TRBP inhibits PKR by direct interaction and also by sequestering the dsRNAs that trigger PKR activation (63, 71). In addition, PACT, which is structurally homologous to TRBP, activates PKR during cellular stress in the absence of dsRNA (72). Conversely, a direct interaction between PACT and TRBP can inhibit the activation of PKR (65, 71, 73). TRBP forms heterodimers with PACT and PKR; these interactions prevent PACT to bind and activate PKR (74, 75). Moreover, TRBP can be phosphorylated in stress conditions, which increases its interaction with PKR and contributes to

cell survival (76). PACT behaves similarly to TRBP and binds to Dicer through its third dsRBD but its function in the context of RNAi is still unclear (77-80).

1.1.3.3 The loading RISC: Ago2

Ago2 belongs to a large group of proteins called *Argonautes (AGO)*. AGO proteins were first described for their critical role in plant development and stem cell division in *Drosophila melanogaster* (81, 82). Other studies found that AGO proteins are relevant for meiotic silencing and DNA degradation in different organisms like fungi or ciliates (83, 84). The most characteristic feature of AGO proteins was demonstrated years later when they were found to participate in the turnover of mRNA by gene silencing, chromosome maintenance and heterochromatin formation (85).

There are three different clades of AGO proteins: The Ago clade, the Piwi clade and the worm-specific WAGO clade (85, 86). The Ago clade includes all AGO proteins that interact with miRNA or siRNA during the post-transcriptional gene silencing. The Piwi clade consists of proteins that interact with Piwi RNAs (piRNAs) expressed exclusively in the testes. piRNAs are expressed mainly in the nucleus and repress transposon's expression. Finally, WAGO proteins are AGO proteins that bind RNA products called 22G-RNAs, which are RNAs of 22 nt lengths with 5'G residues. WAGO proteins and 22G-RNAs silence different sequences at the post-transcriptional or epigenetic level (87).

In humans, there are eight AGO proteins. Four proteins belong to the Piwi clade and four to the Ago clade (85). Chromosome 8 harbors the Ago2 gene, whereas chromosome 1 harbors the Ago1, Ago3 and Ago4 genes (88). Ago2 is the most abundant and the only one that participates in the loading RISC. Ago2 possess endonuclease activity triggered when a miRNA matches perfectly

with an mRNA; the cleavage switches to translational repression in P-bodies when the sequences are not entirely complementary (89, 90).

Ago2 has four domains: the N terminal domain, the Piwi-Argonaute-Zwille (PAZ) domain, the middle domain (MID) and the P element-induced wimpy testes (Piwi) domain alongside two linkers (L1 and L2) that separates PAZ from N and MID (Fig 1.2A), (91). MID and Piwi domains interact actively with miRNAs. The MID domain interacts with the miRNA at the 5' end while Piwi interacts with the 3' end. This interaction exposes the miRNA seed region, which hybridizes with the mRNA (Fig 1.2B) (47, 92, 93).

1.1.4 MiRNA strand selection and pairing

Following Dicer edition and Ago2 loading, the next step is the strand selection of the miRNA duplex that will hybridize to the mRNA. The "guide strand" is the strand that targets the mRNA, and the "passenger strand" is the one that is degraded. The guide strands are chosen based on their thermodynamic characteristics; they are less stable than passenger strands and therefore, easier to be recruited by Ago2. Besides, the guide strands usually contain uracils with weaker interactions at the 5' and more adenines and guanines (A/G) than the passenger strands (94). The high concentration of purines in A/G presumably forms hydrophobic interactions with aromatic compounds in the PAZ domain of Ago2 that favors the selection of the guide strand (95).

The guide strand is functional as long as it satisfies the following conditions: (1) the guide strand has to match perfectly with the target in the seed region located 2 to 8 nt from the 5' end. (2) Bulges or mismatches are tolerated but must be at 9-13 nt from the 5' end of the guide strand and those, must help Ago2 for repression or cleavage. (3) The complementary miRNA region (from

13 to 22) allows bulges or mismatches, but they must be after the sixteenth nt from the 5'. The miRNA functionality may be compromised if those conditions are not met (Fig 1.3) (18).

When Ago2 leaves the loading RISC, the guide strand exposes the seed region and interacts with the target mRNA and gains more stability with the complementary area in nucleotides 13 to 16 (Fig 1.3), (18, 96). Ago2 is subjected to phosphorylation and dephosphorylation cycles in highly conserved amino acids that allow it to bind and unbind to the target mRNA (97). Once Ago2 brings the guide strand to the target mRNA, translational repression begins with the recruitment of the Ago2-miRNA-mRNA complex to P-bodies (Fig 1.1).

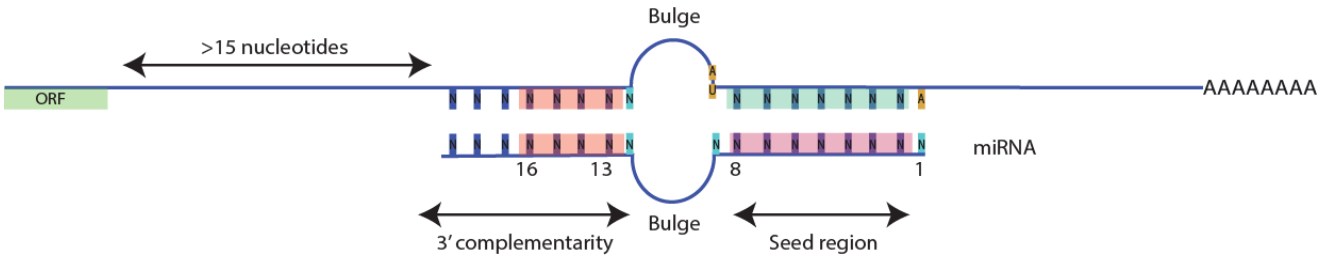

Figure 1. 3 miRNA and mRNA interaction.

The interaction between the miRNA and the mRNA follows specific rules like the perfect pairing in 2 to 8 nt (seed region) from the 5' of the miRNA; bulges are tolerated except in 13-16 nt of the complementary part. If these characteristics are present, the miRNA will silence the mRNA.

1.1.5 P-bodies

P-bodies are ribonucleoproteins that create non-membrane structures where mRNA is stored for its translational repression or degradation (98, 99). The main components of P-bodies can be separated into different groups by their function: (1) proteins of the core, which include decapping enzymes DCP2, decapping activators (DDX6, DCP1) and enhancers (EDC3, EDC4) in addition

to deadenylases (PAN2-PAN3, CCR4-NOT complex) and exonucleases (XRN1) (99-102); (2) MRNA repression factors (Ago2, GW182 and PABPC) and translational activators in P-bodies that act as repression factors (CPEB, Staufen, and eIF4E) (99, 102, 103); (3) Proteins from the nonsense-mediated mRNA decay (NMD) pathway like UPF and SMG (103). The full list of P-bodies components and an extensive review can be consulted in references (99, 102, 104).

P-bodies appear as roundish non-membrane structures with a diameter of ~300 nm in electron microscopy (105). The high concentration of proteins and RNA in P-bodies originates from the liquid-liquid phase separation where proteins like EDC3 harbors intrinsically disordered regions appended to RNA-binding domains. Intrinsically disordered regions can promote phase separation when they interact with RNAs (99, 106). Due to this nature, P-bodies can fuse between them and create more substantial structures with a higher capacity of mRNA retention.

Varying lines of evidence show that mRNA decay occurs mostly within P-bodies. For example, the decapping products are concentrated and the mRNA 3'UTRs co-localize with the exonuclease XRN1 (107). In addition, a large amount of decapping events correlates with a increased size of P-bodies (104). Conversely, in cells under stress mRNA accumulates in P-bodies but shifts to polysomes when the stress is removed (108). Therefore, P-bodies are structures where mRNA repression and degradation occur, but also where mRNA can be stored under particular conditions.

Besides, under stress conditions, cells create stress granules that contain mRNAs stalled in translation initiation associated with diverse RNA binding proteins. Unlike stress granules, P-bodies are generated to control mRNAs but not at the translation initiation level and mostly in the absence of stress (109). P-bodies can assemble *de novo* or be maintained, but this depends on the P-bodies protein concentration and the amount of repressed mRNA (99). *De novo* formation of P-bodies is caused by mRNA repression, which can be triggered by different activators. In yeast

models, the Puf protein binds to the 3'UTR of mRNA transcripts and activates CCR4-NOT ortholog complex, which begins the deadenylation process (110). Another example is the repression of aberrant mRNA sequences that are recognized by UPF1, which recruits other UPF proteins and SMG7 to activate decapping enzymes (104, 111). The RNAi pathway can also trigger mRNA repression and decay.

The mRNA repression and degradation by silencing mechanisms begin with Ago2-miRNA binding to a target mRNA. Consequently, Ago2 recruits GW182 [in humans the protein of Trinucleotide Repeat-Containing gene 6A (TNRC6A, TNRC6B, TNRC6C) gene] through the PIWI domain and the Ago-binding domain (ABD) (112, 113). GW182 interacts with PABPC (it is unclear if PABPC is within P-bodies) repressing the translation of the target mRNA (114). This event makes PABPC recruit deadenylases PAN2, PAN3 and CCR4-NOT complex, which removes adenines and promotes the oligouridylation by TUT4/7 (114-118). These events trigger mRNA decapping and degradation conducted by DCP1-DCP2, DDX6 and XRN1 (Fig 1.4), (47, 118-120).

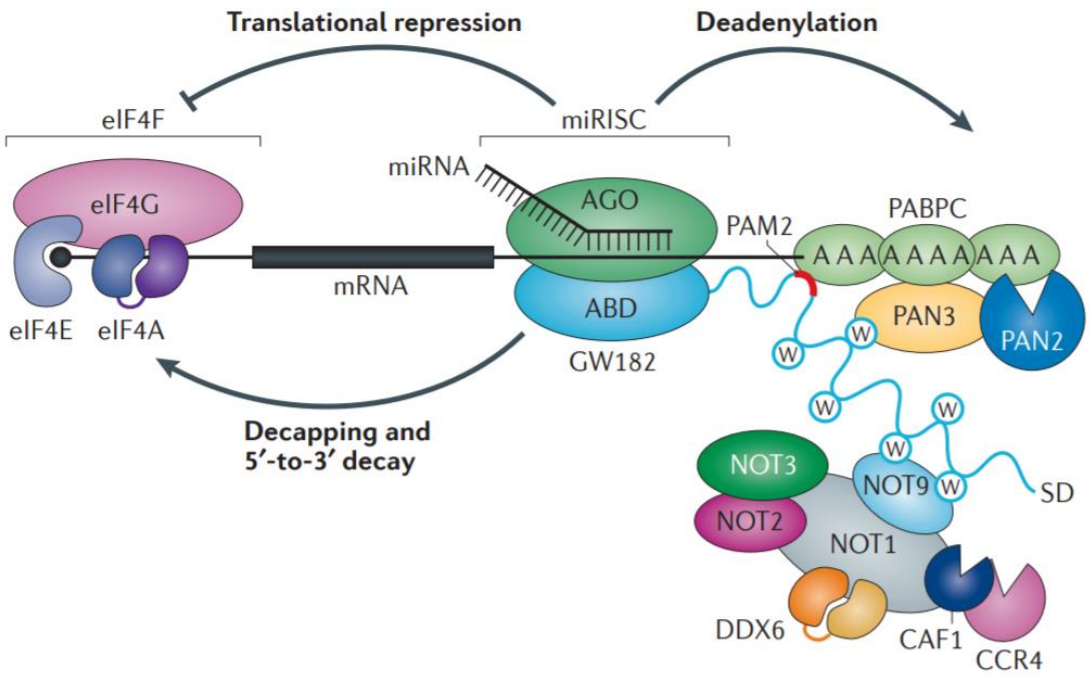

Figure 1. 4 mRNA silencing in P-bodies through miRNAs.

MiRNA silencing can lead the target mRNA to be repressed and degraded. MiRNA silencing and degradation is initiated by the Ago2/GW182 interactions with PABPC and PAN deadenylases. Next, GW182 recruits (CCR4)-NOT complexes to uridylate the mRNA. These events trigger the deadenylation and decapping by DCP1 that enhances its activity in the presence of DDX6. Without cap, XRN1 degrades the mRNA from 5’ to 3’. Reproduced from (102).

1.2 Human immunodeficiency virus

1.2.1 HIV Discovery, origins, and contemporary impacts

Among the hardest challenges in humankind history are the epidemics originated by viruses. The first viral epidemic documented was the Antonine plague; it occurred in the second century around 165 A.D. when the Roman troops returned from the East and brought smallpox to the Roman empire, killing around five million people (121). Another example is the "Spanish" flu that occurred in 1918, likely originated in Kansas (US), and was due to the influenza virus H1N1, causing about 50 to 100 million casualties worlwide (122, 123). The HIV epidemic has lasted for a very long time, with 74.9 million victims since the discovery of the virus (124). Despite the prevention, care and treatment, to date, HIV has not been eradicated. Therefore, it is still necessary to study HIV by exploring new areas of viral and host behaviors.

The identification of HIV epidemics started in the early 1980s when the Centers for Disease Control and Prevention (CDC) and doctors from California and New York found unexplained deficiencies in the immune system in young homosexuals. Consequently, these men developed opportunistic infections (125). Shortly after, more cases of immunodeficiency were reported not only in homosexuals but also in intravenous drug users and blood transfusion recipients. In 1983 Dr. Barré-Sinoussi in Dr. Luc Montagnier's lab characterized a new retrovirus in lymph nodes of affected patients and named it lymphadenopathy associated virus (LAV) (126). In 1984, Dr. Robert Gallo and his team isolated a similar T-lymphotropic retrovirus from a larger pool of samples and set up the conditions to propagate the virus *in vitro* (127). Simultaneously, the group of Dr. Jay Levy in San Francisco, California cultured a similar retrovirus from patients with AIDS and associated the specific antibodies produced from the infected individuals with the causative retrovirus (128). These viruses were variants of the same virus that was later renamed HIV or HIV-

1 (129). By 1986 another retrovirus with similarities was found in patients from West African countries, this virus was later known as HIV-2 (130).

In 1989, the origin of HIV-1 was associated with a Simian immunodeficiency virus (SIV) isolated from two captive chimpanzees (SIV_{cpz}) (131). SIV_{cpz} resulted from the recombination of two SIV, one from the red-capped mangabeys (SIV_{rcm}) and another from greater spot-nosed monkeys (SIV_{gsn}) (132). SIV_{cpz} gave rise to two distinct viruses, the first one was established in gorillas (SIV_{gor}) and the other one in humans (HIV-1) (Fig 1.5). HIV-1 coming from SIV_{cpz} is divided into groups M and N, (133, 134). Group M is responsible for the main HIV-1 pandemic, while group N is confined into 13 individuals in Cameroon and one more in France (133, 135, 136). Group M is sub classified in clades A, B, C, D, F, G, H, J, K, L and 51 circulating recombinant forms (125, 133, 137). On the other hand, SIV_{gor} crossed the interspecies barrier and gave rise to two other groups, O and P of HIV-1. The group O remains in African countries with low prevalence, whereas group P has been identified in two individuals in Yaounde and Cameroon (Fig 1.5) (133). HIV-2 originated from one common ancestor, an SIV from sooty mangabey monkeys (SIV_{smm}) (Fig 1.5) (138). Interestingly, SIV_{smm} infection is asymptomatic in sooty mangabey monkeys, but its adaptation to a different species triggered its virulence (125).

Phylogenetic data estimate that HIV began to be transmitted between humans in early 1900 (139, 140). A complementary study showed that HIV-1 group M and SIV_{cpz} shared a common ancestor that date back between 1799-1904, suggesting that SIV crossed the species barrier at some point around 1853 (141). This transfer to humans probably occurred by contact with SIV-infected blood during the hunt and butchering of chimpanzees (142).

According to UNAIDS, around 75 million people worldwide have been infected with HIV and almost 37 million people currently live with HIV (124). Moreover, there are 5,000 new infections per day, with a total of 1.8 million infections yearly (143). To date, only 59% of infected patients have access to combination antiretroviral therapy (cART) worldwide (143), whose effects only control the disease without resolving it. Furthermore, the financial burden goes over millions of dollars each year for prevention, care and treatment. An estimation in 2015 showed that a person living in the U.S.A. who is infected at 35 years age-old would cost $326,500 U.S in medical care during his/her lifetime (144). Beyond the financial and health issues, infected individuals are highly stigmatized, they have physical and psychological problems that often lead them to turn down diagnosis and healthcare (145). Therefore, it is still necessary to pursue HIV studies for a better understanding of the virus and find additional treatments that will consequently lead us to a cure. Due to the HIV-1 importance and distribution, from this part of the thesis onward, HIV will be referred to as HIV-1 unless it is stated otherwise.

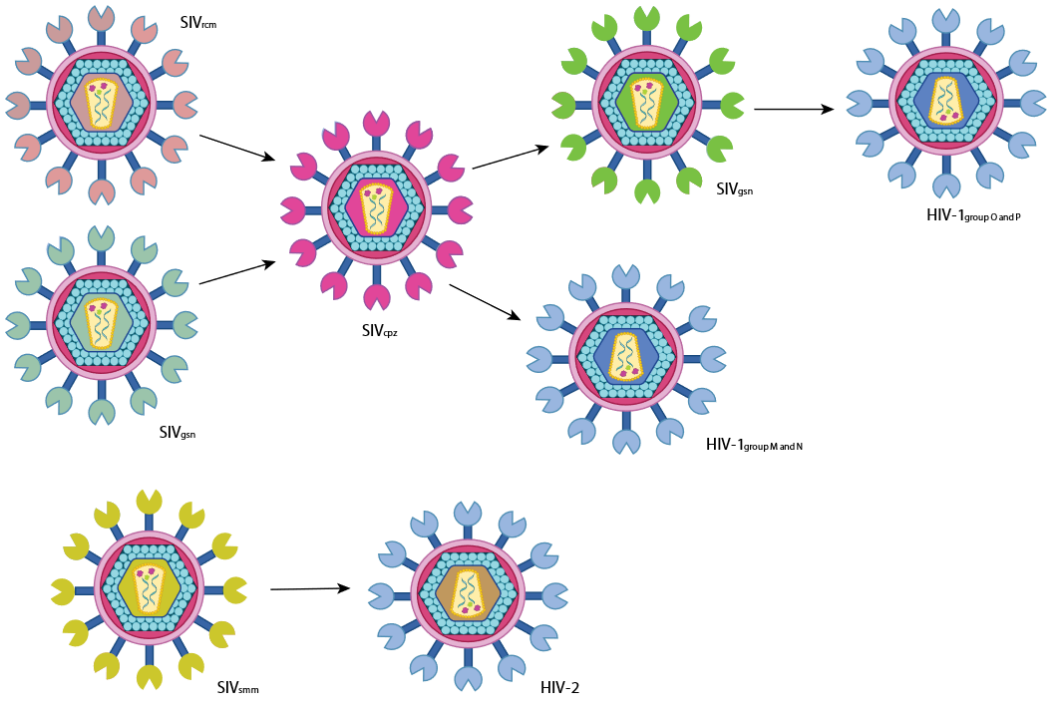

Figure 1. 5 HIV-1 and HIV-2 evolved from SIV.

HIV phylogenic analysis shows that HIV-1 and HIV-2 are SIV viruses adapted to humans. HIV-1 group M and N originated from SIVcpz, whereas HIV-1 group O and P are derived from SIVgsn. HIV-2 evolved exclusively from SIVsmm.

1.2.2 HIV-1 genome and virion structure

HIV-1 belongs to the *Retroviridae* family, of the Lentivirus genus and is classified as being in group IV within the Baltimore classification system (125). The characteristic of the *Retroviridae* family is the fact that these viruses possess a reverse transcriptase (RT) to convert their genomic RNA into DNA to be integrated into the host genome. Lentiviruses are complex retroviruses because their genome codes for several regulatory and accessory (also called auxiliary) proteins in addition to the structural polyproteins group specific antigen (Gag), polymerase (Pol), and envelope (Env) encoded by simple retroviruses. These additional proteins encoded by complex

retroviruses are the result of additional open reading frames (ORF) and alternative splicing (146). HIV-1 virions possess an envelope encoded by the Env gene obtained from the cell membrane during budding after migration of the Env protein to the membrane. Mature virions contain a characteristic cone-shaped core given by the assembly of capsid molecules, which protects the genomic RNA. The virial particle is spherical, typically of ~145nm in size (Fig 1.6A) (147, 148). The genome length of HIV-1 is 10 kb which encodes a total of 16 proteins from 10 transcripts. The genome also includes two long terminal repeats (LTR), one at the 5' end and the other at the 3' end (Fig 1.6B). Each LTR includes a unique region 3 (U3), a repeat region (R) and a unique region 5 (U5) on the proviral DNA. The transcription begins with the R region and starts at +1 with the transactivation response element (TAR), which plays a vital role during the viral transactivation (149). The first protein encoded at the 5' end is the pr55 Gag polyprotein, which can also be translated as pr160 Gag-Pol due to a frameshift in the ORF. The Env polyprotein is translated from the 3' end of the singly spliced RNA.

Gag is a polyprotein composed of different domains such as the matrix (MA) or p17, capsid (CA) or p24, nucleocapsid (NC) p7, P6 and two spacer peptides SP1 and SP2 that flank NC (125). Each protein is eventually cleaved from the Gag and Gag-Pol polyproteins by the protease (PR) or p10 present within the Pol and Gag-Pol polyproteins. These Gag and Gag-Pol polyproteins also include the RT (p66 and p51) and the integrase (IN) or p32 (Fig 1.6B). The Env polyprotein is composed of the glycosylated precursor gp160, which is processed within the Golgi apparatus by cellular furin or furin-like proteases to create the surface gp120 and the transmembrane gp41 (150). Additionally, Env transcripts include the Rev Response Element (RRE), which is necessary for unspliced and partially spliced viral mRNAs to be exported to the cytoplasm (151). Finally,

alternative splicing of viral transcripts generates Vif (23kD), Vpr (15kD), Tat (14kD), Rev (19kD), Vpu (16kD) and Nef (27kD) proteins.

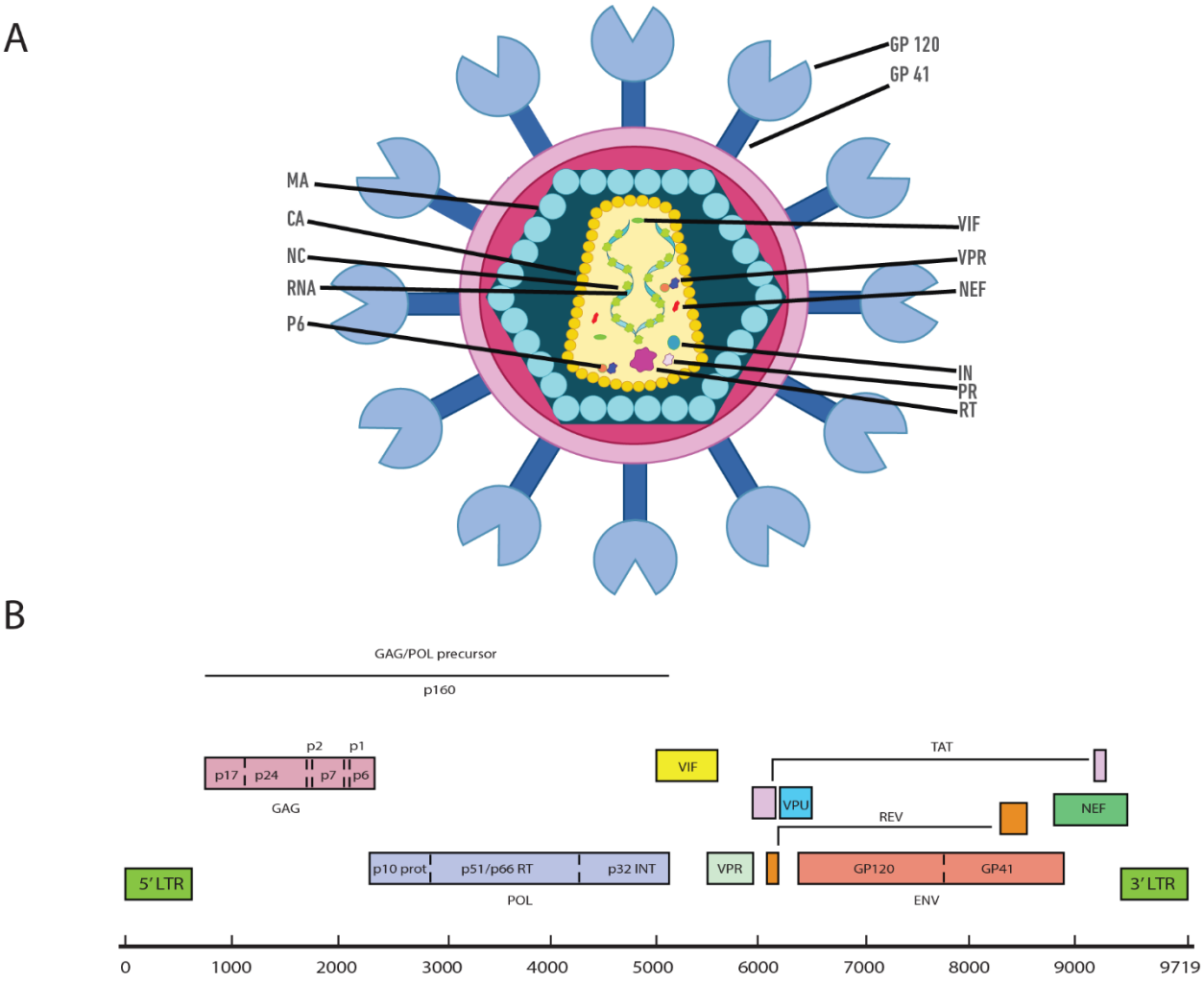

Figure 1. 6 HIV-1 virion architecture and viral genome.

A) HIV-1 acquires the viral envelope from the cell along with Env proteins gp120 and gp41. MA is anchored into the inner leaflet of the viral envelope and right after CA, the main structural protein of the viral core that protects the viral RNA bound to NC. Other viral proteins P6, Vif, Vpr, Nef, IN, RT, and PR are found in the viral core. B) HIV-1 genome consists of 9719 nt that encodes 16 proteins from 10 transcripts due to alternative splicing sites and different open reading frames.

1.2.3 The HIV-1 replication cycle and Gag protein

HIV-1 replication can be divided into early and late phases. In the initial stage, the virus attaches to the cell membrane followed by fusion, entry and uncoating. Retroviral transcription starts in the viral core and continues during uncoating, forming a dsDNA from the viral RNA. This DNA and associated proteins form the pre-integration complex (PIC), which shuttles to the nucleus and the viral DNA is integrated into the host genome to create the provirus (Fig 1.7). In the late phase, the provirus produces the genomic RNA and transcripts that are translated into proteins for the assembly and release. The budded viral particle will mature, creating all the cleaved components necessary for the next round of infection (Fig 1.7).

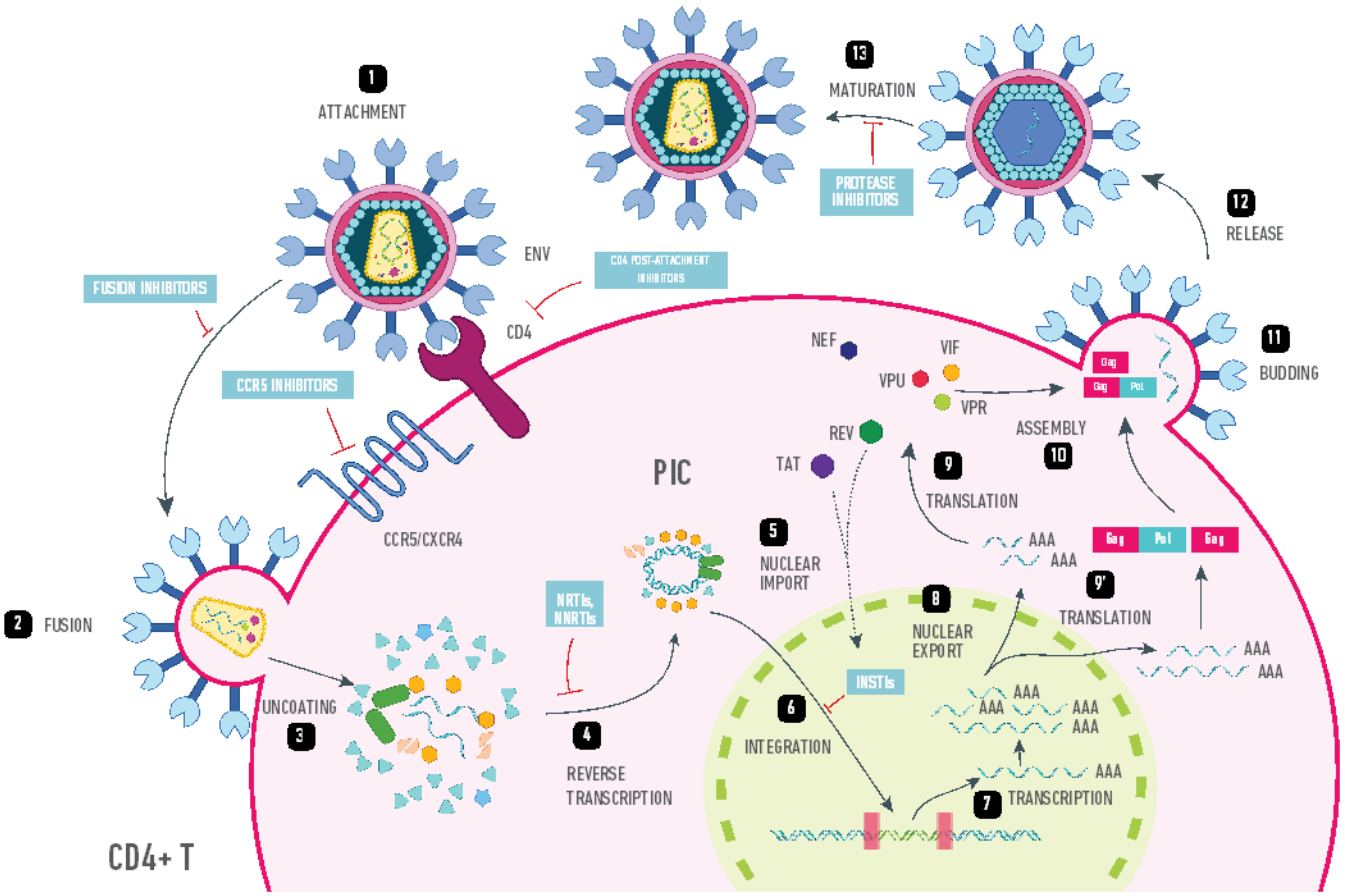

Figure 1. 7 HIV-1 replication cycle.

The early stage of the HIV-1 replication cycle encompasses attachment, binding, uncoating, reverse transcription, nuclear import, and integration. The late phase begins when the provirus produces Tat, Rev, and Nef. Tat and Rev are imported into the nucleus. Tat increases the transcription rate whereas Rev facilitates the export of unspliced and singly spliced viral transcripts to the cytoplasm where they will be translated and also used as the viral genome. Gag protein orchestrates the assembly and RNA packaging on the inner leaflet of the cell membrane, which triggers the virion release and maturation. Different drug strategies to counter the replication cycle are shown in blue squares. Adapted from (152).

1.2.3.1 Virus binding, entry, and the reverse transcription

HIV-1 infects cells that possess cluster of differentiation 4 (CD4) surface receptors and C-C chemokine receptor type 5 (CCR5) or C-X-C Chemokine Receptor Type 4 (CXCR4) co-receptors. The primary targets are $CD4^+$ T lymphocytes ($CD4^+$ T) as well as macrophages and dendritic cells (DC) (153). HIV-1 begins the infection by a non-specific attachment of the protein gp120 on the cell membrane through the interaction with integrins and heparan sulfates (154). This attachment continues until the gp120 encounters a CD4 receptor forming a specific binding (Fig 1.7). Gp120 heterodimers harbor five constant domains (C1-C5) and five variable domains (V1-V5). The contact with CD4 causes conformational changes on both proteins allowing the V3 domain to interact with CCR5/CXCR4 (155). The interaction of gp120 and the co-receptor reveals a gp41 trimer with fusion peptides that are folded in the hinge region. The conformational change exposes the amino-terminal peptides that harpoon the cell membrane while the carboxy-terminal domains remain in the viral envelope. Then, the viral envelope forces the formation of a fusion pore to the cell membrane allowing the access of the viral core (155, 156).

There are three models of virus uncoating at the post-entry events. The first one supports that the uncoating occurs right after the entry and close to the inner cell membrane. The second one proposes that the uncoating gradually occurs while the core goes towards the nucleus and the third model favors the reverse transcription inside of the core until the nucleus is reached (148). Regardless of the uncoating model, the reverse transcription starts after the entry by the retro-transcription complex made by the RT, CA, NC, IN, Vpr and the viral genome. Reverse transcription is the hallmark of the *Retroviridae* family, where the RNA is transcribed into double-stranded DNA (157). The HIV-1 RT is a heterodimer composed by p66 and p55. P66 contains a

polymerase and an RNase H domain, whereas p51 only has the polymerase domain with a more compact structure, which stabilizes the heterodimer (158, 159).

Reverse-transcription uses $tRNA^{Lys3}$ as an initial primer in the 5' viral RNA, which produces a negative single-stranded DNA while the RNA strand is degraded. Only a small sequence in the viral RNA called polypurine tract (ppt) resists the RNase H activity which is then used as a primer for the synthesis of the complementary DNA strand creating a linear double-stranded viral complementary DNA (vcDNA) (157, 158).

1.2.3.2 Integration and transcription

After reverse transcription, the vcDNA harbors CA, Vpr, RT, NC, MA and IN to form the pre-integration complex (PIC). To transport the vcDNA into the nucleus, IN interacts with importin 7 (Imp7), transportin 3 (TNPO3) and Impα3 on the nuclear surface while MA and Vpr assist the import through nuclear localization signals (NLS) and Imp-α (160-162). Within the nucleus, IN removes two nucleotides from the 3' vcDNA in each strand, which generates 3'OH sticky ends that allows a nucleophilic attack into the 5' phosphate target DNA (163). IN and CA tether the vcDNA to the genome by binding the host factors lens epithelium-derived growth factor (LEDGF) and cleavage and polyadenylation specific factor 6(CPSF6). These interactions modulate the integration onto spliced transcriptional regions with a high density of GC and CpG, mostly found in euchromatin (164-166). Once vcDNA is integrated, the PIC is dismantled, and the transferred vcDNA intermediate is repaired by the host machinery (Fig 1.7) (163).

The proviral LTR is divided into U3, R and U5 regions (167). The U3 is subdivided in the modulatory segment (-455 to -104) that possesses the transcription binding signals, the enhancer segment (-109 to -79) that harbors binding sites for the SP1 and the NF-κB transcription factors

and the promoter segment (-78 to -1) that has the TATA box-binding sites (168). The R/U5 region encodes for the TAR element and other regulatory binding sites (169). RNA Pol II generates the first viral transcripts; however, the transcription rate is inefficient (169). The first transcripts are subjected to double splicing and export to the cytoplasm where they produce the first HIV-1 proteins, Tat, Rev, and Nef (Fig 1.7). Tat protein posses a nuclear localization signal (NLS). Tat recruits the positive transcription elongation factor b (P-TEFb) from the 7SK complex (170). 7SK is a conserved and abundant ncRNA of 332 nt localized mainly in the nucleus with few pools in the cytoplasm (171). In addition to the P-TEFb, 7SK harbors other cellular proteins such as La-related protein 7 (LaRP7) and methylphosphate capping enzyme (MePCE) that stabilizes the RNA structure whereas HEXM1/2 binds to P-TEFb and regulates its release (172-174). P-TEFb is composed of cyclin-dependent kinase (Cdk9) and cyclin T1 (CycT1). Tat binds CycT1 and drags it in proximity to the TAR element. Tat binds to the bulge of TAR RNA, whereas CycT1 binds to the loop. This association triggers P-TEFb to hyperphosphorylate RNA Polymerase (Pol) II, making it highly processive and enhancing viral transcripts several hundred-fold (170, 175-177).

HIV-1 produces more than 40 RNA species, which belong to one of the 3 categories: (1) unspliced genomic RNA, coding for Gag, and Gag-Pol, (2) singly spliced RNAs that produce Vif, Vpr, Vpu and Env and (3) doubly spliced RNAs that are translated into Tat, Nef and Rev (125, 146, 178, 179). The unspliced and partially spliced RNAs are restricted for nuclear export. To overcome this stage, HIV-1 uses Rev protein to export viral transcripts. The first step is when Rev gets into the nucleus through the interaction with Imp-β (180). Within the nucleus, Rev binds the RRE contained in the Env region of the unspliced and singly spliced RNAs. The Rev-RRE complex binds to the chromosomal maintenance 1 (CRM1), DEAD-box helicase 3 (DDX3), the host up-

frameshift protein 1 (UPF1), and Ran (GTP) which makes the transcript reach the nuclear pore and exit the nucleus (151, 180-182). In the cytoplasm, Ran(GTP) is dephosphorylated to give rise to Ran(GDP) inducing the release of CRM1 and Rev from RRE, while DDX3 and UPF1 remain associated to the unspliced viral transcript and ensure an efficient association to ribosomes to be translated into Gag and Gag-Pol (181, 183).

1.2.3.3 Gag, viral assembly, release and maturation.

Gag is a structural HIV-1 protein that is essential for creating new viruses. Gag is a 55 kD multidomain protein composed MA, CA, NC, P6, and two spacer peptides SP1, and SP2 flanking NC (Fig 1.8) (184). Gag transcripts are translated in a ratio of 95% versus 5% for Gag-Pol due to a frameshift during the translation (184). MA shows a globular structure with myristoyl group at the N-terminus that permits hydrophobic interactions, and a highly basic region (HBR) that interacts with phosphatidylinositol-4,5 bisphosphate (PIP2) in the inner plasma membrane (185, 186). MA also interacts with lipid rafts that function as a scaffold for the viral assembly and Env recruitment (187, 188). CA is a multifunctional protein that associates itself through the C-terminus and the major homology region (MHR) (189). The N-terminus is rich in prolines that interact with cyclophilin A (CYPA) into nascent viral particles that protect the HIV-1 core from cellular restriction factors like TRIM5α during the entry and the reverse transcription process (190). In addition, individual units of CA form the cone-shaped core in mature viral particles, each virion has 5000 units of CA assembled in pentamers and hexamers that create the fullerene cone (191). NC dimerizes and directs the RNA packaging into viral particles. After the unspliced HIV-1 RNA is exported from the nucleus, the viral RNA can dimerize in the cytosol or at the plasma membrane from the Ψ-region located in the 5’ UTR, specifically at the stem-loop 1 (SL1) contained in the dimerization initiation site (DIS) (186, 192). SL1 selectively promotes the

packaging of unspliced RNAs (151). DIS sequences form RNA dimers that have bound a $tRNA^{Lys3}$. The dimer then associates with NC zinc finger domains that stabilize the structure for the recruitment in nascent viral particles (193, 194). P6 is a small peptide of 55 amino acids (aa) that interact with the endosomal sorting complexes required for transport (ESCRT) machinery, especially with ESCRT-I and ESCRT-III, which are essential for the viral budding on the plasma membrane (195, 196).

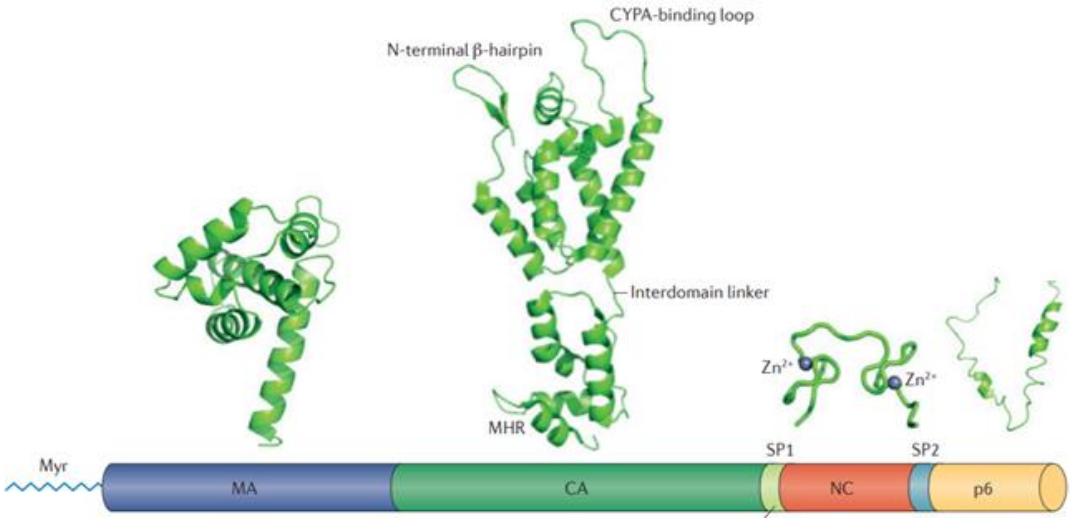

Figure 1. 8 Gag structure.

HIV-1 Gag protein contains multiple domains that assist the virus assembly and release. MA brings Gag to the cell membrane and anchors it to the inner leaflet using myristoyl groups that interact with PIP2. CA mediates Gag multimerization in the inner plasma membrane. CA homodimers interact with each other through the C terminus and the MHR, whereas a loop rich in prolines at the N terminus binds to CYPA. SP1 and SP2 are short domains that flank NC, which interacts with the genomic RNA. P6 recruits ESCRT components for the viral budding on the plasma membrane. Reproduced from (184).

Viral assembly starts with the dimerization of viral genomic RNA through the Ψ-region (192). Gag multimerizes through the CA domain (197) and concomitantly NC domain binds the viral genomic RNA maintaining its dimer structure (193, 194). In proximity to the plasma membrane, MA anchors to the inner leaflet, whereas Env units into the cell membrane are recruited by Gag (184). During assembly, Gag also interacts with different cellular proteins that assist it, such as ABCE1 (198), DDX6 (199) and Staufen1 (200, 201). Indeed, many cellular proteins can interact with Gag, although, their role throughout the infection is unknown (202, 203). Finally, P6 recruits the ESCRT machinery through the conserved motif PTAP for the virion release (Fig 1.9) (195, 196). At this point, Vif, Vpr and cellular proteins are also recruited to the nascent virions (204, 205). It is important to state that most of the assembly events occur on the plasma membrane.

Outside the cell, PR is auto-catalyzed from the Gag-Pol polyprotein generating a free PR that rapidly cleaves in ten different locations in Gag and Gag-Pol producing MA, CA, NC, IN and RT (206). The result creates a mature viral particle with a different architecture, which is ready for the next round of infection (Fig 1.9).

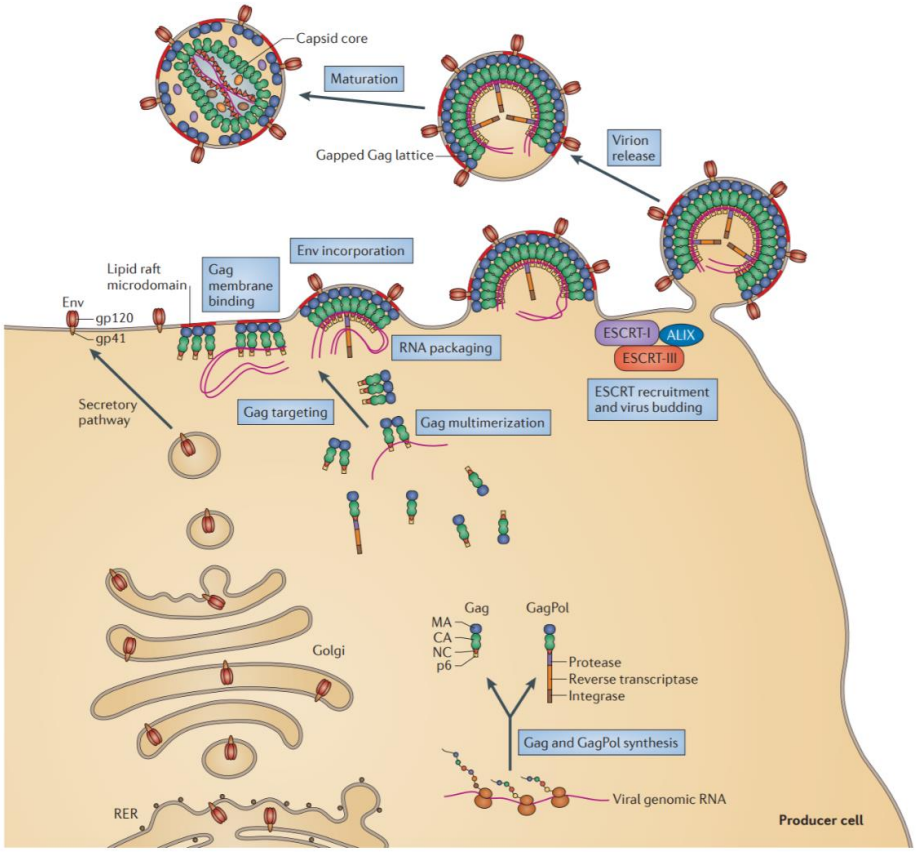

Figure 1. 9 HIV-1 assembly and release.

Gag and Gag-Pol target the inner leaflet of the cell membrane. The binding of Gag and Gag-Pol to the cell membrane by MA triggers mechanisms that recruit Env onto nascent viral particles. Simultaneously, NC recruits genomic RNA and P6 binds the first ESCRT proteins to release the immature virion. Outside of the cell, PR in Gag-Pol cleaves several sites in Gag and Gag-Pol, which induces virion maturation. Reproduced from (184).

1.2.4 HIV-1 infection

HIV-1 is commonly transmitted by sexual intercourse, intravenous inoculations and less frequently, during labor and breastfeeding (143). Nonetheless, the risk of infection by each transmission route is different. A comprehensive literature study in 2014 estimated that blood

transfusion recipients have a 92.5 % probability of acquiring the virus, vertical transmission from mother to child 22.6%, needle sharing 0.63%, percutaneous injuries with needles 0.23%, receptive anal intercourse 1.38%, insertive anal intercourse 0.11%, receptive penile-vaginal intercourse 0.8%, and insertive penile-vaginal intercourse 0.4% (207). The transmission rate can be increased by different factors such as high viral load in blood and genital ulcer disease (207). The transmission rate can also be decreased by ART, pre-exposure prophylaxis, use of condom and circumcision (207). Indeed, heterosexual circumcised individuals lessen by up to 60 % HIV-1 transmission due to a reduction in the activation of the immune response in the inner penis foreskin, which harbors a large number of targets (208, 209).

Independently of the transmission route, when HIV-1 reaches specific epithelium or bloodstream, it targets $CD4^+$ T cells with co-receptors CCR5 (HIV-1 strains R5) or CXCR4 (HIV-1 strains X4) (210). $CD4^+$ T cells have subpopulations depending on the co-receptor's expression. For instance, high expression of CCR5 in $CD4^+$ T cells is linked to memory T cells, whereas low expression represents naïve T cells (211). In the same fashion, there are resting (naïve and memory) and activated T cells, which eventually become memory cells. Resting $CD4^+$ T cells show low expression of CCR5, whereby HIV-1 barely infects these cells (212). The time course in which HIV-1 depletes the majority of $CD4^+$ T cells varies from person to person albeit, three typical stages of infection are recognized: acute or primary infection, chronic infection, and acquired immune deficiency syndrome (AIDS). In the next section, I will describe the cellular events in the acute, chronic and AIDS stages.

1.2.4.1 Acute infection and the founder virus.

During the first hours after the transmission, HIV-1 infects $CD4^+$ T cells in local tissues that also contain DC and macrophages (213). Within a few hours, HIV-1 replicates and infects new cells in the local tissue, disseminating beyond the mucosal barrier in the first days. Infected DCs migrate to the closest lymphoid organs where they spread the virus to naïve and memory $CD4^+$ T cells giving rise to a systemic infection (214, 215). Similarly, infected $CD4^+$ T cells migrate to gut-associated lymphoid tissue (GALT) that houses the primary source of $CD4^+$ CCR5 T cells in the body, which are obliterated within days (216). These events occur continuously during the first 7 to 21 days and this stage is known as the eclipse phase (217). During the first days of the eclipse phase, the virus cannot be detected by conventional techniques until the infection reaches a concentration of 5 RNA copies/mL of plasma (218). The clinical manifestations at this stage are nonspecific and only 50 to 70% of people show fever, headaches, arthralgias myalgias, malaise, maculopapular rash on the face and trunk (219, 220). Eleven or twelve days after infection, laboratory analysis should show a characteristic lymphopenia in $CD4^+$ T cells, an increase of $CD8^+$ T cells and detectable HIV-1 RNA levels (221-223).

HIV-1 is genetically heterogeneous with several mutant viral particles called quasi-species (224). During transmission and acute infection, several quasi-species infect DC or $CD4^+$ T cells in the host mucosa. Mathematical models based on phylogenetic analysis demonstrated that only one virion (the founder virus) is responsible for the infection in 80% of heterosexual cases, 60% in homosexuals and 40% in intravenous inoculations (214, 217). Therefore, individuals that acquired HIV-1 through injections have more heterogeneity than those who obtained the virus through sexual contact. This is explained by HIV-1 being subjected to a bottleneck selection from the donor to the recipient. Briefly, HIV-1 is highly heterogeneous in the donor's blood, but this diversity is

reduced in the donor's mucosa (semen or cervicovaginal mucus) due to lectins and autologous antibodies (225). Only virions adapted to the donor's mucosa are transmitted to the recipient's mucosa wherein the virions are subjected to another round of selection. Viruses that have low fitness genotype or that infect cells with a rough environment for replication will not survive and only the first virus that reaches the perfect target will pass through several rounds of replication and disseminate across the host (225).

1.2.4.2 Chronic infection and AIDS.

After 4 to 12 weeks of primary infection, the immune response controls the infection and establishes a set point with a small recovery of $CD4^+$ T cell population. However, over time HIV-1 population increases while $CD4^+$ T cells population is diminished. The chronic stage lasts for years and seems to be asymptomatic for most individuals, albeit some of them develop symptoms such as night sweats and weight loss as well as illness related to a faint immune response (125). Regardless of the symptoms, a massive immune activation takes over against the virus. This hyper-activation can be observed through immune activation markers like CD38 and human leukocyte antigens (HLA)-B27, HLAB57 for slow progressors and HLA-B35 for individuals that are highly susceptible to the infection (226, 227).

During the chronic stage, depleted $CD4^+$ T cells in GALT provokes translocation of microbial lipopolysaccharide (LPS) to the bloodstream which triggers a persistent activation of the immune response (228). The hyperactivation of the immune system also activates T regulatory cells, which express transforming growth factor-beta 1, augmenting collagen deposits and fibrosis in lymphatic tissue resulting in architecture disruption that further favors $CD4^+$ T cells depletion (229, 230). The constant reduction of $CD4^+$ T cells and activation of the immune system induces the production of T cells with a short lifetime and abnormal regenerative potential (231). The loss of

proper functions and the limited proliferative capacity of T cells leads the immune response to exhaustion and AIDS (232). During AIDS, the $CD4^+$ T cell numbers decrease, reaching 500 cells/mL, 200 cells/mL and even 50 cells/mL allowing opportunistic pathogens and malignancies to take over (125).

AIDS can be reversed and prevented with ART. Currently, HIV-1 infection is no more a fatal disease but a chronic one when ART is prescribed on time. Although ART is beneficial to eliminate all the active virus, viral reservoirs are still the challenge. In the next sections, I will describe the current ART, the viral reservoir and cure strategies.

1.2.5 Current ART

The first antiretroviral drug, a nucleoside analog reverse transcriptase inhibitor (NRTI) known as zidovudine (AZT), was approved in 1987 (233). AZT was taken as monotherapy for some time until people began to have a rebound in the viral load due to HIV-1 drug-resistant quasi-species. By 1990 other NRTIs were developed and started to be used together to boost the treatment's efficacy. By 1995, the combined therapy was named as highly active antiretroviral therapy (HAART) or currently cART (234).

In 1995 with the introduction of the first generation of protease inhibitors (PI) and the non-nucleoside analog reverse transcriptase inhibitors (NNRTI), thousands of people stopped dying (235-237). From 1996 onward HAART started to be used, and other antiretroviral drugs with increased efficacy, decreased toxicity and less virus resistance have been produced and approved (234). As of the last review in October 2018, the Department of Health and Human Services Panel on Antiretroviral Guidelines for Adults and Adolescents recognizes more than 30 antiretroviral drugs divided into 7 classes included NRTIs, NNRTIs, PIs, integrase strand transfer inhibitors

(INSTIs), fusion inhibitors, CCR5 antagonists and CD4 post-attachment inhibitors (Fig 1.7). In addition, ritonavir and cobicistat are used to boost the pharmacokinetics of atazanavir, darunavir and elvitegravir (238).

According to the guidelines for the use of antiretroviral agents in adults and adolescents with HIV (239), infected individuals must initiate ART by taking two NRTIs and one of any INSTI, NNRTI or a boosted PI. Suggested regimens are in Table 1 based on the last guidelines for the use of antiretroviral agents.

Table 1. 1 Initial regimen examples of cART.

Regimen for most people linving with HIV				
Treatment	**Name**	**Cathegory**	**Total pills per day**	**Condition**
	Bictegravir	INSTI		
	Tenofovir alafenamide	NRTI		
1	Emtricitabine	NRTI	3	none
	Dolutegravir	INSTI		
	Abacavir	NRTI		
2	Lamivudine	NRTI	3	HLA-B57 negative
	Raltegravir	INSTI		
	Abacavir	NRTI		
3	Lamivudine	NRTI	3	HLA-B57 negative and HIV RNA <100,000 copies/mL
	Darunavir	PI		
	Ritonavir or Cobicistat	Booster		
	Tenofovir alafenamide	NRTI		
4	Emtricitabine	NRTI	4	none
	Doravirine	NNRTI		
	Tenofovir alafenamide	NRTI		
5	Lamivudine	NRTI	3	none
	Darunavir	PI		
	Ritonavir	Booster		
6	Raltegravir x2	INSTI	4	HIV RNA <100,000 copies/mL, CD4 > 200 cell/mm^3

1.2.6 Latency and viral reservoir

Resting $CD4^+$ T cells can be infected by HIV-1, but the virus cannot complete its replication cycle due to specific cellular factors (240, 241). If these cells are activated shortly after infection, the viral integration will proceed and the replication cycle will be completed (240). In patients under ART the activated $CD4^+$ T cells will enter in a memory-resting mode with negligible viral particle

production (240). Thus, $CD4^+$ T cells that harbor the provirus but do not express it, are called viral reservoirs. The half-life of these cells is around twelve years and only 1 over 10^6 resting $CD4^+$ T cell is a viral reservoir (242). These features make the decay rate so small that it would take approximately 73 years to eliminate all the reservoirs (243-245).

Virus latency is not totally understood, but some mechanisms explain it. The first mechanism could be related to the site and orientation in the genome (246), where host genes occlude the LTR (247, 248). A deficiency in transcription explains the second mechanism due to either the absence of active NF-κB (p50/ReIA), which favors deacetylation, or to a failure in the recruitment of transactivation products like p-TEFb (249, 250). A critical step for virus production is the Tat acetylation, which allows TAR dissociation between early and late phases in the replication cycle. Therefore, the third mechanism of latency is represented by improper Tat acetylation (251). Finally, epigenetic regulation on viral promoters by methylases like MBD2 and deacetylase HDAC2 also contributes to latency (252).

Knowing the mechanisms that govern viral latency, researchers' efforts have focussed on identifying a functional cure. There is one patient that has been completely cured, Timothy Brown, also called the “Berlin patient” (253, 254). A second possible cured person was reported in 2019 in England, but follow-up analyses need to be done to determine if this patient is definitively cured (255). In the next section, I will describe the current cure strategies for HIV-1.

1.2.7 HIV-1 cure strategies

Timothy Brown is the only patient throughout the world in whom no HIV-1 rebound has been observed through the years after a cure treatment. Mr. Brown was infected by HIV-1 and treated by HAART. After several years, he developed myeloid leukemia and underwent allogeneic

hematopoietic stem-cell transplantation (HSCT) from a homozygous donor with a mutation in CCR5 (CCR5Δ/Δ32) (253). The deletion in CCR5 rendered the donor cells refractory to HIV-1 infection and prevented virus resurgence in the patient. Recently a similar case was reported after HSCT where a patient has experienced viral remission for 19 months (255). Although both patients show the feasibility of reaching a cure, both instances were sporadic due to their histocompatibility and tolerance to the donor and they do not represent a strategy that can be widely applied to all patients (256).

Early HAART is explored as part of a functional cure due to temporary viral remission in reported cases like the Mississippi baby, the French VISCONTI cohort and others (257-261). The very early use of HAART could reduce HIV-1 progression up to 75% (262). However, the most promising strategies are related to broadly neutralizing antibodies (bnAb), "shock and kill" and "block and lock" therapies as well as gene therapy.

Among HIV-1 infected individuals, less than 1% are elite controllers (EC) who control plasma viremia at levels of 50 to 400 RNA copies/mL (263). ECs have different characteristics to modulate HIV-1, like the production of bnAbs (263-265). BnAbs are Abs that have a broad range of neutralizing activity in many HIV-1 subtypes and are studied for a functional cure (265). For instance, bnAbs with Toll-like receptor agonists are sufficient to stop or delay viral infection (266). Other strategies focus on improving target recognition with engineered bispecific bnAbs and increasing the number of targeted strains (267, 268).

The "shock and kill" strategy is based on the reactivation of the dormant virus within reservoirs using latency reversing agents (LRA), which may lead to their recognition and destruction by the host immune response (269). LRAs are divided into six categories. (1) Histone post-translational modification modulators, (2) Non-histone chromatin modulators, (3) NF-κB stimulators, (4) Toll-

like receptors (TLR) agonists, (5) extracellular stimulators like TNF-α and (6) miscellaneous compounds whose mechanism of action is not understood (269). The main drawbacks of the "shock and kill" strategy is the weak response to reactivate viral reservoirs, the cytotoxicity in the patient and the inability of the immune response to eliminate reactivated cells (270, 271). "Block and lock" is an alternative strategy, which is based on the use of latency promoting agents (LPAs). LPAs promote deep latency of the provirus by countering viral or host proteins/mechanisms that favor virus replication like Tat (272, 273) and the cellular autophagy regulator mTOR (274-276).

Finally, an alternative option is gene therapy, which consists of transplanted stem cells that were knocked down or knocked out in specific host or viral components like CCR5 gene or viral RNA (277-280).

1.3 Zika virus

1.3.1 Emergence of Zika virus

ZIKV is an emerging virus transmitted by mosquitoes, which causes mild symptoms such as fever, headache, rash, conjunctivitis and arthralgia (281). ZIKV caught the public eye when it was linked to congenital malformations and neuropathological manifestations. ZIKV dissemination from Africa, Asia and the Americas makes it a global health problem. ZIKV historical strain MR766 was first discovered and isolated from sentinel rhesus monkeys in Ziika forest of Uganda in 1947 (282). In 1954, the first ZIKV MR776 was found and isolated from humans in Nigeria (283), and by 1964 to 1970, more infections were reported in Africa (284, 285). Interestingly, ZIKV was found for the first time in Asia in 1966 (286), which gave rise to the first outbreak by 1977-1978 in Indonesia (287).

For more than twenty years, the virus circulated in South Asia without any outbreak until 2007 when the first major outbreak was reported on Yap Island in the Federated States of Micronesia in the Pacific Ocean (288). The circulating virus spread faster, presumably infecting more than 900 people with at least 49 confirmed cases. From 2007 to early 2012, ZIKV remained in south Asia but in late 2012 and 2013, a broader outbreak occurred in French Polynesia with 396 confirmed cases and 29,000 estimated infections (289-291). Between October 2013 and March 2014, ZIKV was introduced into 11 Brazilian cities by tourists from French Polynesia (292).

The Brazilian outbreak was the largest ZIKV outbreak in history; there were 7000 cases only between February and April 2015 (293). Short after, Paraguay, Bolivia, Ecuador, Colombia, Venezuela, all Central America, including Mexico and some regions in the USA reported cases of infected people with ZIKV (293). On December 1st 2015, the Pan American Health Organization (PAHO) and World Health Organization (WHO) announced the association of ZIKV infection

with neurological syndromes and congenital malformations (293). Meanwhile in 2016, another outbreak with local strains was declared in Singapore, Philippines, Vietnam and Thailand (294). Currently, sporadic cases all over the globe have been reported. As of June 2019, the CDC reported 18 new ZIKV cases in North American territories (295). The ZIKV origin and pandemics can be observed in (Fig 1.10). A few years after the first outbreak in Asia, ZIKV rapidly changed and adapted, infecting thousands of people in other countries. Therefore, it is necessary to review the viral architecture, genome, phylogenic and polymorphism to elucidate the sudden expansion from Asia to America.

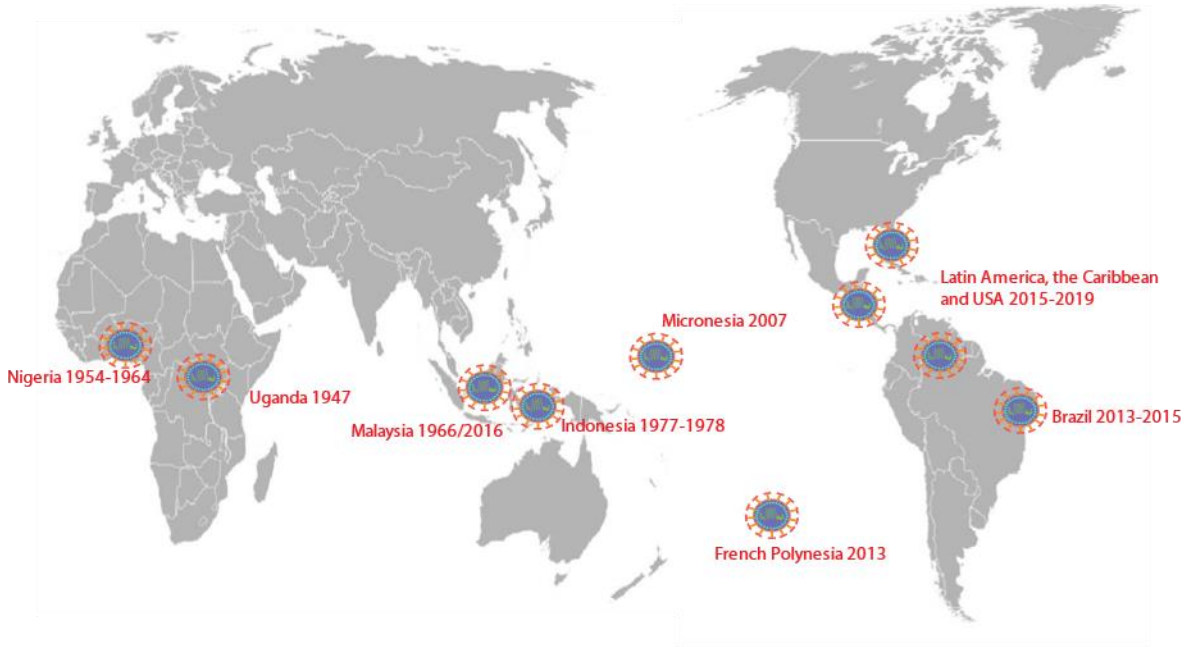

Figure 1. 10 Emergence of ZIKV

ZIKV world map with relevant dates. ZIKV emerged in Uganda in 1947 and disseminated in central Africa. During the 1960s ZIKV reached Asia causing sporadic infection and some outbreaks for more than four decades. The French Polynesia outbreak was pivotal for ZIKV to reach the Americas. In late 2013, ZIKV was brought to Brazil scattering all over Latin America, the Caribbean, and some regions in the USA.

1.3.2 ZIKV and genome

ZIKV belongs to group IV in the Baltimore classification from the *Flaviviridae* family and *Flavivirus* genus, such as Dengue, West Nile, yellow fever and Japanese encephalitis viruses (296). ZIKV posses an ssRNA (+) genome of around 11kb that encodes a single polyprotein, which is processed by cellular and viral proteases into structural proteins (capsid (C), pre-membrane (prM) and envelope (E) and seven non-structural proteins (NS1, NS2A, NS2B, NS3, NS4A, NS4B, NS5) (Fig 1.11A) (297, 298). The 5' UTR is capped, but in the absence of the cap, the 5'UTR can efficiently act as an internal ribosomal entry site (IRES) producing an infection in mammalian or insect cells (299). The 3'UTR is a conserved sequence in ZIKV and other flaviviruses (300). The pathogenicity of flaviviruses seems to be linked to the accumulation of the genomic RNAs and long non-coding RNAs (lncRNA) or also called subgenomic flavivirus RNAs (sfRNA) that embrace only the 3'UTR (301). The sfRNAs are produced by Xrn1 whose exonuclease activity is stopped when it encounters RNA structures at the 3'UTR called Xrn1-resistant RNAs (xrRNAs) (Fig 1.11A) (302).

ZIKV structural proteins form the nascent viral particle with a size of ~ 50 nm (297). The C protein binds tightly to the genomic RNA, whereas E and prM mediate the binding and fusion to the cellular membrane followed by the entry in the cell (Fig 1.11B) (297, 303, 304). The NS proteins have not thoroughly been studied but because of the similarity to other flaviviruses, the comparison is possible. NS1 is a multifunctional glycoprotein involved in the formation of the replication complex, virus assembly, modulation of the innate immune response from the host and it is also secreted (305-307). In addition, NS1 activates the transmission from human to mosquitoes (308). NS2A recruits viral genomic RNA, contributes to virus assembly and destabilizes the adherent junction complex impairing the cell-cell junctions (294, 309).

NS2B is the cofactor of NS3 (NS2B/NS3), the ZIKV protease, essential for the polyprotein cleavage (310). The main function of NS4A is to rearrange the cytoplasmic membrane, Golgi and remodel ER but its precise role is unknown (311, 312). NS4B has also a critical role in remodeling the ER and in the formation of induced membrane structures during the replication (313). Together, NS4A and NS4B inhibit the neurogenesis by inducing autophagy via mTOR signaling (314).

Finally, NS5 is the RNA-dependent RNA polymerase (RdRp) that catalyzes the RNA synthesis through the N domain while the methyltransferase domain in the C terminus adds the cap for translation (315). Of note, NS proteins interact together and this interaction results essential for virus replication (NS3-NS5; NS3-NS4B; NS4A-NS4B; NS4B-NS4B; NS1-NS4B; NS1-NS4A-4B precursor).

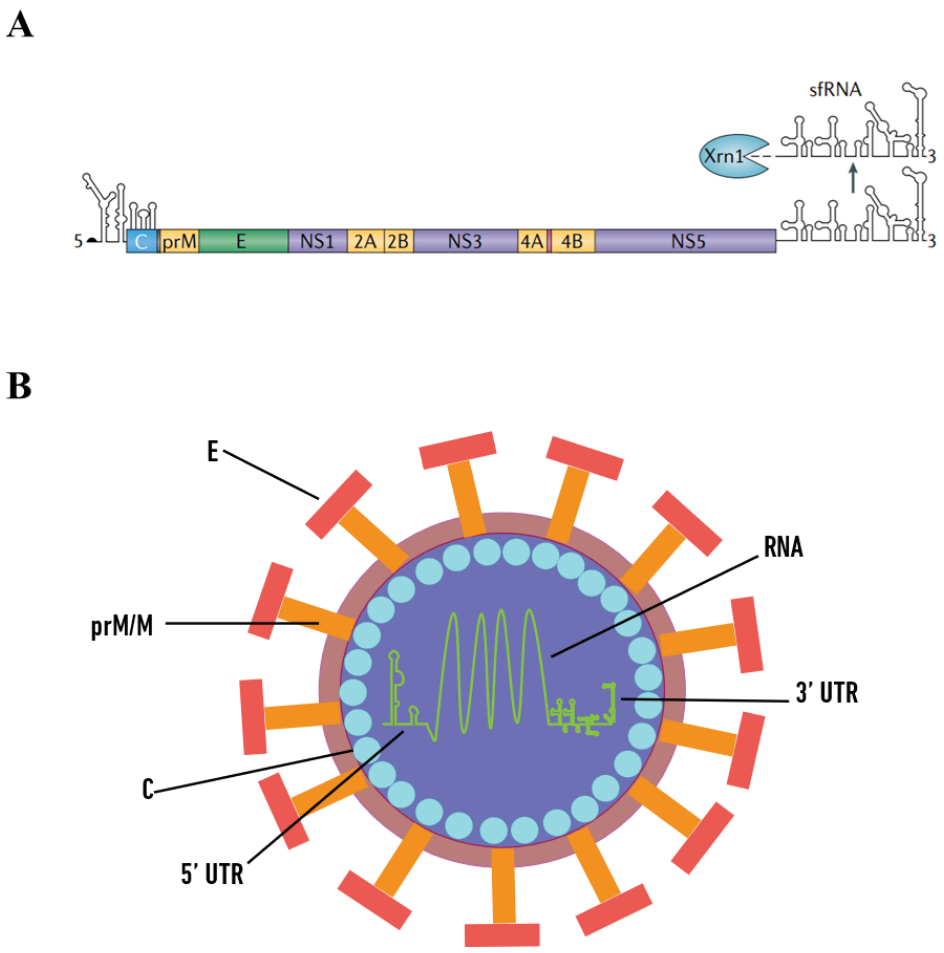

Figure 1. 11 ZIKV genome and viral architecture.

A) ZIKV genome is a monocistronic positive RNA of ~ 10,794 nt, which encodes a single polyprotein that is cleaved in structural (C, prM, and E) and non-structural proteins (NS1, NS2A, NS2B, NS3, NS4A, NS4B, NS5). The 5' UTR is a capped conserved site. A high RNA transcription activates the cellular endonuclease XRN1 that partially degrades the genomic RNA leaving only a 3'UTR fragment (sfRNA). Reproduced from (291). B) ZIKV virion structure showing protein E and prM in the envelope and a capsid protein C surrounding the RNA genome.

1.3.3 ZIKV replication cycle

The complete replication cycle of ZIKV has not been widely studied, but the resemblance with other flaviviruses has contributed to the elucidation of most of the steps. Here, I will break down the replication cycle into (1), binding, entry, fusion and release. (2), translation, polyprotein cleavage and RNA replication. (3), virus assembly and release (Fig 1.12).

1.3.3.1 Binding, entry, fusion and release

ZIKV infects a significant number of cell types (316-319) but since the emergence of the Asian strains, ZIKV preferentially infects neuroprogenitor cells (NPC) within the brain (320-322). ZIKV E protein binds to different receptors on the cell membrane like the tyrosine-protein kinase receptor AXL, Tyro3, DC-SIGN and TIM-1 (316). The binding triggers clathrin-mediated endocytosis, which internalizes the virus into clathrin-coated vesicles. These vesicles are transported through the cytoplasm and fuse with early endosomes to generate late endosomes. The low pH in late endosomes induces a conformational change in E protein from 90 dimers to 60 trimers followed by the exposure of the fusion peptide, which is then inserted into the endosome membrane creating a pore where the capsid passes through and reach the cytoplasm (323, 324).

1.3.3.2 Translation, polyprotein cleavage and RNA replication

It is not well documented whether the capsid dissociates immediately after entering the cytoplasm or if it is brought to the rough endoplasmic reticulum (RER). Regardless of the localization of its dissociation, ZIKV genomic RNA is transported to the RER and its 5'UTR is recognized by ribosomes, which translate the sequence into a single polyprotein. The nascent polyprotein contains hydrophobic signal recognition particles in its C terminus, which allows its translocation to the RER (303, 325). After the ZIKV polyprotein is inserted into the RER, the NS3 protease and

its cofactor NS2B are activated along with cellular peptidases that cleave the polyprotein in specific locations for the generation of all the structural and nonstructural mature proteins (Fig 1.11A), (325). The cleavage of the polyprotein induces convoluted membranes and vesicle packets better known as flaviviral replication complexes constituted by NS1, NS2A, NS3, NS4A, NS4B and NS5 (325, 326). Inside the replication complex, NS5 recognizes the genomic RNA (+) from the 5' UTR stem-loop A (SLA) sequence and uses the 3'UTR SL sequence as the initial position to produce a negative uncapped ssRNA (-) (327). To initiate the synthesis of the negative genome, the vRNA adopts a circularized form through the interaction between the 5' and 3' UTRs (300). Thus, NS5 uses this negative-strand as a template for the overproduction of RNA (+). During the synthesis, the first new RNAs (+) replaces the old RNA (+) that helped to create the RNA (-) (328).

The RNA (-) is produced only at the early stages, during the formation of the replication complex, the production of the RNA (+) occurs in the late stage of viral replication (329, 330). The replication process takes place within ER which derives in viral replication factories, more precisely within replication packets, an ultrastructure common to all tested flaviviruses (300).

1.3.3.3 Assembly and release

The nascent RNAs (+) and C proteins associate on the cytoplasmic face of the RER, where a single RNA (+) is associated with several C units (331). The prM and E associate in trimers along with C proteins and the RNA (+). This association triggers the formation of invaginations towards the RER lumen and alterations of the cytoskeleton. The alteration of the cytoskeleton is linked to replication factories in their whole. This includes structures related to both replication and virus accumulation within virus bags (332). Virus bags contain assembled immature viral particles, which are transported for a proteolytic cleavage.

ZIKV immature particles are strictly intraluminal and need to cooperate with cargo proteins, possibly with the secretory complex COPII to be transported from the luminal side of the RER to the trans-Golgi (333). The acidic environment in the trans-Golgi rearranges and aligns the E protein homodimers on the viral envelope, exposing the junction peptide of the prM, which is recognized by the cellular protease furin. The cleavage generates a mature M protein with traces of prM on the external leaflet of the viral membrane (333-335). Mature virions reach the intracellular plasma membrane where they interact with an octameric protein complex called EXOCYST, which tethers viral particles to the plasma membrane and facilitates their secretion (333, 336). Interestingly, ZIKV is highly dependent on low temperature for its secretion, which is favored at 28°C and decreased at 37°C (337, 338). This characteristic explains the high virus titer in insect cells (339).

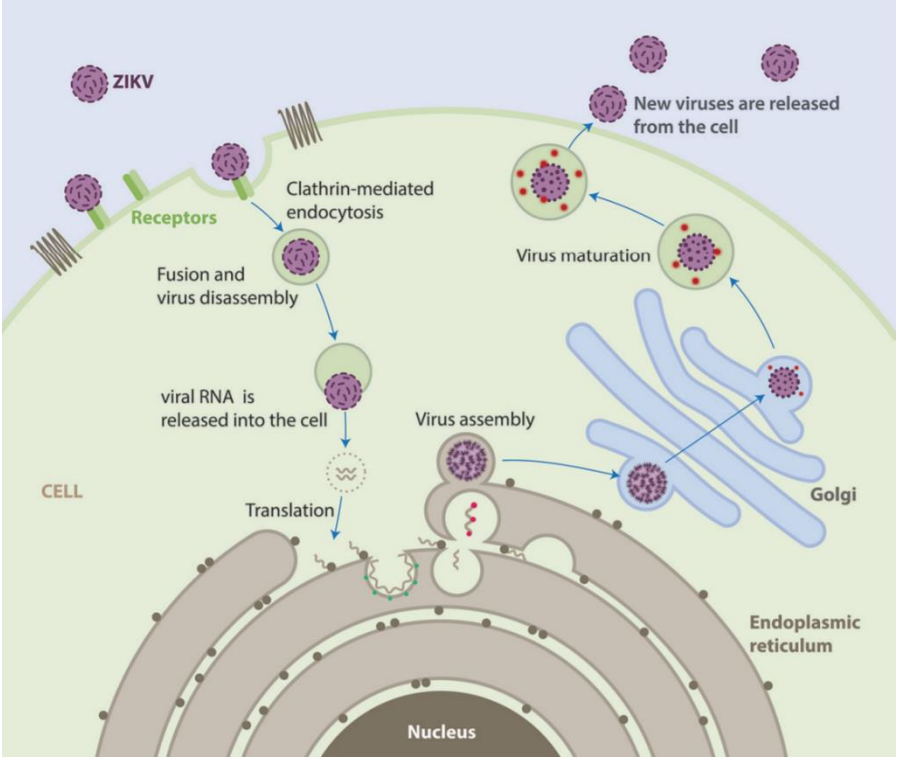

Figure 1. 12 ZIKV replication cycle.

ZIKV binds to cellular tyrosine-protein kinase receptors that trigger clathrin-mediated endocytosis. The acidic environment of late endosomes allows the viral envelope to fuse with the endosomal membrane and release the capsid. The capsid is dismantled, releasing the genomic RNA (+), which is translated into the polyprotein that becomes anchored to the RER. The polyprotein is cleaved by viral and cellular enzymes producing all the ZIKV proteins. The NS proteins create an RNA (-) strand that is used as a template for the RNA (+) amplification. The C, E and prM along with a single copy of RNA (+) detach from the RER in vesicles that form immature virions. Immature ZIKV particles encounter the trans-Golgi that rearrange the E and prM to the mature forms. The virions are transported to the inner leaflet of the cell membrane, where the EXOCYST complex exports them out of the cell. Reproduced from (340).

1.3.4. ZIKV phylogenomics and pathogenesis

ZIKV has two main lineages: African and Asian (341, 342). The African ZIKV lineage was reported for the first time in humans in 1952 and since then, sporadic cases have been circulating in West Africa (282, 285, 343). The most representative strain of the African lineage is the MR766, which possesses a higher infection capacity *in vitro* and *in vivo* in neurons than the Asian lineage (344, 345). However, there are no reports of large-scale outbreaks or severe consequences like congenital ZIKV syndrome (CZVS) or Guillain-Barré syndrome (GBS). A ZIKV variant was isolated in Malaysia in 1966. The virus then spread to the Pacific Islands and is considered the origin of the Asian epidemic, with the first large-scale outbreak in the Yap islands in 2007 (286, 288). A few years later, the Asian strain reached French Polynesia by 2012-2013 until it reached the Americas in late 2013 (292, 293, 295). Multiple studies have tried to understand why pandemics with Asian strains had more severe consequences such as CZVS and GBS compared to African strains.

Recent Asian isolates have three distinctive mutations associated to the pathogenesis. The first mutation located in the prM, at position S139N, is related to neurotropism (341, 346). Experiments made in mouse and human NPCs showed that the single substitution S139N was sufficient to increase the replication rate, to induce cell apoptosis and to contribute to microcephaly in fetal mice (346). The S139N mutation was also found in the virus that was linked to microcephaly cases in 2013 in French Polynesia, (291). The second one is harbored in the NS1 protein, at the amino acid 982 (A982V) (291). The consequence of this mutation produces the binding between NS1 and Tank-binding kinase 1 (TBK1) followed by a reduction of its phosphorylation and consequently a decrease of active IFN-β, which likely decreases the immune response against the virus (347). The third mutation is a substitution in the NS5 at position M2634V, found only in

viruses that were isolated in the Americas (American strains) (291), which might contribute to viral fitness (291). Conversely, other authors observed that this mutation does not help viral pathogenesis and replication (348).

There are additional mutations that enhance ZIKV pathogenesis and cytopathicity. Our lab showed that a Brazilian strain possesses the prM S139N and NS5 M2634V and other substitutions compared to an early Asian one. The increased cytopathicity and higher RNA accumulation of this Brazilian strain in different cell types might be related to the various mutations across the genome (349).

1.3.5. ZIKV transmission

ZIKV entry receptors are ubiquitous on cell membranes allowing the virus to infect many cell types. ZIKV main vectors are mosquitoes *Aedes aegypti*, *Aedes albopictus*, and potentially *Culex quinquefasciatus* that live in urban, rural and countryside areas (350). EM pictures in mosquitoes artificially fed with ZIKV showed salivary glands as viral targets (350). The infected cells are impaired with disruptions in the ER as a consequence of viral replication (350). The production in salivary glands facilitates the transmission to humans, non-human primates and other mammals (Fig 1.13). ZIKV can infect humans, macaques, apes, mice and recently, serological evidence demonstrates that horses are also affected (351, 352). The high concentration of mosquitoes throughout the world suggest that around 400 million people could be at risk to contract ZIKV (353).

ZIKV transmission occurs mainly through mosquito bites but is not limited to this route. Brian Foy from Colorado University traveled in 2008 to Senegal, when he came back, he and his wife developed Dengue like symptoms. Both were tested for Dengue Ab, but he was the only one in

the couple to have Ab against Dengue. Two years later, Andrew Haddow, an entomologist at the University of Texas Medical Branch at Galveston, tested the saved serum from Brian and his wife for ZIKV Abs, which were both positive (354). Since then, other reports have been disclosed showing that ZIKV transmission could occur through sexual intercourses in male to male, female to male and most commonly from male to female (355-358). ZIKV seems to be hidden in the genital tract. In semen, ZIKV has been cultured after 80 days from the initial symptoms and detection of viral RNA after six months (359, 360). In male mice, ZIKV infection is associated with infertility (361).

ZIKV vertical transmission from mother to child was suspected for the first time on October 30th, 2015, when the state of Pernambuco, Brazil reported an increase of new cases of babies born with congenital microcephaly during the outbreak. By November 2015, ZIKV was found in the amniotic fluid of pregnant women (362). Multiple fetal malformations associated with ZIKV were later described along with the intrauterine transmission (363-365). Finally, the presence of ZIKV RNA in breast milk in nursing mothers suggests another route of infection. However, there is not enough supporting evidence to state that breastfeeding is a route of transmission in newborns (366). Therefore, depending on the transmission in the infected individual, the symptomatology and the clinical features will vary.

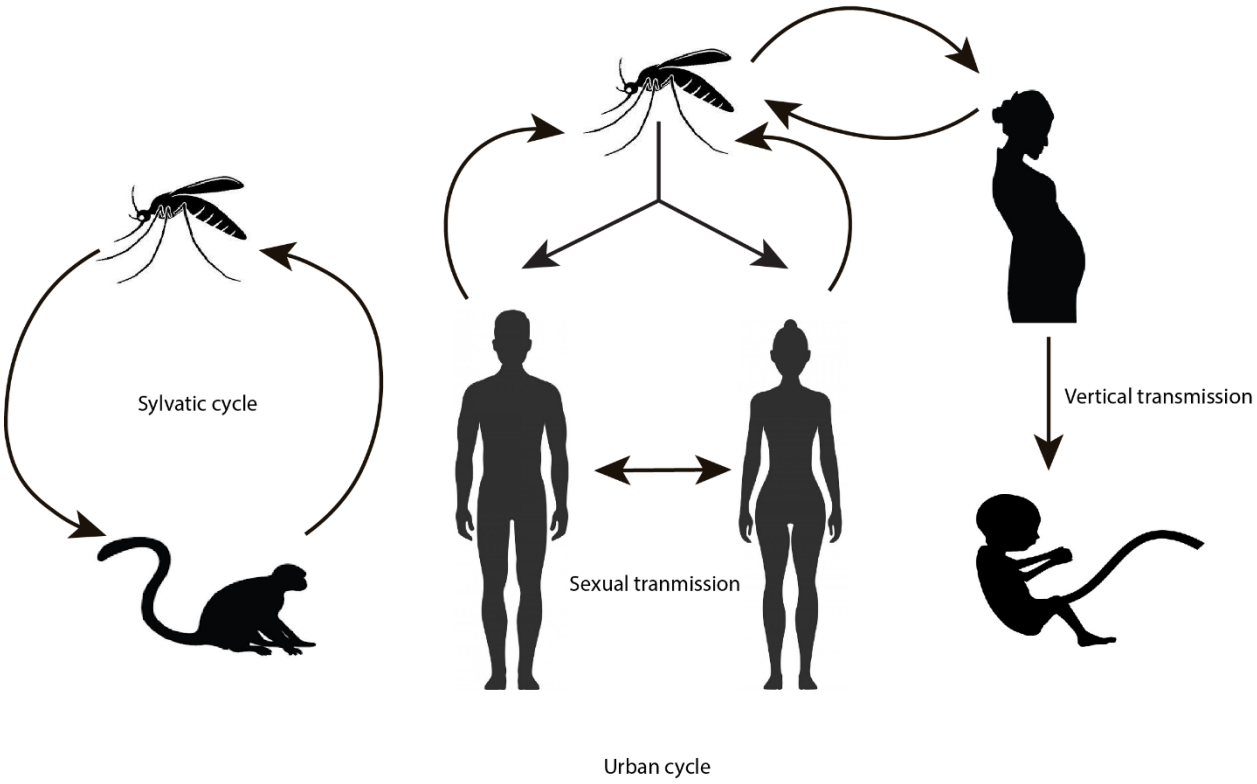

Figure 1. 13 ZIKV transmission cycles.

Schematic representation of sylvatic and urban cycles. The urban cycle of ZIKV embraces transmission by vectors, including *Aedes aegypti, Aedes albopictus and Culex quinquefasciatus*. Additionally, sexual and vertical transmission (mother to child) are considered as part of the urban cycle. The sylvatic cycle is commonly found in tropical forests where mosquitoes spread the virus in different monkeys like rhesus macaques.

1.3.6 ZIKV pathology

ZIKV is mainly transmitted by mosquito bites with an incubation time of 3-12 days. The symptoms are frequently absent or mild, but they included fever, headache, rash, conjunctivitis, retro-orbital pain and arthralgia (281, 367). Vertical ZIKV transmission pathology differs from the horizontal

transmission in whose case produces CZVS in neonates, which encompass neurologic, ocular, musculoskeletal, genitourinary, and other congenital disabilities (362).

1.3.6.1 CZVS, neurologic abnormalities

Evidence accumulated during the Brazilian outbreak brought out in April 2016, the recognition of ZIKV by the CDC as a pathogen that causes brain abnormalities in neonates (368). Indeed, ZIKV vertical transmission induces abnormal brain development in neonates and the main symptom is microcephaly. Microcephaly is diagnosed when the occipitofrontal circumference of the head is smaller than the average of babies at the same age, and it must show two standard deviations. Severe microcephaly shows smaller heads than the regular microcephaly and this exceeds three standard deviations (369). Microcephaly is not the only neurologic abnormality in neonates produced by ZIKV; it also produces malformations such as hydrocephalus, complete Agrya of lateral ventricles, micrencephaly, dystrophic calcifications, cortical displacement and focal inflammation (370). The broad range of abnormalities in the brain and head caused by ZIKV seems to be multifactorial. Microscopy analysis of brain tissue demonstrates significant loss of neurons, glial cells, as well as axonal rarefaction and inflammatory cell, infiltrates that contribute to the apoptosis and necrosis (371). Of note, distinct studies have demonstrated that children with no apparent defects at birth presented a delay in neurodevelopment years after being exposed to ZIKV (372, 373).

1.3.6.2 CZVS, ocular and other abnormalities

First reports of children with microcephaly associated with CZVS also presented macular atrophy in the eyes. A follow-up with a more significant cohort demonstrated other abnormalities such as optic nerve hypoplasia, alterations in the cup to disk ratio, foveal reflex loss and chorioretinal

macular atrophy (364, 374). These characteristics of CZVS in the eye were further explored using *in vivo* models where mice presented conjunctivitis, infection in the cornea, retina, iris, optic nerve and RNA was detected in tears (375). Another study showed mice with uveitis, destruction of photoreceptor neurons, and retinal ganglion cells (376). ZIKV infects retinal pigment epithelium and Müller cells in early stages of development when the blood-retinal barrier and the immune response are not fully formed (376). Other malformations due to CZVS are craniofacial malformations, limb abnormalities, congenital joint contracture in all limbs, severe flexion of the hips and hydrocephaly (377). In addition, other reports point out respiratory, genitourinary, digestive and heart dysfunctionality (362, 378). Currently, there is no medication for ZIKV infection and there are only preventive measures against mosquitoes bites. Therefore, it is necessary to develop treatments and potential vaccines.

1.3.7. ZIKV, potential treatments and vaccines

As of today, no treatment or vaccine is effective against ZIKV albeit several compounds are being tested to target different steps of the replication cycle. The entry can be targeted with compounds that can block the attachment. Suramin is a drug used initially to treat *Trypanosoma brucei* (379). Recent evidence showed that suramin is effective in inhibiting viral attachment and viral release in low concentrations and limited toxicity in cell lines (380). The mechanism of action has not been defined for ZIKV, but sumarin may bind glycosaminoglycans, therefore interfering with the attachment of the E protein (381, 382). The entry of ZIKV can also be stopped by blocking the mechanism that governs clathrin-mediated endocytosis. Nanchangmycin is a polyether produced by *Streptomyces nanchagensis* that inhibits the uptake of cargo proteins during flavivirus infection (383).

The viral protease NS2B-NS3 can be targeted with compounds like novobiocin that increase the survival rate with low side effects in immunosuppressed mice infected with ZIKV (384). Docking analysis suggests that novobiocin interact at HIS51 of the NS2B-NS3, which is a conserved residue necessary for cleavage (384). Sofosbuvir, a nucleotide inhibitor that mimics the natural substrate of the NS5B and is used in Hepatitis C treatment (385), has also been tested in human hepatoma, placental cells, and neuronal stem cells and *in vivo* models with different ZIKV strains. The results show that sofosbuvir could inhibit ZIKV infection and replication with low toxicity *in vitro* and *in vivo* (386). Furthermore, other cellular proteins and functions essential for viral replication are being tested, like the modulation of lipid metabolism and the cellular protein Hsp70 (387, 388).

ZIKV vaccines are under development in clinical or pre-clinical phases. Some of them are promising using purified inactivated virus and confirmed by adoptive transfer studies with purified IgG, DNA vaccine, and adenoviruses vector-based prM and E proteins as immunogens (389).

Table 1. 2 Examples of ZIKV vaccines in clinical development. Table adapted from (390).

Vaccine	Antigen	Induction of neutralizing antibodies	Immunocompetence	Clinical trial
ZPIV	Not applicable	yes	competent	Phase I
DNA	prM-E	yes	competent	Phase I/II
Ad	prM-E	yes	competent/deficient	Phase I
mRNA	prM-E	yes	competent/deficient	Phase I/II
MVA	NS1	yes	competent	Phase I
MV	prM-E	yes	not reported	Phase I
ZIKV-LAV	Not applicable	yes	competent/deficient	Not applicable

ZIPV, ZIKV purified inactivated virus vaccine; Ad, adenovirus-based vaccine; MVA, modified vaccinia virus Ankara, MV; measles virus-based vaccine; ZIKV-LAV, live attenuated Zika virus vaccine.

1.4. RNAi and viruses interplay, HIV-1 and ZIKV

The relationship between miRNAs and viruses in mammalian cells is complex and it remains debatable whether cellular miRNAs impair viruses or not (391). Furthermore, different viruses can produce miRNA from their genomes. DNA viruses like herpes viruses encode vmiRNAs and they regulate triggering mechanisms of replication or latency (391). γ Herpes viruses like Kaposi's sarcoma-associated herpesvirus encodes 18 mature vmiRNAs located within the latency-associated region (392). α-Herpes viruses like Herpes simplex virus 1 and 2 produce vmiRNAs during latency (393, 394). The polyomavirus simian virus 40 generates vmiRNAs from the 3'UTR, which regulates the expression of its T antigen during genome replication. Consequently, the virus avoids recognition from the immune system (43).

The role of vmiRNAs in RNA viruses remains unclear, mainly because of the controversy to demonstrate their existence (395). RNA viruses with replication cycles in the cytoplasm cannot generate vmiRNAs due to the following reasons: 1) They do not reach the nucleus and do not have contact with Drosha and DGCR8 to produce pre-miRNAs and 2) most of the ssRNA viruses encode a polyprotein transcript. MiRNAs are generated from endonucleolytic activity, thereby compromises its own genome for unproductive cleavage seems to be disadvantageous to the virus (395). Nonetheless, RNA viruses co-opt the RNAi pathway and miRNAs. For example, pestiviruses bind miR-17 and let-7 at the 3' UTR, which increases stability for translation (396). Likewise, miR-122 in hepatocytes amplifies the accumulation and replication of hepatitis C virus (HCV) several hundredfolds. MiR-122 binds the 5'UTR in the HCV genomic RNA, preventing decay and stabilizing the structure, which facilitates the accumulation and translation of the viral RNA (397, 398).

In the context of RNAi proteins, viruses can also impair the pathway affecting the generation of miRNAs. For example, Ebola VP40 protein degrades Drosha, DGCR8, Dicer and Ago1 in human cell lines (399). Human T-lymphotropic virus type 1 Tax protein interacts with Drosha in the nucleus affecting pri-miRNAs cleavage and changing the global miRNA expression within cells (400). Also, the expression of E6/E7 oncoproteins from human papillomavirus enhances the concentration of Drosha and Dicer, therefore dysregulating a proportion of miRNAs, which contributes to cancer development (401). HIV-1 and ZIKV also modulate the RNAi pathway and miRNAs; in the following section, I will describe specific examples of dysregulation induced by each virus.

1.4.1 miRNAs and HIV-1

The interplay between HIV-1 and miRNAs has been described under different aspects. In this section, I will break down how miRNA, vmiRNAs, and RNAi protein components interact with HIV-1.

1.4.1.1 Encoded vmiRNAs by HIV-1

There is still controversy whether HIV-1 produces vmiRNAs or not. Hypothetically, HIV-1 has access to the miRNA machinery in the nucleus and cytoplasm. Bioinformatic prediction analyses have shown different regions on the HIV-1 genome with possible sites for vmiRNA synthesis, especially in areas where stem-loops have resemblance with pri-miRNAs or pre-miRNAs. The 5' and 3'LTR, Gag-CA, Gag-Pol and Nef harbor sites for the potential vmiRNAs (402). Prediction studies of vmiRNAs have shown the possible implications that favor cycles of replication or latency. For instance, vmiRNA miR-H1 encoded from viral 3'LTR down-regulates the apoptosis antagonizing transcription factor (AATF) gene and the expression of the cellular miR-149, which

targets Vpr (403). However, a follow-up study showed that there are more than 1000 variants of miR-H1 in *ex vivo* analysis, reducing the possibilities to this viral RNA of being a real miRNA (404).

Another example is the vmiRNA miR-N367 sequence cleaved from the Nef sequence, decreases Nef expression and may contribute to viral latency (39). However, further analysis of HIV-1 miRNAs by next generation sequencing failed to retrieve it, thereby miR-N367 is currently controversial (405, 406). Deep sequencing experiments in infected SupT1 with HIV-1 showed that one percent of total small RNAs could map with the HIV-1 RNA genome (407). Conversely, another study made in cell lines and primary cells infected with HIV-1 did not find any small RNA that originates from the virus (408). TAR element is 50 nt stem-loop that has resemblance to Dicer substrates and was predicted to interact with Dicer (402). Confirmatory experiments have shown that TAR is processed by Dicer into TAR-miR-5p and 3p of 21 nt in length, where TAR-miR-3p had silencing activity through Ago2 (409-411). More experiments using new approaches like immunoprecipitation of the RNAi components or single-cell sequencing are necessary to elucidate and confirm the HIV-1 vmiRNAs.

1.4.1.2 miRNAs that directly target HIV-1 RNA

A single miRNA can target hundreds of mRNAs (412) and not surprisingly, cellular miRNAs can hybridize with HIV-1 RNA. Resting $CD4^+$ T cells are susceptible but not permissive to HIV-1 (240, 241). This resiliency correlated with miR-28, miR-125b, miR-150, miR-223 and miR-382 that bind viral RNA and are highly produced only in resting $CD4^+$ T cells (413). Monocytes are also less susceptible and less permissive to HIV-1 infection than macrophages. This may be due in part to the high expression of anti-HIV miRNAs, miR-28, miR-150, miR-223 and miR-382 in monocytes compared to macrophages. Indeed, a decrease of these miRNAs in monocytes

increased HIV-1 replication, whereas their overexpression in macrophages reduced HIV-1 replication (414). MiR-29a reduces viral replication by targeting Nef sequence (415). Furthermore, miR-29a overexpression increased HIV-1 RNA bound to Ago2 purified from P-bodies (416). To date, there are potentially 16 cellular miRNAs that hybridize in different regions of HIV-1 RNA like, Gag, Pol, Vif, Env, Nef and the 3'UTR (Fig 1.14).

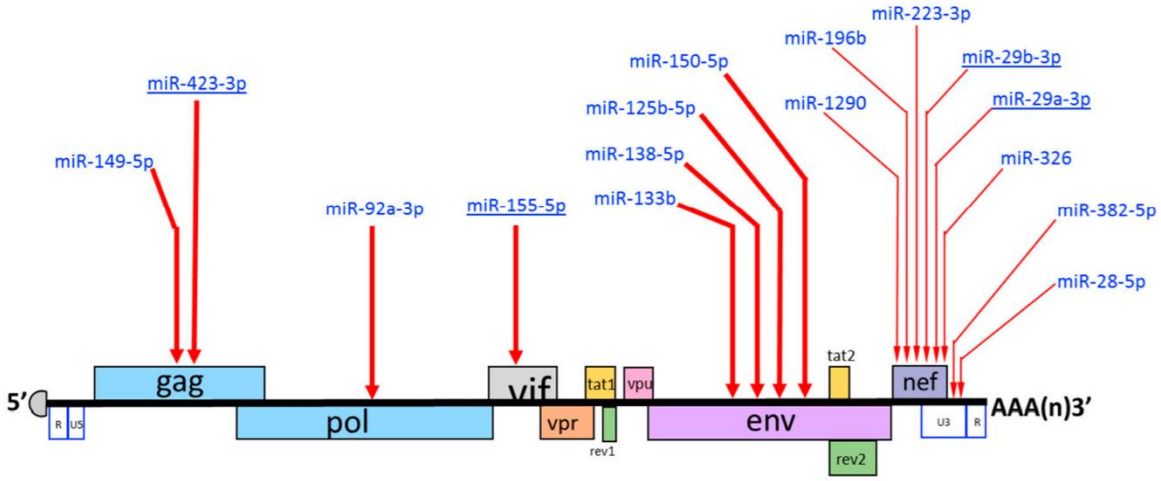

Figure 1. 14 Cellular miRNA that directly targets HIV-1 RNA.

There are potentially 16 miRNAs that target different positions through the genome. Reproduced from (406).

1.4.1.3 miRNAs that impair HIV-1 through host dependency factors

HIV-1 requires cellular factors to complete its replication; these host proteins are called host dependency factors (HDF) and are critical for HIV-1. HDF can be involved at any stage of the replication cycle and be countered through gene regulation by miRNAs. For example, within the

late phase, HIV-1 expresses Tat protein, which recruits p-TEFb (Cdk9 and CycT1), an HDF that will mediate Tat-mediated transactivation (170). Monocytes express low levels of CycT1 until differentiation into macrophages; this property is correlated to the generation of miR-198 that controls CycT1 and consequently represses HIV-1 expression (417). Likewise, resting $CD4^+$ T cells produces miR-27b, which also targets and downregulates CycT1. The activation of $CD4^+$ T cells downregulates miR-27b favoring viral replication (418). Another Tat-HDF is Pur-α protein, which binds TAR/Tat and increases viral transcription by several hundred folds (419). Endogenously, monocytes can down-regulate Pur-α by synthesizing miR-15a, miR-15b, miR-16, miR-20a, miR-106b, and miR-93 and repress HIV-1 expression (420). Interestingly, the use of a combination of all miRNAs is required to silence Pur-α; individual miRNAs do not dramatically impair HIV-1. Conversely, single miRNAs can also restrict HIV-1 replication. Upon the activation of TLR3/4 by a stimulation, macrophages can produce miR-155 that drastically reduces HIV-1 replication by targeting several HDF such as a disintegrin and metalloproteinase domain-containing protein (ADAM) 10, TNPO3, nucleoporin (NUP)153, LEDGF/p75, necessary during the integration (421). The viral entry can also be affected by miRNAs targeting HDF. MiR-221 and miR-222 decrease CD4 synthesis by a direct binding at the 3'UTR mRNA in macrophages, which could explain why these cells are more resilient to the infection (422).

1.4.1.4 miRNAs that promote HIV-1 replication

Some cellular factors can restrict the HIV-1 expression, but at the same time, cellular miRNAs can silence these restrictions, promoting viral replication. Activated $CD4^+$ T cells express a high concentration of miR-132 that downregulates MeCP2, a cellular protein that represses viral integration presumably by an antagonistic competition with LEDGF (423). P21 is an HIV-1

restriction factor that indirectly controls the pool of deoxyribonucleotide triphosphate (dNTPs) necessary for HIV-1 replication (424). TWIK-related acid-sensitive K (TASK)1, another HIV-1 restriction factor targets Vpu and degrades it (425). Following HIV-1 infection, both restriction factors are affected by the augmented levels of Let-7c which downregulates p21 and miR34a and miR-124a that decrease TASK1 translation (426). Likewise, sirtuin-1 (SIRT1) a deacetylase that acts over NF-κB and consequently impairs HIV-1 transactivation (427) can be countered by overproduction of miR-34a and miR-217 upregulated by Tat HIV-1 (428, 429). Therefore, miRNAs' production can be modified upon HIV-1 infection and favors its replication cycle by degrading host restriction factors.

1.4.2 RNAi proteins and HIV-1

The interactome of HIV-1 is defined by the interaction of cellular proteins with viral proteins (202, 203). Some proteins of the RNAi pathway interact directly with viral proteins and some others are indirectly related to the HIV-1 infection. Drosha has not been observed to interact with any viral protein, but there is evidence of its importance during HIV-1 infection. For instance, decreased protein levels of Drosha in peripheral mononuclear blood cells (PBMCs) infected with HIV-1 demonstrated that the viral replication rate is faster than in not infected cells (430). Besides, reduced levels of Drosha showed that 11 miRNAs are upregulated upon HIV-1 infection. Among those, the cluster miR-12/92 presented antiviral activity by targeting PCAF, an essential Tat cofactor (430). Likewise, Drosha's cofactor DGCR8 seems to control virus replication. Experiments in where DGCR8 was knocked down in PBMCs of patients under HAART, showed that the lack of this protein is pivotal for virus reactivation. Thereby, DGCR8 might contribute to virus latency (431). Exportin-5, whose function is to transport pre-miRNAs from the nucleus to

the cytoplasm, it has been found to bind HIV-1 Vpu (202). There is no information about the effects of this interaction.

Outside of the nucleus, Dicer, TRBP and Ago2 interact with HIV-1 components. Host-HIV-1 interactome shows that Dicer interacts with Gag and recently, our lab demonstrated that the interaction of specific miRNAs with Dicer are increased in the presence of Gag (202, 432). Rev and Tat harbor NLS that help both proteins to shuttle into the nucleus and mediate the transactivation and nuclear export process of HIV-1 mRNA (170, 175, 176, 181). These NLS are made of arginine-rich motifs that may act as an RNA silencing suppressor (RSS) to decrease Dicer activity (433, 434). Tat also showed interaction with Dicer through RNAs (435). However, a more recent study demonstrated that neither Tat nor Rev act as RSS. In contrast, TAR and RRE are RSS by competing miRNA-bound to TRBP (436). Vpr is an accessory protein of HIV-1 that can recruit $CRL4^{DCAF1}$ ubiquitin ligase complex and degrade cellular proteins through the proteasome pathway (437, 438). Vpr binds Dicer and impairs its functionality through its degradation. Dicer's decay occurs through the assembly of Dicer-Vpr-$CRL4^{DCAF1,}$ (439).

TRBP also has interactions with HIV-1 components. Indeed, TRBP was discovered by its association with the association with TAR element (48). This interaction needs a 24 amino acids peptide in TRBP to bind the upper stem-loop of TAR (48, 51, 440). TRBP also contributes to Tat-mediated transactivation by amplifying gene expression and consequently enhancing virion production (48, 440, 441). A decrease of TRBP expression impairs HIV-1 production in permissive cells (442).

HIV-1 structural and non-structural proteins also target Ago2. Nef is a primary determinant in the viral pathogenesis and the progress to AIDS due to its modulation of many cellular factors like CD4, HLA, CCR5, CXCR4 and others (443, 444). Among the cellular factors, Nef binds Ago2

through two conserved glycine-tryptophan motifs; the interaction relocalizes Ago2 into viral multivesicular bodies that presumably work as sites of assembly (445). The Nef interaction also inhibits the endonucleolytic cleavage properties of Ago2 and along with GW182 suppresses the RNAi activity (445). Gag also binds Ago2; this interaction is independent of RNAs but is heightened in the presence of miRNAs and mediates Ago2 recruitment to spliced and unspliced viral RNA (446). Gag has no impact on the Ago2 silencing function but seems to be beneficial for assembly and virion formation (446). Further experiments using CLIP-seq analysis confirmed that Ago2 binds to different regions on viral unspliced RNAs adjacent to splicing donor sites, the authors concluded that Ago2 contributes to the viral splicing and the effective virion production (447).

During the mRNA repression and degradation in the RNAi pathway, P-body components can also be targeted by distinct viral proteins. GW182 is relocalized through Ago2/Nef interaction to multivesicular bodies, restricting miRNA-mediated mRNA silencing (445). HIV-1 interactome displays the helicase DDX6 to interact with Env although the function is unknown (202). DDX6 also associates with Gag, which favors its multimerization and viral assembly at the plasma membrane (199). DCP1 and DCP2 have been reported to interact with Gag, in co-immunoprecipitation assays (199, 446). BioID-Gag experiments showed that XRN1 binds to Gag by the MA domain suggesting that this interaction may lessen the effectiveness of XRN1 endonuclease activity, which might promote higher availability of viral transcripts (448). Figure 1.15 shows the HIV-1 components that can interact with proteins of the RNAi pathway.

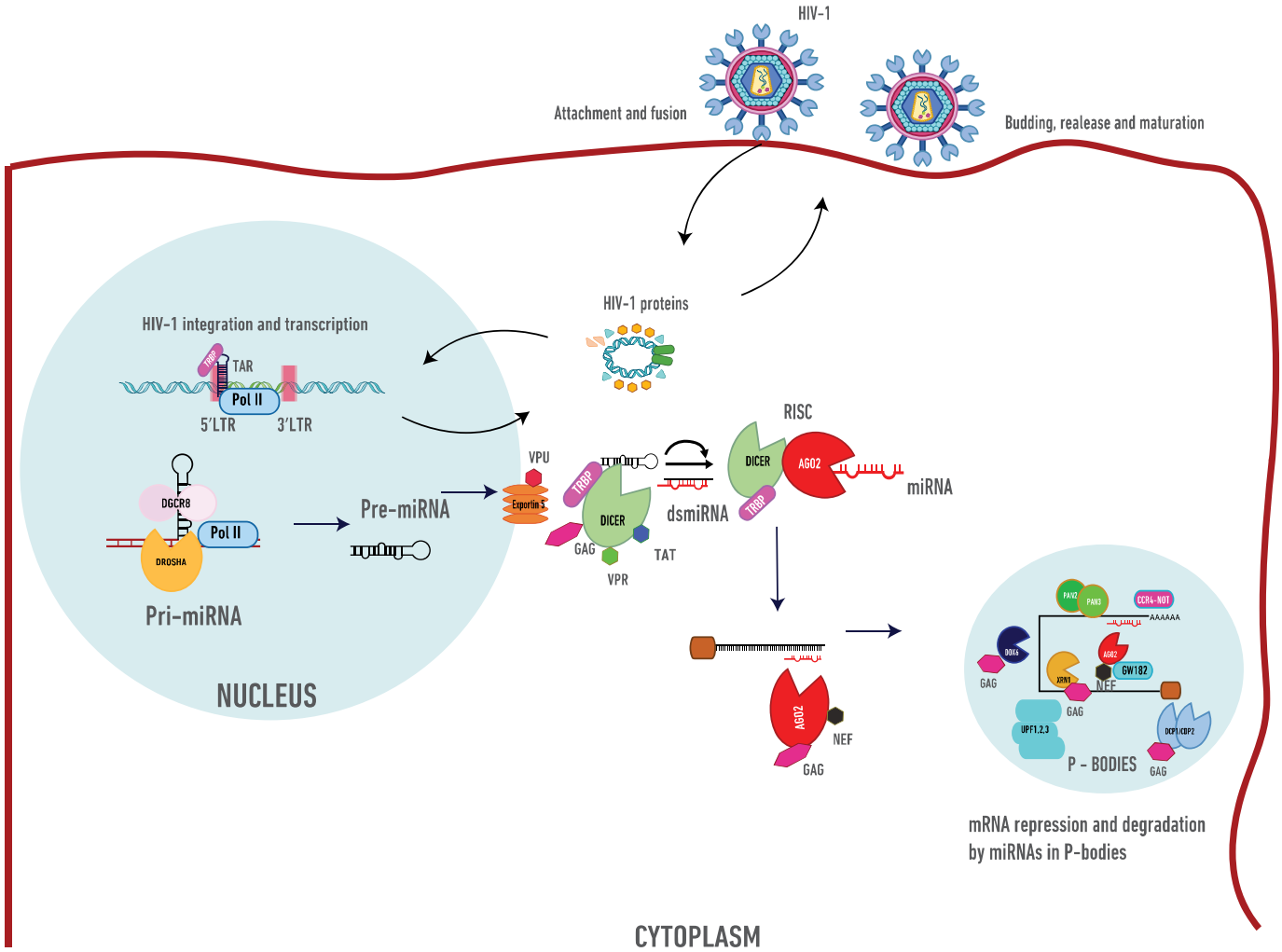

Figure 1. 15 HIV-1 and RNAi protein interactions.

Specific RNAi components have been reported to interact with various HIV-1 proteins. During HIV-1 replication, TRBP associates to HIV-1 TAR element. Exportin 5 binds to Vpu. In the cytoplasm, Dicer is targeted by the viral proteins Tat, Gag, and Vpr. Ago2 is also targeted by viral Gag and Nef, whereas P-bodies components like XRN1, DCP1-DCP2 and DDX6 are targeted by Gag.

1.4.3 miRNAs and ZIKV

Many reports have been published on ZIKV but only a few have studied the interplay between RNAi and ZIKV. The dsRNA formation during ZIKV replication cycle triggers antiviral factors like IFN and other cytokines that usually end up in the elimination of the virus or apoptosis. Neurological damage of ZIKV in newborns has been associated with the high tropism of ZIKV to NPCs. Interestingly, NPCs cannot use the IFN pathway to eradicate the virus but they have alternative paths to counter viral infections. Human NPCs have been observed to mount an antiviral response mediated by siRNAs (vsiRNAs) (449). The evidence of RNAi as an antiviral response in these cells lies in different facts. 1) Deep sequencing and Northern blot analysis show that most of the RNAs transcribed by the presence of ZIKV have a size of 18-28 nt where the majority of them have 22 nt with siRNA characteristics. 2) Downregulation or complete abrogation of Dicer or Ago2 significantly increases viral replication. Furthermore, viral suppressors of Dicer cleavage heightens the virus production. 3) Boosters of RNAi like enoxacin remarkably shows elimination of ZIKV (449, 450).

MiRNA profile analysis of neurons from mice fetuses has found a downregulation in several miRNAs that regulate inflammatory responses (451). Only a few miRNAs that were upregulated such as miR-155, miR-203, and miR29b have previously been shown to have antiviral activity (451-454). Consistently, miRNAs screening in neuroblastoma cell lines infected with a Brazilian ZIKV strain generated a similar response with miRNAs mostly being downregulated and with only a few upregulations, like miR-145 and miR-148. Follow-up experiments found that these miRNAs were also upregulated in postmortem tissue of children with CZVS (455). Recently, a study of miRNA-mRNA dynamics during ZIKV infection using Ago2-CLIP seq in human NPCs, showed dysregulation of genes implicated in neurogenesis, stem cell maintenance and metabolism by

miRNAs (456). Particularly, miR-let7c and miR-124-3p that are linked to microcephaly development were singularly more bound to Ago2 during the infection.

Likewise, mosquito cells are deficient in IFN but they possess a strong RNAi response. During ZIKV infection in mosquito cells, the miRNA profile changes. A comparative study between infected and noninfected mosquito cells with a contemporary ZIKV strain revealed that 17 miRNAs were differentially expressed (457). Predicted targets of *Aedes aegypti* (aae)-miR263a-5p, aae-miR-286, aae-miR-305-5p, aae-miR308-5p, aae-miR-989 and aae-miR-980-3p exhibit ZIKV RNA affinity (457). Moreover, infected astrocytes unveil a general downregulation of miRNAs with a small upregulated group like miR-30, miR-296, miR-431 and miR-17, which manifest antiviral activity and regulation of the unfolded protein response pathway, essential for protein folding in the ER (458). Strikingly, ZIKV infection in astrocytes downregulates *dicer1* transcripts, which disturbs the RNAi pathway (458). Similarly, Drosha, Dicer and Ago2 have had low transcript concentration in liver, lung and kidney cells after ZIKV infection (459). Indeed, protein networks between different ZIKV proteins and neuroblastoma proteins indicate that there is a possible interaction between viral capsid and proteins of the loading RISC like Dicer and TRBP and also some of the proteins within P-bodies (460).

The complex relationship between RNAi and ZIKV remains poorly understood and many topics still need to be addressed like the interactomics with miRNA processors in the nucleus, proteins of the loading RISC and the outcomes of possible interactions with proteins that belong to P-bodies. Unlike HIV-1, ZIKV might be impaired by miRNAs and the modulation of RNAi seems to be strictly necessary, especially in cells like NPC or other stem cells that are deficient in IFN.

1.5 REFERENCES

1. Friedman RC, Farh KK, Burge CB, Bartel DP. 2009. Most mammalian mRNAs are conserved targets of microRNAs. Genome Res 19:92-105.
2. Guo S, Kemphues KJ. 1995. par-1, a gene required for establishing polarity in C. elegans embryos, encodes a putative Ser/Thr kinase that is asymmetrically distributed. Cell 81:611-20.
3. Fire A, Xu S, Montgomery MK, Kostas SA, Driver SE, Mello CC. 1998. Potent and specific genetic interference by double-stranded RNA in Caenorhabditis elegans. Nature 391:806-11.
4. Elbashir SM, Lendeckel W, Tuschl T. 2001. RNA interference is mediated by 21- and 22-nucleotide RNAs. Genes Dev 15:188-200.
5. Rivas FV, Tolia NH, Song JJ, Aragon JP, Liu J, Hannon GJ, Joshua-Tor L. 2005. Purified Argonaute2 and an siRNA form recombinant human RISC. Nat Struct Mol Biol 12:340-9.
6. Hammond SM. 2005. Dicing and slicing: the core machinery of the RNA interference pathway. FEBS Lett 579:5822-9.
7. Fareh M, Yeom KH, Haagsma AC, Chauhan S, Heo I, Joo C. 2016. TRBP ensures efficient Dicer processing of precursor microRNA in RNA-crowded environments. Nat Commun 7:13694.
8. Elbashir SM, Harborth J, Lendeckel W, Yalcin A, Weber K, Tuschl T. 2001. Duplexes of 21-nucleotide RNAs mediate RNA interference in cultured mammalian cells. Nature 411:494-8.
9. Moore CB, Guthrie EH, Huang MT, Taxman DJ. 2010. Short hairpin RNA (shRNA): design, delivery, and assessment of gene knockdown. Methods Mol Biol 629:141-58.
10. Alles J, Fehlmann T, Fischer U, Backes C, Galata V, Minet M, Hart M, Abu-Halima M, Grasser FA, Lenhof HP, Keller A, Meese E. 2019. An estimate of the total number of true human miRNAs. Nucleic Acids Res 47:3353-3364.
11. Lee Y, Kim M, Han J, Yeom KH, Lee S, Baek SH, Kim VN. 2004. MicroRNA genes are transcribed by RNA polymerase II. Embo j 23:4051-60.
12. Han J, Lee Y, Yeom KH, Nam JW, Heo I, Rhee JK, Sohn SY, Cho Y, Zhang BT, Kim VN. 2006. Molecular basis for the recognition of primary microRNAs by the Drosha-DGCR8 complex. Cell 125:887-901.
13. Adams L. 2017. Non-coding RNA: Pri-miRNA processing: structure is key. Nat Rev Genet 18:145.
14. Kim VN. 2005. MicroRNA biogenesis: coordinated cropping and dicing. Nat Rev Mol Cell Biol 6:376-85.
15. Daniels SM, Gatignol A. 2012. The multiple functions of TRBP, at the hub of cell responses to viruses, stress, and cancer. Microbiol Mol Biol Rev 76:652-66.
16. Kim Y, Yeo J, Lee JH, Cho J, Seo D, Kim JS, Kim VN. 2014. Deletion of human tarbp2 reveals cellular microRNA targets and cell-cycle function of TRBP. Cell Rep 9:1061-74.
17. Lund E, Dahlberg JE. 2006. Substrate selectivity of exportin 5 and Dicer in the biogenesis of microRNAs. Cold Spring Harb Symp Quant Biol 71:59-66.

18. Filipowicz W, Bhattacharyya SN, Sonenberg N. 2008. Mechanisms of post-transcriptional regulation by microRNAs: are the answers in sight? Nat Rev Genet 9:102-14.
19. Daniels SM, Melendez-Pena CE, Scarborough RJ, Daher A, Christensen HS, El Far M, Purcell DF, Laine S, Gatignol A. 2009. Characterization of the TRBP domain required for dicer interaction and function in RNA interference. BMC Mol Biol 10:38.
20. Tian Y, Simanshu DK, Ma JB, Park JE, Heo I, Kim VN, Patel DJ. 2014. A phosphate-binding pocket within the platform-PAZ-connector helix cassette of human Dicer. Mol Cell 53:606-16.
21. Lau PW, Guiley KZ, De N, Potter CS, Carragher B, MacRae IJ. 2012. The molecular architecture of human Dicer. Nat Struct Mol Biol 19:436-40.
22. Sinha NK, Iwasa J, Shen PS, Bass BL. 2018. Dicer uses distinct modules for recognizing dsRNA termini. Science 359:329-334.
23. MacRae IJ, Zhou K, Doudna JA. 2007. Structural determinants of RNA recognition and cleavage by Dicer. Nat Struct Mol Biol 14:934-40.
24. Wang HW, Noland C, Siridechadilok B, Taylor DW, Ma E, Felderer K, Doudna JA, Nogales E. 2009. Structural insights into RNA processing by the human RISC-loading complex. Nat Struct Mol Biol 16:1148-53.
25. Macrae IJ, Li F, Zhou K, Cande WZ, Doudna JA. 2006. Structure of Dicer and mechanistic implications for RNAi. Cold Spring Harb Symp Quant Biol 71:73-80.
26. Hutvagner G, McLachlan J, Pasquinelli AE, Balint E, Tuschl T, Zamore PD. 2001. A cellular function for the RNA-interference enzyme Dicer in the maturation of the let-7 small temporal RNA. Science 293:834-8.
27. Park JE, Heo I, Tian Y, Simanshu DK, Chang H, Jee D, Patel DJ, Kim VN. 2011. Dicer recognizes the 5' end of RNA for efficient and accurate processing. Nature 475:201-5.
28. Song MS, Rossi JJ. 2017. Molecular mechanisms of Dicer: endonuclease and enzymatic activity. Biochem J 474:1603-1618.
29. Lee YS, Shibata Y, Malhotra A, Dutta A. 2009. A novel class of small RNAs: tRNA-derived RNA fragments (tRFs). Genes Dev 23:2639-49.
30. Cole C, Sobala A, Lu C, Thatcher SR, Bowman A, Brown JW, Green PJ, Barton GJ, Hutvagner G. 2009. Filtering of deep sequencing data reveals the existence of abundant Dicer-dependent small RNAs derived from tRNAs. Rna 15:2147-60.
31. Kawaji H, Nakamura M, Takahashi Y, Sandelin A, Katayama S, Fukuda S, Daub CO, Kai C, Kawai J, Yasuda J, Carninci P, Hayashizaki Y. 2008. Hidden layers of human small RNAs. BMC Genomics 9:157.
32. Falaleeva M, Stamm S. 2013. Processing of snoRNAs as a new source of regulatory non-coding RNAs: snoRNA fragments form a new class of functional RNAs. Bioessays 35:46-54.
33. Brameier M, Herwig A, Reinhardt R, Walter L, Gruber J. 2011. Human box C/D snoRNAs with miRNA like functions: expanding the range of regulatory RNAs. Nucleic Acids Res 39:675-86.
34. Ender C, Krek A, Friedlander MR, Beitzinger M, Weinmann L, Chen W, Pfeffer S, Rajewsky N, Meister G. 2008. A human snoRNA with microRNA-like functions. Mol Cell 32:519-28.

35. Heras SR, Macias S, Plass M, Fernandez N, Cano D, Eyras E, Garcia-Perez JL, Caceres JF. 2013. The Microprocessor controls the activity of mammalian retrotransposons. Nat Struct Mol Biol 20:1173-81.
36. Yang N, Kazazian HH, Jr. 2006. L1 retrotransposition is suppressed by endogenously encoded small interfering RNAs in human cultured cells. Nat Struct Mol Biol 13:763-71.
37. Hellwig S, Bass BL. 2008. A starvation-induced noncoding RNA modulates expression of Dicer-regulated genes. Proc Natl Acad Sci U S A 105:12897-902.
38. Ouellet DL, Plante I, Landry P, Barat C, Janelle ME, Flamand L, Tremblay MJ, Provost P. 2008. Identification of functional microRNAs released through asymmetrical processing of HIV-1 TAR element. Nucleic Acids Res 36:2353-65.
39. Omoto S, Ito M, Tsutsumi Y, Ichikawa Y, Okuyama H, Brisibe EA, Saksena NK, Fujii YR. 2004. HIV-1 nef suppression by virally encoded microRNA. Retrovirology 1:44.
40. Klase Z, Kale P, Winograd R, Gupta MV, Heydarian M, Berro R, McCaffrey T, Kashanchi F. 2007. HIV-1 TAR element is processed by Dicer to yield a viral micro-RNA involved in chromatin remodeling of the viral LTR. BMC Mol Biol 8:63.
41. Zhu Y, Haecker I, Yang Y, Gao SJ, Renne R. 2013. gamma-Herpesvirus-encoded miRNAs and their roles in viral biology and pathogenesis. Curr Opin Virol 3:266-75.
42. Kincaid RP, Sullivan CS. 2012. Virus-encoded microRNAs: an overview and a look to the future. PLoS Pathog 8:e1003018.
43. Sullivan CS, Grundhoff AT, Tevethia S, Pipas JM, Ganem D. 2005. SV40-encoded microRNAs regulate viral gene expression and reduce susceptibility to cytotoxic T cells. Nature 435:682-6.
44. Moon SL, Dodd BJ, Brackney DE, Wilusz CJ, Ebel GD, Wilusz J. 2015. Flavivirus sfRNA suppresses antiviral RNA interference in cultured cells and mosquitoes and directly interacts with the RNAi machinery. Virology 485:322-9.
45. Liu Z, Wang J, Cheng H, Ke X, Sun L, Zhang QC, Wang HW. 2018. Cryo-EM Structure of Human Dicer and Its Complexes with a Pre-miRNA Substrate. Cell 173:1549-1550.
46. Tahbaz N, Kolb FA, Zhang H, Jaronczyk K, Filipowicz W, Hobman TC. 2004. Characterization of the interactions between mammalian PAZ PIWI domain proteins and Dicer. EMBO Rep 5:189-94.
47. Gebert LFR, MacRae IJ. 2018. Regulation of microRNA function in animals. Nat Rev Mol Cell Biol doi:10.1038/s41580-018-0045-7.
48. Gatignol A, Buckler-White A, Berkhout B, Jeang KT. 1991. Characterization of a human TAR RNA-binding protein that activates the HIV-1 LTR. Science 251:1597-600.
49. Gatignol A, Duarte M, Daviet L, Chang YN, Jeang KT. 1996. Sequential steps in Tat trans-activation of HIV-1 mediated through cellular DNA, RNA, and protein binding factors. Gene Expr 5:217-28.
50. Bannwarth S, Talakoub L, Letourneur F, Duarte M, Purcell DF, Hiscott J, Gatignol A. 2001. Organization of the human tarbp2 gene reveals two promoters that are repressed in an astrocytic cell line. J Biol Chem 276:48803-13.
51. Daviet L, Erard M, Dorin D, Duarte M, Vaquero C, Gatignol A. 2000. Analysis of a binding difference between the two dsRNA-binding domains in TRBP reveals the modular function of a KR-helix motif. Eur J Biochem 267:2419-31.
52. Laraki G, Clerzius G, Daher A, Melendez-Pena C, Daniels S, Gatignol A. 2008. Interactions between the double-stranded RNA-binding proteins TRBP and PACT define the Medipal domain that mediates protein-protein interactions. RNA Biol 5:92-103.

53. Du Z, Lee JK, Tjhen R, Stroud RM, James TL. 2008. Structural and biochemical insights into the dicing mechanism of mouse Dicer: a conserved lysine is critical for dsRNA cleavage. Proc Natl Acad Sci U S A 105:2391-6.
54. Li S, Liu L, Zhuang X, Yu Y, Liu X, Cui X, Ji L, Pan Z, Cao X, Mo B, Zhang F, Raikhel N, Jiang L, Chen X. 2013. MicroRNAs inhibit the translation of target mRNAs on the endoplasmic reticulum in Arabidopsis. Cell 153:562-74.
55. Barman B, Bhattacharyya SN. 2015. mRNA Targeting to Endoplasmic Reticulum Precedes Ago Protein Interaction and MicroRNA (miRNA)-mediated Translation Repression in Mammalian Cells. J Biol Chem 290:24650-6.
56. Stalder L, Heusermann W, Sokol L, Trojer D, Wirz J, Hean J, Fritzsche A, Aeschimann F, Pfanzagl V, Basselet P, Weiler J, Hintersteiner M, Morrissey DV, Meisner-Kober NC. 2013. The rough endoplasmatic reticulum is a central nucleation site of siRNA-mediated RNA silencing. Embo j 32:1115-27.
57. Antoniou A, Khudayberdiev S, Idziak A, Bicker S, Jacob R, Schratt G. 2018. The dynamic recruitment of TRBP to neuronal membranes mediates dendritogenesis during development. EMBO Rep 19:e44853.
58. Hornstein E. 2018. When TRBP leaves Dicer at the alt-'ER. EMBO Rep 19.
59. Ma E, MacRae IJ, Kirsch JF, Doudna JA. 2008. Autoinhibition of human dicer by its internal helicase domain. J Mol Biol 380:237-43.
60. Chakravarthy S, Sternberg SH, Kellenberger CA, Doudna JA. 2010. Substrate-specific kinetics of Dicer-catalyzed RNA processing. J Mol Biol 404:392-402.
61. Lee HY, Doudna JA. 2012. TRBP alters human precursor microRNA processing in vitro. Rna 18:2012-9.
62. Masliah G, Maris C, Konig SL, Yulikov M, Aeschimann F, Malinowska AL, Mabille J, Weiler J, Holla A, Hunziker J, Meisner-Kober N, Schuler B, Jeschke G, Allain FH. 2018. Structural basis of siRNA recognition by TRBP double-stranded RNA binding domains. Embo j 37:e97089.
63. Park H, Davies MV, Langland JO, Chang HW, Nam YS, Tartaglia J, Paoletti E, Jacobs BL, Kaufman RJ, Venkatesan S. 1994. TAR RNA-binding protein is an inhibitor of the interferon-induced protein kinase PKR. Proc Natl Acad Sci U S A 91:4713-7.
64. Sanghvi VR, Steel LF. 2011. The cellular TAR RNA binding protein, TRBP, promotes HIV-1 replication primarily by inhibiting the activation of double-stranded RNA-dependent kinase PKR. J Virol 85:12614-21.
65. Patel RC, Sen GC. 1998. PACT, a protein activator of the interferon-induced protein kinase, PKR. Embo j 17:4379-90.
66. Zhang F, Romano PR, Nagamura-Inoue T, Tian B, Dever TE, Mathews MB, Ozato K, Hinnebusch AG. 2001. Binding of double-stranded RNA to protein kinase PKR is required for dimerization and promotes critical autophosphorylation events in the activation loop. J Biol Chem 276:24946-58.
67. Lemaire PA, Anderson E, Lary J, Cole JL. 2008. Mechanism of PKR Activation by dsRNA. J Mol Biol 381:351-60.
68. Radetskyy R, Daher A, Gatignol A. 2018. ADAR1 and PKR, interferon stimulated genes with clashing effects on HIV-1 replication. Cytokine Growth Factor Rev 40:48-58.
69. Katze MG. 1995. Regulation of the interferon-induced PKR: can viruses cope? Trends Microbiol 3:75-8.

70. Samuel CE. 1993. The eIF-2 alpha protein kinases, regulators of translation in eukaryotes from yeasts to humans. J Biol Chem 268:7603-6.
71. Benkirane M, Neuveut C, Chun RF, Smith SM, Samuel CE, Gatignol A, Jeang KT. 1997. Oncogenic potential of TAR RNA binding protein TRBP and its regulatory interaction with RNA-dependent protein kinase PKR. Embo j 16:611-24.
72. Li S, Peters GA, Ding K, Zhang X, Qin J, Sen GC. 2006. Molecular basis for PKR activation by PACT or dsRNA. Proc Natl Acad Sci U S A 103:10005-10.
73. Patel CV, Handy I, Goldsmith T, Patel RC. 2000. PACT, a stress-modulated cellular activator of interferon-induced double-stranded RNA-activated protein kinase, PKR. J Biol Chem 275:37993-8.
74. Daher A, Laraki G, Singh M, Melendez-Pena CE, Bannwarth S, Peters AH, Meurs EF, Braun RE, Patel RC, Gatignol A. 2009. TRBP control of PACT-induced phosphorylation of protein kinase R is reversed by stress. Mol Cell Biol 29:254-65.
75. Daher A, Longuet M, Dorin D, Bois F, Segeral E, Bannwarth S, Battisti PL, Purcell DF, Benarous R, Vaquero C, Meurs EF, Gatignol A. 2001. Two dimerization domains in the trans-activation response RNA-binding protein (TRBP) individually reverse the protein kinase R inhibition of HIV-1 long terminal repeat expression. J Biol Chem 276:33899-905.
76. Chukwurah E, Patel RC. 2018. Stress-induced TRBP phosphorylation enhances its interaction with PKR to regulate cellular survival. Sci Rep 8:1020.
77. Lee Y, Hur I, Park SY, Kim YK, Suh MR, Kim VN. 2006. The role of PACT in the RNA silencing pathway. Embo j 25:522-32.
78. Lee HY, Zhou K, Smith AM, Noland CL, Doudna JA. 2013. Differential roles of human Dicer-binding proteins TRBP and PACT in small RNA processing. Nucleic Acids Res 41:6568-76.
79. Wilson RC, Tambe A, Kidwell MA, Noland CL, Schneider CP, Doudna JA. 2015. Dicer-TRBP complex formation ensures accurate mammalian microRNA biogenesis. Mol Cell 57:397-407.
80. Kok KH, Ng MH, Ching YP, Jin DY. 2007. Human TRBP and PACT directly interact with each other and associate with dicer to facilitate the production of small interfering RNA. J Biol Chem 282:17649-57.
81. Lin H, Spradling AC. 1997. A novel group of pumilio mutations affects the asymmetric division of germline stem cells in the Drosophila ovary. Development 124:2463-76.
82. Bohmert K, Camus I, Bellini C, Bouchez D, Caboche M, Benning C. 1998. AGO1 defines a novel locus of Arabidopsis controlling leaf development. Embo j 17:170-80.
83. Lee DW, Pratt RJ, McLaughlin M, Aramayo R. 2003. An argonaute-like protein is required for meiotic silencing. Genetics 164:821-8.
84. Mochizuki K, Fine NA, Fujisawa T, Gorovsky MA. 2002. Analysis of a piwi-related gene implicates small RNAs in genome rearrangement in tetrahymena. Cell 110:689-99.
85. Hutvagner G, Simard MJ. 2008. Argonaute proteins: key players in RNA silencing. Nat Rev Mol Cell Biol 9:22-32.
86. Meister G. 2013. Argonaute proteins: functional insights and emerging roles. Nat Rev Genet 14:447-59.
87. Guo D, Barry L, Lin SS, Huang V, Li LC. 2014. RNAa in action: from the exception to the norm. RNA Biol 11:1221-5.
88. Hock J, Meister G. 2008. The Argonaute protein family. Genome Biol 9:210.

89. Diederichs S, Haber DA. 2007. Dual role for argonautes in microRNA processing and posttranscriptional regulation of microRNA expression. Cell 131:1097-108.
90. Liu J, Carmell MA, Rivas FV, Marsden CG, Thomson JM, Song JJ, Hammond SM, Joshua-Tor L, Hannon GJ. 2004. Argonaute2 is the catalytic engine of mammalian RNAi. Science 305:1437-41.
91. Sheu-Gruttadauria J, MacRae IJ. 2017. Structural Foundations of RNA Silencing by Argonaute. J Mol Biol 429:2619-2639.
92. Wang Y, Sheng G, Juranek S, Tuschl T, Patel DJ. 2008. Structure of the guide-strand-containing argonaute silencing complex. Nature 456:209-13.
93. Schirle NT, MacRae IJ. 2012. The crystal structure of human Argonaute2. Science 336:1037-40.
94. Meijer HA, Smith EM, Bushell M. 2014. Regulation of miRNA strand selection: follow the leader? Biochem Soc Trans 42:1135-40.
95. Hu HY, Yan Z, Xu Y, Hu H, Menzel C, Zhou YH, Chen W, Khaitovich P. 2009. Sequence features associated with microRNA strand selection in humans and flies. BMC Genomics 10:413.
96. Grimson A, Farh KK, Johnston WK, Garrett-Engele P, Lim LP, Bartel DP. 2007. MicroRNA targeting specificity in mammals: determinants beyond seed pairing. Mol Cell 27:91-105.
97. Golden RJ, Chen B, Li T, Braun J, Manjunath H, Chen X, Wu J, Schmid V, Chang TC, Kopp F, Ramirez-Martinez A, Tagliabracci VS, Chen ZJ, Xie Y, Mendell JT. 2017. An Argonaute phosphorylation cycle promotes microRNA-mediated silencing. Nature 542:197-202.
98. Standart N, Weil D. 2018. P-Bodies: Cytosolic Droplets for Coordinated mRNA Storage. Trends Genet 34:612-626.
99. Luo Y, Na Z, Slavoff SA. 2018. P-Bodies: Composition, Properties, and Functions. Biochemistry 57:2424-2431.
100. Piccirillo C, Khanna R, Kiledjian M. 2003. Functional characterization of the mammalian mRNA decapping enzyme hDcp2. Rna 9:1138-47.
101. Franks TM, Lykke-Andersen J. 2008. The control of mRNA decapping and P-body formation. Mol Cell 32:605-15.
102. Jonas S, Izaurralde E. 2015. Towards a molecular understanding of microRNA-mediated gene silencing. Nat Rev Genet 16:421-33.
103. Eulalio A, Behm-Ansmant I, Schweizer D, Izaurralde E. 2007. P-body formation is a consequence, not the cause, of RNA-mediated gene silencing. Mol Cell Biol 27:3970-81.
104. Parker R, Sheth U. 2007. P bodies and the control of mRNA translation and degradation. Mol Cell 25:635-46.
105. Souquere S, Mollet S, Kress M, Dautry F, Pierron G, Weil D. 2009. Unravelling the ultrastructure of stress granules and associated P-bodies in human cells. J Cell Sci 122:3619-26.
106. Shin Y, Brangwynne CP. 2017. Liquid phase condensation in cell physiology and disease. Science 357:eaaf4382.
107. Sheth U, Parker R. 2003. Decapping and decay of messenger RNA occur in cytoplasmic processing bodies. Science 300:805-8.
108. Brengues M, Teixeira D, Parker R. 2005. Movement of eukaryotic mRNAs between polysomes and cytoplasmic processing bodies. Science 310:486-9.

109. Valiente-Echeverria F, Melnychuk L, Mouland AJ. 2012. Viral modulation of stress granules. Virus Res 169:430-7.
110. Goldstrohm AC, Hook BA, Seay DJ, Wickens M. 2006. PUF proteins bind Pop2p to regulate messenger RNAs. Nat Struct Mol Biol 13:533-9.
111. Isken O, Kim YK, Hosoda N, Mayeur GL, Hershey JW, Maquat LE. 2008. Upf1 phosphorylation triggers translational repression during nonsense-mediated mRNA decay. Cell 133:314-27.
112. Lian SL, Li S, Abadal GX, Pauley BA, Fritzler MJ, Chan EK. 2009. The C-terminal half of human Ago2 binds to multiple GW-rich regions of GW182 and requires GW182 to mediate silencing. Rna 15:804-13.
113. Zipprich JT, Bhattacharyya S, Mathys H, Filipowicz W. 2009. Importance of the C-terminal domain of the human GW182 protein TNRC6C for translational repression. Rna 15:781-93.
114. Braun JE, Huntzinger E, Fauser M, Izaurralde E. 2011. GW182 proteins directly recruit cytoplasmic deadenylase complexes to miRNA targets. Mol Cell 44:120-33.
115. Chen CY, Zheng D, Xia Z, Shyu AB. 2009. Ago-TNRC6 triggers microRNA-mediated decay by promoting two deadenylation steps. Nat Struct Mol Biol 16:1160-6.
116. Behm-Ansmant I, Rehwinkel J, Doerks T, Stark A, Bork P, Izaurralde E. 2006. mRNA degradation by miRNAs and GW182 requires both CCR4:NOT deadenylase and DCP1:DCP2 decapping complexes. Genes Dev 20:1885-98.
117. Fabian MR, Cieplak MK, Frank F, Morita M, Green J, Srikumar T, Nagar B, Yamamoto T, Raught B, Duchaine TF, Sonenberg N. 2011. miRNA-mediated deadenylation is orchestrated by GW182 through two conserved motifs that interact with CCR4-NOT. Nat Struct Mol Biol 18:1211-7.
118. Iwakawa HO, Tomari Y. 2015. The Functions of MicroRNAs: mRNA Decay and Translational Repression. Trends Cell Biol 25:651-665.
119. Braun JE, Truffault V, Boland A, Huntzinger E, Chang CT, Haas G, Weichenrieder O, Coles M, Izaurralde E. 2012. A direct interaction between DCP1 and XRN1 couples mRNA decapping to 5' exonucleolytic degradation. Nat Struct Mol Biol 19:1324-31.
120. Mathys H, Basquin J, Ozgur S, Czarnocki-Cieciura M, Bonneau F, Aartse A, Dziembowski A, Nowotny M, Conti E, Filipowicz W. 2014. Structural and biochemical insights to the role of the CCR4-NOT complex and DDX6 ATPase in microRNA repression. Mol Cell 54:751-65.
121. Saez A. 2016. [The Antonine plague: A global pestilence in the II century d.C]. Rev Chilena Infectol 33:218-21.
122. Morens DM, Taubenberger JK. 2018. Influenza Cataclysm, 1918. N Engl J Med 379:2285-2287.
123. Luthy IA, Ritacco V, Kantor IN. 2018. [One hundred years after the "Spanish" flu]. Medicina (B Aires) 78:113-118.
124. UNAIDS. 2019. Global HIV & AIDS statistics — 2019 fact sheet. https://www.unaids.org/en/resources/fact-sheet. Accessed
125. Knipe DM, Howley PM. 2013. Fields virology, 6th ed. Wolters Kluwer/Lippincott Williams & Wilkins Health, Philadelphia, PA.
126. Barre-Sinoussi F, Chermann JC, Rey F, Nugeyre MT, Chamaret S, Gruest J, Dauguet C, Axler-Blin C, Vezinet-Brun F, Rouzioux C, Rozenbaum W, Montagnier L. 1983.

Isolation of a T-lymphotropic retrovirus from a patient at risk for acquired immune deficiency syndrome (AIDS). Science 220:868-71.
127. Gallo RC, Salahuddin SZ, Popovic M, Shearer GM, Kaplan M, Haynes BF, Palker TJ, Redfield R, Oleske J, Safai B, et al. 1984. Frequent detection and isolation of cytopathic retroviruses (HTLV-III) from patients with AIDS and at risk for AIDS. Science 224:500-3.
128. Levy JA, Hoffman AD, Kramer SM, Landis JA, Shimabukuro JM, Oshiro LS. 1984. Isolation of lymphocytopathic retroviruses from San Francisco patients with AIDS. Science 225:840-2.
129. Coffin J, Haase A, Levy JA, Montagnier L, Oroszlan S, Teich N, Temin H, Toyoshima K, Varmus H, Vogt P, et al. 1986. Human immunodeficiency viruses. Science 232:697.
130. Clavel F, Guetard D, Brun-Vezinet F, Chamaret S, Rey MA, Santos-Ferreira MO, Laurent AG, Dauguet C, Katlama C, Rouzioux C, et al. 1986. Isolation of a new human retrovirus from West African patients with AIDS. Science 233:343-6.
131. Peeters M, Honore C, Huet T, Bedjabaga L, Ossari S, Bussi P, Cooper RW, Delaporte E. 1989. Isolation and partial characterization of an HIV-related virus occurring naturally in chimpanzees in Gabon. Aids 3:625-30.
132. Bailes E, Gao F, Bibollet-Ruche F, Courgnaud V, Peeters M, Marx PA, Hahn BH, Sharp PM. 2003. Hybrid origin of SIV in chimpanzees. Science 300:1713.
133. Hemelaar J. 2012. The origin and diversity of the HIV-1 pandemic. Trends Mol Med 18:182-92.
134. Sharp PM, Hahn BH. 2010. The evolution of HIV-1 and the origin of AIDS. Philos Trans R Soc Lond B Biol Sci 365:2487-94.
135. Vallari A, Bodelle P, Ngansop C, Makamche F, Ndembi N, Mbanya D, Kaptue L, Gurtler LG, McArthur CP, Devare SG, Brennan CA. 2010. Four new HIV-1 group N isolates from Cameroon: Prevalence continues to be low. AIDS Res Hum Retroviruses 26:109-15.
136. Delaugerre C, De Oliveira F, Lascoux-Combe C, Plantier JC, Simon F. 2011. HIV-1 group N: travelling beyond Cameroon. Lancet 378:1894.
137. Yamaguchi J, McArthur C, Vallari A, Sthreshley L, Cloherty GA, Berg MG, Rodgers MA. 2019. Complete genome sequence of CG-0018a-01 establishes HIV-1 subtype L. J Acquir Immune Defic Syndr 83:319-322.
138. Hirsch VM, Olmsted RA, Murphey-Corb M, Purcell RH, Johnson PR. 1989. An African primate lentivirus (SIVsm) closely related to HIV-2. Nature 339:389-92.
139. Korber B, Muldoon M, Theiler J, Gao F, Gupta R, Lapedes A, Hahn BH, Wolinsky S, Bhattacharya T. 2000. Timing the ancestor of the HIV-1 pandemic strains. Science 288:1789-96.
140. Worobey M, Gemmel M, Teuwen DE, Haselkorn T, Kunstman K, Bunce M, Muyembe JJ, Kabongo JM, Kalengayi RM, Van Marck E, Gilbert MT, Wolinsky SM. 2008. Direct evidence of extensive diversity of HIV-1 in Kinshasa by 1960. Nature 455:661-4.
141. Wertheim JO, Worobey M. 2009. Dating the age of the SIV lineages that gave rise to HIV-1 and HIV-2. PLoS Comput Biol 5:e1000377.
142. Parsyan AE. 2005. Protective correlates against HIVs may have evolved in human populations in the areas of historic occurrence of primate-to-man transmissions of SIVs ancestral to HIVs: studies in these populations may provide crucial insights for treatment and prevention of HIV infection. Med Hypotheses 64:433-7.

143. Services USDoHH. 2018. Global HIV/AIDS Overview. https://www.hiv.gov/federal-response/pepfar-global-aids/global-hiv-aids-overview. Accessed
144. Schackman BR, Fleishman JA, Su AE, Berkowitz BK, Moore RD, Walensky RP, Becker JE, Voss C, Paltiel AD, Weinstein MC, Freedberg KA, Gebo KA, Losina E. 2015. The lifetime medical cost savings from preventing HIV in the United States. Med Care 53:293-301.
145. Prinsloo CD, Greeff M, Kruger A, Khumalo IP. 2017. HIV stigma experiences and stigmatisation before and after a HIV stigma-reduction community "hub" intervention. Afr J AIDS Res 16:203-213.
146. Peterlin BM, Trono D. 2003. Hide, shield and strike back: how HIV-infected cells avoid immune eradication. Nat Rev Immunol 3:97-107.
147. Briggs JA, Wilk T, Welker R, Krausslich HG, Fuller SD. 2003. Structural organization of authentic, mature HIV-1 virions and cores. Embo j 22:1707-15.
148. Arhel N. 2010. Revisiting HIV-1 uncoating. Retrovirology 7:96.
149. Das AT, Klaver B, Berkhout B. 1998. The 5' and 3' TAR elements of human immunodeficiency virus exert effects at several points in the virus life cycle. J Virol 72:9217-23.
150. Vollenweider F, Benjannet S, Decroly E, Savaria D, Lazure C, Thomas G, Chretien M, Seidah NG. 1996. Comparative cellular processing of the human immunodeficiency virus (HIV-1) envelope glycoprotein gp160 by the mammalian subtilisin/kexin-like convertases. Biochem J 314 (Pt 2):521-32.
151. Fernandes J, Jayaraman B, Frankel A. 2012. The HIV-1 Rev response element: an RNA scaffold that directs the cooperative assembly of a homo-oligomeric ribonucleoprotein complex. RNA Biol 9:6-11.
152. Engelman A, Cherepanov P. 2012. The structural biology of HIV-1: mechanistic and therapeutic insights. Nat Rev Microbiol 10:279-90.
153. Clapham PR, McKnight A. 2001. HIV-1 receptors and cell tropism. Br Med Bull 58:43-59.
154. Connell BJ, Lortat-Jacob H. 2013. Human immunodeficiency virus and heparan sulfate: from attachment to entry inhibition. Front Immunol 4:385.
155. Wilen CB, Tilton JC, Doms RW. 2012. HIV: cell binding and entry. Cold Spring Harb Perspect Med 2:a006866.
156. Melikyan GB. 2008. Common principles and intermediates of viral protein-mediated fusion: the HIV-1 paradigm. Retrovirology 5:111.
157. Sarafianos SG, Marchand B, Das K, Himmel DM, Parniak MA, Hughes SH, Arnold E. 2009. Structure and function of HIV-1 reverse transcriptase: molecular mechanisms of polymerization and inhibition. J Mol Biol 385:693-713.
158. Hu WS, Hughes SH. 2012. HIV-1 reverse transcription. Cold Spring Harb Perspect Med 2:a006882.
159. London RE. 2019. HIV-1 Reverse Transcriptase: A Metamorphic Protein with Three Stable States. Structure 27:420-426.
160. Ao Z, Huang G, Yao H, Xu Z, Labine M, Cochrane AW, Yao X. 2007. Interaction of human immunodeficiency virus type 1 integrase with cellular nuclear import receptor importin 7 and its impact on viral replication. J Biol Chem 282:13456-67.

161. Christ F, Thys W, De Rijck J, Gijsbers R, Albanese A, Arosio D, Emiliani S, Rain JC, Benarous R, Cereseto A, Debyser Z. 2008. Transportin-SR2 imports HIV into the nucleus. Curr Biol 18:1192-202.
162. Jayappa KD, Ao Z, Yao X. 2012. The HIV-1 passage from cytoplasm to nucleus: the process involving a complex exchange between the components of HIV-1 and cellular machinery to access nucleus and successful integration. Int J Biochem Mol Biol 3:70-85.
163. Lusic M, Siliciano RF. 2017. Nuclear landscape of HIV-1 infection and integration. Nat Rev Microbiol 15:69-82.
164. Singh PK, Plumb MR, Ferris AL, Iben JR, Wu X, Fadel HJ, Luke BT, Esnault C, Poeschla EM, Hughes SH, Kvaratskhelia M, Levin HL. 2015. LEDGF/p75 interacts with mRNA splicing factors and targets HIV-1 integration to highly spliced genes. Genes Dev 29:2287-97.
165. Sowd GA, Serrao E, Wang H, Wang W, Fadel HJ, Poeschla EM, Engelman AN. 2016. A critical role for alternative polyadenylation factor CPSF6 in targeting HIV-1 integration to transcriptionally active chromatin. Proc Natl Acad Sci U S A 113:E1054-63.
166. Albanese A, Arosio D, Terreni M, Cereseto A. 2008. HIV-1 pre-integration complexes selectively target decondensed chromatin in the nuclear periphery. PLoS One 3:e2413.
167. Pereira LA, Bentley K, Peeters A, Churchill MJ, Deacon NJ. 2000. A compilation of cellular transcription factor interactions with the HIV-1 LTR promoter. Nucleic Acids Res 28:663-8.
168. Mbondji-Wonje C, Dong M, Wang X, Zhao J, Ragupathy V, Sanchez AM, Denny TN, Hewlett I. 2018. Distinctive variation in the U3R region of the 5' Long Terminal Repeat from diverse HIV-1 strains. PLoS One 13:e0195661.
169. Ne E, Palstra RJ, Mahmoudi T. 2018. Transcription: Insights From the HIV-1 Promoter. Int Rev Cell Mol Biol 335:191-243.
170. Muniz L, Egloff S, Ughy B, Jady BE, Kiss T. 2010. Controlling cellular P-TEFb activity by the HIV-1 transcriptional transactivator Tat. PLoS Pathog 6:e1001152.
171. Faust TB, Li Y, Bacon CW, Jang GM, Weiss A, Jayaraman B, Newton BW, Krogan NJ, D'Orso I, Frankel AD. 2018. The HIV-1 Tat protein recruits a ubiquitin ligase to reorganize the 7SK snRNP for transcriptional activation. Elife 7.
172. Markert A, Grimm M, Martinez J, Wiesner J, Meyerhans A, Meyuhas O, Sickmann A, Fischer U. 2008. The La-related protein LARP7 is a component of the 7SK ribonucleoprotein and affects transcription of cellular and viral polymerase II genes. EMBO Rep 9:569-75.
173. Jeronimo C, Forget D, Bouchard A, Li Q, Chua G, Poitras C, Therien C, Bergeron D, Bourassa S, Greenblatt J, Chabot B, Poirier GG, Hughes TR, Blanchette M, Price DH, Coulombe B. 2007. Systematic analysis of the protein interaction network for the human transcription machinery reveals the identity of the 7SK capping enzyme. Mol Cell 27:262-74.
174. Russo AA, Tong L, Lee JO, Jeffrey PD, Pavletich NP. 1998. Structural basis for inhibition of the cyclin-dependent kinase Cdk6 by the tumour suppressor p16INK4a. Nature 395:237-43.
175. Gibellini D, Vitone F, Schiavone P, Re MC. 2005. HIV-1 tat protein and cell proliferation and survival: a brief review. New Microbiol 28:95-109.
176. Debaisieux S, Rayne F, Yezid H, Beaumelle B. 2012. The ins and outs of HIV-1 Tat. Traffic 13:355-63.

177. Gatignol A. 2007. Transcription of HIV: Tat and cellular chromatin. Adv Pharmacol 55:137-59.
178. Stoltzfus CM. 2009. Chapter 1. Regulation of HIV-1 alternative RNA splicing and its role in virus replication. Adv Virus Res 74:1-40.
179. Purcell DF, Martin MA. 1993. Alternative splicing of human immunodeficiency virus type 1 mRNA modulates viral protein expression, replication, and infectivity. J Virol 67:6365-78.
180. Pollard VW, Malim MH. 1998. The HIV-1 Rev protein. Annu Rev Microbiol 52:491-532.
181. Dayton AI. 2004. Within you, without you: HIV-1 Rev and RNA export. Retrovirology 1:35.
182. Ajamian L, Abel K, Rao S, Vyboh K, Garcia-de-Gracia F, Soto-Rifo R, Kulozik AE, Gehring NH, Mouland AJ. 2015. HIV-1 Recruits UPF1 but Excludes UPF2 to Promote Nucleocytoplasmic Export of the Genomic RNA. Biomolecules 5:2808-39.
183. Toro-Ascuy D, Rojas-Araya B, Valiente-Echeverria F, Soto-Rifo R. 2016. Interactions between the HIV-1 Unspliced mRNA and Host mRNA Decay Machineries. Viruses 8.
184. Freed EO. 2015. HIV-1 assembly, release and maturation. Nat Rev Microbiol 13:484-96.
185. Olety B, Ono A. 2014. Roles played by acidic lipids in HIV-1 Gag membrane binding. Virus Res 193:108-15.
186. Mailler E, Bernacchi S, Marquet R, Paillart JC, Vivet-Boudou V, Smyth RP. 2016. The Life-Cycle of the HIV-1 Gag-RNA Complex. Viruses 8.
187. Hogue IB, Grover JR, Soheilian F, Nagashima K, Ono A. 2011. Gag induces the coalescence of clustered lipid rafts and tetraspanin-enriched microdomains at HIV-1 assembly sites on the plasma membrane. J Virol 85:9749-66.
188. Nguyen DH, Hildreth JE. 2000. Evidence for budding of human immunodeficiency virus type 1 selectively from glycolipid-enriched membrane lipid rafts. J Virol 74:3264-72.
189. Gamble TR, Yoo S, Vajdos FF, von Schwedler UK, Worthylake DK, Wang H, McCutcheon JP, Sundquist WI, Hill CP. 1997. Structure of the carboxyl-terminal dimerization domain of the HIV-1 capsid protein. Science 278:849-53.
190. Berthoux L, Sebastian S, Sokolskaja E, Luban J. 2005. Cyclophilin A is required for TRIM5{alpha}-mediated resistance to HIV-1 in Old World monkey cells. Proc Natl Acad Sci U S A 102:14849-53.
191. Campbell EM, Hope TJ. 2015. HIV-1 capsid: the multifaceted key player in HIV-1 infection. Nat Rev Microbiol 13:471-83.
192. Moore MD, Nikolaitchik OA, Chen J, Hammarskjold ML, Rekosh D, Hu WS. 2009. Probing the HIV-1 genomic RNA trafficking pathway and dimerization by genetic recombination and single virion analyses. PLoS Pathog 5:e1000627.
193. van Bel N, Das AT, Cornelissen M, Abbink TE, Berkhout B. 2014. A short sequence motif in the 5' leader of the HIV-1 genome modulates extended RNA dimer formation and virus replication. J Biol Chem 289:35061-74.
194. Brigham BS, Kitzrow JP, Reyes JC, Musier-Forsyth K, Munro JB. 2019. Intrinsic conformational dynamics of the HIV-1 genomic RNA 5'UTR. Proc Natl Acad Sci U S A 116:10372-10381.
195. Morita E, Sandrin V, McCullough J, Katsuyama A, Baci Hamilton I, Sundquist WI. 2011. ESCRT-III protein requirements for HIV-1 budding. Cell Host Microbe 9:235-242.

196. Huang M, Orenstein JM, Martin MA, Freed EO. 1995. p6Gag is required for particle production from full-length human immunodeficiency virus type 1 molecular clones expressing protease. J Virol 69:6810-8.
197. Inamdar K, Floderer C, Favard C, Muriaux D. 2019. Monitoring HIV-1 Assembly in Living Cells: Insights from Dynamic and Single Molecule Microscopy. Viruses 11.
198. Lingappa JR, Dooher JE, Newman MA, Kiser PK, Klein KC. 2006. Basic residues in the nucleocapsid domain of Gag are required for interaction of HIV-1 gag with ABCE1 (HP68), a cellular protein important for HIV-1 capsid assembly. J Biol Chem 281:3773-84.
199. Reed JC, Molter B, Geary CD, McNevin J, McElrath J, Giri S, Klein KC, Lingappa JR. 2012. HIV-1 Gag co-opts a cellular complex containing DDX6, a helicase that facilitates capsid assembly. J Cell Biol 198:439-56.
200. Mouland AJ, Mercier J, Luo M, Bernier L, DesGroseillers L, Cohen EA. 2000. The double-stranded RNA-binding protein Staufen is incorporated in human immunodeficiency virus type 1: evidence for a role in genomic RNA encapsidation. J Virol 74:5441-51.
201. Chatel-Chaix L, Clement JF, Martel C, Beriault V, Gatignol A, DesGroseillers L, Mouland AJ. 2004. Identification of Staufen in the human immunodeficiency virus type 1 Gag ribonucleoprotein complex and a role in generating infectious viral particles. Mol Cell Biol 24:2637-48.
202. Jager S, Cimermancic P, Gulbahce N, Johnson JR, McGovern KE, Clarke SC, Shales M, Mercenne G, Pache L, Li K, Hernandez H, Jang GM, Roth SL, Akiva E, Marlett J, Stephens M, D'Orso I, Fernandes J, Fahey M, Mahon C, O'Donoghue AJ, Todorovic A, Morris JH, Maltby DA, Alber T, Cagney G, Bushman FD, Young JA, Chanda SK, Sundquist WI, et al. 2011. Global landscape of HIV-human protein complexes. Nature 481:365-70.
203. Engeland CE, Brown NP, Borner K, Schumann M, Krause E, Kaderali L, Muller GA, Krausslich HG. 2014. Proteome analysis of the HIV-1 Gag interactome. Virology 460-461:194-206.
204. Ott DE. 2008. Cellular proteins detected in HIV-1. Rev Med Virol 18:159-75.
205. Swanson CM, Malim MH. 2008. SnapShot: HIV-1 proteins. Cell 133:742, 742.e1.
206. Huang L, Chen C. 2013. Understanding HIV-1 protease autoprocessing for novel therapeutic development. Future Med Chem 5:1215-29.
207. Patel P, Borkowf CB, Brooks JT, Lasry A, Lansky A, Mermin J. 2014. Estimating per-act HIV transmission risk: a systematic review. Aids 28:1509-19.
208. Tobian AA, Kacker S, Quinn TC. 2014. Male circumcision: a globally relevant but under-utilized method for the prevention of HIV and other sexually transmitted infections. Annu Rev Med 65:293-306.
209. Prodger JL, Kaul R. 2017. The biology of how circumcision reduces HIV susceptibility: broader implications for the prevention field. AIDS Res Ther 14:49.
210. Swanstrom R, Coffin J. 2012. HIV-1 pathogenesis: the virus. Cold Spring Harb Perspect Med 2:a007443.
211. Deeks SG, Overbaugh J, Phillips A, Buchbinder S. 2015. HIV infection. Nat Rev Dis Primers 1:15035.
212. Zhang Z, Schuler T, Zupancic M, Wietgrefe S, Staskus KA, Reimann KA, Reinhart TA, Rogan M, Cavert W, Miller CJ, Veazey RS, Notermans D, Little S, Danner SA, Richman

DD, Havlir D, Wong J, Jordan HL, Schacker TW, Racz P, Tenner-Racz K, Letvin NL, Wolinsky S, Haase AT. 1999. Sexual transmission and propagation of SIV and HIV in resting and activated CD4+ T cells. Science 286:1353-7.
213. Manches O, Frleta D, Bhardwaj N. 2014. Dendritic cells in progression and pathology of HIV infection. Trends Immunol 35:114-22.
214. Cohen MS, Shaw GM, McMichael AJ, Haynes BF. 2011. Acute HIV-1 Infection. N Engl J Med 364:1943-54.
215. Lackner AA, Lederman MM, Rodriguez B. 2012. HIV pathogenesis: the host. Cold Spring Harb Perspect Med 2:a007005.
216. Brenchley JM, Schacker TW, Ruff LE, Price DA, Taylor JH, Beilman GJ, Nguyen PL, Khoruts A, Larson M, Haase AT, Douek DC. 2004. CD4+ T cell depletion during all stages of HIV disease occurs predominantly in the gastrointestinal tract. J Exp Med 200:749-59.
217. Lee HY, Giorgi EE, Keele BF, Gaschen B, Athreya GS, Salazar-Gonzalez JF, Pham KT, Goepfert PA, Kilby JM, Saag MS, Delwart EL, Busch MP, Hahn BH, Shaw GM, Korber BT, Bhattacharya T, Perelson AS. 2009. Modeling sequence evolution in acute HIV-1 infection. J Theor Biol 261:341-60.
218. Palmer S, Wiegand AP, Maldarelli F, Bazmi H, Mican JM, Polis M, Dewar RL, Planta A, Liu S, Metcalf JA, Mellors JW, Coffin JM. 2003. New real-time reverse transcriptase-initiated PCR assay with single-copy sensitivity for human immunodeficiency virus type 1 RNA in plasma. J Clin Microbiol 41:4531-6.
219. Kahn JO, Walker BD. 1998. Acute human immunodeficiency virus type 1 infection. N Engl J Med 339:33-9.
220. Daar ES, Little S, Pitt J, Santangelo J, Ho P, Harawa N, Kerndt P, Glorgi JV, Bai J, Gaut P, Richman DD, Mandel S, Nichols S. 2001. Diagnosis of primary HIV-1 infection. Los Angeles County Primary HIV Infection Recruitment Network. Ann Intern Med 134:25-9.
221. Cooper DA, Tindall B, Wilson EJ, Imrie AA, Penny R. 1988. Characterization of T lymphocyte responses during primary infection with human immunodeficiency virus. J Infect Dis 157:889-96.
222. Lindback S, Karlsson AC, Mittler J, Blaxhult A, Carlsson M, Briheim G, Sonnerborg A, Gaines H. 2000. Viral dynamics in primary HIV-1 infection. Karolinska Institutet Primary HIV Infection Study Group. Aids 14:2283-91.
223. Branson BM. 2019. HIV Diagnostics: Current Recommendations and Opportunities for Improvement. Infect Dis Clin North Am 33:611-628.
224. Nowak MA. 1992. What is a quasispecies? Trends Ecol Evol 7:118-21.
225. Joseph SB, Swanstrom R, Kashuba AD, Cohen MS. 2015. Bottlenecks in HIV-1 transmission: insights from the study of founder viruses. Nat Rev Microbiol 13:414-25.
226. Liu Z, Cumberland WG, Hultin LE, Prince HE, Detels R, Giorgi JV. 1997. Elevated CD38 antigen expression on CD8+ T cells is a stronger marker for the risk of chronic HIV disease progression to AIDS and death in the Multicenter AIDS Cohort Study than CD4+ cell count, soluble immune activation markers, or combinations of HLA-DR and CD38 expression. J Acquir Immune Defic Syndr Hum Retrovirol 16:83-92.
227. McMichael AJ, Rowland-Jones SL. 2001. Cellular immune responses to HIV. Nature 410:980-7.
228. Lackner AA, Mohan M, Veazey RS. 2009. The gastrointestinal tract and AIDS pathogenesis. Gastroenterology 136:1965-78.

229. Estes JD, Wietgrefe S, Schacker T, Southern P, Beilman G, Reilly C, Milush JM, Lifson JD, Sodora DL, Carlis JV, Haase AT. 2007. Simian immunodeficiency virus-induced lymphatic tissue fibrosis is mediated by transforming growth factor beta 1-positive regulatory T cells and begins in early infection. J Infect Dis 195:551-61.
230. Douek DC, McFarland RD, Keiser PH, Gage EA, Massey JM, Haynes BF, Polis MA, Haase AT, Feinberg MB, Sullivan JL, Jamieson BD, Zack JA, Picker LJ, Koup RA. 1998. Changes in thymic function with age and during the treatment of HIV infection. Nature 396:690-5.
231. Grossman Z, Meier-Schellersheim M, Paul WE, Picker LJ. 2006. Pathogenesis of HIV infection: what the virus spares is as important as what it destroys. Nat Med 12:289-95.
232. Khaitan A, Unutmaz D. 2011. Revisiting immune exhaustion during HIV infection. Curr HIV/AIDS Rep 8:4-11.
233. Fischl MA, Richman DD, Grieco MH, Gottlieb MS, Volberding PA, Laskin OL, Leedom JM, Groopman JE, Mildvan D, Schooley RT, et al. 1987. The efficacy of azidothymidine (AZT) in the treatment of patients with AIDS and AIDS-related complex. A double-blind, placebo-controlled trial. N Engl J Med 317:185-91.
234. Laskey SB, Siliciano RF. 2014. A mechanistic theory to explain the efficacy of antiretroviral therapy. Nat Rev Microbiol 12:772-80.
235. Services USDoHH. 2019. A Timeline of HIV and AIDS. https://www.hiv.gov/hiv-basics/overview/history/hiv-and-aids-timeline. Accessed
236. Lv Z, Chu Y, Wang Y. 2015. HIV protease inhibitors: a review of molecular selectivity and toxicity. HIV AIDS (Auckl) 7:95-104.
237. Usach I, Melis V, Peris JE. 2013. Non-nucleoside reverse transcriptase inhibitors: a review on pharmacokinetics, pharmacodynamics, safety and tolerability. J Int AIDS Soc 16:1-14.
238. Tseng A, Hughes CA, Wu J, Seet J, Phillips EJ. 2017. Cobicistat Versus Ritonavir: Similar Pharmacokinetic Enhancers But Some Important Differences. Ann Pharmacother 51:1008-1022.
239. AIDSinfo. 2019. Guidelines for the Use of Antiretroviral Agents in Adults and Adolescents with HIV. https://aidsinfo.nih.gov/guidelines. Accessed
240. Han Y, Lassen K, Monie D, Sedaghat AR, Shimoji S, Liu X, Pierson TC, Margolick JB, Siliciano RF, Siliciano JD. 2004. Resting CD4+ T cells from human immunodeficiency virus type 1 (HIV-1)-infected individuals carry integrated HIV-1 genomes within actively transcribed host genes. J Virol 78:6122-33.
241. Korin YD, Zack JA. 1999. Nonproductive human immunodeficiency virus type 1 infection in nucleoside-treated G0 lymphocytes. J Virol 73:6526-32.
242. Golob JL, Stern J, Holte S, Kitahata MM, Crane HM, Coombs RW, Goecker E, Woolfrey AE, Harrington RD. 2018. HIV DNA levels and decay in a cohort of 111 long-term virally suppressed patients. Aids 32:2113-2118.
243. Chun TW, Stuyver L, Mizell SB, Ehler LA, Mican JA, Baseler M, Lloyd AL, Nowak MA, Fauci AS. 1997. Presence of an inducible HIV-1 latent reservoir during highly active antiretroviral therapy. Proc Natl Acad Sci U S A 94:13193-7.
244. Finzi D, Hermankova M, Pierson T, Carruth LM, Buck C, Chaisson RE, Quinn TC, Chadwick K, Margolick J, Brookmeyer R, Gallant J, Markowitz M, Ho DD, Richman DD, Siliciano RF. 1997. Identification of a reservoir for HIV-1 in patients on highly active antiretroviral therapy. Science 278:1295-300.

245. Siliciano JD, Kajdas J, Finzi D, Quinn TC, Chadwick K, Margolick JB, Kovacs C, Gange SJ, Siliciano RF. 2003. Long-term follow-up studies confirm the stability of the latent reservoir for HIV-1 in resting CD4+ T cells. Nat Med 9:727-8.
246. Ruelas DS, Greene WC. 2013. An integrated overview of HIV-1 latency. Cell 155:519-29.
247. Greger IH, Demarchi F, Giacca M, Proudfoot NJ. 1998. Transcriptional interference perturbs the binding of Sp1 to the HIV-1 promoter. Nucleic Acids Res 26:1294-301.
248. Lewinski MK, Bisgrove D, Shinn P, Chen H, Hoffmann C, Hannenhalli S, Verdin E, Berry CC, Ecker JR, Bushman FD. 2005. Genome-wide analysis of chromosomal features repressing human immunodeficiency virus transcription. J Virol 79:6610-9.
249. Zhong H, May MJ, Jimi E, Ghosh S. 2002. The phosphorylation status of nuclear NF-kappa B determines its association with CBP/p300 or HDAC-1. Mol Cell 9:625-36.
250. Barboric M, Nissen RM, Kanazawa S, Jabrane-Ferrat N, Peterlin BM. 2001. NF-kappaB binds P-TEFb to stimulate transcriptional elongation by RNA polymerase II. Mol Cell 8:327-37.
251. Ott M, Dorr A, Hetzer-Egger C, Kaehlcke K, Schnolzer M, Henklein P, Cole P, Zhou MM, Verdin E. 2004. Tat acetylation: a regulatory switch between early and late phases in HIV transcription elongation. Novartis Found Symp 259:182-93; discussion 193-6, 223-5.
252. Kauder SE, Bosque A, Lindqvist A, Planelles V, Verdin E. 2009. Epigenetic regulation of HIV-1 latency by cytosine methylation. PLoS Pathog 5:e1000495.
253. Hutter G, Nowak D, Mossner M, Ganepola S, Mussig A, Allers K, Schneider T, Hofmann J, Kucherer C, Blau O, Blau IW, Hofmann WK, Thiel E. 2009. Long-term control of HIV by CCR5 Delta32/Delta32 stem-cell transplantation. N Engl J Med 360:692-8.
254. Allers K, Hutter G, Hofmann J, Loddenkemper C, Rieger K, Thiel E, Schneider T. 2011. Evidence for the cure of HIV infection by CCR5Delta32/Delta32 stem cell transplantation. Blood 117:2791-9.
255. Gupta RK, Abdul-Jawad S, McCoy LE, Mok HP, Peppa D, Salgado M, Martinez-Picado J, Nijhuis M, Wensing AMJ, Lee H, Grant P, Nastouli E, Lambert J, Pace M, Salasc F, Monit C, Innes AJ, Muir L, Waters L, Frater J, Lever AML, Edwards SG, Gabriel IH, Olavarria E. 2019. HIV-1 remission following CCR5Delta32/Delta32 haematopoietic stem-cell transplantation. Nature 568:244-248.
256. Scarborough RJ, Goguen RP, Gatignol A. 2019. A second patient cured of HIV infection: hopes and limitations. Virologie (Montrouge) 23:1-4.
257. Persaud D, Gay H, Ziemniak C, Chen YH, Piatak M, Jr., Chun TW, Strain M, Richman D, Luzuriaga K. 2013. Absence of detectable HIV-1 viremia after treatment cessation in an infant. N Engl J Med 369:1828-35.
258. Luzuriaga K, Gay H, Ziemniak C, Sanborn KB, Somasundaran M, Rainwater-Lovett K, Mellors JW, Rosenbloom D, Persaud D. 2015. Viremic relapse after HIV-1 remission in a perinatally infected child. N Engl J Med 372:786-8.
259. Rainwater-Lovett K, Luzuriaga K, Persaud D. 2015. Very early combination antiretroviral therapy in infants: prospects for cure. Curr Opin HIV AIDS 10:4-11.
260. Saez-Cirion A, Bacchus C, Hocqueloux L, Avettand-Fenoel V, Girault I, Lecuroux C, Potard V, Versmisse P, Melard A, Prazuck T, Descours B, Guergnon J, Viard JP, Boufassa F, Lambotte O, Goujard C, Meyer L, Costagliola D, Venet A, Pancino G,

Autran B, Rouzioux C. 2013. Post-treatment HIV-1 controllers with a long-term virological remission after the interruption of early initiated antiretroviral therapy ANRS VISCONTI Study. PLoS Pathog 9:e1003211.
261. Check Hayden E. 2015. French teenager healthy 12 years after ceasing HIV treatment. Nature 523:393.
262. Violari A, Cotton MF, Gibb DM, Babiker AG, Steyn J, Madhi SA, Jean-Philippe P, McIntyre JA. 2008. Early antiretroviral therapy and mortality among HIV-infected infants. N Engl J Med 359:2233-44.
263. Cortes FH, Passaes CP, Bello G, Teixeira SL, Vorsatz C, Babic D, Sharkey M, Grinsztejn B, Veloso V, Stevenson M, Morgado MG. 2015. HIV controllers with different viral load cutoff levels have distinct virologic and immunologic profiles. J Acquir Immune Defic Syndr 68:377-385.
264. Okulicz JF, Lambotte O. 2011. Epidemiology and clinical characteristics of elite controllers. Curr Opin HIV AIDS 6:163-8.
265. Kumar R, Qureshi H, Deshpande S, Bhattacharya J. 2018. Broadly neutralizing antibodies in HIV-1 treatment and prevention. Ther Adv Vaccines Immunother 6:61-68.
266. Borducchi EN, Liu J, Nkolola JP, Cadena AM, Yu WH, Fischinger S, Broge T, Abbink P, Mercado NB, Chandrashekar A, Jetton D, Peter L, McMahan K, Moseley ET, Bekerman E, Hesselgesser J, Li W, Lewis MG, Alter G, Geleziunas R, Barouch DH. 2018. Antibody and TLR7 agonist delay viral rebound in SHIV-infected monkeys. Nature 563:360-364.
267. Sun M, Pace CS, Yao X, Yu F, Padte NN, Huang Y, Seaman MS, Li Q, Ho DD. 2014. Rational design and characterization of the novel, broad and potent bispecific HIV-1 neutralizing antibody iMabm36. J Acquir Immune Defic Syndr 66:473-83.
268. Wu X, Guo J, Niu M, An M, Liu L, Wang H, Jin X, Zhang Q, Lam KS, Wu T, Wang H, Wang Q, Du Y, Li J, Cheng L, Tang HY, Shang H, Zhang L, Zhou P, Chen Z. 2018. Tandem bispecific neutralizing antibody eliminates HIV-1 infection in humanized mice. J Clin Invest 128:2239-2251.
269. Abner E, Jordan A. 2019. HIV "shock and kill" therapy: In need of revision. Antiviral Res 166:19-34.
270. Rato S, Rausell A, Munoz M, Telenti A, Ciuffi A. 2017. Single-cell analysis identifies cellular markers of the HIV permissive cell. PLoS Pathog 13:e1006678.
271. Battivelli E, Dahabieh MS, Abdel-Mohsen M, Svensson JP, Tojal Da Silva I, Cohn LB, Gramatica A, Deeks S, Greene WC, Pillai SK, Verdin E. 2018. Distinct chromatin functional states correlate with HIV latency reactivation in infected primary CD4(+) T cells. Elife 7:e34655.
272. Mousseau G, Clementz MA, Bakeman WN, Nagarsheth N, Cameron M, Shi J, Baran P, Fromentin R, Chomont N, Valente ST. 2012. An analog of the natural steroidal alkaloid cortistatin A potently suppresses Tat-dependent HIV transcription. Cell Host Microbe 12:97-108.
273. Kessing CF, Nixon CC, Li C, Tsai P, Takata H, Mousseau G, Ho PT, Honeycutt JB, Fallahi M, Trautmann L, Garcia JV, Valente ST. 2017. In Vivo Suppression of HIV Rebound by Didehydro-Cortistatin A, a "Block-and-Lock" Strategy for HIV-1 Treatment. Cell Rep 21:600-611.

274. Sagnier S, Daussy CF, Borel S, Robert-Hebmann V, Faure M, Blanchet FP, Beaumelle B, Biard-Piechaczyk M, Espert L. 2015. Autophagy restricts HIV-1 infection by selectively degrading Tat in CD4+ T lymphocytes. J Virol 89:615-25.
275. Zhao F, Huang W, Zhang Z, Mao L, Han Y, Yan J, Lei M. 2016. Triptolide induces protective autophagy through activation of the CaMKKbeta-AMPK signaling pathway in prostate cancer cells. Oncotarget 7:5366-82.
276. Besnard E, Hakre S, Kampmann M, Lim HW, Hosmane NN, Martin A, Bassik MC, Verschueren E, Battivelli E, Chan J, Svensson JP, Gramatica A, Conrad RJ, Ott M, Greene WC, Krogan NJ, Siliciano RF, Weissman JS, Verdin E. 2016. The mTOR Complex Controls HIV Latency. Cell Host Microbe 20:785-797.
277. Scarborough RJ, Gatignol A. 2017. RNA Interference Therapies for an HIV-1 Functional Cure. Viruses 10:8.
278. Goguen RP, Malard CM, Scarborough RJ, Gatignol A. 2019. Small RNAs to treat human immunodeficiency virus type 1 infection by gene therapy. Curr Opin Virol 38:10-20.
279. Xu L, Yang H, Gao Y, Chen Z, Xie L, Liu Y, Liu Y, Wang X, Li H, Lai W, He Y, Yao A, Ma L, Shao Y, Zhang B, Wang C, Chen H, Deng H. 2017. CRISPR/Cas9-Mediated CCR5 Ablation in Human Hematopoietic Stem/Progenitor Cells Confers HIV-1 Resistance In Vivo. Mol Ther 25:1782-1789.
280. Wang Z, Wang W, Cui YC, Pan Q, Zhu W, Gendron P, Guo F, Cen S, Witcher M, Liang C. 2018. HIV-1 Employs Multiple Mechanisms To Resist Cas9/Single Guide RNA Targeting the Viral Primer Binding Site. J Virol 92:e01135-18.
281. Ferraris P, Yssel H, Misse D. 2019. Zika virus infection: an update. Microbes Infect doi:10.1016/j.micinf.2019.04.005.
282. Dick GW, Kitchen SF, Haddow AJ. 1952. Zika virus. I. Isolations and serological specificity. Trans R Soc Trop Med Hyg 46:509-20.
283. Macnamara FN. 1954. Zika virus: a report on three cases of human infection during an epidemic of jaundice in Nigeria. Trans R Soc Trop Med Hyg 48:139-45.
284. Simpson DI. 1964. ZIKA VIRUS INFECTION IN MAN. Trans R Soc Trop Med Hyg 58:335-8.
285. Moore DL, Causey OR, Carey DE, Reddy S, Cooke AR, Akinkugbe FM, David-West TS, Kemp GE. 1975. Arthropod-borne viral infections of man in Nigeria, 1964-1970. Ann Trop Med Parasitol 69:49-64.
286. Marchette NJ, Garcia R, Rudnick A. 1969. Isolation of Zika virus from Aedes aegypti mosquitoes in Malaysia. Am J Trop Med Hyg 18:411-5.
287. Olson JG, Ksiazek TG, Suhandiman, Triwibowo. 1981. Zika virus, a cause of fever in Central Java, Indonesia. Trans R Soc Trop Med Hyg 75:389-93.
288. Duffy MR, Chen TH, Hancock WT, Powers AM, Kool JL, Lanciotti RS, Pretrick M, Marfel M, Holzbauer S, Dubray C, Guillaumot L, Griggs A, Bel M, Lambert AJ, Laven J, Kosoy O, Panella A, Biggerstaff BJ, Fischer M, Hayes EB. 2009. Zika virus outbreak on Yap Island, Federated States of Micronesia. N Engl J Med 360:2536-43.
289. Hancock WT, Marfel M, Bel M. 2014. Zika virus, French Polynesia, South Pacific, 2013. Emerg Infect Dis 20:1960.
290. Ioos S, Mallet HP, Leparc Goffart I, Gauthier V, Cardoso T, Herida M. 2014. Current Zika virus epidemiology and recent epidemics. Med Mal Infect 44:302-7.
291. Liu ZY, Shi WF, Qin CF. 2019. The evolution of Zika virus from Asia to the Americas. Nat Rev Microbiol 17:131-139.

292. Massad E, Burattini MN, Khan K, Struchiner CJ, Coutinho FAB, Wilder-Smith A. 2017. On the origin and timing of Zika virus introduction in Brazil. Epidemiol Infect 145:2303-2312.
293. Kindhauser MK, Allen T, Frank V, Santhana RS, Dye C. 2016. Zika: the origin and spread of a mosquito-borne virus. Bull World Health Organ 94:675-686c.
294. Lim SK, Lim JK, Yoon IK. 2017. An Update on Zika Virus in Asia. Infect Chemother 49:91-100.
295. CDC. 2019. 2019 Case Counts in the US. https://www.cdc.gov/zika/reporting/2019-case-counts.html. Accessed
296. Heinz FX, Stiasny K. 2017. The Antigenic Structure of Zika Virus and Its Relation to Other Flaviviruses: Implications for Infection and Immunoprophylaxis. Microbiol Mol Biol Rev 81:e00055-16.
297. Shi Y, Gao GF. 2017. Structural Biology of the Zika Virus. Trends Biochem Sci 42:443-456.
298. Ye Q, Liu ZY, Han JF, Jiang T, Li XF, Qin CF. 2016. Genomic characterization and phylogenetic analysis of Zika virus circulating in the Americas. Infect Genet Evol 43:43-9.
299. Song Y, Mugavero J, Stauft CB, Wimmer E. 2019. Dengue and Zika Virus 5' Untranslated Regions Harbor Internal Ribosomal Entry Site Functions. MBio 10.
300. Mazeaud C, Freppel W, Chatel-Chaix L. 2018. The Multiples Fates of the Flavivirus RNA Genome During Pathogenesis. Front Genet 9:595.
301. Pijlman GP, Funk A, Kondratieva N, Leung J, Torres S, van der Aa L, Liu WJ, Palmenberg AC, Shi PY, Hall RA, Khromykh AA. 2008. A highly structured, nuclease-resistant, noncoding RNA produced by flaviviruses is required for pathogenicity. Cell Host Microbe 4:579-91.
302. Schneider AB, Wolfinger MT. 2019. Musashi binding elements in Zika and related Flavivirus 3'UTRs: A comparative study in silico. Sci Rep 9:6911.
303. Mukhopadhyay S, Kuhn RJ, Rossmann MG. 2005. A structural perspective of the flavivirus life cycle. Nat Rev Microbiol 3:13-22.
304. Lazear HM, Diamond MS. 2016. Zika Virus: New Clinical Syndromes and Its Emergence in the Western Hemisphere. J Virol 90:4864-4875.
305. Youn S, Ambrose RL, Mackenzie JM, Diamond MS. 2013. Non-structural protein-1 is required for West Nile virus replication complex formation and viral RNA synthesis. Virol J 10:339.
306. Crook KR, Miller-Kittrell M, Morrison CR, Scholle F. 2014. Modulation of innate immune signaling by the secreted form of the West Nile virus NS1 glycoprotein. Virology 458-459:172-82.
307. Scaturro P, Cortese M, Chatel-Chaix L, Fischl W, Bartenschlager R. 2015. Dengue Virus Non-structural Protein 1 Modulates Infectious Particle Production via Interaction with the Structural Proteins. PLoS Pathog 11:e1005277.
308. Liu J, Liu Y, Nie K, Du S, Qiu J, Pang X, Wang P, Cheng G. 2016. Flavivirus NS1 protein in infected host sera enhances viral acquisition by mosquitoes. Nat Microbiol 1:16087.
309. Zhang X, Xie X, Xia H, Zou J, Huang L, Popov VL, Chen X, Shi PY. 2019. Zika Virus NS2A-Mediated Virion Assembly. mBio 10.

310. Shiryaev SA, Farhy C, Pinto A, Huang CT, Simonetti N, Elong Ngono A, Dewing A, Shresta S, Pinkerton AB, Cieplak P, Strongin AY, Terskikh AV. 2017. Characterization of the Zika virus two-component NS2B-NS3 protease and structure-assisted identification of allosteric small-molecule antagonists. Antiviral Res 143:218-229.
311. Miller S, Kastner S, Krijnse-Locker J, Buhler S, Bartenschlager R. 2007. The non-structural protein 4A of dengue virus is an integral membrane protein inducing membrane alterations in a 2K-regulated manner. J Biol Chem 282:8873-82.
312. Roosendaal J, Westaway EG, Khromykh A, Mackenzie JM. 2006. Regulated cleavages at the West Nile virus NS4A-2K-NS4B junctions play a major role in rearranging cytoplasmic membranes and Golgi trafficking of the NS4A protein. J Virol 80:4623-32.
313. Kaufusi PH, Kelley JF, Yanagihara R, Nerurkar VR. 2014. Induction of endoplasmic reticulum-derived replication-competent membrane structures by West Nile virus non-structural protein 4B. PLoS One 9:e84040.
314. Liang Q, Luo Z, Zeng J, Chen W, Foo SS, Lee SA, Ge J, Wang S, Goldman SA, Zlokovic BV, Zhao Z, Jung JU. 2016. Zika Virus NS4A and NS4B Proteins Deregulate Akt-mTOR Signaling in Human Fetal Neural Stem Cells to Inhibit Neurogenesis and Induce Autophagy. Cell Stem Cell 19:663-671.
315. Zhao B, Yi G, Du F, Chuang YC, Vaughan RC, Sankaran B, Kao CC, Li P. 2017. Structure and function of the Zika virus full-length NS5 protein. Nat Commun 8:14762.
316. Hamel R, Dejarnac O, Wichit S, Ekchariyawat P, Neyret A, Luplertlop N, Perera-Lecoin M, Surasombatpattana P, Talignani L, Thomas F, Cao-Lormeau VM, Choumet V, Briant L, Despres P, Amara A, Yssel H, Misse D. 2015. Biology of Zika Virus Infection in Human Skin Cells. J Virol 89:8880-96.
317. Kim JA, Seong RK, Son SW, Shin OS. 2019. Insights into ZIKV-Mediated Innate Immune Responses in Human Dermal Fibroblasts and Epidermal Keratinocytes. J Invest Dermatol 139:391-399.
318. Sun X, Hua S, Chen HR, Ouyang Z, Einkauf K, Tse S, Ard K, Ciaranello A, Yawetz S, Sax P, Rosenberg ES, Lichterfeld M, Yu XG. 2017. Transcriptional Changes during Naturally Acquired Zika Virus Infection Render Dendritic Cells Highly Conducive to Viral Replication. Cell Rep 21:3471-3482.
319. Foo SS, Chen W, Chan Y, Bowman JW, Chang LC, Choi Y, Yoo JS, Ge J, Cheng G, Bonnin A, Nielsen-Saines K, Brasil P, Jung JU. 2017. Asian Zika virus strains target CD14(+) blood monocytes and induce M2-skewed immunosuppression during pregnancy. Nat Microbiol 2:1558-1570.
320. Tang H, Hammack C, Ogden SC, Wen Z, Qian X, Li Y, Yao B, Shin J, Zhang F, Lee EM, Christian KM, Didier RA, Jin P, Song H, Ming GL. 2016. Zika Virus Infects Human Cortical Neural Progenitors and Attenuates Their Growth. Cell Stem Cell 18:587-90.
321. Garcez PP, Loiola EC, Madeiro da Costa R, Higa LM, Trindade P, Delvecchio R, Nascimento JM, Brindeiro R, Tanuri A, Rehen SK. 2016. Zika virus impairs growth in human neurospheres and brain organoids. Science 352:816-8.
322. Lee I, Bos S, Li G, Wang S, Gadea G, Despres P, Zhao RY. 2018. Probing Molecular Insights into Zika Virus(-)Host Interactions. Viruses 10:233.
323. Smit JM, Moesker B, Rodenhuis-Zybert I, Wilschut J. 2011. Flavivirus cell entry and membrane fusion. Viruses 3:160-71.

324. Zhang X, Sheng J, Austin SK, Hoornweg TE, Smit JM, Kuhn RJ, Diamond MS, Rossmann MG. 2015. Structure of acidic pH dengue virus showing the fusogenic glycoprotein trimers. J Virol 89:743-50.
325. Barrows NJ, Campos RK, Liao KC, Prasanth KR, Soto-Acosta R, Yeh SC, Schott-Lerner G, Pompon J, Sessions OM, Bradrick SS, Garcia-Blanco MA. 2018. Biochemistry and Molecular Biology of Flaviviruses. Chem Rev 118:4448-4482.
326. Westaway EG, Mackenzie JM, Khromykh AA. 2003. Kunjin RNA replication and applications of Kunjin replicons. Adv Virus Res 59:99-140.
327. Saeedi BJ, Geiss BJ. 2013. Regulation of flavivirus RNA synthesis and capping. Wiley Interdiscip Rev RNA 4:723-35.
328. Selisko B, Wang C, Harris E, Canard B. 2014. Regulation of Flavivirus RNA synthesis and replication. Curr Opin Virol 9:74-83.
329. Brinton MA. 2013. Replication cycle and molecular biology of the West Nile virus. Viruses 6:13-53.
330. Welsch S, Miller S, Romero-Brey I, Merz A, Bleck CK, Walther P, Fuller SD, Antony C, Krijnse-Locker J, Bartenschlager R. 2009. Composition and three-dimensional architecture of the dengue virus replication and assembly sites. Cell Host Microbe 5:365-75.
331. Byk LA, Gamarnik AV. 2016. Properties and Functions of the Dengue Virus Capsid Protein. Annu Rev Virol 3:263-281.
332. Cortese M, Goellner S, Acosta EG, Neufeldt CJ, Oleksiuk O, Lampe M, Haselmann U, Funaya C, Schieber N, Ronchi P, Schorb M, Pruunsild P, Schwab Y, Chatel-Chaix L, Ruggieri A, Bartenschlager R. 2017. Ultrastructural Characterization of Zika Virus Replication Factories. Cell Rep 18:2113-2123.
333. Sager G, Gabaglio S, Sztul E, Belov GA. 2018. Role of Host Cell Secretory Machinery in Zika Virus Life Cycle. Viruses 10:559.
334. Pierson TC, Diamond MS. 2012. Degrees of maturity: the complex structure and biology of flaviviruses. Curr Opin Virol 2:168-75.
335. Sirohi D, Kuhn RJ. 2017. Zika Virus Structure, Maturation, and Receptors. J Infect Dis 216:S935-s944.
336. Wu B, Guo W. 2015. The Exocyst at a Glance. J Cell Sci 128:2957-64.
337. Mossenta M, Marchese S, Poggianella M, Slon Campos JL, Burrone OR. 2017. Role of N-glycosylation on Zika virus E protein secretion, viral assembly and infectivity. Biochem Biophys Res Commun 492:579-586.
338. Chen Z, Lin X, Zhang Z, Huang J, Fu S, Huang R. 2011. EXO70 protein influences dengue virus secretion. Microbes Infect 13:143-50.
339. Barreto-Vieira DF, Jacome FC, da Silva MAN, Caldas GC, de Filippis AMB, de Sequeira PC, de Souza EM, Andrade AA, Manso PPA, Trindade GF, Lima SMB, Barth OM. 2017. Structural investigation of C6/36 and Vero cell cultures infected with a Brazilian Zika virus. PLoS One 12:e0184397.
340. Acosta-Ampudia Y, Monsalve DM, Castillo-Medina LF, Rodriguez Y, Pacheco Y, Halstead S, Willison HJ, Anaya JM, Ramirez-Santana C. 2018. Autoimmune Neurological Conditions Associated With Zika Virus Infection. Front Mol Neurosci 11:116.

341. Pettersson JH, Eldholm V, Seligman SJ, Lundkvist A, Falconar AK, Gaunt MW, Musso D, Nougairede A, Charrel R, Gould EA, de Lamballerie X. 2016. How Did Zika Virus Emerge in the Pacific Islands and Latin America? MBio 7:e01239-16.
342. Musso D, Gubler DJ. 2016. Zika Virus. Clin Microbiol Rev 29:487-524.
343. Herrera BB, Chang CA, Hamel DJ, Mboup S, Ndiaye D, Imade G, Okpokwu J, Agbaji O, Bei AK, Kanki PJ. 2017. Continued Transmission of Zika Virus in Humans in West Africa, 1992-2016. J Infect Dis 215:1546-1550.
344. Shao Q, Herrlinger S, Zhu YN, Yang M, Goodfellow F, Stice SL, Qi XP, Brindley MA, Chen JF. 2017. The African Zika virus MR-766 is more virulent and causes more severe brain damage than current Asian lineage and dengue virus. Development 144:4114-4124.
345. Sanchez-San Martin C, Li T, Bouquet J, Streithorst J, Yu G, Paranjpe A, Chiu CY. 2018. Differentiation enhances Zika virus infection of neuronal brain cells. Sci Rep 8:14543.
346. Yuan L, Huang XY, Liu ZY, Zhang F, Zhu XL, Yu JY, Ji X, Xu YP, Li G, Li C, Wang HJ, Deng YQ, Wu M, Cheng ML, Ye Q, Xie DY, Li XF, Wang X, Shi W, Hu B, Shi PY, Xu Z, Qin CF. 2017. A single mutation in the prM protein of Zika virus contributes to fetal microcephaly. Science 358:933-936.
347. Xia H, Luo H, Shan C, Muruato AE, Nunes BTD, Medeiros DBA, Zou J, Xie X, Giraldo MI, Vasconcelos PFC, Weaver SC, Wang T, Rajsbaum R, Shi PY. 2018. An evolutionary NS1 mutation enhances Zika virus evasion of host interferon induction. Nat Commun 9:414.
348. Zhao F, Xu Y, Lavillette D, Zhong J, Zou G, Long G. 2018. Negligible contribution of M2634V substitution to ZIKV pathogenesis in AG6 mice revealed by a bacterial promoter activity reduced infectious clone. Sci Rep 8:10491.
349. Alpuche-Lazcano SP, McCullogh CR, Del Corpo O, Rance E, Scarborough RJ, Mouland AJ, Sagan SM, Teixeira MM, Gatignol A. 2018. Higher Cytopathic Effects of a Zika Virus Brazilian Isolate from Bahia Compared to a Canadian-Imported Thai Strain. Viruses 10:53.
350. Guedes DR, Paiva MH, Donato MM, Barbosa PP, Krokovsky L, Rocha S, Saraiva K, Crespo MM, Rezende TM, Wallau GL, Barbosa RM, Oliveira CM, Melo-Santos MA, Pena L, Cordeiro MT, Franca RFO, Oliveira AL, Peixoto CA, Leal WS, Ayres CF. 2017. Zika virus replication in the mosquito Culex quinquefasciatus in Brazil. Emerg Microbes Infect 6:e69.
351. Morrison TE, Diamond MS. 2017. Animal Models of Zika Virus Infection, Pathogenesis, and Immunity. J Virol 91:e00009-17.
352. Beck C, Leparc-Goffart I, Desoutter D, Deberge E, Bichet H, Lowenski S, Dumarest M, Gonzalez G, Migne C, Vanhomwegen J, Zientara S, Durand B, Lecollinet S. 2019. Serological evidence of infection with dengue and Zika viruses in horses on French Pacific Islands. PLoS Negl Trop Dis 13:e0007162.
353. Bhatt S, Gething PW, Brady OJ, Messina JP, Farlow AW, Moyes CL, Drake JM, Brownstein JS, Hoen AG, Sankoh O, Myers MF, George DB, Jaenisch T, Wint GR, Simmons CP, Scott TW, Farrar JJ, Hay SI. 2013. The global distribution and burden of dengue. Nature 496:504-7.
354. Foy BD, Kobylinski KC, Chilson Foy JL, Blitvich BJ, Travassos da Rosa A, Haddow AD, Lanciotti RS, Tesh RB. 2011. Probable non-vector-borne transmission of Zika virus, Colorado, USA. Emerg Infect Dis 17:880-2.

355. D'Ortenzio E, Matheron S, Yazdanpanah Y, de Lamballerie X, Hubert B, Piorkowski G, Maquart M, Descamps D, Damond F, Leparc-Goffart I. 2016. Evidence of Sexual Transmission of Zika Virus. N Engl J Med 374:2195-8.
356. Hastings AK, Fikrig E. 2017. Zika Virus and Sexual Transmission: A New Route of Transmission for Mosquito-borne Flaviviruses. Yale J Biol Med 90:325-330.
357. Davidson A, Slavinski S, Komoto K, Rakeman J, Weiss D. 2016. Suspected Female-to-Male Sexual Transmission of Zika Virus - New York City, 2016. MMWR Morb Mortal Wkly Rep 65:716-7.
358. Deckard DT, Chung WM, Brooks JT, Smith JC, Woldai S, Hennessey M, Kwit N, Mead P. 2016. Male-to-Male Sexual Transmission of Zika Virus--Texas, January 2016. MMWR Morb Mortal Wkly Rep 65:372-4.
359. Matheron S, d'Ortenzio E, Leparc-Goffart I, Hubert B, de Lamballerie X, Yazdanpanah Y. 2016. Long-Lasting Persistence of Zika Virus in Semen. Clin Infect Dis 63:1264.
360. Nicastri E, Castilletti C, Liuzzi G, Iannetta M, Capobianchi MR, Ippolito G. 2016. Persistent detection of Zika virus RNA in semen for six months after symptom onset in a traveller returning from Haiti to Italy, February 2016. Euro Surveill 21:30314.
361. de La Vega MA, Piret J, Griffin BD, Rheaume C, Venable MC, Carbonneau J, Couture C, das Neves Almeida R, Tremblay RR, Magalhaes KG, Park YK, Roberts CC, Maslow JN, Sardesai NY, Kim JJ, Muthumani K, Weiner DB, Kobinger GP, Boivin G. 2019. Zika-Induced Male Infertility in Mice Is Potentially Reversible and Preventable by Deoxyribonucleic Acid Immunization. J Infect Dis 219:365-374.
362. Alvarado MG, Schwartz DA. 2017. Zika Virus Infection in Pregnancy, Microcephaly, and Maternal and Fetal Health: What We Think, What We Know, and What We Think We Know. Arch Pathol Lab Med 141:26-32.
363. Oliveira Melo AS, Malinger G, Ximenes R, Szejnfeld PO, Alves Sampaio S, Bispo de Filippis AM. 2016. Zika virus intrauterine infection causes fetal brain abnormality and microcephaly: tip of the iceberg? Ultrasound Obstet Gynecol 47:6-7.
364. Ventura CV, Maia M, Bravo-Filho V, Gois AL, Belfort R, Jr. 2016. Zika virus in Brazil and macular atrophy in a child with microcephaly. Lancet 387:228.
365. Campos AG, Lira RP, Arantes TE. 2016. Optical coherence tomography of macular atrophy associated with microcephaly and presumed intrauterine Zika virus infection. Arq Bras Oftalmol 79:400-401.
366. Colt S, Garcia-Casal MN, Pena-Rosas JP, Finkelstein JL, Rayco-Solon P, Weise Prinzo ZC, Mehta S. 2017. Transmission of Zika virus through breast milk and other breastfeeding-related bodily-fluids: A systematic review. PLoS Negl Trop Dis 11:e0005528.
367. Hamel R, Liegeois F, Wichit S, Pompon J, Diop F, Talignani L, Thomas F, Despres P, Yssel H, Misse D. 2016. Zika virus: epidemiology, clinical features and host-virus interactions. Microbes Infect 18:441-9.
368. Rasmussen SA, Jamieson DJ, Honein MA, Petersen LR. 2016. Zika Virus and Birth Defects--Reviewing the Evidence for Causality. N Engl J Med 374:1981-7.
369. CDC. 2017. Facts about Microcephaly. https://www.cdc.gov/ncbddd/birthdefects/microcephaly.html. Accessed
370. Mlakar J, Korva M, Tul N, Popovic M, Poljsak-Prijatelj M, Mraz J, Kolenc M, Resman Rus K, Vesnaver Vipotnik T, Fabjan Vodusek V, Vizjak A, Pizem J, Petrovec M, Avsic Zupanc T. 2016. Zika Virus Associated with Microcephaly. N Engl J Med 374:951-8.

371. Schwartz DA. 2017. Autopsy and Postmortem Studies Are Concordant: Pathology of Zika Virus Infection Is Neurotropic in Fetuses and Infants With Microcephaly Following Transplacental Transmission. Arch Pathol Lab Med 141:68-72.
372. Nielsen-Saines K, Brasil P, Kerin T, Vasconcelos Z, Gabaglia CR, Damasceno L, Pone M, Abreu de Carvalho LM, Pone SM, Zin AA, Tsui I, Salles TRS, da Cunha DC, Costa RP, Malacarne J, Reis AB, Hasue RH, Aizawa CYP, Genovesi FF, Einspieler C, Marschik PB, Pereira JP, Gaw SL, Adachi K, Cherry JD, Xu Z, Cheng G, Moreira ME. 2019. Delayed childhood neurodevelopment and neurosensory alterations in the second year of life in a prospective cohort of ZIKV-exposed children. Nat Med 25:1213-1217.
373. Pecanha PM, Gomes Junior SC, Pone SM, Pone M, Vasconcelos Z, Zin A, Vilibor RHH, Costa RP, Meio M, Nielsen-Saines K, Brasil P, Brickley E, Lopes Moreira ME. 2020. Neurodevelopment of children exposed intra-uterus by Zika virus: A case series. PLoS One 15:e0229434.
374. Ventura CV, Maia M, Ventura BV, Linden VV, Araujo EB, Ramos RC, Rocha MA, Carvalho MD, Belfort R, Jr., Ventura LO. 2016. Ophthalmological findings in infants with microcephaly and presumable intra-uterus Zika virus infection. Arq Bras Oftalmol 79:1-3.
375. Miner JJ, Sene A, Richner JM, Smith AM, Santeford A, Ban N, Weger-Lucarelli J, Manzella F, Ruckert C, Govero J, Noguchi KK, Ebel GD, Diamond MS, Apte RS. 2016. Zika Virus Infection in Mice Causes Panuveitis with Shedding of Virus in Tears. Cell Rep 16:3208-3218.
376. Zhao Z, Yang M, Azar SR, Soong L, Weaver SC, Sun J, Chen Y, Rossi SL, Cai J. 2017. Viral Retinopathy in Experimental Models of Zika Infection. Invest Ophthalmol Vis Sci 58:4355-4365.
377. Perez S, Tato R, Cabrera JJ, Lopez A, Robles O, Paz E, Coira A, Sanchez-Seco MP, Vazquez A, Carballo R, Quintas C, Pousa A. 2016. Confirmed case of Zika virus congenital infection, Spain, March 2016. Euro Surveill 21:30261.
378. Costello A, Dua T, Duran P, Gulmezoglu M, Oladapo OT, Perea W, Pires J, Ramon-Pardo P, Rollins N, Saxena S. 2016. Defining the syndrome associated with congenital Zika virus infection. Bull World Health Organ 94:406-406a.
379. Babokhov P, Sanyaolu AO, Oyibo WA, Fagbenro-Beyioku AF, Iriemenam NC. 2013. A current analysis of chemotherapy strategies for the treatment of human African trypanosomiasis. Pathog Glob Health 107:242-52.
380. Albulescu IC, Kovacikova K, Tas A, Snijder EJ, van Hemert MJ. 2017. Suramin inhibits Zika virus replication by interfering with virus attachment and release of infectious particles. Antiviral Res 143:230-236.
381. Chen Y, Maguire T, Hileman RE, Fromm JR, Esko JD, Linhardt RJ, Marks RM. 1997. Dengue virus infectivity depends on envelope protein binding to target cell heparan sulfate. Nat Med 3:866-71.
382. Kim SY, Zhao J, Liu X, Fraser K, Lin L, Zhang X, Zhang F, Dordick JS, Linhardt RJ. 2017. Interaction of Zika Virus Envelope Protein with Glycosaminoglycans. Biochemistry 56:1151-1162.
383. Rausch K, Hackett BA, Weinbren NL, Reeder SM, Sadovsky Y, Hunter CA, Schultz DC, Coyne CB, Cherry S. 2017. Screening Bioactives Reveals Nanchangmycin as a Broad Spectrum Antiviral Active against Zika Virus. Cell Rep 18:804-815.

384. Yuan S, Chan JF, den-Haan H, Chik KK, Zhang AJ, Chan CC, Poon VK, Yip CC, Mak WW, Zhu Z, Zou Z, Tee KM, Cai JP, Chan KH, de la Pena J, Perez-Sanchez H, Ceron-Carrasco JP, Yuen KY. 2017. Structure-based discovery of clinically approved drugs as Zika virus NS2B-NS3 protease inhibitors that potently inhibit Zika virus infection in vitro and in vivo. Antiviral Res 145:33-43.
385. McQuaid T, Savini C, Seyedkazemi S. 2015. Sofosbuvir, a Significant Paradigm Change in HCV Treatment. J Clin Transl Hepatol 3:27-35.
386. Bullard-Feibelman KM, Govero J, Zhu Z, Salazar V, Veselinovic M, Diamond MS, Geiss BJ. 2017. The FDA-approved drug sofosbuvir inhibits Zika virus infection. Antiviral Res 137:134-140.
387. Wichit S, Hamel R, Bernard E, Talignani L, Diop F, Ferraris P, Liegeois F, Ekchariyawat P, Luplertlop N, Surasombatpattana P, Thomas F, Merits A, Choumet V, Roques P, Yssel H, Briant L, Misse D. 2017. Imipramine Inhibits Chikungunya Virus Replication in Human Skin Fibroblasts through Interference with Intracellular Cholesterol Trafficking. Sci Rep 7:3145.
388. Taguwa S, Yeh MT, Rainbolt TK, Nayak A, Shao H, Gestwicki JE, Andino R, Frydman J. 2019. Zika Virus Dependence on Host Hsp70 Provides a Protective Strategy against Infection and Disease. Cell Rep 26:906-920.e3.
389. Abbink P, Larocca RA, De La Barrera RA, Bricault CA, Moseley ET, Boyd M, Kirilova M, Li Z, Ng'ang'a D, Nanayakkara O, Nityanandam R, Mercado NB, Borducchi EN, Agarwal A, Brinkman AL, Cabral C, Chandrashekar A, Giglio PB, Jetton D, Jimenez J, Lee BC, Mojta S, Molloy K, Shetty M, Neubauer GH, Stephenson KE, Peron JP, Zanotto PM, Misamore J, Finneyfrock B, et al. 2016. Protective efficacy of multiple vaccine platforms against Zika virus challenge in rhesus monkeys. Science 353:1129-32.
390. Abbink P, Stephenson KE, Barouch DH. 2018. Zika virus vaccines. Nat Rev Microbiol 16:594-600.
391. Bruscella P, Bottini S, Baudesson C, Pawlotsky JM, Feray C, Trabucchi M. 2017. Viruses and miRNAs: More Friends than Foes. Front Microbiol 8:824.
392. Plaisance-Bonstaff K, Renne R. 2011. Viral miRNAs. Methods Mol Biol 721:43-66.
393. Peng W, Henderson G, Inman M, BenMohamed L, Perng GC, Wechsler SL, Jones C. 2005. The locus encompassing the latency-associated transcript of herpes simplex virus type 1 interferes with and delays interferon expression in productively infected neuroblastoma cells and trigeminal Ganglia of acutely infected mice. J Virol 79:6162-71.
394. Umbach JL, Wang K, Tang S, Krause PR, Mont EK, Cohen JI, Cullen BR. 2010. Identification of viral microRNAs expressed in human sacral ganglia latently infected with herpes simplex virus 2. J Virol 84:1189-92.
395. Swaminathan G, Martin-Garcia J, Navas-Martin S. 2013. RNA viruses and microRNAs: challenging discoveries for the 21st century. Physiol Genomics 45:1035-48.
396. Scheel TK, Luna JM, Liniger M, Nishiuchi E, Rozen-Gagnon K, Shlomai A, Auray G, Gerber M, Fak J, Keller I, Bruggmann R, Darnell RB, Ruggli N, Rice CM. 2016. A Broad RNA Virus Survey Reveals Both miRNA Dependence and Functional Sequestration. Cell Host Microbe 19:409-23.
397. Machlin ES, Sarnow P, Sagan SM. 2011. Masking the 5' terminal nucleotides of the hepatitis C virus genome by an unconventional microRNA-target RNA complex. Proc Natl Acad Sci U S A 108:3193-8.

398. Schult P, Roth H, Adams RL, Mas C, Imbert L, Orlik C, Ruggieri A, Pyle AM, Lohmann V. 2018. microRNA-122 amplifies hepatitis C virus translation by shaping the structure of the internal ribosomal entry site. Nat Commun 9:2613.
399. Pleet ML, Mathiesen A, DeMarino C, Akpamagbo YA, Barclay RA, Schwab A, Iordanskiy S, Sampey GC, Lepene B, Nekhai S, Aman MJ, Kashanchi F. 2016. Ebola VP40 in Exosomes Can Cause Immune Cell Dysfunction. Front Microbiol 7:1765.
400. Van Duyne R, Guendel I, Klase Z, Narayanan A, Coley W, Jaworski E, Roman J, Popratiloff A, Mahieux R, Kehn-Hall K, Kashanchi F. 2012. Localization and sub-cellular shuttling of HTLV-1 tax with the miRNA machinery. PLoS One 7:e40662.
401. Harden ME, Munger K. 2017. Perturbation of DROSHA and DICER expression by human papillomavirus 16 oncoproteins. Virology 507:192-198.
402. Bennasser Y, Le SY, Yeung ML, Jeang KT. 2004. HIV-1 encoded candidate micro-RNAs and their cellular targets. Retrovirology 1:43.
403. Kaul D, Ahlawat A, Gupta SD. 2009. HIV-1 genome-encoded hiv1-mir-H1 impairs cellular responses to infection. Mol Cell Biochem 323:143-8.
404. Lamers SL, Fogel GB, McGrath MS. 2010. HIV-miR-H1 evolvability during HIV pathogenesis. Biosystems 101:88-96.
405. Pfeffer S, Sewer A, Lagos-Quintana M, Sheridan R, Sander C, Grasser FA, van Dyk LF, Ho CK, Shuman S, Chien M, Russo JJ, Ju J, Randall G, Lindenbach BD, Rice CM, Simon V, Ho DD, Zavolan M, Tuschl T. 2005. Identification of microRNAs of the herpesvirus family. Nat Methods 2:269-76.
406. Balasubramaniam M, Pandhare J, Dash C. 2018. Are microRNAs Important Players in HIV-1 Infection? An Update. Viruses 10:110.
407. Schopman NC, Willemsen M, Liu YP, Bradley T, van Kampen A, Baas F, Berkhout B, Haasnoot J. 2012. Deep sequencing of virus-infected cells reveals HIV-encoded small RNAs. Nucleic Acids Res 40:414-27.
408. Whisnant AW, Bogerd HP, Flores O, Ho P, Powers JG, Sharova N, Stevenson M, Chen CH, Cullen BR. 2013. In-depth analysis of the interaction of HIV-1 with cellular microRNA biogenesis and effector mechanisms. MBio 4:e000193.
409. Klase Z, Winograd R, Davis J, Carpio L, Hildreth R, Heydarian M, Fu S, McCaffrey T, Meiri E, Ayash-Rashkovsky M, Gilad S, Bentwich Z, Kashanchi F. 2009. HIV-1 TAR miRNA protects against apoptosis by altering cellular gene expression. Retrovirology 6:18.
410. Harwig A, Jongejan A, van Kampen AH, Berkhout B, Das AT. 2016. Tat-dependent production of an HIV-1 TAR-encoded miRNA-like small RNA. Nucleic Acids Res 44:4340-53.
411. Ouellet DL, Vigneault-Edwards J, Letourneau K, Gobeil LA, Plante I, Burnett JC, Rossi JJ, Provost P. 2013. Regulation of host gene expression by HIV-1 TAR microRNAs. Retrovirology 10:86.
412. Liu W, Wang X. 2019. Prediction of functional microRNA targets by integrative modeling of microRNA binding and target expression data. Genome Biol 20:18.
413. Huang J, Wang F, Argyris E, Chen K, Liang Z, Tian H, Huang W, Squires K, Verlinghieri G, Zhang H. 2007. Cellular microRNAs contribute to HIV-1 latency in resting primary CD4+ T lymphocytes. Nat Med 13:1241-7.

414. Wang X, Ye L, Hou W, Zhou Y, Wang YJ, Metzger DS, Ho WZ. 2009. Cellular microRNA expression correlates with susceptibility of monocytes/macrophages to HIV-1 infection. Blood 113:671-4.
415. Frattari G, Aagaard L, Denton PW. 2017. The role of miR-29a in HIV-1 replication and latency. J Virus Erad 3:185-191.
416. Nathans R, Chu CY, Serquina AK, Lu CC, Cao H, Rana TM. 2009. Cellular microRNA and P bodies modulate host-HIV-1 interactions. Mol Cell 34:696-709.
417. Sung TL, Rice AP. 2009. miR-198 inhibits HIV-1 gene expression and replication in monocytes and its mechanism of action appears to involve repression of cyclin T1. PLoS Pathog 5:e1000263.
418. Chiang K, Sung TL, Rice AP. 2012. Regulation of cyclin T1 and HIV-1 Replication by microRNAs in resting CD4+ T lymphocytes. J Virol 86:3244-52.
419. White MK, Johnson EM, Khalili K. 2009. Multiple roles for Puralpha in cellular and viral regulation. Cell Cycle 8:1-7.
420. Shen CJ, Jia YH, Tian RR, Ding M, Zhang C, Wang JH. 2012. Translation of Pur-alpha is targeted by cellular miRNAs to modulate the differentiation-dependent susceptibility of monocytes to HIV-1 infection. Faseb j 26:4755-64.
421. Swaminathan G, Rossi F, Sierra LJ, Gupta A, Navas-Martin S, Martin-Garcia J. 2012. A role for microRNA-155 modulation in the anti-HIV-1 effects of Toll-like receptor 3 stimulation in macrophages. PLoS Pathog 8:e1002937.
422. Lodge R, Ferreira Barbosa JA, Lombard-Vadnais F, Gilmore JC, Deshiere A, Gosselin A, Wiche Salinas TR, Bego MG, Power C, Routy JP, Ancuta P, Tremblay MJ, Cohen EA. 2017. Host MicroRNAs-221 and -222 Inhibit HIV-1 Entry in Macrophages by Targeting the CD4 Viral Receptor. Cell Rep 21:141-153.
423. Swaminathan G, Navas-Martin S, Martin-Garcia J. 2014. MicroRNAs and HIV-1 infection: antiviral activities and beyond. J Mol Biol 426:1178-97.
424. Allouch A, David A, Amie SM, Lahouassa H, Chartier L, Margottin-Goguet F, Barre-Sinoussi F, Kim B, Saez-Cirion A, Pancino G. 2013. p21-mediated RNR2 repression restricts HIV-1 replication in macrophages by inhibiting dNTP biosynthesis pathway. Proc Natl Acad Sci U S A 110:E3997-4006.
425. Hsu K, Seharaseyon J, Dong P, Bour S, Marban E. 2004. Mutual functional destruction of HIV-1 Vpu and host TASK-1 channel. Mol Cell 14:259-67.
426. Farberov L, Herzig E, Modai S, Isakov O, Hizi A, Shomron N. 2015. MicroRNA-mediated regulation of p21 and TASK1 cellular restriction factors enhances HIV-1 infection. J Cell Sci 128:1607-16.
427. Pinzone MR, Cacopardo B, Condorelli F, Di Rosa M, Nunnari G. 2013. Sirtuin-1 and HIV-1: an overview. Curr Drug Targets 14:648-52.
428. Zhang HS, Chen XY, Wu TC, Sang WW, Ruan Z. 2012. MiR-34a is involved in Tat-induced HIV-1 long terminal repeat (LTR) transactivation through the SIRT1/NFkappaB pathway. FEBS Lett 586:4203-7.
429. Zhang HS, Wu TC, Sang WW, Ruan Z. 2012. MiR-217 is involved in Tat-induced HIV-1 long terminal repeat (LTR) transactivation by down-regulation of SIRT1. Biochim Biophys Acta 1823:1017-23.
430. Triboulet R, Mari B, Lin YL, Chable-Bessia C, Bennasser Y, Lebrigand K, Cardinaud B, Maurin T, Barbry P, Baillat V, Reynes J, Corbeau P, Jeang KT, Benkirane M. 2007.

Suppression of microRNA-silencing pathway by HIV-1 during virus replication. Science 315:1579-82.
431. Chable-Bessia C, Meziane O, Latreille D, Triboulet R, Zamborlini A, Wagschal A, Jacquet JM, Reynes J, Levy Y, Saib A, Bennasser Y, Benkirane M. 2009. Suppression of HIV-1 replication by microRNA effectors. Retrovirology 6:26.
432. Alpuche-Lazcano SP, Scarborough RJ, Daniels SM, Rance E, Mouland AJ, Gatignol A. 2020. HIV-1 Gag interacts with Dicer and increases its binding to specific microRNAs. submitted.
433. Ponia SS, Arora S, Kumar B, Banerjea AC. 2013. Arginine rich short linear motif of HIV-1 regulatory proteins inhibits dicer dependent RNA interference. Retrovirology 10:97.
434. Bennasser Y, Le SY, Benkirane M, Jeang KT. 2005. Evidence that HIV-1 encodes an siRNA and a suppressor of RNA silencing. Immunity 22:607-19.
435. Bennasser Y, Jeang KT. 2006. HIV-1 Tat interaction with Dicer: requirement for RNA. Retrovirology 3:95.
436. Daniels SM, Sinck L, Ward NJ, Melendez-Pena CE, Scarborough RJ, Azar I, Rance E, Daher A, Pang KM, Rossi JJ, Gatignol A. 2015. HIV-1 RRE RNA acts as an RNA silencing suppressor by competing with TRBP-bound siRNAs. RNA Biol 12:123-35.
437. Fenard D, Houzet L, Bernard E, Tupin A, Brun S, Mougel M, Devaux C, Chazal N, Briant L. 2009. Uracil DNA Glycosylase 2 negatively regulates HIV-1 LTR transcription. Nucleic Acids Res 37:6008-18.
438. Schrofelbauer B, Yu Q, Zeitlin SG, Landau NR. 2005. Human immunodeficiency virus type 1 Vpr induces the degradation of the UNG and SMUG uracil-DNA glycosylases. J Virol 79:10978-87.
439. Casey Klockow L, Sharifi HJ, Wen X, Flagg M, Furuya AK, Nekorchuk M, de Noronha CM. 2013. The HIV-1 protein Vpr targets the endoribonuclease Dicer for proteasomal degradation to boost macrophage infection. Virology 444:191-202.
440. Gatignol A, Buckler C, Jeang KT. 1993. Relatedness of an RNA-binding motif in human immunodeficiency virus type 1 TAR RNA-binding protein TRBP to human P1/dsI kinase and Drosophila staufen. Mol Cell Biol 13:2193-202.
441. Battisti PL, Daher A, Bannwarth S, Voortman J, Peden KW, Hiscott J, Mouland AJ, Benarous R, Gatignol A. 2003. Additive activity between the trans-activation response RNA-binding protein, TRBP2, and cyclin T1 on HIV type 1 expression and viral production in murine cells. AIDS Res Hum Retroviruses 19:767-78.
442. Christensen HS, Daher A, Soye KJ, Frankel LB, Alexander MR, Laine S, Bannwarth S, Ong CL, Chung SW, Campbell SM, Purcell DF, Gatignol A. 2007. Small interfering RNAs against the TAR RNA binding protein, TRBP, a Dicer cofactor, inhibit human immunodeficiency virus type 1 long terminal repeat expression and viral production. J Virol 81:5121-31.
443. Kestler HW, 3rd, Ringler DJ, Mori K, Panicali DL, Sehgal PK, Daniel MD, Desrosiers RC. 1991. Importance of the nef gene for maintenance of high virus loads and for development of AIDS. Cell 65:651-62.
444. Pereira EA, daSilva LL. 2016. HIV-1 Nef: Taking Control of Protein Trafficking. Traffic 17:976-96.
445. Aqil M, Naqvi AR, Bano AS, Jameel S. 2013. The HIV-1 Nef protein binds argonaute-2 and functions as a viral suppressor of RNA interference. PLoS One 8:e74472.

446. Bouttier M, Saumet A, Peter M, Courgnaud V, Schmidt U, Cazevieille C, Bertrand E, Lecellier CH. 2012. Retroviral GAG proteins recruit AGO2 on viral RNAs without affecting RNA accumulation and translation. Nucleic Acids Res 40:775-86.
447. Eckenfelder A, Segeral E, Pinzon N, Ulveling D, Amadori C, Charpentier M, Nidelet S, Concordet JP, Zagury JF, Paillart JC, Berlioz-Torrent C, Seitz H, Emiliani S, Gallois-Montbrun S. 2017. Argonaute proteins regulate HIV-1 multiply spliced RNA and viral production in a Dicer independent manner. Nucleic Acids Res 45:4158-4173.
448. Ritchie C, Cylinder I, Platt EJ, Barklis E. 2015. Analysis of HIV-1 Gag protein interactions via biotin ligase tagging. J Virol 89:3988-4001.
449. Xu YP, Qiu Y, Zhang B, Chen G, Chen Q, Wang M, Mo F, Xu J, Wu J, Zhang RR, Cheng ML, Zhang NN, Lyu B, Zhu WL, Wu MH, Ye Q, Zhang D, Man JH, Li XF, Cui J, Xu Z, Hu B, Zhou X, Qin CF. 2019. Zika virus infection induces RNAi-mediated antiviral immunity in human neural progenitors and brain organoids. Cell Res 29:265-273.
450. Xie X, Shi PY. 2019. Anti-Zika virus RNAi in neural progenitor cells. Cell Res 29:261-262.
451. Azouz F, Arora K, Krause K, Nerurkar VR, Kumar M. 2019. Integrated MicroRNA and mRNA Profiling in Zika Virus-Infected Neurons. Viruses 11:162.
452. Pareek S, Roy S, Kumari B, Jain P, Banerjee A, Vrati S. 2014. MiR-155 induction in microglial cells suppresses Japanese encephalitis virus replication and negatively modulates innate immune responses. J Neuroinflammation 11:97.
453. Thounaojam MC, Kaushik DK, Kundu K, Basu A. 2014. MicroRNA-29b modulates Japanese encephalitis virus-induced microglia activation by targeting tumor necrosis factor alpha-induced protein 3. J Neurochem 129:143-54.
454. Zhang S, Li J, Li J, Yang Y, Kang X, Li Y, Wu X, Zhu Q, Zhou Y, Hu Y. 2018. Up-regulation of microRNA-203 in influenza A virus infection inhibits viral replication by targeting DR1. Sci Rep 8:6797.
455. Castro FL, Geddes VEV, Monteiro FLL, Goncalves R, Campanati L, Pezzuto P, Paquin-Proulx D, Schamber-Reis BL, Azevedo GS, Goncalves AL, Cunha DP, Moreira MEL, Vasconcelos ZFM, Chimeli L, Melo A, Tanuri A, Nixon DF, Ribeiro-Alves M, Aguiar RS. 2019. MicroRNAs 145 and 148a Are Upregulated During Congenital Zika Virus Infection. ASN Neuro 11:1759091419850983.
456. Dang JW, Tiwari SK, Qin Y, Rana TM. 2019. Genome-wide Integrative Analysis of Zika-Virus-Infected Neuronal Stem Cells Reveals Roles for MicroRNAs in Cell Cycle and Stemness. Cell Rep 27:3618-3628.e5.
457. Saldana MA, Etebari K, Hart CE, Widen SG, Wood TG, Thangamani S, Asgari S, Hughes GL. 2017. Zika virus alters the microRNA expression profile and elicits an RNAi response in Aedes aegypti mosquitoes. PLoS Negl Trop Dis 11:e0005760.
458. Kozak RA, Majer A, Biondi MJ, Medina SJ, Goneau LW, Sajesh BV, Slota JA, Zubach V, Severini A, Safronetz D, Hiebert SL, Beniac DR, Booth TF, Booth SA, Kobinger GP. 2017. MicroRNA and mRNA Dysregulation in Astrocytes Infected with Zika Virus. Viruses 9:297.
459. Ferreira RN, Holanda GM, Pinto Silva EV, Casseb SMM, Melo KFL, Carvalho CAM, Lima JA, Vasconcelos PFC, Cruz ACR. 2018. Zika Virus Alters the Expression Profile of microRNA-Related Genes in Liver, Lung, and Kidney Cell Lineages. Viral Immunol 31:583-588.

460. Scaturro P, Stukalov A, Haas DA, Cortese M, Draganova K, Plaszczyca A, Bartenschlager R, Gotz M, Pichlmair A. 2018. An orthogonal proteomic survey uncovers novel Zika virus host factors. Nature 561:253-257.

1.6 Rationale and hypothesis

Viruses use different mechanisms to infect cells. During the infection process, viruses disrupt key mechanisms and pathways within the cell to complete the replication cycle. RNAi is a crucial pathway for cells to regulate gene production. Different evidence accumulated during the years has demonstrated that viruses can impair or use the RNAi pathway to complete their replication cycle. Here, using two different viruses (HIV-1 and ZIKV), we hypothesized that the interplay between these viruses and RNAi, leads to abnormal modulation of miRNAs.

1.6.1 Objectives

The general objective of this thesis was to evaluate the relationships between the RNAi pathway and HIV-1 or ZIKV infection. This investigation started from observations that showed that HIV-1 did not impair RNAi activity and did not change the localization of proteins from the RNAi pathway. As a follow-up, we observed a co-localization and interaction between Gag and Dicer and analyzed their consequences on the miRNA profile described in chapter II (1). For a better understanding of the RNAi pathway, miRNAs and the changes produced during other viral infections, we decided to study ZIKV, a highly relevant emergent virus. Because of the lack of information in 2014-2015 about this virus, we evaluated the cytopathicity a Brazilian isolate of ZIKV compared to an early Asian strain in different cell types. Our observations are described in chapter III (2). Furthermore, we analyzed the transcriptome and miRNA profiles in primary mice neurons infected with the ZIKV. An integrative approach revealed an association between dysregulated miRNAs and mRNAs described in chapter IV.

Objective 1: Consequences of HIV-1 infection in the RNAi pathway.

Our first objective was to evaluate the interplay between HIV-1 and the RNAi pathway and consequently the production of miRNAs. Our priority was to discover novel miRNAs that disrupt or are disrupted upon HIV-1 infection. We also evaluated the components of RNAi and its association with viral proteins. Novel associations might mean disruption or modification of the RNAi pathway.

Objective 2: Evaluation of ZIKV cytopathicity between an imported Canadian isolate and a Brazilian one causative of CZVS.

We first assessed the cytopathicity of a ZIKV isolate from Bahia, Brazil and compared it with a Thai strain isolated from a Canadian patient. Bahia isolates have been related to the Brazilian outbreak and with cases of ZIKV congenital syndrome (3-5). We hypothesized that the Brazilian isolate is more cytopathic than the Thai one regardless of the cell type. The effects in different cells showed more accumulation of viral RNA, an increase in virus titer and more cell death.

Objective 3: Consequences of ZIKV infection on the transcriptome and miRNAome in infected primary murine neurons.

We carried on our investigation assessing the transcriptome and miRNA profile of primary infected murine neurons with the Brazilian ZIKV. We hypothesized that distinct mRNAs may change their concentration during the infection and some of those should be related to changes in

miRNAs. Thus, an integrative analysis of miRNAs and mRNAs was performed to discover the interrelationship between them and ZIKV.

1.6.2 References

1. Alpuche-Lazcano SP, Scarborough RJ, Daniels SM, Rance E, Mouland AJ, Gatignol A. 2020. HIV-1 Gag interacts with Dicer and increases its binding to specific microRNAs. submitted.
2. Alpuche-Lazcano SP, McCullogh CR, Del Corpo O, Rance E, Scarborough RJ, Mouland AJ, Sagan SM, Teixeira MM, Gatignol A. 2018. Higher Cytopathic Effects of a Zika Virus Brazilian Isolate from Bahia Compared to a Canadian-Imported Thai Strain. Viruses 10:53.
3. Camargos VN, Foureaux G, Medeiros DC, da Silveira VT, Queiroz-Junior CM, Matosinhos ALB, Figueiredo AFA, Sousa CDF, Moreira TP, Queiroz VF, Dias ACF, Santana KTO, Passos I, Real A, Silva LC, Mourao FAG, Wnuk NT, Oliveira MAP, Macari S, Silva T, Garlet GP, Jackman JA, Soriani FM, Moraes MFD, Mendes E, Ribeiro FM, Costa GMJ, Teixeira AL, Cho NJ, Oliveira ACP, et al. 2019. In-depth characterization of congenital Zika syndrome in immunocompetent mice: Antibody-dependent enhancement and an antiviral peptide therapy. EBioMedicine 44:516-529.
4. Sarno M, Aquino M, Pimentel K, Cabral R, Costa G, Bastos F, Brites C. 2017. Progressive lesions of central nervous system in microcephalic fetuses with suspected congenital Zika virus syndrome. Ultrasound Obstet Gynecol 50:717-722.
5. Campos GS, Bandeira AC, Sardi SI. 2015. Zika Virus Outbreak, Bahia, Brazil. Emerg Infect Dis 21:1885-6.

CHAPTER II

HIV-1 Gag interacts with Dicer and increases its binding to specific microRNAs.

This chapter is adapted from the following manuscript: Alpuche-Lazcano SP, Scarborough RJ, Daniels SM, Rance E, Mouland AJ and Gatignol A. 2020. “HIV-1 Gag interacts with Dicer and increases its binding to specific microRNAs” Manuscript submitted.

2.1 PREFACE

This chapter shows a new scope of the interplay between RNAi and HIV-1. Here, we demonstrated that miRNA expression is not impaired in HIV-1 expressing cells. Instead, we obtained novel evidence where a viral protein modifies miRNAs interactions without affecting the total concentration. This evidence contributes to the understanding of HIV-1 molecular behavior and provides new miRNA candidates that might modulate essential factors for the virus replication. Some of these miRNAs might be further investigated for future strategies towards the HIV-1 cure.

CONFLICT OF INTEREST:

The authors declare that they have no conflicts of interest with the contents of this article.

ACKNOWLEDGMENTS

We thank Dr. Eric Lécuyer (IRCM, Montreal, QC, Canada) for his valuable insight and review of the manuscript, James Saliba (LDI and McGill University) for helping in the qRT-PCR analysis. Anne Monette (LDI) for her insight in confocal microscopy analysis and Valerie Le Sage for PLA assays, José Héctor Gálvez López and François Lefebvre (Canadian Centre for Computational Genomics, Montréal) for the bioinformatic analysis. We are grateful to Dr. Witold Filipowicz for providing GST-Dicer and anti-Dicer 349 and Dr. Marvin Fritzler for providing the human 18033 serum. We are also thankful for expert technical assistance from Aïcha Daher and Meijuan Niu. The following reagent was obtained through the NIH AIDS Reagent Program, Division of AIDS, NIAID, NIH: Anti-HIV-1 SF2 p24 Polyclonal.

This study was supported by grants from the Canadian Institutes of Health Research (CIHR) (HBF-143163 and PJT-148704 to AG), (MOP-56974 to AJM) and by the Canadian HIV Cure Enterprise Team Grant HIG-133050 (to AG and AJM) from the CIHR in partnership with the Canadian Foundation for AIDS research (CANFAR) and the International AIDS Society (IAS).-SPAL was supported by a Doctoral fellowship from the Consejo Nacional de Ciencia y Tecnologia (CONACYT) (Mexico). RJS is a recipient of a post-doctoral fellowship from the Richard and Edith Strauss Canadian Foundation through the McGill University Department of Medicine.

2.2 ABSTRACT

Viruses interfere with the RNA interference (RNAi) pathway at different levels and modify the expression or function of micro RNAs (miRNAs). Human Dicer protein is part of the RNAi pathway, in which it catalyzes the processing of precursor miRNAs (pre-miRNAs) into mature miRNAs. In this study, we evaluated the extent to which human immunodeficiency virus type 1 (HIV-1) affects the RNAi pathway. We identified that RNAi remains functional in infected cells, but RNAi components can be modulated by HIV-1 proteins. We showed by immunofluorescence, immunoprecipitation (IP) and proximity ligation assay that HIV-1 $pr55^{Gag}$ (Gag) colocalizes and is found in complex with Dicer in an RNA-independent manner. Gag did not affect pre-miRNA processing by Dicer but RNA IP and sequencing analyses (RIP-seq) identified selected miRNAs that associated with Dicer exclusively in the presence of Gag. Gag enhanced the abundance of miR642a 3p, miR766 5p and 3p in Dicer IP analyses. This study identified that HIV-1 co-opts the RNAi machinery by enhancing recruitment and processing of miRNAs leading to possible changes in host cell function.

Keywords: Dicer/Gag/HIV-1/miRNAs/RNA interference.

2.3 INTRODUCTION

Post-transcriptional gene regulation in eukaryotes is mediated in part through microRNAs (miRNAs), which are 20-22 nucleotides (nt) double-stranded (ds)RNAs in a process called the RNA interference (RNAi) pathway (1, 2). In the nucleus, RNA polymerase II transcribes primary miRNAs, which are cleaved by Drosha and DGCR8, producing precursor miRNAs (pre-miRNAs) that will be exported to the cytoplasm by exportin-5 (2-5). In the cytoplasm, pre-miRNAs are processed by the Ribonuclease III-like Dicer bound to the TAR RNA-binding protein (TRBP) into ~22 nt mature miRNAs (2, 6). The TRBP-Dicer complex recruits Argonaute 2 (Ago2) to assemble the RNA-induced silencing complex (RISC) (6, 7). The RISC mediates the strand separation of the miRNA and the guide strand hybridizes to a target mRNA sequence to mediate its cleavage or translational repression. In cells, mRNA degradation is subsequently completed in cytoplasmic foci called GW or processing (P)-bodies (8, 9). Ago2 and GW182 are recruited to P-bodies and DDX6 (previously called Rck or p54) is an integral component of these structures (10, 11). To date, the miRNome size is of 2300 miRNAs that control approximately 60% of all protein-coding genes in humans (12, 13).

RNAi is highly dependent on the Dicer enzyme. Knocking out the dicer-1 (dcr-1) gene in mice leads to embryonic lethality (14), but conditional or targeted deletions identifies deficiency in multiple organ development including heart, brain, reproductive organs and hematopoiesis (15-17). Dcr1 knockout in mouse embryonic stem cells inactivates RNAi giving rise to cells defective in differentiation and DNA damage repair (18, 19). The interaction between Dicer and TRBP is required for correct pre-miRNA processing and occurs through the ATPase/Helicase Dicer domain and the C4 motif in the Medipal domain of TRBP (7, 20). In the absence of TRBP, Dicer loses its accuracy during pre-miRNAs cleavage and thus, the mRNA targets of each miRNA are

inaccurately targeted for degradation or translational arrest. (21). Dicer also binds directly to Ago2 to mediate post-transcriptional silencing either by RNA cleavage or by translational repression (22).

Viruses use and affect cellular pathways during their replication cycle. The human immunodeficiency virus type 1 (HIV-1) depends on highly regulated processes, which require several viral and cellular proteins (23). The structural proteins of HIV-1 are synthesized as a 55kDa viral precursor polyprotein $pr55^{Gag}$ also called Gag, which is sufficient to assemble viral-like particles, and Gag-Pol, which also contains HIV-1 enzymes, protease, reverse transcriptase and integrase. During the late phase of the HIV-1 replication cycle, the unspliced viral RNA harboring the Rev Response Element (RRE) is bound by the Rev protein and exported out of the nucleus. It will then be translated into Gag and Gag-Pol in the cytoplasm (24-26). During maturation Gag is cleaved by the HIV-1 protease into the matrix (MA), capsid (CA), nucleocapsid (NC) and P6 proteins along with spacer peptides SP1 and SP2 flanking NC (27).

A significant amount of crosstalk exists between HIV-1 and miRNAs, having both proviral and antiviral outcomes. miRNAs can directly bind HIV-1 RNA and affect its translation or they can target cellular factors that are essential for virus replication or latency (28, 29). Cellular miRNAs can also enhance viral production by targeting HIV-1 negative regulators and some HIV-1 derived miRNAs can modulate viral replication (30, 31). Furthermore, HIV-1 proteins and RNAs can interact with proteins from the RISC and consequently affect their function in the RNAi pathway (32-35). For instance, HIV-1 Tat has an RNA-dependent interaction with Dicer but does not interfere with RNAi function (32, 33). HIV-1 TAR and RRE structures act as RNAi suppressors by competing with miRNAs bound to TRBP, but this function is masked in the context of the entire HIV-1 (33). In contrast, the HIV-1 auxiliary protein, Vpr interacts with Dicer, which brings

the ubiquitin ligase E3 complex in proximity, inducing Dicer degradation via the proteasome and enhancing HIV-1 infection in macrophages (34). An HIV-1 Gag mass spectrometry analysis showed different cellular interacting proteins, including some of the RISC proteins (36, 37). Indeed, Gag recruits Ago2 through the RNA packaging signals to contribute to the retroviral replication cycle of HIV-1 and primate foamy virus 1 with no involvement in miRNAs translational repression (35). Similarly, Ago1 and Ago2 repress the production of multiply spliced HIV-1 transcripts in a Dicer independent fashion and enhance virus production (38).

To investigate how HIV-1 impacts the RNAi pathway, we analyzed RNAi function and the localization of the RISC proteins in HIV-1-producing cells. We characterized that RNAi remains functional in the presence of HIV-1. Using immunofluorescence (IF), immunoprecipitation (IP) and proximity ligation assays (PLA), we found that Gag colocalizes and interacts with human Dicer. RNA sequencing (RNA seq) of small RNAs after Dicer IP showed that the Dicer/Gag complex increases the binding of specific miRNAs compared to Dicer. Specifically, mature miR632a and miR766 have a stronger affinity to Dicer/Gag than to Dicer alone. These miRNAs target many genes from the HIV-1 interactome involved in cell function.

2.4 RESULTS

2.4.1 RNA interference remains functional in cells expressing HIV-1

Several studies suggested that RNAi is suppressed or altered by HIV-1 components but others indicated that it is not the case in HIV-1-replicating cells (33, 39-42). To solve this issue, we first evaluated whether the RNAi pathway is functional or partially altered in cells expressing HIV-1. To assess the function of the RNAi pathway, we first assayed a small interfering (si)RNA and an miRNA against EGFP, as we previously showed that they were functional in HeLa cells and sensitive to RNAi dysfunction in TRBP knock-out and knock-down cells (20). We found that the extent of EGFP decrease by siGFP or miGFP was similar whether the cells were transfected by the HIV-1 molecular clone pNL4-3 or a control plasmid (Fig 2.1A).

We next determined the functionality of RNAi on endogenous genes using a short hairpin (sh)RNA targeting GAPDH and evaluated the decrease of the protein whether it was expressed from a transfected plasmid (GAPDH-PL) or endogenously expressed (GAPDH) (Fig 2.1B). We simultaneously performed the assay in control (pcDNA3) or pNL4-3 transfected cells and observed that the expression of HIV-1 did not alter the extent of the decrease of GAPDH with the corresponding shGAPDH.

To further determine RNAi function of endogenous miRNAs, we used a reporter assay by transfecting a plasmid encoding EGFP with the complementary sequence to cellular miRNA Let7 inserted into its 3'UTR (33). We assessed the knock-down of EGFP by the endogenous miRNA Let7 in the presence and absence of transfected HIV-1 pNL4-3 (Fig 2.1C left) and in HIV-1 infected HeLa-based MAGI cells (Fig 2.1C right). Again, no difference was observed in the efficiency of EGFP knock-down by Let7 indicating that the endogenous RNAi is functional in HIV-1-replicating cells.

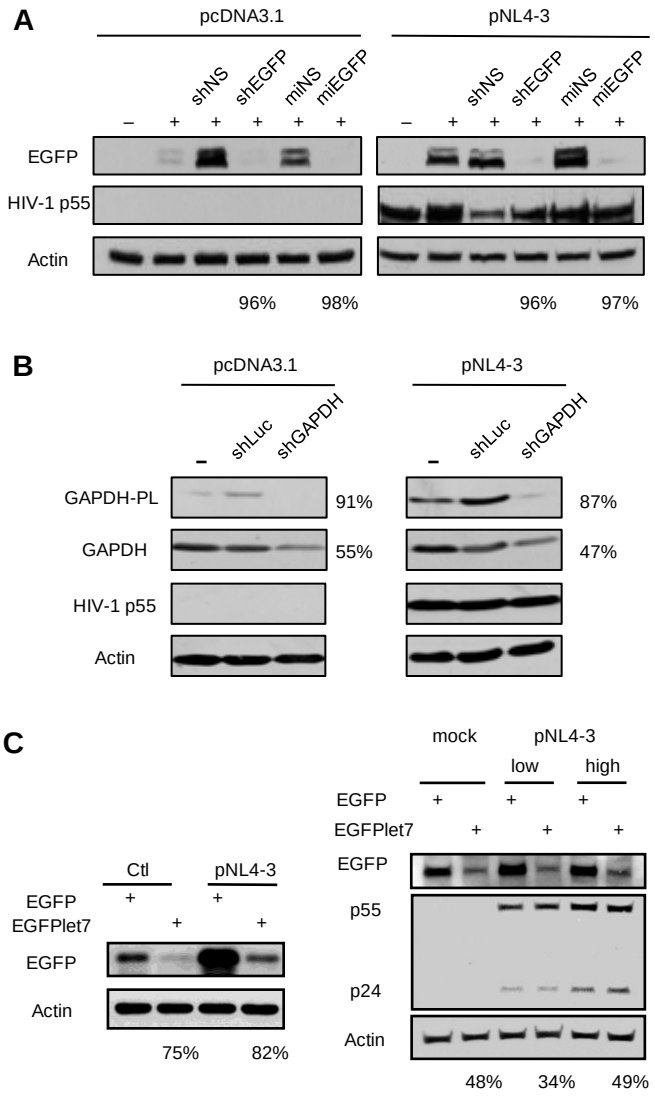

Figure 2. 1 RNAi is functional in HIV-expressing cells.

A) Inhibition of EGFP expression by siGFP and miGFP is functional in HIV-expressing cells. HeLa cells were cotransfected with 2µg pcDNA3 or pNL4-3, 1µg pEGFP-C1 and 4µg shRNA-NS or shRNA-EGFP or miRNA-NS or miRNA-EGFP as indicated. Effects on knock-down of EGFP by shRNA or miRNA, HIV-1 Gag and actin expression were observed by immunoblot and quantified by densitometry analysis. B) Inhibition of endogenous and transfected GAPDH expression by shGAPDH is functional in HIV-expressing cells. HeLa cells were cotransfected with 2µg pcDNA3 or pNL4-3, 1µg GAPDH-ProLabel (Clontech) and 1µg pSIREN-shRNA-LucIRR

(Clontech) or pSIREN-shRNA-GAPDHB (Clontech). Effects on knock-down of GAPDH by shRNA, HIV Gag and actin expression were observed by immunoblot and quantified by densitometry analysis. C) Inhibition of EGFP expression by Let7 is functional in HIV-expressing or replicating cells. (left) HeLa cells were cotransfected with 0.4µg of pEGFP or pEGFP-Let7, and 1µg of either pcDNA3 or pNL4-3 as indicated. (right) MAGI cells were not infected (lanes 1, 2), infected with pNL4-3 one million RT cpms (lanes 3, 4) or 2 million RT cpms (lanes 5, 6) of supernatant. They were cotransfected with pEGFP or pEGFP-Let7 24 h later. Effects on knock-down of EGFP by miRNA Let7 were observed by immunoblot and quantified by densitometry analysis.

2.4.2 HIV-1 expression in human cells does not change the localization of RISC proteins in the cytoplasm

Considering that the RNAi is functional in HIV-1-producing cells, we next questioned if differences could exist with only minor consequences on the function. We evaluated whether HIV-1 could change the cellular localization of RISC proteins. HeLa cells were transfected with the HIV-1 molecular clone pNL4-3 and images were generated 48 h post-transfection using antibodies targeting the HIV-1 CA protein (p24), the human autoimmune 18033 serum, that recognizes Ge1 and GW182 proteins and considered a P-body marker, as well as different RISC proteins (TRBP, Dicer, Ago2 and DDX6). We first compared the number of P-bodies in HIV-1-expressing cells using the 18033 serum in HIV-1-expressing and non-expressing cells (Fig 2.2). Although there were variations in the number and size of P-bodies in different cells, there were no apparent differences between p24 positive and negative cells. We then verified the presence of known P-body markers in HIV-1-expressing cells and found that DDX6 and Ago2 both co-localized to P-bodies in HIV-1-expressing and non-expressing cells (Fig 2.2A, B). The localization of TRBP and Dicer was also similar in cells staining positive and negative for HIV-1 p24 expression with a

preferential cytoplasmic distribution outside P-bodies. We also found a partial colocalization between Dicer and Gag observed by the cyan color in HIV-1-expressing cells (Fig 2.2C, D). We conclude that the cytoplasmic distribution of the RISC components TRBP, Dicer, Ago2 and DDX6 remains unchanged in HIV-1 expressing HeLa cells and that Gag partially colocalizes with Dicer as seen by the cyan color (Fig 2.2D right).

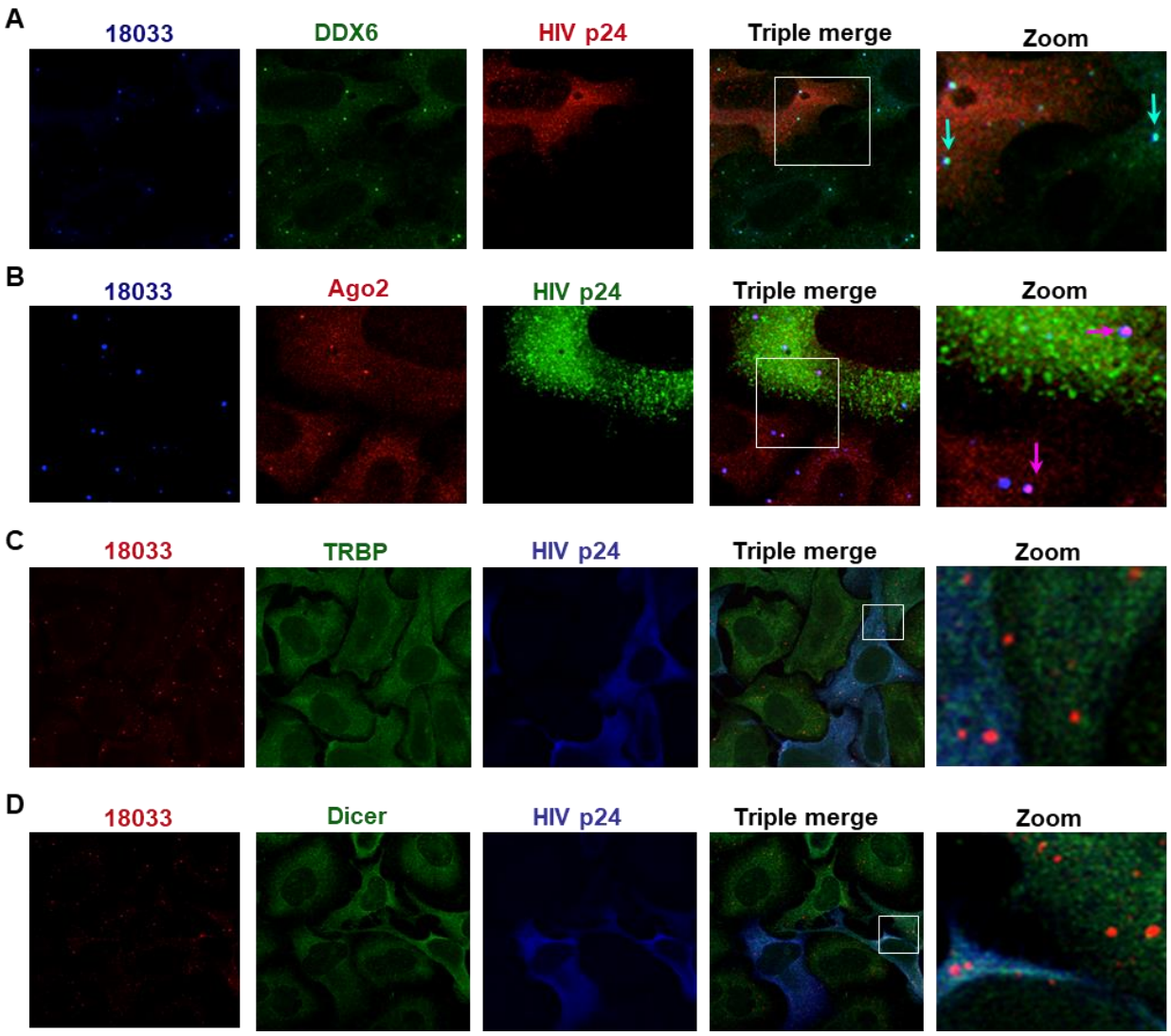

Figure 2. 2 HIV-1 expression in human cells does not change the localization of RISC proteins in the cytoplasm.

HeLa cells were transfected with 0.2 µg of HIV-1 pNL4-3. A) Cells were fixed and stained 48 h later with the P-body marker, human sera 18033, HIV-1 p24 antibody and antibodies against DDX6. B) Cells were fixed and stained 48 h later with the P-body marker, human sera 18033, HIV-1 p24 antibody and antibodies against Ago2. C) Cells were fixed and stained 48 h later with the P-body marker, human sera 18033, HIV-1 p24 antibody and antibodies against TRBP. D) Cells were fixed and stained 48 h later with the P-body marker, human sera 18033, HIV-1 p24 antibody and antibodies against Dicer. Digitally zoomed images of the merged channels are shown on the far right, with arrows highlighting colocalization between the P-body marker 18033 and DDX6 or Ago2, shown as cyan or purple dots, respectively.

2.4.3 Viral Gag colocalizes with Dicer in HIV-1 producing cells.

To further evaluate the colocalization between Dicer and HIV-1 Gag observed in Fig 2D, we performed IF analyses using a commercial Dicer antibody (Abcam) to confirm any possible co-localization with Gag, and we next performed microscopy analyses (Fig 2.3). We transfected cells with the HIV-1 molecular clone pNL4-3 and observed a colocalization between Dicer and Gag at 24 h using a p24 antibody (Fig 2.3, 24 h). A 36, 48 and 72 h time course post-transfection showed that Dicer/Gag colocalization is maintained throughout the experiment (Fig 2.3). Using Imaris and Fiji software packages, we counted a total of twenty co-transfected cells and calculated the Pearson coefficient for each time point, which shows a maximum colocalization at 48 h (Fig 2.3).

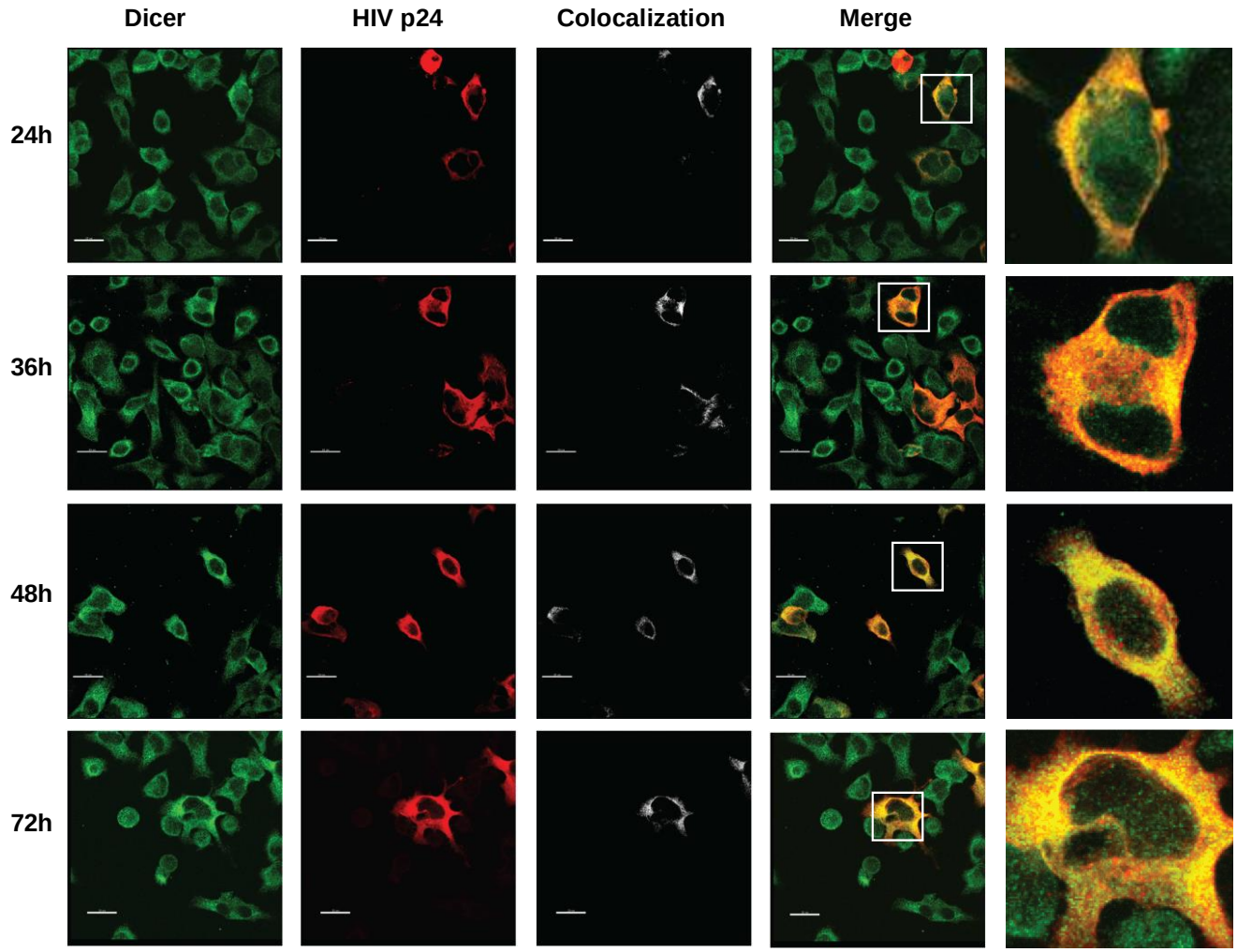

Figure 2. 3 Viral Gag protein colocalizes with Dicer in HIV-1 producing cells.

HeLa cells were transfected with 0.2 µg of HIV-1 pNL4-3. Cells were subjected to transfection time points of 24 h, 36 h, 48 h and 72 h. After each time point, cells were fixed and stained with mouse anti-Dicer 13D1 (green) and rabbit anti-p24 (red). The size scale is 20 µm and is shown in each picture on the bottom left. Digitally zoomed images of the merged channels are shown on the far right. A colocalization channel was built using Imaris software and is displayed in the third lane. The calculated Pearson coefficient for each time point is the average from 5 cells ± standard error of the mean (SEM) and is: 0.5420 ± 0.0532 at 24 h; 0.5320 ± 0.0258 at 36 h; 0.6380 ± 0.0290 at 48 h; 0.5560 ± 0.0660 at 72 h.

2.4.4 Dicer and HIV-1 Gag interaction is independent of RNA.

Because Dicer and Gag colocalize, we next wanted to determine if the two proteins interact in cells. We transfected human embryonic kidney (HEK) 293T cells with pNL4-3 and performed IP with a Dicer antibody. Our results show that endogenous Dicer pulls down Gag from HIV-1 transfected cells, which was not observed with an isotype antibody (Fig 2.4A, B). To further determine the specificity of this interaction, we co-transfected HEK 293T with GST-Dicer and Flag-Gag or GST-Dicer and the empty vector pFlag. Co-IP with a GST antibody showed a 55 kDa band corresponding to Flag-Gag (Fig 2.4C) even after RNases treatment (Fig 2.4D). We therefore conclude that Dicer and Gag interact in human cells and that this interaction occurs independently of RNA.

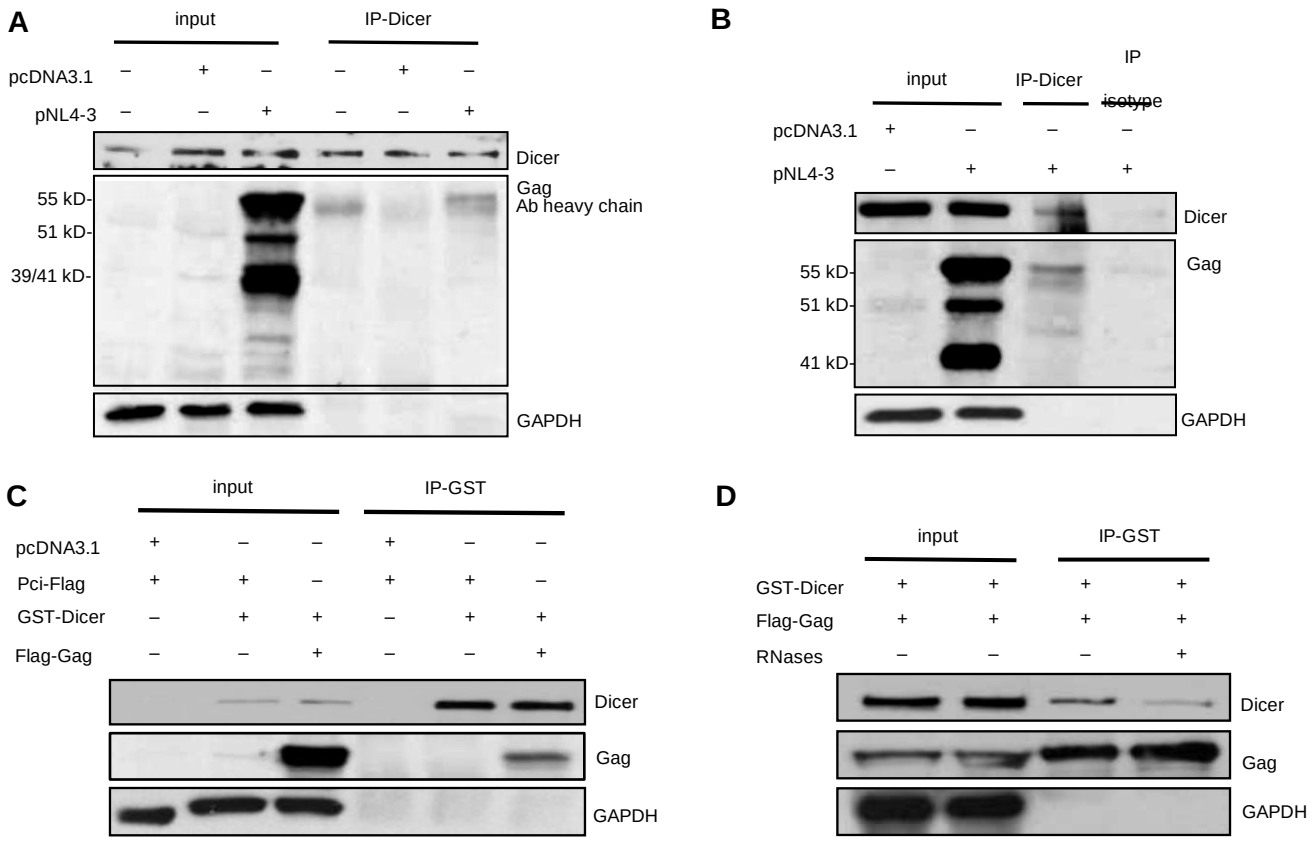

Figure 2. 4 Dicer and HIV-1 Gag interaction is independent of RNA.

A) Transfected HEK 293T cells with pNL4-3 or pcDNA 3.1 for 48 h were subjected to IP-Dicer. In the 3rd lane (input) is observed Dicer and Gag as part of the transfection as well as in the 6th lane (output) where Dicer is immunoprecipitated. B) In IP-Dicer of transfected cells with pNL4-3, it was added an isotype Ab to discard any possible non-specific interaction. The 2nd lane (input) and 3rd lane (IP-Dicer) have partial Gag cleaved products. C) HEK 293T cells were co-transfected for 48h with GST-Dicer/pFlag, GST-Dicer/Flag-Gag, or mock. The 3rd lane shows the co-expression of Dicer and Gag in the input. Lane 6 shows the interaction between Dicer and the Gag in an IP-GST. D) HEK 293T cells were co-transfected with GST-Dicer/Flag-Gag and RNases treatment was added during the IP (lane 4).

2.4.5 Dicer and Gag are in close proximity in both the nucleus and cytoplasm

To further characterize the interaction between Dicer and Gag, we also performed in situ PLA assays. PLA is a powerful assay that detects proximity between epitopes/ antibodies at a maximum distance of 40 nm (43). PLA was performed in HeLa cells transfected with Flag-Gag, pNL4-3 or mock after 24 h and we analyzed the results using the Imaris software. Dicer/Gag colocalization can be visualized as green dots in cells harboring pNL4-3 or Flag-Gag. Our results confirm the presence of Dicer/Gag complexes throughout the cells transfected with pNL4-3 ($n=100$, $p< 0.0001$) or Flag-Gag ($n=100$, $p< 0.0001$) (Fig 2.5A, B and C). We also evaluated Dicer/Gag (green dots) colocalization with DAPI using the intensity mean (Fig 2.5A, B, DAPI-colocalization) and observed that there are Dicer/Gag complexes localized into the cell nucleus ($n>10$, $P< 0.01$) (Fig 2.5D). Therefore, we determined that Dicer/Gag interaction occurs in HIV-1 and Gag expressing cells predominantly in the cytoplasm but also in the nucleus.

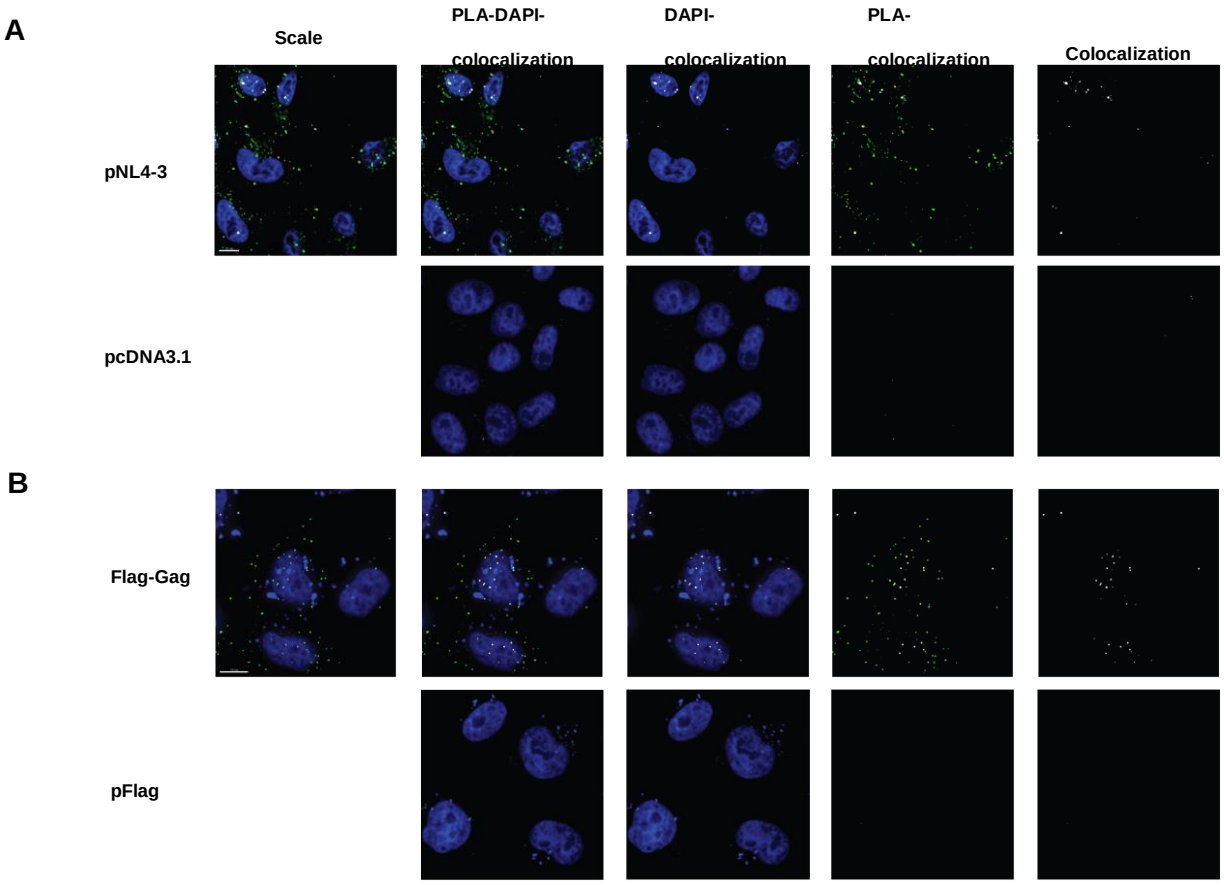
A
Scale
PLA-DAPI-colocalization
DAPI-colocalization
PLA-colocalization
Colocalization
pNL4-3
pcDNA3.1
B
Flag-Gag
pFlag

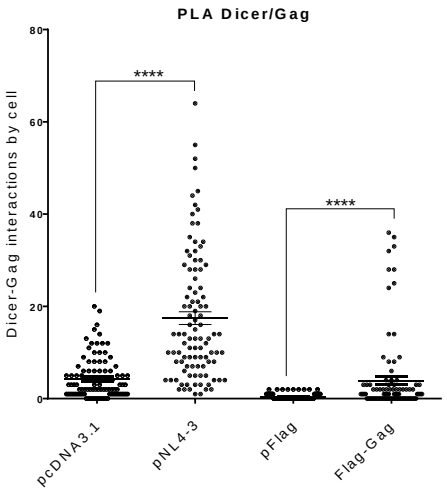
C
PLA Dicer/Gag
Dicer-Gag interactions by cell
80
60
40
20
0
****
****
pcDNA3.1
pNL4-3
pFlag
Flag-Gag

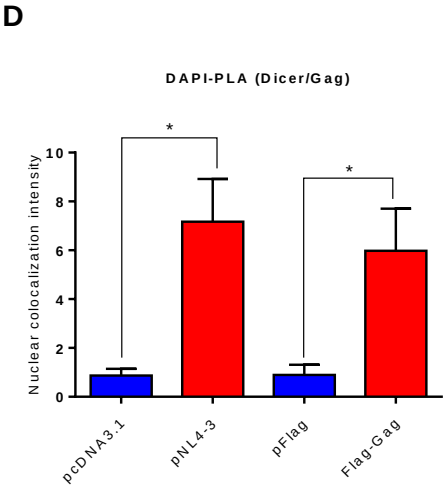
D
DAPI-PLA (Dicer/Gag)
Nuclear colocalization intensity
10
8
6
4
2
0
*
*
pcDNA3.1
pNL4-3
pFlag
Flag-Gag

Figure 2. 5 Dicer-Gag is localized in the cell nucleus and cytoplasm.

PLA determined localization and quantification of Dicer/Gag interaction. Images shown are representative of 100 cells. A) HeLa cells transfected with pNL4-3 or mock. B) HeLa cells transfected with Flag-Gag or mock. A, B from left to right: the first column corresponds to the size scale which is 10 µm and is shown in the bottom left. The second column shows the merged channel of PLA-DAPI-colocalization. The third column shows DAPI and PLA signal in the nucleus (DAPI-colocalization). The fourth column shows PLA and colocalization without DAPI. The fifth column shows only the colocalization. C) Scatter plot with T-test of Dicer/Gag PLA of transfected cells with pNL4-3 ($p< 0.0001$) or Flag-Gag ($p< 0.0001$). D) Comparison and T-test analysis of Dicer/Gag DAPI-PLA with pNL4-3 ($n>10$, $p=0.0273$) or Flag-Gag ($n>10$, $p=0.0101$)

2.4.6 Dicer catalytic activity on pre-miRNA Let7c and pre-miRNA29a is maintained in the presence of Gag

To determine if Gag interaction with Dicer affects its catalytic activity, we performed a Dicer cleavage assay with pre-miRNAs (44). We evaluated the cleavage of pre-miRLet7c as a control for the technique (44) and pre-miR29a because it targets a sequence in the Nef coding region of HIV-1 RNA (45). Our assay was carried out using α-^{32}P UTP to label the pre-miRNAs and IP with an antibody against GST tag that was attached or not to Dicer (Fig 2.6). The pre-miRLet7c and pre-miR29a (Fig 2.6 lanes 1,2,8,9) incubated with GST-Dicer gave rise to a 22 nt band corresponding to the mature miRLet7c (lanes 3, 6) and miR29a (lanes 10, 13). IP of GST-Dicer in the presence of Flag-Gag showed no changes in the production of mature miRLet7c and miR29a (lanes 4, 7, 11, 14) suggesting that the production of the mature miRLet7c and miR29a by Dicer is maintained in the presence of Gag.

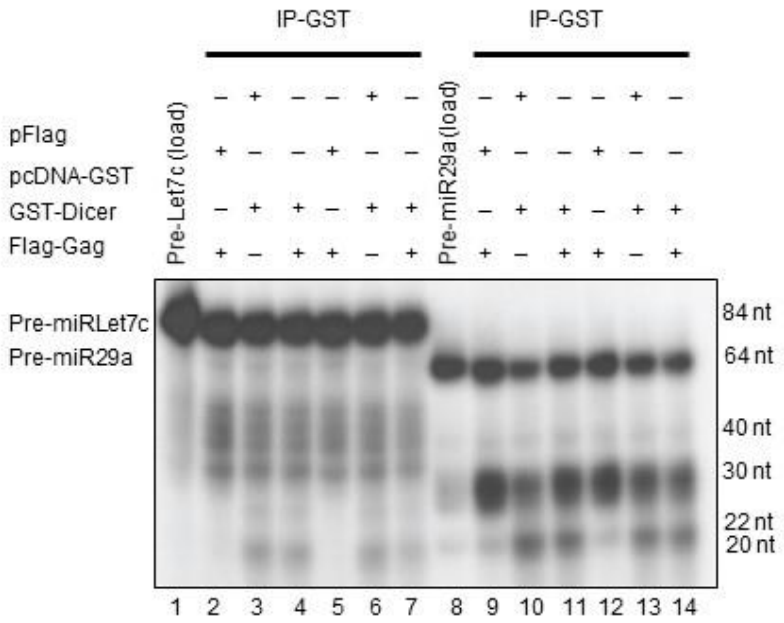

Figure 2. 6 Dicer catalytic activity on pre-miRNA Let 7c and pre-miRNA29a is maintained in the presence of Gag.

Pre-miRNA Let-7c and pre-miRNA 29a were evaluated in IP-GST-Dicer cleavage assay to determine changes in Dicer cleavage capacity in the presence of HIV-1 Gag. Lanes 1-7 show pre-miRNA Let 7c catalytic activity where lanes 5,6,7 are duplicates. Lanes 8-14 show Dicer activity in pre-miRNA 29a where lanes 12,13,14 are duplicates.

2.4.7 Dicer/Gag interaction results in higher binding of specific miRNAs.

Our results and previous studies point out that HIV-1 does not induce major dysfunctions of the RNAi pathway (33, 46). In contrast, subtle differences in the concentration of miRNAs exist in HIV-1-infected cells or patients and could be due to either their expression, stability or incorporation into the RISC (45, 47-51). Because Dicer and Gag interact in cells, we investigated if this binding could induce modifications in miRNAs loaded on Dicer. To test this hypothesis, we performed RNA IP followed by sequencing analysis (RIP-seq) experiments in cells expressing

Dicer (HA-Dicer) and/or Gag (Flag-Gag) followed by a pull down of small RNAs bound to Dicer in each condition.

RNA was extracted from HA-Dicer/pFlag, HA-Dicer/Flag-Gag or HA/Flag-Gag transfected cells and IP performed with HA antibody or isotype control. The small RNAs were isolated, sequenced and analyzed to determine the profile of non-coding (nc)RNAs bound to Dicer vs ncRNAs bound to Dicer in Gag expressing cells (Fig 2.7). The consensus peaksets of the replicates in the occupancy analysis produced 175 potential ncRNAs with HA-Dicer alone and 121 potential ncRNAs with HA-Dicer/Flag-Gag. 105 potential ncRNAs were specific to HA-Dicer and 51 specific to HA-Dicer/Flag-Gag. Thus, we found 70 likely ncRNAs present in both conditions (Fig 2.7A). RNA annotation demonstrated that 22 ncRNAs in both conditions were named as miRNAs (Fig 2.7B). Based on the miRNA database (52) we chose miRNAs that had an alignment score over 105 for further normalization (Fig 2.7C). After confirmation of the normalized sequences to the controls and total reads, we observed that more miRNAs were bound to Dicer/Gag than to Dicer alone. Specifically, miR642a, miR187, miR30a5p, miR766-3p, miR766-5p, miR3127-5p, miR339 were more present on Dicer/Gag, whereas miR455-5p, 3p and Let7i were slightly lower and miR4661, miR3127-3p, miR378a-3p, miR30a-3p were close to equal in both conditions (Fig 2.7C).

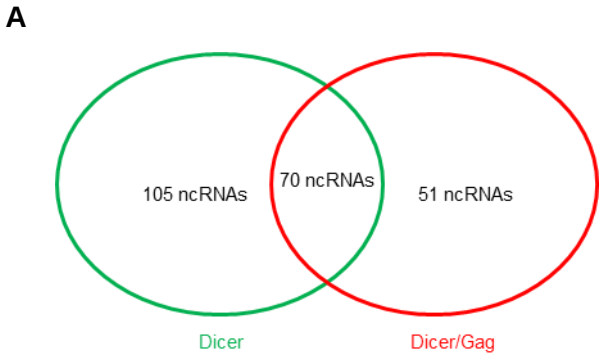

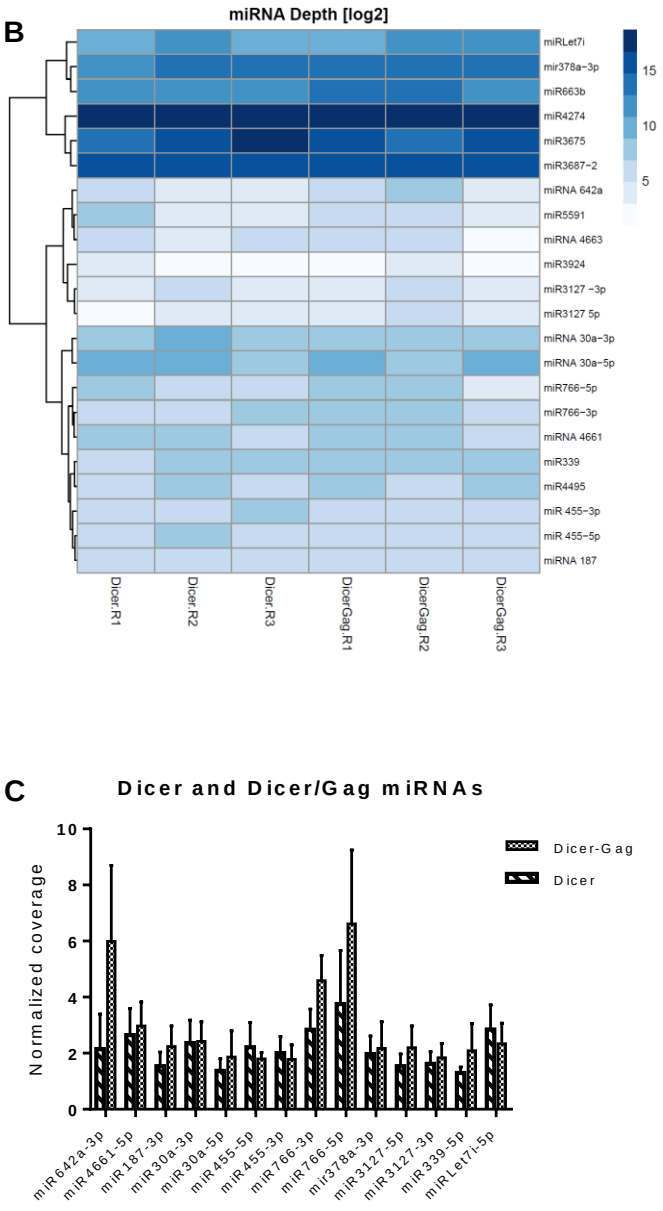

Figure 2. 7 Dicer/Gag interaction results in higher binding of specific miRNAs.

Transfected HEK 293T cells with HA-Dicer/pFlag or HA-Dicer/Flag-Gag were subjected to RIP-seq. Sequencing data were analyzed as described in materials and methods. A) Venn's diagram of ncRNAs found by group after the consensus peaksets. Dicer in green and Dicer/Gag in red outline. B) Heatmap of miRNAs in log2 scale was generated with R studio based on occupancy analysis data of miRNAs that were found in IP-HA-Dicer/pFlag and IP-HA-Dicer/Flag-Gag. R1, R2, R3 stand for replicates. C) After normalization of total reads, controls and alignment scores, 14 miRNAs were generated and graphed as Dicer or Dicer/Gag. Data represent the mean ± SEM.

2.4.8 Increased binding of miR642a 3p, miR766 5p and miR766 3p to Dicer when HIV-1 Gag is co-expressed.

To determine if the RIP-seq results reflect the mature miRNA concentration or a specific binding to Dicer or Dicer/Gag, we evaluated their amount in either the input or IP-HA by quantitative reverse transcription polymerase chain reaction (qRT-PCR), as performed previously (53), in transfected cells with HA-Dicer alone or HA-Dicer/Gag. We chose to further validate miR642a, miR766-3p and miR766-5p because they have the highest binding increase in the presence of Gag (Fig 2.7C). We also analyzed miR378a-3p because it is predicted to target HIV-1 Vpu (54) and miR30a5p because it is involved in the control of SAMHD1 expression, an HIV-1 restriction factor (55). The primers used for each miRNA are shown in Table 2.1. To accurately evaluate the binding of miRNAs to Dicer and Dicer/Gag, we first determined if their expression was changed in cells by the presence of Gag. We observed that the normalized expression of these miRNAs was similar with no significant difference ($p > 0.05$) (Fig 2.8 A-E). We next quantified their levels after IP with or without Gag. We observed that all 5 miRNAs were statistically more abundant after IP with Dicer and Gag compared to Dicer alone (Fig 2.8 F-J). Among those, miR642a 3p showed a 3-fold increase with a highly significant difference ($p<0.001$) (Fig 2.8 F). miR766 5p and miR766 3p showed a two-fold increased binding in the presence of Gag, which also corroborates the RNA-Seq data (Fig 2.8 G-H). Although miR30a 5p and miR378a 3p were also more abundant in the Dicer IP when Gag was present, the comparison with the expression level shows similarities suggesting that the small difference in binding could reflect the difference in expression (Fig 2.8 I-J compared to D-E). Overall, the highest retention in Dicer-Gag compared to Dicer alone was most significant for miR642a 3p, and significant for miR766 5p and miR766 3p.

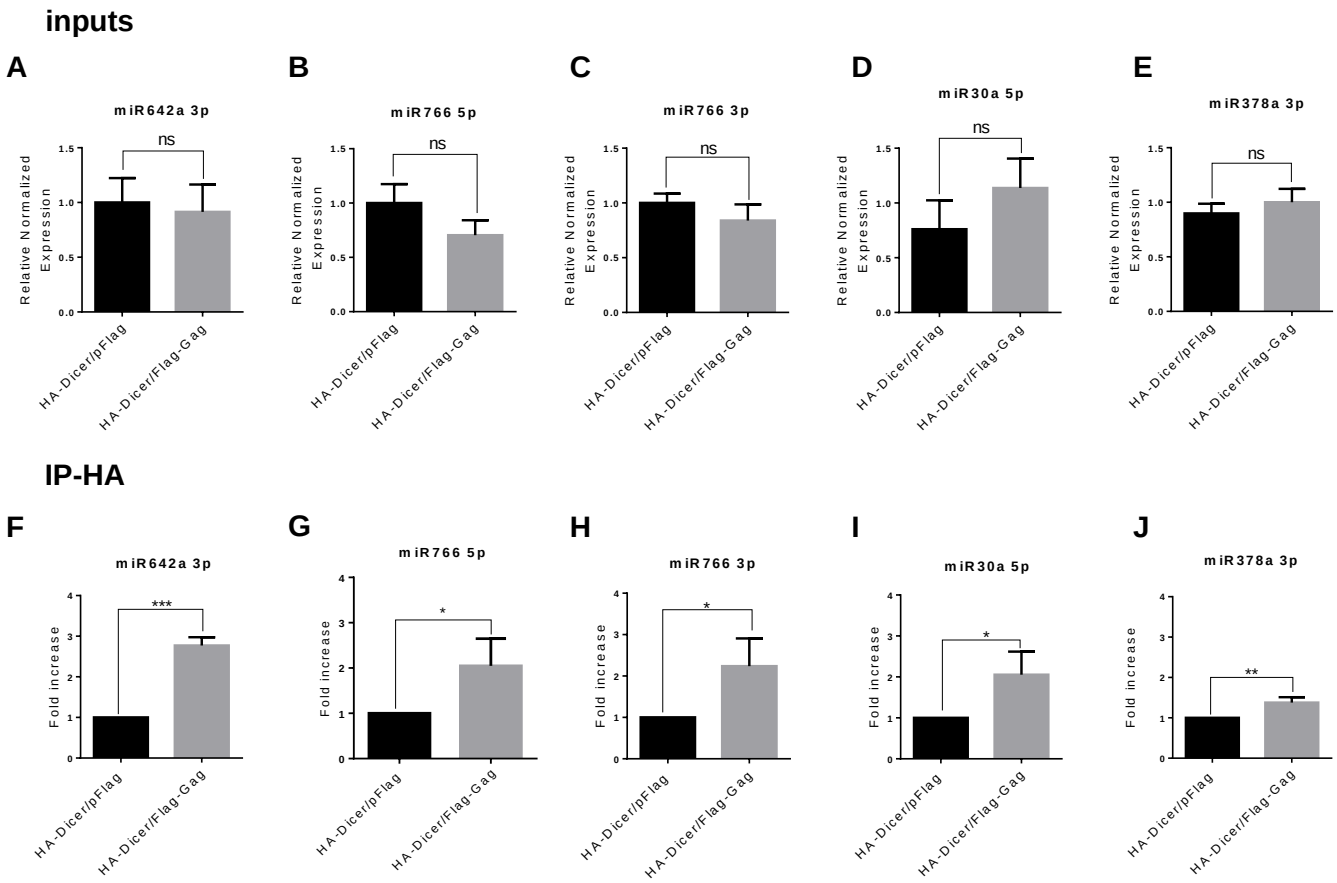

Figure 2. 8 Higher concentration of miR642a 3p, miR766 5p miR766 3p, miR30a 5p and miR 378a 3p into Dicer when HIV-1 Gag is bound.

The RIP-qRT-PCR validation process of miR642a 3p, miR766 5p miR766 3p, miR30a 5p and miR 378a 3p was carried out in IP-HA-Dicer/Flag or IP-HA-Dicer/Flag-Gag. A-E) MiRNA ΔΔCq values of the input for miR642a 3p, miR766 5p, miR766 3p, miR30a 5p, miR378a 3p. F-J) Fold increase of the output for miR642a 3p (p=0.0001), miR766 5p (p=0.0392), miR766 3p (p=0.0323), miR30a 5p (p=0.0254), miR378a 3p (p=0.0064). The generated p-values were calculated through T-test.

Table 2. 1 Primer sequences to evaluate selected miRNAs.

miRNA	Forward 5' to 3'	Reverse 5' to 3'
miR642a 3p	CGCAGAGACACATTTGGAGAG	CAGGTCCAGTTTTTTTTTTTTTTTGGTTCC
miR766 5p	GCAGAGGAGGAATTGGTGCT	CAGGTCCAGTTTTTTTTTTTTTTTAAGACC
miR766 3p	AGACTCCAGCCCCACAGC	CAGGTCCAGTTTTTTTTTTTTTTTGCTGAG
miRNA 30a 5p	CGCAGTGTAAACATCCTCGACT	CAGGTCCAGTTTTTTTTTTTTTTTCTTCC
miR-378a 3p	CGCAGACTGGACTTGGAGTCA	CAGGTCCAGTTTTTTTTTTTTTTTGCCTTC

2.4.9 HIV-1 interacting cellular genes are targeted by miR642a 3p, miR766 5p and miR766 3p

To evaluate the importance of a higher number of mature miRNA transcripts bound to Dicer/Gag compared to Dicer, we used miRDB database (56, 57) to predict the targets of miR642a 3p, miR766 5p and miR766 3p. MiRDB predicted 564 targets for miR642a 3p, 1043 for miR766 5p and 916 for miR766 3p. Due to the high number of targets, we further analyzed those with a prediction of 95% or more in the target score. We kept 14 targets for miR642a, 21 for miR766 5p and 15 for miR766 3p. Among those, we next looked for cellular genes coding for a protein with a known interaction with HIV-1 proteins in the NCBI gene database (interactome). In addition, for those that were not found in the HIV-1 interactome, we further analyzed them to determine if they have a relationship with HIV-1 replication. Within 14 predicted targets for miR642a 3p, we found AF4/FMR2 family member 4 (AFF4) that interacts with Tat (37, 58) and the nuclear receptor corepressor 1 (NCOR1) that interacts with Vif (37). The poly(A) binding protein nuclear 1 (PABPN1) is part of the Staufen complex together with Env, Gag, GagPol and Nef (59) and superoxide dismutase 2 (SOD2) is related to Env, Tat and Vif function (60-62) (Fig 2.9A). MiR766 5p targets phosphatidylinositol-4,5-bisphosphate 4-phosphatase 1 (PIP4P1) which is part of the

HIV-1 interactome (37). MiR766 5p also has predicted targets in genes coding for proteins involved in an HIV-1 related functions including EPH receptor B2 (EPBHB2), protein phosphatase 1 regulatory subunit 10 (PPPIR10), GTP cyclohydrolase 1 (GCH1), GLIS family zinc finger 2 (GLIS2), E2F transcription factor 3 (E2F3) and POU class 2 associating factor 1 (POU2AF1 OR OBF1) (Fig 2.9B). Finally, miR766 3p had 3 predicted targets that were related to HIV-1, glycerol-3-phosphate dehydrogenase 2 (GPD2), mitofusin 2 (MFN2) and BBX, HMG-box containing (BBX) (Fig 2.9C). Interestingly, miR766 3p targets the mRNA coding for 6 zinc finger proteins, which regulate gene transcription.

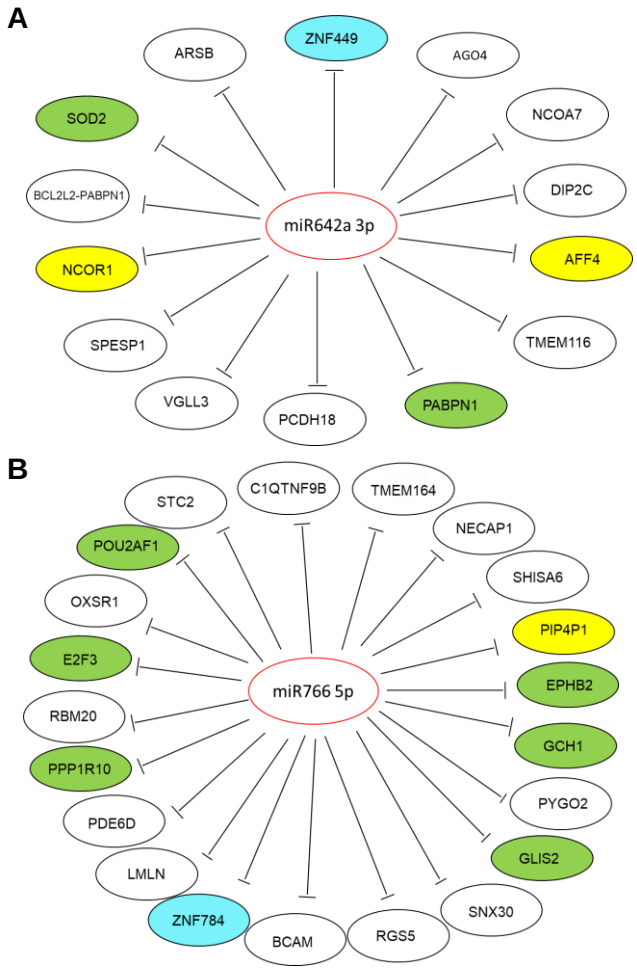

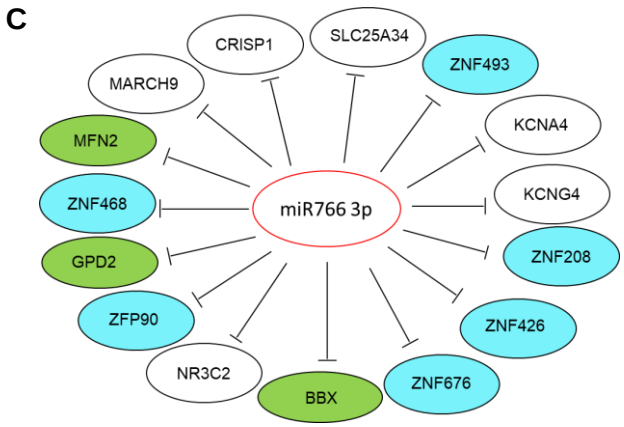

Figure 2. 9 MiRNA high ranked targetome.

Schematics of high ranked predicted targets for miRNAs with high affinity to Dicer/Gag. A) mir642a 3p shows 14 predicted targets with ≥ 95% target score where 2 (yellow) interact with HIV-1 components, 2 are related to HIV-1 (green) and 1 is part of zinc finger transcription factors (blue). B) miR 755 5 p shows 21 targets with a high score where 1 (yellow) interact with HIV-1 components, 6 are related to HIV-1 (green) and 1 is a zinc finger transcription factor (blue). C) 15 scored predicted targets were identified for miR755 3p where 6 belong to zinc finger transcription factors (blue) and 3 are related to HIV-1 (green).

2.5 DISCUSSION

In the context of HIV-1, the role of RNAi components on HIV-1 replication, the antiviral role of RNAi and the activity of RNAi suppressors have been conflicting (32, 33, 39-42, 63-66). In a previous study, we identified that RRE RNA can suppress RNAi, but this function is masked in HIV-1-producing cells (33). We have expanded this view by showing that RNAi mediated by exogenous or endogenous si-, sh- or miRNAs remains functional in HIV-1 replicating cells, whether they are transfected or infected by HIV-1 (Fig 2.1). Furthermore, we also found no

modification of the localization of the RISC proteins TRBP, Dicer, Ago2 and DDX6 in HIV-1-producing cells nor of their localization in or outside of P-bodies (Fig 2.2). These results are compatible with the use of siRNAs or shRNAs against the virus shown in several studies and applicable in a gene therapy setting (67-69).

Unexpectedly, IF images showed that Gag and Dicer partially co-localize in cells (Fig 2.2D). This observation prompted us to verify this colocalization using time points of HIV-1 production and interaction of these two proteins using IP assays and we characterized an RNA-independent interaction between Gag and Dicer (Fig 2.3, 2.4). Dicer's primary function is to generate miRNAs in the cytoplasm after its association with TRBP and this association mediates accurate pre-miRNAs processing (7, 20, 21, 70). Dicer then associates with an Argonaute protein to constitute the loading RISC that will mediate miRNA-mediated mRNA cleavage or translational repression (7, 22). Dicer also interacts with 5-lipoxygenase that modulates Dicer pre-miRNA cleavage (71) and with CLIMP-63 in the endoplasmic reticulum, which helps stabilize Dicer and maintain its function (72). The interaction with Gag may change these interactions and functions.

Furthermore, PLA assays showed a very close association between the two proteins, mainly in the cytoplasm but also in the nucleus (Fig 2.5). The nuclear localization may be related to Dicer's association with NUP153 in the nuclear periphery and may contribute to its transfer to the nucleus in some conditions (73). In addition, viral proteins can also affect Dicer such as I7 protease from vaccinia virus which degrades Dicer (74) or HIV-1 Vpr, which also targets Dicer for degradation (34). Dicer was identified in mass spectrometry screens using Gag as bait, but no further functional characterization was pursued (36, 37). Our interaction and co-localization studies on Dicer/Gag complement previous interactions identified with Dicer and suggest that it may impact its function.

Several modifications of miRNA expression have been described either in HIV-1-replicating cells or in patients in various conditions suggesting that HIV-1 replication impacts miRNA production, processing and/or function. Specific miRNAs can be involved in maintaining latency in primary lymphocytes (45), downregulated in HIV-1 multiply exposed uninfected persons (49), or differentially expressed in chronically infected patients or elite controllers vs. healthy donors (50). We therefore hypothesized that the interaction between Dicer and Gag might contribute to these changes. Because our results indicate that Gag does not modify Dicer processing activity on two pre-miRNA substrates pre-miRLet7c or pre-miR29a (Fig 2.6), we explored if the consequences of Dicer-Gag interactions may be in loading miRNAs to the Dicer/Gag complex.

Previous RIP-seq analyses for the identification of miRNAs were performed with Ago2 because the protein concentrates mature miRNAs but none were done with Dicer (38, 75, 76). From our readouts of Dicer RIP-seq experiments, we found that mature miRNAs were more prevalent than pre-miRNAs and we retained the most significant for further analysis (Fig 2.7). Overall, Gag mainly increases the binding of specific miRNAs. Through RIP-qRT-PCR we observed that miR642a 3p, miR766 5p and miR766 3p were more bound to Dicer/Gag than to Dicer (Fig 2.8 F, G, H) with no similar increase in the global expression (Fig 2.8 A, B, C). miR30a 5p and miR 378a were also increased in the Dicer/Gag IP, but this could reflect the observed increased expression (Fig 2.8 I, J compared to D, E). These findings open the possibility of miRNA regulation mediated by the HIV-1 Gag/Dicer interaction.

Most of the research done so far is focused on probing the up- or down-regulation of specific miRNAs. Here, we showed that miR642a 3p, miR766 5p and 3p do not have alterations of their production in HIV-1 expressing cells but might be functionally impaired or enhanced by Gag's interaction with Dicer during HIV-1 expression. The modification of miRNAs loaded onto Dicer

could be related to the fact that other proteins can bind miRNAs and affect Dicer. For instance, Lin28a, a cellular RNA binding protein interferes selectively with the processing of pre-miRLet7 by Dicer (77, 78). Lin28a shares homology into conserved motifs with NC in their Zn-knuckle domain that differ by only one proline, this domain recognizes GGAG and GGUG sequences (79). Interestingly GGAG and GGUG sequences are present in miR642a and miR766 and NC could recognize them through these motifs. Overall, two possible scenarios are possible: 1) the Dicer/Gag interaction could sequester miRNAs, which will make them unavailable for the function or 2) Gag/Dicer complex could overload Dicer with miRNAs to increase their activity.

MiRNAs bind to several gene transcripts and control their expression through the mRNA translational repression and degradation. To understand the importance of miR642a 3p, miR766 5p and 3p increased binding to Dicer/Gag, we analyzed their predicted mRNA targets using miRDB. Within the top-ranked targets of miR642a 3p, we found that two genes were coding for HIV-1 interactome components and two had related functions with HIV-1 (Fig 2.9A). In addition, seven targets for miR766 5p and three for miR766 3p were among the HIV-1 interactome or had functions regulated by or regulating HIV-1. Any of the predicted targets could change the replication kinetics of HIV-1. Among them, miR642a 3p targets AFF4, which is essential for transcriptional elongation (80, 81). A stronger decrease of AFF4 expression by miR642a 3p could affect the efficiency of viral transcription as observed with other inhibitors of AFF4 (80-82). Potentially, the retention or overload of miR642a-3p by Dicer and Gag interaction would be determinant for HIV-1 transactivation through AFF4 availability. In the same fashion, miR766 5p and miR766 3p retention or overload may affect distinct stages of HIV-1 life cycle depending on the potency to repress the distinct targets.

In summary, our results show that HIV-1 Gag binds to Dicer and increases its retention capacity to specific miRNAs. Changing the availability of these miRNAs will modify the targeted mRNAs and consequently cellular processes and HIV-1 replication.

2.6 MATERIALS AND METHODS

2.6.1 Plasmid constructions

The HIV-1 molecular clone pNL4-3 was previously described (83, 84). GST-Dicer was donated by Dr. W. Filipowicz (7). To construct pCMV2-HA-Dicer (HA-Dicer), GST-Dicer was used as a template. The whole gene was amplified by PCR using 5'AGCGGTCGACCATGAAAAGCCCTGCTTTG3' as a forward primer and 5'ATATAGCGGCCGCTCAGCTATTGGGAACCTG3' as a reverse primer. The PCR products cut by SalI and NotI were subcloned in frame into pCMV2-HA (Clontech) cut by the same enzymes. PCDNA3.1 was purchased from Invitrogen and Flag-Gag was previously described (85). ShRNA and miRNA against EGFP and EGFPlet7 were previously described (20, 33). GAPDH-ProLabel, pSIREN-shRNA-LucIRR and pSIREN-shRNA GAPDHHB were purchased from Clontech.

2.6.2 Cell culture and transfections

HeLa and HEK 293T cells were maintained in Dulbecco's modified Eagle's medium (DMEM) with high glucose (Hyclone) supplemented with 10% fetal bovine serum (FBS) (Hyclone), 50 U/ml Penicillin and 50 µg/ml Streptomycin (Thermo Fisher Scientific).

For Western blots, RNA extraction and IP, 2.6 x 10^6 cells were seeded in 10 cm culture plates 12 h prior to transfection whereas 5 x 10^4 cells were seeded for indirect IF assays. Cells were transfected with 9 µg of total DNA using polyethyleneimine (PEI) in a ratio of 3:1 total DNA. Co-transfections were performed using the same amount of DNA for each plasmid. Forty-eight h after transfection cells were fixed or lysed.

2.6.3 Immunoblotting

Cells were plated in 6-well plates 24 h prior to transfection by using TransIT-LT1 transfection reagent (Mirus) at a 1:3 DNA/TransIT ratio. Forty-eight h after transfection, cells were washed twice with phosphate-buffered saline (PBS) (Wisent) and lysed in cold lysis buffer (50mM Tris-HCl pH7.4, 150mM NaCl, 5mM EDTA pH8.0, 10% Glycerol, 1% Nonidet (N) P-40) with protease inhibitor cocktail (Roche). The lysates were then chilled on ice and centrifuged for 15 min at 13,000 rpm. Proteins were quantified in supernatants by Bradford assay (Bio-Rad). 40 µg of protein mixed with Laemmli sample buffer were incubated for 5 min at 95°C. Proteins were separated by sodium dodecyl sulfate polyacrylamide gel electrophoresis (SDS-PAGE) and wet-transferred overnight at 150 mA to Hybond nitrocellulose membranes (Bio-Rad) as described (33, 83). Membranes were blocked for 1 h with 5% milk in 0.1% Tris-buffered saline tween 20 (TBS-T) followed by three washes with TBS-T. The membranes were incubated overnight at 4°C with anti-EGFP (Santa Cruz) antibody at 1/1000 dilution, anti-GST (GE Healthcare) antibody at 1/1000 dilution, anti-GAPDH antibody (Clontech) at 1/2500 dilution, anti-actin (Chemicon) antibody at 1/10000 dilution, anti-Dicer 13D1 (Abcam) antibody at 1/1000 dilution or anti-HIV-1 p24 183-H12-5C at a 1/10000 dilution (33, 84, 86). After three washes with TBS-T, membranes were incubated with horseradish peroxidase-conjugated secondary antibodies (Amersham or Rockland

Immunochemicals) at a 1:5000 dilution. After three washes with TBS-T, the bands were visualized with Western Lightning Plus-ECL reagent (Perkin-Elmer).

2.6.4 Immunofluorescence and imaging

HeLa cells transfected with pNL4-3 were subjected to IF at different time points (24, 48, 36 and 72h). Cells were washed with PBS (Wisent) and fixed with paraformaldehyde 4% / sucrose 4% for 20 min. Cells were washed once with PBS and incubated with 0.1M glycine for 20 min. Cells were washed once again with PBS and permeabilized with 0.2% Triton X-100 for 5 min. After permeabilization, cells were washed with PBS and blocked with bovine serum albumin (BSA) 3%. The cells were incubated with the primary antibodies for 1 h at 37°C using mouse monoclonal anti-p24 (183-H12-5C) (83)at a 1/400 or 1/1000 dilution, rabbit anti-p24 (from Dr. L. Kleiman) at a 1/1000 dilution, rabbit anti-Rck/p54/DDX6 (Bethyl labs) at a 1/1000 dilution, mouse anti-Ago2 (Wako 4G8) at a 1/100 dilution, rabbit anti-TRBP673 (87) at a 1/250 dilution, rabbit anti-Dicer 349 (7) at a 1/250 dilution, mouse monoclonal anti-Dicer 13D1 antibody (Abcam) at a 1/500 dilution and human autoimmune serum 18033 (88) at a 1/5000 dilution. Cells were washed 5 times for 5 min with rinse solution (PBS, tween 20 0.3%, BSA 0.1 %) followed by incubation with Alexa 488, 546 or 647 (Invitrogen) secondary antibodies in total darkness for 1 h on a rocking platform and rinsed again in darkness 5 times for 5 min. This was followed by mounting the cell's coverslips with Immu-Mount (Thermo-electron corporation). Imaging was performed using a Zeiss Pascal confocal LSM with a 65X objective. Image acquisition was done using LSM AIM Pascal acquisition Software. Image processing and analysis were performed by Imaris software (version 8.4.1 Bitplane Andor) and Pearson's R-value (no threshold) was calculated using Fiji image processing package of image J (89). Imaging experiments were performed at least three times.

2.6.5 Co-immunoprecipitations (co-IPs)

HEK-293T cells were transfected with GST-Dicer, HA-Dicer and/or Flag-Gag. After 48 h cells were washed once with PBS and lysed with lysis buffer. Total proteins were quantified by Bradford assay (Bio-Rad). For each condition, 1000 µg of proteins were cleared with agarose protein A beads (Millipore) at 4°C for 1.5 h on a rocking platform. Samples were centrifuged at 8000 rpm for 1 min and the supernatant was collected. Two µl of either anti-GST (GE Healthcare) antibody, anti-HA (Sigma H6908) or anti-Dicer 13D1 were added to the supernatant and incubated with constant shaking at 4°C overnight. 30 µl of Dynabeads protein A (Thermo Fisher) or Sepharose protein G (Sigma) were added and further incubated with shaking for 3 h at room temperature. Samples were centrifuged and washed 3 times for 5 min with lysis buffer. All supernatants were discarded and 30 µl of Laemmli sample buffer was added and incubated for 5 min at 95°C. Samples were loaded for SDS-PAGE analysis and analyzed by immunoblotting.

2.6.6 In situ protein-protein interaction assay (DuoLink®)

HeLa cells were transfected with Flag-Gag or pNL4-3 for 48 h followed by in situ PLA using the DUOLINK II in Situ kit (Duolink) according to the manufacturer's protocol. PLA is based on two primary antibodies from different species that target the proteins of interest, followed by secondary antibodies that carry oligonucleotides. The oligonucleotides will then hybridize, ligate and amplify as rolling circles if they are at a maximum distance of 40 nm. Finally, the addition of labeled oligos will hybridize the amplicon giving a signal which is visualized as dots, where each dot represents one colocalization event. PLA conditions were previously described (90, 91). Mouse monoclonal anti-Dicer 13D1 antibody was used at a 1:500 dilution and rabbit polyclonal anti-HIV-1 SF2 p24 (National Institute of Health AIDS reagent program) was used at a 1/400 dilution. The antibodies

were detected using DuoLink II Detection Reagent Red, Duolink II PLA Probe Anti-Mouse MINUS, and DuoLink II PLA Probe anti-rabbit PLUS. Imaging acquisition was performed on a confocal laser scanning microscopy Leica DM1600B equipped with WaveFX spinning disk confocal head (Quorum Technologies). The analysis was done as described (91, 92) using Imaris software (version 8.4.1 Bitplane Andor). T-tests were carried out in Graph-Pad Prism V6.

2.6.7 Dicer catalytic activity in the presence of HIV-1 Gag

IPs or co-IPs were performed with Sepharose protein G beads. The evaluation of Dicer catalytic activity was performed according to (44). Briefly, to analyze Dicer catalytic activity we transcribed T7 promoter-pre-Let7c 5'GCTCCUUGGUUUGCTUGUUGGTTGTUCUGTTUUCTCCCUGGGTGTUUCTCTUUUC CUTUCUUCCTUCTUCCTCUUCCCGGUTGCCCTATAGTGTGAGTCGTATTA 3' and T7-promoter-pre-miR29a 5'ATAACCGATTTCAGATGGTGCTAGAAAATTATATTGACTCTGAACACCAAAAGAA ATCAGTCCCTATAGTGAGTCGTATTA3' using the T7 high yield RNA synthesis kit (BioLabs) with α^{32}P UTP (Perkin Elmer) at 800-6000 Ci/mmol ≥ 10mCi/mL. Pre-miRNAs were cleared from the DNA template using DNase I (QIAGEN) for 15 min and 20 µl of GLB II (Thermo Fisher Scientific) mixed and loaded on a denaturing 10% polyacrylamide gel (19:1)/ 7M urea. Pre-miRNAs were purified from the gel followed by heating and slow cooling for proper folding. 45,000 cpm of labeled RNA were incubated with Dicer IP complexes attached to Sepharose protein G beads for 1 h at 37°C. RNA was extracted and concentrated by TRizol and ethanol precipitated with Glycogen and yeast tRNA (Thermo Fisher Scientific). Products were subjected to denaturing PAGE and visualized in X-ray films after incubation at -80°C for 48 h.

2.6.8 RNA immunoprecipitation sequencing (RIP-seq) for small RNAs detection

RIP-seq experiments were based on (93) with modifications. Briefly, HEK 293T cells were transfected with HA-Dicer/pFlag, HA-Dicer/Flag-Gag, HA/Flag-Gag (negative control) and after 48 h cells were washed once with PBS and lysed with RNA extraction buffer [150 mM NaCl, 50 mM Tris, pH 7.5, 5 mM EDTA, 0.5% Nonidet P-40, 0.5% of RNaseOUT (Invitrogen), 0.2% of Vanadyl (NEB), 100mM of DTT (Invitrogen) protease and phosphatase inhibitor cocktail (Roche)]. 30 µl of agarose protein A beads (Millipore) washed with RNA extraction buffer were added to 1 mg of protein lysate for a 1.5 h incubation at 4°C on a rocking platform. After centrifugation, the supernatant was incubated with 50 µl of 1% BSA blocked Pierce anti-HA magnetic beads (Thermo Fisher) or 1% BSA blocked Pierce NHS-activated magnetic beads (Thermo Fisher) with mouse monoclonal IgG1 isotype antibody overnight at 4°C with agitation. Samples were centrifugated at 8000 rpm for 1 min and the supernatant was discarded. The beads were washed 3 times with RNA extraction buffer and separated in two samples for protein and RNA analysis. For protein analysis, 30 µl of Laemmli sample buffer was added to the beads and incubated 5 min at 95°C. RNA extraction was performed on the second sample of the beads after adding Trizol reagent and purified with miRNeasy mini kit (QIAGEN). RNase-free DNase set (QIAGEN) was loaded onto the miRNeasy columns to avoid any DNA contamination. Libraries were synthesized from 300 ng of total RNA with New England BioLabs NEBNext® Small RNA Library Prep Set for Illumina®. Libraries were run in Illumina HiSeq2500, SR50 sequencing lane at Genome Quebec, Canada.

2.6.9 Small non-coding RNA analysis

RNA bioinformatics was performed at the Canadian Centre for Computational Genomics (McGill University). Briefly, reads were trimmed from the 3' end to have a phred score of at least 30.

Illumina sequencing adapters were removed from the reads. Trimming and clipping were performed using Trimmomatic (94). The filtered reads were aligned to *Homo_sapiens* assembly GRCh37. Each readset was aligned using STAR (95). Then, all readset BAM files from the same sample were merged into a single global BAM file using Picard (96). All control samples (HA/Flag-Gag and the isotype antibody sample) were merged into a single file as well to use with the peak-calling software. Peaks were called using MACSv2 software (97). The mfold parameter used in the model building step was estimated from a peak enrichment diagnosis run. The estimated mfold lower bound was 5 and the estimated upper bound was 50. Nmodel and extsize were adjusted to better reflect the condition of the experiment. Peak call strategy was based in pooled samples (differences between the samples could be compensated during peak calling, producing a smaller but more robust set of peaks) and individual samples to increase the sensitivity.

All called peaksets files were annotated using annotatePeaks.pl from Homer (98). The information used to annotate the peaks came from the Ensembl 75 (99) which includes information on gene transcript as well as the position of 9,459 miRNA, 5,783 snRNAs, and 54,912 ncRNAs. To determine the statistical differences between peaks from both experimental conditions, a Differential Binding Analysis was carried out using the R package DiffBind (100). The purpose of this package is to find overlapping peaks between the samples, merging the peak sets and then counting reads in the overlapping intervals of the peak sets. The Differential binding analysis was carried on by an exploratory step to determine the potential occupancy of a specific locus (occupancy analysis). A heatmap of miRNAs was made using R package. Each annotated miRNA was confirmed manually using IGV (101) from the BAM files. Each annotated miRNA was looked up at miRBase (52) and only those that had more than 105 alignment score were further analyzed.

The chosen miRNAs from HA-Dicer/pFlag and HA-Dicer/Flag-Gag coverage were normalized to the total reads and the internal controls.

2.6.10 RIP qRT-PCR

For RIP qRT-PCR experiments, 2.6 x10^6 HEK-293T cells were co-transfected with a total of 9 µg of HA-Dicer and Flag-Gag. Cells were collected 48 h post-transfection, washed once with PBS and lysed with RNA extraction buffer for 15 min at 4℃. The lysate was centrifuged at 13,200 rpm at 4℃ for 15 min, the supernatant was kept, and 2.2 mg of protein was used for the IP and 1% of it was kept as the input. 30 µl of agarose protein A beads (Millipore) were taken and washed once with RNA extraction buffer. The protein A beads were diluted with 25 µl of RNA extraction buffer and were added to the 2.2 mg of protein with constant agitation for 1.5 h at 4℃. The sample was centrifuged at 8000 rpm for 1 min, and the supernatant was kept and incubated with 2 µl of the HA antibody or 1 µl of control rabbit serum overnight. 50 µl of pre-blocked Dynabeads protein A with 1 % BSA RNA extraction buffer was added to the beads and incubated with constant agitation for 3 h at 4℃. The supernatant was discarded, and the beads were washed 3 times with RNA extraction buffer (without RNaseOUT) for 5 min with a magnetic stand. After the final wash, 700 µl of TRIzol reagent and 140 µl of chloroform were added to the beads. To extract the RNA, miRNeasy mini kit was used according to the manufacturer's protocol. RNase-free DNase set was loaded onto the RNeasy columns to avoid any DNA contamination and due to the low abundance of RNAs in IPs we used isopropanol protocol described by QIAGEN for a better recovery of RNAs. The RNA was diluted from the columns in 60 µl of ultrapure distilled water. The IP RNA was concentrated by precipitating the RNA with 50 µl of ammonium acetate, 5 µl of Glycogen and 700 µl of ice-cold ethanol 100% at -80 ℃ for one hour followed by 30 min of centrifugation at 13,200 rpm. The pellet was washed once with ice-cold ethanol 70%, dried and diluted in 11.5

µl of ultrapure distilled water. 1.5 µl were used to measure the RNA in a Spectrophotometer/Fluorometer (DeNovix, DS-11 FX+). Our yield of RNA in IPs was HA-Dicer/pFlag (40-60 ng/µl) and HA-Dicer/Flag-Gag (50-75 ng/µl). 200 ng of total RNA was used to synthesized cDNA. The protocol to detect miRNA was based on (53, 102). Table 2 shows the primers to track specific miRNAs. Data Cq acquisition and analysis were performed using Bio-Rad CFX96 and CFX maestro software respectively. Actin was used to calculate $\Delta\Delta Cq$ and percent input method [100*2^ (Adjusted input - Ct (IP)] for the abundance of miRNAs in IPs. The calculated abundance was transformed from percentage to fold change and T-tests were carried out in Graph-Pad Prism V6.

2.6.10 Mir642a 3p, miR766 5p and miR766 3p predicted targets.

miR642a 3p, miR766 5p and miR766 3p target prediction was performed using miRDB (56, 57). Due to the high number of targets, we kept targets with a score higher than 95%. Predicted targets were analyzed in the NCBI gene database (103) to find any interaction with HIV-1 proteins. Genes not known to be related to HIV-1 replication had a second round of extensive research in PubMed journal database (104) to find any relationship with HIV-1.

2.7 REFERENCES

1. Bartel DP. 2009. MicroRNAs: target recognition and regulatory functions. Cell 136:215-33.
2. Kim VN. 2005. MicroRNA biogenesis: Coordinated cropping and dicing. Nature Reviews Molecular Cell Biology 6:376-385.
3. Abdelfattah AM, Park C, Choi MY. 2014. Update on non-canonical microRNAs. Biomol Concepts 5:275-87.
4. Lee Y, Kim M, Han J, Yeom KH, Lee S, Baek SH, Kim VN. 2004. MicroRNA genes are transcribed by RNA polymerase II. Embo j 23:4051-60.
5. Zeng Y, Yi R, Cullen BR. 2005. Recognition and cleavage of primary microRNA precursors by the nuclear processing enzyme Drosha. Embo j 24:138-48.
6. Daniels SM, Gatignol A. 2012. The multiple functions of TRBP, at the hub of cell responses to viruses, stress, and cancer. Microbiol Mol Biol Rev 76:652-66.
7. Haase AD, Jaskiewicz L, Zhang H, Laine S, Sack R, Gatignol A, Filipowicz W. 2005. TRBP, a regulator of cellular PKR and HIV-1 virus expression, interacts with Dicer and functions in RNA silencing. EMBO Rep 6:961-7.
8. Sheth U, Parker R. 2003. Decapping and decay of messenger RNA occur in cytoplasmic processing bodies. Science 300:805-8.
9. Moser JJ, Fritzler MJ. 2010. Cytoplasmic ribonucleoprotein (RNP) bodies and their relationship to GW/P bodies. Int J Biochem Cell Biol 42:828-43.
10. Pare JM, Tahbaz N, Lopez-Orozco J, LaPointe P, Lasko P, Hobman TC. 2009. Hsp90 regulates the function of argonaute 2 and its recruitment to stress granules and P-bodies. Mol Biol Cell 20:3273-84.
11. Luo Y, Na Z, Slavoff SA. 2018. P-Bodies: Composition, Properties, and Functions. Biochemistry 57:2424-2431.
12. Alles J, Fehlmann T, Fischer U, Backes C, Galata V, Minet M, Hart M, Abu-Halima M, Grasser FA, Lenhof HP, Keller A, Meese E. 2019. An estimate of the total number of true human miRNAs. Nucleic Acids Res 47:3353-3364.
13. Friedman RC, Farh KK, Burge CB, Bartel DP. 2009. Most mammalian mRNAs are conserved targets of microRNAs. Genome Res 19:92-105.
14. Bernstein E, Kim SY, Carmell MA, Murchison EP, Alcorn H, Li MZ, Mills AA, Elledge SJ, Anderson KV, Hannon GJ. 2003. Dicer is essential for mouse development. Nat Genet 35:215-7.
15. Zindy F, Lee Y, Kawauchi D, Ayrault O, Merzoug LB, Li Y, McKinnon PJ, Roussel MF. 2015. Dicer Is Required for Normal Cerebellar Development and to Restrain Medulloblastoma Formation. PLoS One 10:e0129642.
16. Otsuka M, Zheng M, Hayashi M, Lee JD, Yoshino O, Lin S, Han J. 2008. Impaired microRNA processing causes corpus luteum insufficiency and infertility in mice. J Clin Invest 118:1944-54.
17. Chen JF, Murchison EP, Tang R, Callis TE, Tatsuguchi M, Deng Z, Rojas M, Hammond SM, Schneider MD, Selzman CH, Meissner G, Patterson C, Hannon GJ, Wang DZ. 2008. Targeted deletion of Dicer in the heart leads to dilated cardiomyopathy and heart failure. Proc Natl Acad Sci U S A 105:2111-6.

18. Kanellopoulou C, Muljo SA, Kung AL, Ganesan S, Drapkin R, Jenuwein T, Livingston DM, Rajewsky K. 2005. Dicer-deficient mouse embryonic stem cells are defective in differentiation and centromeric silencing. Genes Dev 19:489-501.
19. Swahari V, Nakamura A, Baran-Gale J, Garcia I, Crowther AJ, Sons R, Gershon TR, Hammond S, Sethupathy P, Deshmukh M. 2016. Essential Function of Dicer in Resolving DNA Damage in the Rapidly Dividing Cells of the Developing and Malignant Cerebellum. Cell Rep 14:216-24.
20. Daniels SM, Melendez-Pena CE, Scarborough RJ, Daher A, Christensen HS, El Far M, Purcell DF, Laine S, Gatignol A. 2009. Characterization of the TRBP domain required for dicer interaction and function in RNA interference. BMC Mol Biol 10:38.
21. Kim Y, Yeo J, Lee JH, Cho J, Seo D, Kim JS, Kim VN. 2014. Deletion of human tarbp2 reveals cellular microRNA targets and cell-cycle function of TRBP. Cell Rep 9:1061-74.
22. Tahbaz N, Kolb FA, Zhang H, Jaronczyk K, Filipowicz W, Hobman TC. 2004. Characterization of the interactions between mammalian PAZ PIWI domain proteins and Dicer. EMBO Rep 5:189-94.
23. Brass AL, Dykxhoorn DM, Benita Y, Yan N, Engelman A, Xavier RJ, Lieberman J, Elledge SJ. 2008. Identification of host proteins required for HIV infection through a functional genomic screen. Science 319:921-6.
24. Malim MH, Hauber J, Le SY, Maizel JV, Cullen BR. 1989. The HIV-1 rev trans-activator acts through a structured target sequence to activate nuclear export of unspliced viral mRNA. Nature 338:254-7.
25. Daly TJ, Cook KS, Gray GS, Maione TE, Rusche JR. 1989. Specific binding of HIV-1 recombinant Rev protein to the Rev-responsive element in vitro. Nature 342:816-9.
26. Fornerod M, Ohno M, Yoshida M, Mattaj IW. 1997. CRM1 is an export receptor for leucine-rich nuclear export signals. Cell 90:1051-60.
27. Freed EO. 2015. HIV-1 assembly, release and maturation. Nat Rev Microbiol 13:484-96.
28. Rice AP. 2015. Roles of microRNAs and long-noncoding RNAs in human immunodeficiency virus replication. Wiley Interdiscip Rev RNA 6:661-70.
29. Sun B, Yang R, Mallardo M. 2016. Roles of microRNAs in HIV-1 Replication and Latency. Microrna 5:120-123.
30. Swaminathan G, Navas-Martin S, Martin-Garcia J. 2014. MicroRNAs and HIV-1 infection: antiviral activities and beyond. J Mol Biol 426:1178-97.
31. Zhang X, Ma X, Jing S, Zhang H, Zhang Y. 2018. Non-coding RNAs and retroviruses. Retrovirology 15:20.
32. Bennasser Y, Jeang KT. 2006. HIV-1 Tat interaction with Dicer: requirement for RNA. Retrovirology 3:95.
33. Daniels SM, Sinck L, Ward NJ, Melendez-Pena CE, Scarborough RJ, Azar I, Rance E, Daher A, Pang KM, Rossi JJ, Gatignol A. 2015. HIV-1 RRE RNA acts as an RNA silencing suppressor by competing with TRBP-bound siRNAs. RNA Biol 12:123-35.
34. Casey Klockow L, Sharifi HJ, Wen X, Flagg M, Furuya AK, Nekorchuk M, de Noronha CM. 2013. The HIV-1 protein Vpr targets the endoribonuclease Dicer for proteasomal degradation to boost macrophage infection. Virology 444:191-202.
35. Bouttier M, Saumet A, Peter M, Courgnaud V, Schmidt U, Cazevieille C, Bertrand E, Lecellier CH. 2012. Retroviral GAG proteins recruit AGO2 on viral RNAs without affecting RNA accumulation and translation. Nucleic Acids Res 40:775-86.

36. Engeland CE, Brown NP, Borner K, Schumann M, Krause E, Kaderali L, Muller GA, Krausslich HG. 2014. Proteome analysis of the HIV-1 Gag interactome. Virology 460-461:194-206.
37. Jager S, Cimermancic P, Gulbahce N, Johnson JR, McGovern KE, Clarke SC, Shales M, Mercenne G, Pache L, Li K, Hernandez H, Jang GM, Roth SL, Akiva E, Marlett J, Stephens M, D'Orso I, Fernandes J, Fahey M, Mahon C, O'Donoghue AJ, Todorovic A, Morris JH, Maltby DA, Alber T, Cagney G, Bushman FD, Young JA, Chanda SK, Sundquist WI, et al. 2011. Global landscape of HIV-human protein complexes. Nature 481:365-70.
38. Eckenfelder A, Segeral E, Pinzon N, Ulveling D, Amadori C, Charpentier M, Nidelet S, Concordet JP, Zagury JF, Paillart JC, Berlioz-Torrent C, Seitz H, Emiliani S, Gallois-Montbrun S. 2017. Argonaute proteins regulate HIV-1 multiply spliced RNA and viral production in a Dicer independent manner. Nucleic Acids Res 45:4158-4173.
39. Bennasser Y, Le SY, Benkirane M, Jeang KT. 2005. Evidence that HIV-1 encodes an siRNA and a suppressor of RNA silencing. Immunity 22:607-19.
40. Qian S, Zhong X, Yu L, Ding B, de Haan P, Boris-Lawrie K. 2009. HIV-1 Tat RNA silencing suppressor activity is conserved across kingdoms and counteracts translational repression of HIV-1. Proc Natl Acad Sci U S A 106:605-10.
41. Lin J, Cullen BR. 2007. Analysis of the interaction of primate retroviruses with the human RNA interference machinery. J Virol 81:12218-26.
42. Triboulet R, Mari B, Lin YL, Chable-Bessia C, Bennasser Y, Lebrigand K, Cardinaud B, Maurin T, Barbry P, Baillat V, Reynes J, Corbeau P, Jeang KT, Benkirane M. 2007. Suppression of microRNA-silencing pathway by HIV-1 during virus replication. Science 315:1579-82.
43. Soderberg O, Gullberg M, Jarvius M, Ridderstrale K, Leuchowius KJ, Jarvius J, Wester K, Hydbring P, Bahram F, Larsson LG, Landegren U. 2006. Direct observation of individual endogenous protein complexes in situ by proximity ligation. Nat Methods 3:995-1000.
44. Perron MP, Landry P, Plante I, Provost P. 2011. Detection of human Dicer and Argonaute 2 catalytic activity. Methods Mol Biol 725:121-41.
45. Ahluwalia JK, Khan SZ, Soni K, Rawat P, Gupta A, Hariharan M, Scaria V, Lalwani M, Pillai B, Mitra D, Brahmachari SK. 2008. Human cellular microRNA hsa-miR-29a interferes with viral nef protein expression and HIV-1 replication. Retrovirology 5:117.
46. Nathans R, Chu CY, Serquina AK, Lu CC, Cao H, Rana TM. 2009. Cellular microRNA and P bodies modulate host-HIV-1 interactions. Mol Cell 34:696-709.
47. Lodge R, Ferreira Barbosa JA, Lombard-Vadnais F, Gilmore JC, Deshiere A, Gosselin A, Wiche Salinas TR, Bego MG, Power C, Routy JP, Ancuta P, Tremblay MJ, Cohen EA. 2017. Host MicroRNAs-221 and -222 Inhibit HIV-1 Entry in Macrophages by Targeting the CD4 Viral Receptor. Cell Rep 21:141-153.
48. Ortega PAS, Saulle I, Mercurio V, Ibba SV, Lori EM, Fenizia C, Masetti M, Trabattoni D, Caputo SL, Vichi F, Mazzotta F, Clerici M, Biasin M. 2018. Interleukin 21 (IL-21)/microRNA-29 (miR-29) axis is associated with natural resistance to HIV-1 infection. Aids 32:2453-2461.
49. Bignami F, Pilotti E, Bertoncelli L, Ronzi P, Gulli M, Marmiroli N, Magnani G, Pinti M, Lopalco L, Mussini C, Ruotolo R, Galli M, Cossarizza A, Casoli C. 2012. Stable changes in CD4+ T lymphocyte miRNA expression after exposure to HIV-1. Blood 119:6259-67.

50. Reynoso R, Laufer N, Hackl M, Skalicky S, Monteforte R, Turk G, Carobene M, Quarleri J, Cahn P, Werner R, Stoiber H, Grillari-Voglauer R, Grillari J. 2014. MicroRNAs differentially present in the plasma of HIV elite controllers reduce HIV infection in vitro. Sci Rep 4:5915.
51. Balasubramaniam M, Pandhare J, Dash C. 2018. Are microRNAs Important Players in HIV-1 Infection? An Update. Viruses 10:110.
52. database mtm. 2018. miRBase. http://www.mirbase.org/. Accessed Sept, 2018.
53. Balcells I, Cirera S, Busk PK. 2011. Specific and sensitive quantitative RT-PCR of miRNAs with DNA primers. BMC Biotechnol 11:70.
54. Hariharan M, Scaria V, Pillai B, Brahmachari SK. 2005. Targets for human encoded microRNAs in HIV genes. Biochem Biophys Res Commun 337:1214-8.
55. Riess M, Fuchs NV, Idica A, Hamdorf M, Flory E, Pedersen IM, Konig R. 2017. Interferons Induce Expression of SAMHD1 in Monocytes through Down-regulation of miR-181a and miR-30a. J Biol Chem 292:264-277.
56. Wong N, Wang X. 2015. miRDB: an online resource for microRNA target prediction and functional annotations. Nucleic Acids Res 43:D146-52.
57. Liu W, Wang X. 2019. Prediction of functional microRNA targets by integrative modeling of microRNA binding and target expression data. Genome Biol 20:18.
58. Schulze-Gahmen U, Upton H, Birnberg A, Bao K, Chou S, Krogan NJ, Zhou Q, Alber T. 2013. The AFF4 scaffold binds human P-TEFb adjacent to HIV Tat. Elife 2:e00327.
59. Milev MP, Ravichandran M, Khan MF, Schriemer DC, Mouland AJ. 2012. Characterization of staufen1 ribonucleoproteins by mass spectrometry and biochemical analyses reveal the presence of diverse host proteins associated with human immunodeficiency virus type 1. Front Microbiol 3:367.
60. Kapasi AA, Coscia SA, Pandya MP, Singhal PC. 2004. Morphine modulates HIV-1 gp160-induced murine macrophage and human monocyte apoptosis by disparate ways. J Neuroimmunol 148:86-96.
61. Kim DY, Kwon E, Hartley PD, Crosby DC, Mann S, Krogan NJ, Gross JD. 2013. CBFbeta stabilizes HIV Vif to counteract APOBEC3 at the expense of RUNX1 target gene expression. Mol Cell 49:632-44.
62. Woollard SM, Bhargavan B, Yu F, Kanmogne GD. 2014. Differential effects of Tat proteins derived from HIV-1 subtypes B and recombinant CRF02_AG on human brain microvascular endothelial cells: implications for blood-brain barrier dysfunction. J Cereb Blood Flow Metab 34:1047-59.
63. Christensen HS, Daher A, Soye KJ, Frankel LB, Alexander MR, Laine S, Bannwarth S, Ong CL, Chung SW, Campbell SM, Purcell DF, Gatignol A. 2007. Small interfering RNAs against the TAR RNA binding protein, TRBP, a Dicer cofactor, inhibit human immunodeficiency virus type 1 long terminal repeat expression and viral production. J Virol 81:5121-31.
64. Maillard PV, van der Veen AG, Poirier EZ, Reis ESC. 2019. Slicing and dicing viruses: antiviral RNA interference in mammals. Embo j 38:e100941.
65. Petitjean O, Montavon T, Pfeffer S, . 2018. En avoir ou pas, l'interférence par l'ARN comme défense antivirale chez les mammifères. Virologie 22:251-260.
66. tenOever BR. 2017. Questioning antiviral RNAi in mammals. Nat Microbiol 2:17052.
67. Chung J, DiGiusto DL, Rossi JJ. 2013. Combinatorial RNA-based gene therapy for the treatment of HIV/AIDS. Expert Opin Biol Ther 13:437-45.

68. Herrera-Carrillo E, Berkhout B. 2015. Gene therapy strategies to block HIV-1 replication by RNA interference. Adv Exp Med Biol 848:71-95.
69. Goguen RP, Malard CM, Scarborough RJ, Gatignol A. 2019. Small RNAs to treat human immunodeficiency virus type 1 infection by gene therapy. Curr Opin Virol 38:10-20.
70. Wilson RC, Tambe A, Kidwell MA, Noland CL, Schneider CP, Doudna JA. 2015. Dicer-TRBP complex formation ensures accurate mammalian microRNA biogenesis. Mol Cell 57:397-407.
71. Dincbas-Renqvist V, Pepin G, Rakonjac M, Plante I, Ouellet DL, Hermansson A, Goulet I, Doucet J, Samuelsson B, Radmark O, Provost P. 2009. Human Dicer C-terminus functions as a 5-lipoxygenase binding domain. Biochim Biophys Acta 1789:99-108.
72. Pepin G, Perron MP, Provost P. 2012. Regulation of human Dicer by the resident ER membrane protein CLIMP-63. Nucleic Acids Res 40:11603-17.
73. Ando Y, Tomaru Y, Morinaga A, Burroughs AM, Kawaji H, Kubosaki A, Kimura R, Tagata M, Ino Y, Hirano H, Chiba J, Suzuki H, Carninci P, Hayashizaki Y. 2011. Nuclear pore complex protein mediated nuclear localization of dicer protein in human cells. PLoS One 6:e23385.
74. Chen JS, Li HC, Lin SI, Yang CH, Chien WY, Syu CL, Lo SY. 2015. Cleavage of Dicer protein by I7 protease during vaccinia virus infection. PLoS One 10:e0120390.
75. Tichy D, Pickl JMA, Benner A, Sultmann H. 2018. Experimental design and data analysis of Ago-RIP-Seq experiments for the identification of microRNA targets. Brief Bioinform 19:918-929.
76. Petri R, Jakobsson J. 2018. Identifying miRNA Targets Using AGO-RIPseq. Methods Mol Biol 1720:131-140.
77. Desjardins A, Bouvette J, Legault P. 2014. Stepwise assembly of multiple Lin28 proteins on the terminal loop of let-7 miRNA precursors. Nucleic Acids Res 42:4615-28.
78. Lightfoot HL, Bugaut A, Armisen J, Lehrbach NJ, Miska EA, Balasubramanian S. 2011. A LIN28-dependent structural change in pre-let-7g directly inhibits dicer processing. Biochemistry 50:7514-21.
79. Mayr F, Heinemann U. 2013. Mechanisms of Lin28-mediated miRNA and mRNA regulation--a structural and functional perspective. Int J Mol Sci 14:16532-53.
80. Chou S, Upton H, Bao K, Schulze-Gahmen U, Samelson AJ, He N, Nowak A, Lu H, Krogan NJ, Zhou Q, Alber T. 2013. HIV-1 Tat recruits transcription elongation factors dispersed along a flexible AFF4 scaffold. Proc Natl Acad Sci U S A 110:E123-31.
81. Li Z, Lu H, Zhou Q. 2016. A Minor Subset of Super Elongation Complexes Plays a Predominant Role in Reversing HIV-1 Latency. Mol Cell Biol 36:1194-205.
82. Krasnopolsky S, Marom L, Victor RA, Kuzmina A, Schwartz JC, Fujinaga K, Taube R. 2019. Fused in sarcoma silences HIV gene transcription and maintains viral latency through suppressing AFF4 gene activation. Retrovirology 16:16.
83. Battisti PL, Daher A, Bannwarth S, Voortman J, Peden KW, Hiscott J, Mouland AJ, Benarous R, Gatignol A. 2003. Additive activity between the trans-activation response RNA-binding protein, TRBP2, and cyclin T1 on HIV type 1 expression and viral production in murine cells. AIDS Res Hum Retroviruses 19:767-78.
84. Scarborough RJ, Levesque MV, Boudrias-Dalle E, Chute IC, Daniels SM, Ouellette RJ, Perreault JP, Gatignol A. 2014. A Conserved Target Site in HIV-1 Gag RNA is Accessible to Inhibition by Both an HDV Ribozyme and a Short Hairpin RNA. Mol Ther Nucleic Acids 3:e178.

85. Cinti A, Le Sage V, Ghanem M, Mouland AJ. 2016. HIV-1 Gag Blocks Selenite-Induced Stress Granule Assembly by Altering the mRNA Cap-Binding Complex. MBio 7:e00329.
86. Clerzius G, Shaw E, Daher A, Burugu S, Gelinas JF, Ear T, Sinck L, Routy JP, Mouland AJ, Patel RC, Gatignol A. 2013. The PKR activator, PACT, becomes a PKR inhibitor during HIV-1 replication. Retrovirology 10:96.
87. Duarte M, Graham K, Daher A, Battisti PL, Bannwarth S, Segeral E, Jeang KT, Gatignol A. 2000. Characterization of TRBP1 and TRBP2. Stable stem-loop structure at the 5' end of TRBP2 mRNA resembles HIV-1 TAR and is not found in its processed pseudogene. J Biomed Sci 7:494-506.
88. Moser JJ, Eystathioy T, Chan EK, Fritzler MJ. 2007. Markers of mRNA stabilization and degradation, and RNAi within astrocytoma GW bodies. J Neurosci Res 85:3619-31.
89. Schindelin J, Arganda-Carreras I, Frise E, Kaynig V, Longair M, Pietzsch T, Preibisch S, Rueden C, Saalfeld S, Schmid B, Tinevez JY, White DJ, Hartenstein V, Eliceiri K, Tomancak P, Cardona A. 2012. Fiji: an open-source platform for biological-image analysis. Nat Methods 9:676-82.
90. Le Sage V, Cinti A, McCarthy S, Amorim R, Rao S, Daino GL, Tramontano E, Branch DR, Mouland AJ. 2017. Ebola virus VP35 blocks stress granule assembly. Virology 502:73-83.
91. Rao S, Cinti A, Temzi A, Amorim R, You JC, Mouland AJ. 2018. HIV-1 NC-induced stress granule assembly and translation arrest are inhibited by the dsRNA binding protein Staufen1. Rna 24:219-236.
92. Valiente-Echeverria F, Melnychuk L, Vyboh K, Ajamian L, Gallouzi IE, Bernard N, Mouland AJ. 2014. eEF2 and Ras-GAP SH3 domain-binding protein (G3BP1) modulate stress granule assembly during HIV-1 infection. Nat Commun 5:4819.
93. Keene JD, Komisarow JM, Friedersdorf MB. 2006. RIP-Chip: the isolation and identification of mRNAs, microRNAs and protein components of ribonucleoprotein complexes from cell extracts. Nat Protoc 1:302-7.
94. Bolger AM, Lohse M, Usadel B. 2014. Trimmomatic: a flexible trimmer for Illumina sequence data. Bioinformatics 30:2114-20.
95. Dobin A, Davis CA, Schlesinger F, Drenkow J, Zaleski C, Jha S, Batut P, Chaisson M, Gingeras TR. 2013. STAR: ultrafast universal RNA-seq aligner. Bioinformatics 29:15-21.
96. passing Pb. 2019. Picard. https://broadinstitute.github.io/picard/. Accessed Mar, 2018.
97. Zhang Y, Liu T, Meyer CA, Eeckhoute J, Johnson DS, Bernstein BE, Nusbaum C, Myers RM, Brown M, Li W, Liu XS. 2008. Model-based analysis of ChIP-Seq (MACS). Genome Biol 9:R137.
98. Heinz S, Benner C, Spann N, Bertolino E, Lin YC, Laslo P, Cheng JX, Murre C, Singh H, Glass CK. 2010. Simple combinations of lineage-determining transcription factors prime cis-regulatory elements required for macrophage and B cell identities. Mol Cell 38:576-89.
99. GRCh37 E. 2019. Ensembl Release 75 data. https://grch37.ensembl.org/index.html. Accessed Mar, 2018.
100. Ross-Innes CS, Stark R, Teschendorff AE, Holmes KA, Ali HR, Dunning MJ, Brown GD, Gojis O, Ellis IO, Green AR, Ali S, Chin SF, Palmieri C, Caldas C, Carroll JS. 2012. Differential oestrogen receptor binding is associated with clinical outcome in breast cancer. Nature 481:389-93.

101. Viewer IG. 2018. IGV. https://software.broadinstitute.org/software/igv/home. Accessed Mar, 2018.
102. Alpuche-Lazcano SP, McCullogh CR, Del Corpo O, Rance E, Scarborough RJ, Mouland AJ, Sagan SM, Teixeira MM, Gatignol A. 2018. Higher Cytopathic Effects of a Zika Virus Brazilian Isolate from Bahia Compared to a Canadian-Imported Thai Strain. Viruses 10:53.
103. NCBI. 2019. Gene. https://www.ncbi.nlm.nih.gov/gene. Accessed Feb, 2019.
104. NCBI. 2019. PubMed. https://www.ncbi.nlm.nih.gov/pubmed/. Accessed Apr, 2019.

CHAPTER III

Higher Cytopathic Effects of a Zika Virus Brazilian Isolate from Bahia Compared to a Canadian-Imported Thai Strain

This chapter was adapted from the following published manuscript:

Alpuche-Lazcano SP, McCullogh CR, Del Corpo O, Rance E, Scarborough RJ, Mouland AJ, Sagan SM, Teixeira MM, Gatignol A. 2018. "Higher Cytopathic Effects of a Zika Virus Brazilian Isolate from Bahia Compared to a Canadian-Imported Thai Strain."

Viruses 2018. 10: 53

3.1 PREFACE

To understand the dysregulation of miRNAs and mRNAs caused by another virus type, we chose ZIKV. Because of the lack of information about this emergent virus, we investigated a Brazilian ZIKV isolate isolated during the outbreak in 2014-2015 and compared its cytopathicity with an early ZIKV strain. This comparison was necessary to further investigate the interplay between RNAi/mRNAs and ZIKV infection. The collected information in this paper allowed us to carry on our investigation with the Brazilian strain, which is still a current priority for virologists.

CONFLICTS OF INTEREST: The authors declare no conflict of interest.

ACKNOWLEDGMENTS

This work was supported by grants HBF-143163 and PJT-133050 from the Canadian Institutes of Health Research (to Anne Gatignol) and MOP-56974 (to Andrew J. Mouland). Sergio P. Alpuche-Lazcano is supported by a Doctoral fellowship from the Consejo Nacional de Ciencia y Tecnologia (CONACYT) (Mexico). Olivier Del Corpo was supported by a Canada Graduate scholarship (CGM). Robert J. Scarborough was a recipient of the Wares Family post-doctoral award and is a recipient of a post-doctoral fellowship from the Richard and Edith Strauss Canadian Foundation through the McGill University Faculty of Medicine. We thank Marc Fabian (Lady Davis Institute, LDI and McGill University, Montréal) for the neuroblastoma SH-SY5Y cell line, Maria Petropavlovskaya (LDI and McGill University, Montréal, QC, Canada) for the use of the Bio-Rad CFX96 and James Saliba (LDI and McGill University, Montréal, QC, Canada) for his technical help in the qRT-PCR set up and analysis.

3.2 ABSTRACT

Zika virus (ZIKV) is an emerging pathogen from the *Flaviviridae* family. It represents a significant threat to global health due to its neurological and fetal pathogenesis (including microcephaly and congenital malformations), and its rapid dissemination across Latin America in recent years. The virus has spread from Africa to Asia, the Pacific islands and the Americas with limited knowledge about the pathogenesis associated with infection in recent years. Herein, we compared the ability of the Canadian-imported Thai strain PLCal_ZV and the Brazilian isolate HS-2015-BA-01 from Bahia to produce infectious ZIKV particles and cytopathic effects in a cell proliferation assay. We also compared the intracellular viral RNA accumulation of the two strains by quantitative RT-PCR (reverse transcription polymerase chain reaction) analyses. Our observations show that HS-2015-BA-01 is more cytopathic than PLCal_ZV in proliferation assays in Vero, Human Embryonic Kidney HEK 293T and neuroblastoma SH-SY5Y cells. Quantitative RT-PCR shows that the level of viral RNA is higher with HS-2015-BA-01 than with PLCal_ZV in two cell lines, but similar in a neuroblastoma cell line. The two strains have 13 amino acids polymorphisms and we analyzed their predicted protein secondary structure. The increased cytopathicity and RNA accumulation of the Brazilian ZIKV isolate compared to the Thai isolate could contribute to the increased pathogenicity observed during the Brazilian epidemic.

Keywords: Zika virus; predicted protein structure; qRT-PCR; cytopathicity; viral titer

3.3 INTRODUCTION

Zika virus (ZIKV) is an emerging arthropod-borne flavivirus transmitted mainly through *Aedes sp.* mosquito bites. In addition, sexual and maternofetal transmissions have also been documented in recent outbreaks (1). ZIKV was first identified as a filterable transmissible agent from the serum of a febrile sentinel rhesus macaque in the Ziika forest (later renamed Zika) of Uganda in 1947 (2). The first human cases of ZIKV infection were reported in 1952, and since then it has slowly spread through Southeast Asia with the first Asian lineage isolate, P6-740, identified in Malaysia in 1966 (3, 4). A large outbreak occurred in 2007 on several islands in the State of Yap, Micronesia, in the Western Pacific, followed by epidemics in French Polynesia, Easter Island, the Cook Islands and New Caledonia in 2013–2015 (5, 6). It reached South America in 2014 resulting in a large outbreak across Brazil in 2015 where ZIKV RNA was detected in people with exanthematous illness and arthralgia (7, 8).

In the early epidemics, ZIKV infection was considered a mild disease. Symptoms included a rash, conjunctivitis and mild fever while many infected people had no symptoms (9, 10). By December 2015, the Minister of Health in Brazil revealed increased incidence of neurological complications like Guillain-Barré syndrome (GBS), and a large increase in the number of microcephaly cases in babies born from infected mothers, specifically in areas of high endemic ZIKV circulation (11-14). A retrospective analysis in French Polynesia showed that ZIKV-related GBS and microcephaly also occurred, while there were no or few such reports from the epidemic in Asia (15-17). ZIKV increased pathogenicity and rapid ability to spread in tropical areas of the Americas raise questions regarding whether there is a genetic basis for these changes between the early Asian ZIKV strains and the contemporary Brazilian isolates (17, 18).

ZIKV is a flavivirus from the *Flaviviridae* family with similar genome organization to other members such as Dengue, West Nile, yellow fever and Japanese encephalitis viruses (3). The ZIKV genome is a monocistronic 11 kb positive-sense RNA, which is translated into a single polyprotein. The polyprotein is cleaved by host and viral proteases into three structural proteins (C, prM, E) and seven non-structural proteins (NS1, NS2A, NS2B, NS3, NS4A, NS4B and NS5) (19, 20). The virion size is approximately 50 nm, in which the capsid is surrounded by the structural membrane protein prM/M and the viral envelope E (19). Compared to other flaviviruses the virion is thermostable and has a more compact surface, which may contribute to its stability in body fluids, such as saliva, urine or semen (21). Dermal fibroblasts, epidermal keratinocytes and dendritic cells are the first cells to be infected by ZIKV after a mosquito bite (22). ZIKV also infects human microglia, neural progenitors and astrocytes, as well as human fetal endothelial cells through interactions with the Gas6 ligand and its cellular receptor, AXL. Receptor interactions trigger clathrin-mediated endocytosis and ZIKV capsids are released through the fusion of the viral envelope with the endosomal membrane (23-25). While the ZIKV replication cycle proceeds in a similar manner to the related flaviviruses, the specific host-virus interactions important for ZIKV infection are not yet clear (7).

Based on phylogenetic analyses, the current circulating ZIKV strains have evolved from the common African ancestor, MR766, representing the African lineage. A breaking point occurred with strain P6-740 from Malaysia that determined the beginning of the Asian lineage and the current ZIKV circulating in the Americas have spread from Asia (26, 27). Due to the changes between the early Asian disease and the Americas' epidemics, we studied the virus characteristics of one example from each epidemic (26) to determine if they could bring some explanation to the increased pathogenicity and dissemination. In this paper, we compared the cytopathicity of a

Canadian-imported Thai strain of ZIKV representing the early Asian lineage to a Brazilian strain isolated from Bahia in 2015. The Brazilian isolate generated higher cytopathicity and intracellular RNA accumulation in the simian Vero and the human HEK 293T cell lines but higher cytopathicity with similar intracellular RNA accumulation in a neuroblastoma cell line. We performed an amino acid (aa) sequence comparison and predicted α-helices, β-strands and coils content between strains. Further examination of the specific aa polymorphisms may provide some insights on the underlying causes of these phenotypic differences observed in cell culture.

3.4 RESULTS

3.4.1 Protein Comparison between the Canadian-Imported Thai Strain and the Brazilian Isolate from Bahia Identifies Amino Acid Polymorphisms across the ZIKV Polyproteins

Based on previous phylogenetic nucleotide analyses, the Canadian-imported Thai strain PLCal_ZV of ZIKV represents an early Asian isolate of the virus before the French Polynesian outbreak (28-31). It is far separated from the Brazilian strain HS-2015-BA-01 (26), which is closely related to other isolates from Bahia in the Asian lineage (32). To investigate the aa difference between these two strains, we first compared the whole sequence of the two polyproteins (Fig S3.1). This comparison showed that there are only 13 aa polymorphisms between the PLCal_ZV and HS-2015-BA-01 isolates (Figure 3.1).

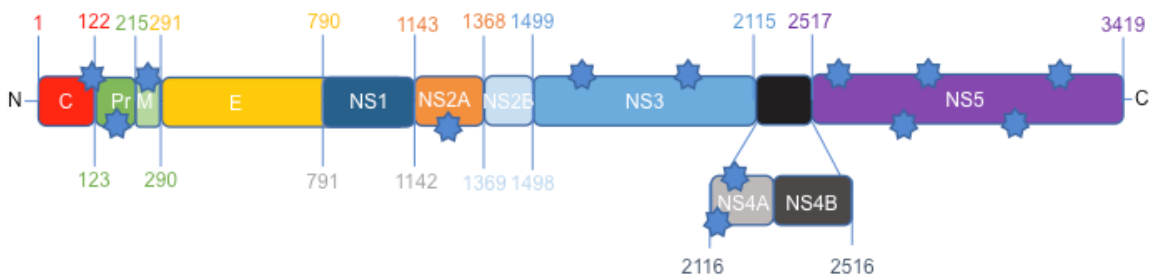

Figure 3. 1 Zika virus (ZIKV) genome representation.

Stars through the genome represent the position of aa differences between the Canadian-imported Thai strain PLCal_ZV and the Brazilian strain HS-2015-BA-01.

The African MR766 reference strain, which is much more divergent, was used for comparison at each of these polymorphisms between PLCal_ZV vs. HS-2015-BA-01 (Table 3.1). We found 13 aa polymorphisms between the two isolates, and the Brazilian isolate has five of those aa that were identical to the African reference strain. The aa variation between the Thai and Brazilian isolates are in the ER anchor of the C, Pr/PrM, NS2A, NS3, NS4A and NS5 proteins. Interestingly, no difference was found in the viral E protein, which is the main component for viral-cell recognition (Table 3.1).

Table 3. 1. Amino acid comparison of ZIKV MR766 at the point mutations between PLCal_ZV and HS-2015-BA-01.

Strain	Amino acid position												
MR-766	A106	A139	S273	A1263	D1622	Y2086	L2123	L2167	Y2594	M2634	V2842	V2894	P3162
PLCal_ZV	T106	S139	S273	A1263	D1622	Y2086	F2123	L2167	Y2594	M2634	I2842	I2894	S3162
HS-2015-BA-01	A106	N139	R273	V1263	G1622	H2086	L2123	M2167	H2594	V2634	V2842	V2894	P3162
Protein	ER anchor	pr/prM	prM	NS2A	NS3	NS3	NS4A	NS4A	NS5	NS5	NS5	NS5	NS5

Red: amino acid (aa) that differ from MR766. Blue: ZIKV proteins.

3.4.2 ZIKV Brazilian Isolate Demonstrates Increased Cytopathic Effects When Compared to the Asian Thai Strain in Three Different Cell Lines

ZIKV has a tropism for different cells and has neuronal cytopathic effects (24, 33-35). To compare the cytopathicity and the viral titer between the Thai and Brazilian isolates we evaluated their capacity to induce cell death and to generate new viruses in three different cell lines, Vero, HEK 293T and neuroblastoma SH-SY5Y cells. We first performed a time point infection in each cell

line and visualized the cells for 6, 12, 24 and 48 h post-infection (Figure 3.2A). We observed that the cytopathic effects were highly visible starting at 24 h in Vero cells infected by the HS-2015-BA-01 with the majority of Vero cells lysed at 48 h post-infection. In contrast, Vero cell lysis was not observed with the PLCal_ZV strain under these conditions (Figure 3.2A). We did not observe any modification of HEK 293T or SH-SY5Y cell morphology before 48 h of infection with HS-2015-BA-01. At that time there was cell detachment with partial cell death of HEK 293T and complete cell death of SH-SY5Y. RNA extraction and quantification could not be performed at 48 h due to cell death and the optimal time for further assays was set-up at 24 h.

To amplify and quantify cell lysis, the supernatant of infected cells was collected at 24 h post-infection and used for plaque assays in Vero cells. An example of this assay from the supernatant of Vero cells is shown in Figure 3.2B. From the virus collected at 24 h, we observed that PLCal_ZV gave plaques at 10^{-1} dilution of virus and no plaques were observed at higher dilution. With HS-2015-BA-01, cells were all lysed with the higher concentrations and plaques were countable only after a 10^{-6} dilution. The shape of the plaques was also different. In the infected Vero cells with PLCal_ZV, the plaques had reproducibly more fuzzy, indefinite boundaries and mostly as a shape of a comet. In contrast, the plaques with HS-2015-BA-01 were consistently round with sharp distinct boundaries, as circles, (Figure 3.2B, zoomed fields).

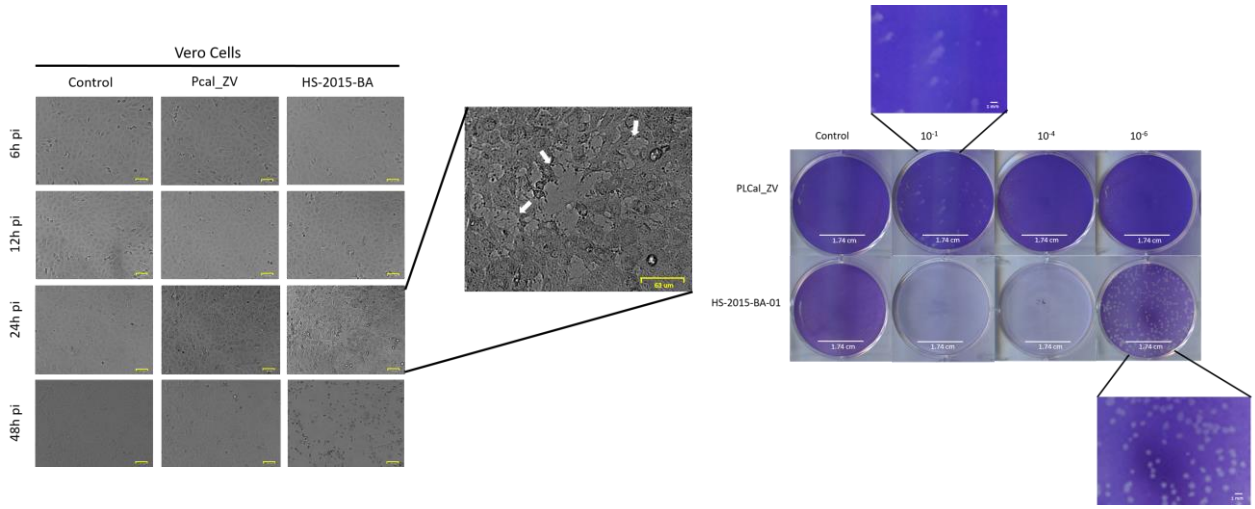

(A) **(B)**

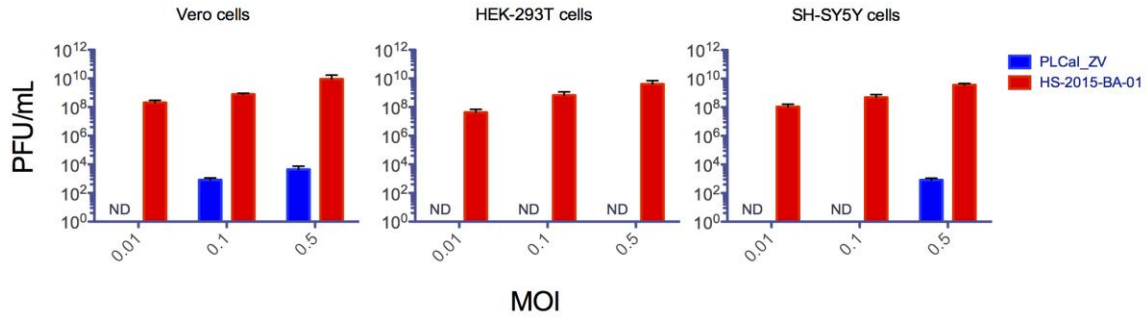

(C)

Figure 3. 2 ZIKV HS-2015-BA is more cytopathic than PLCal_ZV in Vero, HEK 293T and SH-SY5Y cells.

(**A**) Kinetics of cytopathicity of ZIKV in Vero cells. Vero cells were infected at multiplicity of infection (MOI) 0.1 with mock, PLCal_ZV or HS-2015-BA-01 as indicated. Live cells were photographed under the microscope after 6, 12, 24 and 48 h post-infection, scale bar = 63 µm. White arrows show the cytopathic effect of HS-2015-BA on Vero cells (**B**) plaque assay in Vero cells of ZIKV PLCal_ZV and HS-2015-BA-01 after infection with 10^{-1}, 10^{-4} and 10^{-6} dilution of virus from Vero cell supernatants,

scale bar = 1.74 cm in the plates and 1 mm in the zoomed pictures; (**C**) quantification of ZIKV plaque forming units (PFUs) formed by PLCal_ZV and HS-2015-BA-01 produced in Vero, HEK 293T and SH-SY5Y cell lines. Supernatant from each infected cell line at MOI of 0.01, 0.1 or 0.5 was collected and filtered on a 0.45 μm pore membrane. The generated supernatant was used to infect new batches of Vero cells and calculate the PFUs for every cell line. Detection limit is 400 PFUs/mL. ND = not detected. The graphs represent the average of three independent experiments ± standard error of the mean (SEM).

Because the two ZIKV strains showed different plaque production at a similar MOI, we quantified the viral cytopathicity generated by both viruses in each cell line at different MOIs (Figure 3.2C). We observed large differences in viral PFUs generated between PLCal_ZV and HS-2015-BA-01 in all three cell lines with the Brazilian isolate that consistently generated plaque numbers several logs higher at all MOIs. Overall the results show that HS-2015-BA-01 induces higher cytopathic effects than PLCal_ZV in three different cell lines. To determine if the extent of cell killing correlates with RNA accumulation, we next used qRT-PCR to quantify the RNA from the cells infected by each ZIKV strain.

3.4.3 ZIKV Brazilian Isolate Infection Results in Higher Viral RNA Accumulation Compared to Infection with the Thai Strain in Two Cell Lines

To further evaluate phenotypic differences between the two ZIKV isolates, we quantified the intracellular viral RNA levels in each of the three cell lines used in Figure 3.2. We designed primers to target the NS5 domain in ZIKV (nucleotides 7871–7962) to amplify similarly

PLCal_ZV and HS-2015-BA-01 viral RNAs by qRT-PCR assay and quantified viral RNA accumulation at 24 h post-infection (Figure 3.3).

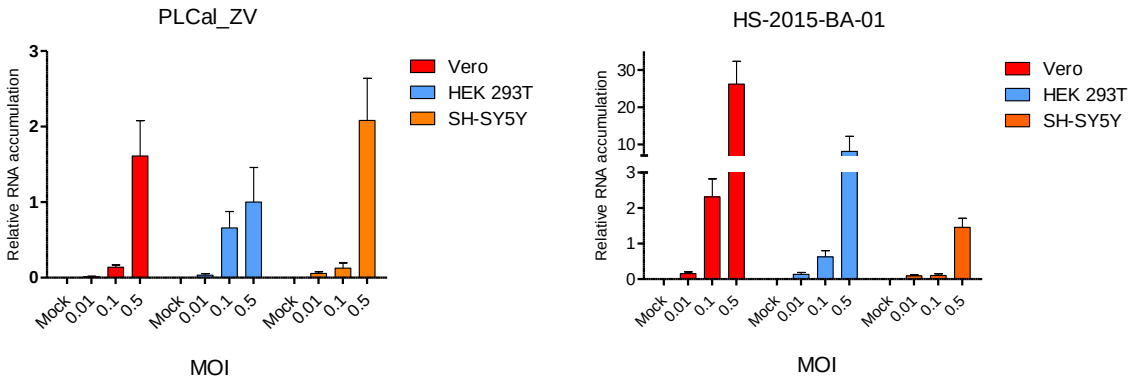

(**A**) (**B**)

Figure 3. 3 ZIKV intracellular RNA accumulation.

Vero (red), HEK 293T (blue) and SH-SY5Y (orange) cells were mock infected or infected with PLCal_ZV (**A**) or HS-2015-BA-01 (**B**) at MOI 0.01, 0.1 or 0.5 as indicated. RNA accumulation was quantified by quantitative reverse transcription polymerase chain reaction (qRT-PCR) at 24 h post-infection. The amount of ZIKV RNA was analyzed by the threshold cycle (Ct) comparative method and normalized to the reference genes TATA-box binding protein (TBP) and Peptidylprolyl isomerase A (PPIA) RNAs using Bio-Rad CFX software. The graphs represent an average of three independent experiments ± standard error of the mean (SEM). GraphPad Prism was used to calculate P-values for effects on RNA accumulation between PLCal_ZV and HS-2015-BA-01 in the different cell lines. Results from a two-way ANOVA were: $p < 0.0001$ for Vero cells, $p < 0.05$ for HEK293T cells and not significant for SH-SY5Y cells.

Our results show that in Vero and HEK 293T cell lines infected with HS-2015-BA-01, the amount of viral genomic RNA was higher than with PLCal_ZV at all MOIs. Interestingly, the RNA level at MOI 0.5 was 16 times higher in Vero cells and 10 times higher in HEK 293T cells with HS-

2015-BA-01 than with PLCal_ZV. Despite the increased cytopathicity of HS-2015-BA-01 in the SH-SY5Y cell line (Figure 3.2), the RNA accumulation from the two viral strains was similar at 24 h post-infection. Overall, the level of viral RNA is higher with HS-2015-BA-01 than with PLCal_ZV at 24 h in Vero and HEK 293T cells, but no apparent difference was observed by qRT-PCR in SH-SY5Y. Therefore, the cytopathicity may involve another parameter different from RNA accumulation, at least in the neuroblastoma SH-SY5Y cells.

3.4.4 ZIKV Brazilian Isolate Decreases Cell Viability More than the Thai Strain in All Three Cell Lines

A different way to assess cytopathicity of the ZIKV strains is to measure their effect on the cellular metabolism. We used a cell viability assay based on the cleavage of the tetrazolium salt, WST-1, into a formazan dye. This reaction is dependent on NAD(P)H and is only intact in metabolically active cells. Vero, HEK 293T and SH-SY5Y cells were infected with PLCal_ZV and HS-2015-BA-01 viruses at increasing MOI. We observed that the HS-2015-BA-01 decreases cell viability of Vero cells more than the PLCal_ZV at 24 h, while the differences between the two strains were negligible for the HEK 293T and SH-SY5Y cells (Figure 3.4A–C). At 48 h, we see a large difference between the two strains in all three cell lines tested, most notably in the Vero cells (Figure 3.4D–F). This result shows an increased effect of HS-2015-BA-01 on reducing cell viability compared to PLCal_ZV and is consistent with results from plaque assays (Figure 3.2C) and from qRT-PCR (Figure 3.3).

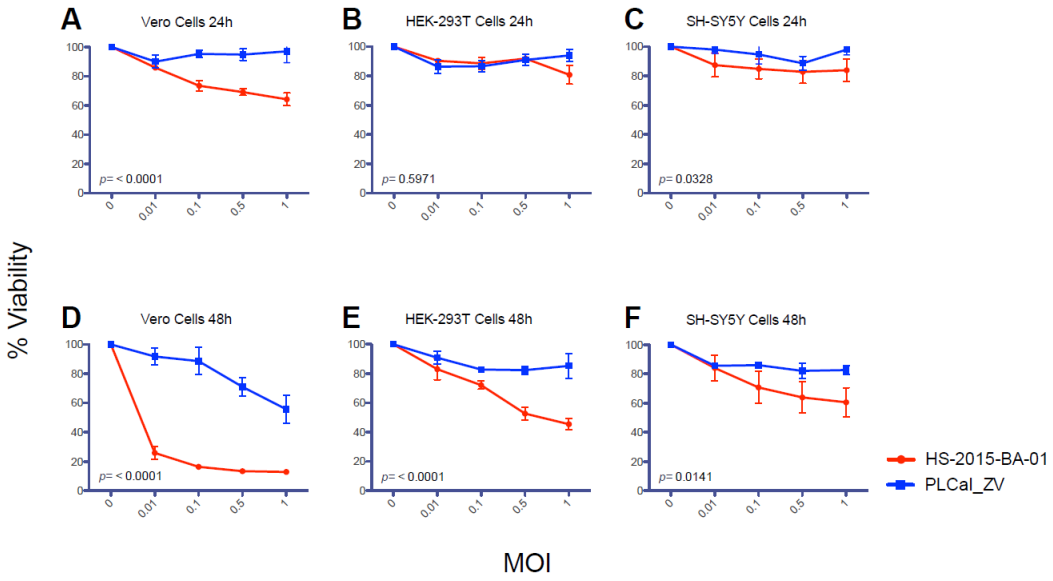

Figure 3. 4 Cellular viability assays in different cells infected with PLCal_ZV or HS-2015-BA-01.

Cells were infected with PLCal_ZV (blue) or HS-2015-BA-01 (red). (**A**–**C**) Cell viability was measured at 24 h in Vero (**A**); HEK 293T (**B**) and SH-SY5Y (**C**); (**D**–**F**) Cell viability assays at 48 h in Vero (**D**); HEK 293T (**E**) and SH-SY5Y (**F**). The OD 450 nm of the mock was set as 100% viability, and each condition was expressed as a percentage of the mock. The values are the average of three independent experiments ± standard error of the mean (SEM). GraphPad Prism was used to calculate *p*-values for effects on cell viability between PLCal_ZV and HS-2015-BA-01. Results from a two-way ANOVA are shown on each graph, **A**–**F**.

3.4.5 ZIKV Secondary Structure of prM, NS2A, NS3, and NS5 Produce Different Patterns of Predicted α-Helices, β-Strands and Coils

To determine if the aa differences between the two ZIKV strains could change the structure of the corresponding proteins, we analyzed the predicted protein secondary structure using a protein prediction program (http://bioinf.cs.ucl.ac.uk/psipred/). The structures were analyzed by

comparing the α-helices, β-strands and coils between proteins of PLCal_ZV and HS-2015-BA-01 (Table 3.2 and Figure S3.2).

Table 3. 2. Changes in predicted protein structure between PLCal_ZV and HS-2015-BA-01 ZIKV.

Observed changes in PLCal_ZV and HS-2015-BA-01			
Protein	*AA Variant position*	*PL Cal_ZV structure*	*HS-2015-BA-01 structure*
pr/prM	139,	Coil (171-174,187,202,203)	β-strand (171-174,187,202,203)
	273	β-strand (235, 236)	Coil (235, 236)
NSA2	1263	α-helix (1172, 1214)	Coil (1172, 1214)
		Coil (1232)	α-helix (1232)
NS3	1622,	β-strand (1508,1520,1524,1565,1614,1641,1642,1788,1947-1949,2095)	Coil (1508,1520,1524,1565,1614,1641,1642,1788,1947-1949,2095)
	2086	α-helix (1773,1854,1855, 1994-1997)	Coil (1773,1854,1855, 1994-1997)
		Coil (1625, 2066)	β-strand (1625, 2066)
		Coil (1794, 1958)	α-helix (1794, 1958)
		α-helix (1998,1999)	β-strand (1998,1999)
NS5	2594	β-strand (2554,2555,2600,2970,2997,3237,3240, 3241)	Coil (2554,2555,2600,2970,2997,3237,3240, 3241)
	2634	Coil (2607,2608,3270,3271,3287)	α-helix (2607,2608,3270,3271,3287)
	2842, 2894	Coil (3110)	β-strand (3110)
	3162	α-helix (3159,3160)	Coil (3159,3160)

The aa modifications in the ER anchor of the Core protein (T106A) and in the NS4A protein (F2123L and L2167M) induced no change of their predicted secondary structures and have little chances to change their properties. The two aa changes in prM (S139N and S273R) and one in NS2A (A1263V) induced several predicted modifications in the secondary structures with several inversions between β-strands and coils (prM) or α-helices and coils (NS2A). Furthermore, the two aa changes in NS3 and five in NS5 induced many differences between predicted coils, α-helices or β-strands. Interestingly, in several cases the aa variation induced an upstream or downstream modification of the predicted secondary structure suggesting that the substructures are interconnected and could affect overall protein folding.

3.5 DISCUSSION

The rapid dissemination of ZIKV and increased pathogenicity between the early Asian strains and the contemporary American isolates prompted us to determine if a difference in cytopathicity and viral RNA accumulation could provide some insight into novel neurological pathogenesis observed (11-14, 17, 18). We therefore chose to study the Canadian-imported Thai strain PLCal_ZV, which belongs to the early Asian lineage and HS-2015-BA-01, a recent Brazilian isolate from Bahia, a region where fetal pathogenesis was detected early in the epidemic (18, 32, 33, 36, 37). An aa comparison between the two strains identified 13 aa polymorphism that may contribute to strain phenotypic variations (Figure 3.1).

ZIKV has a tropism for many human cells and tissues (38). It can infect the skin fibroblasts, keratinocytes and dendritic cells (22), monocytes (39, 40), retinal epithelium (41), brain cells including neural progenitors, neurons, astrocytes and glial cells (23, 42, 43), uterine fibroblasts (44), placental cells (45) and testicular cells (46, 47). In cell culture, insect C6/36 and monkey epithelial Vero cell lines have been widely used to amplify ZIKV (48, 49), whereas human fibroblasts MRC-5, hepatic Huh7, lung epithelial cells A549, astrocytic U251MG, neuronal stem cells and neuroblastoma SK-N-SH and SH-SY5Y cell lines are permissive for ZIKV infection (34, 49-52). Human epithelial HEK 293T cells were found to be moderately permissive to ZIKV infection (22, 34). To better understand the cytopathicity of the two different ZIKV strains, we infected the monkey epithelial Vero and the human epithelial HEK 293T cell lines. Because the main concern about ZIKV is its neurological consequences in fetuses and adults, we used the human SH-SY5Y neuroblastoma cell line as a model for neuronal infection and cytopathicity (16, 43, 53). These cellular models showed greater cytopathic effects with HS-2015-BA-01 than with PLCal_ZV as noticed by live cell observation at different time points and quantification of cell

lysis (Figure 3.2). Furthermore, measurement of cell viability demonstrated that HS-2015-BA-01 induced more metabolic damage than PLCal_ZV in all three cell lines (Figure 3.4). One explanation could be a different tropism related to the entry receptors. AXL is the main ZIKV candidate receptor, present in several cell types such as keratinocytes, HEK 293T, neuronal stem cells, astrocytes, oligodendrocyte precursor cells, microglia and endothelial cells, but its removal does not protect from ZIKV infection suggesting that others are involved (22, 23, 25, 42, 54-56). Indeed, Tyro3 and T-cell immunoglobulin and mucin domain (TIM)1 could be part of the ZIKV entry receptors or co-receptors that enhance the virus entry either alone or with AXL (38, 45). However, the fact that the E protein has no aa polymorphism does not favor this hypothesis. The intracellular milieu may also influence the cytopathic effects of the virus by interactions with cellular components. Those include helper or restriction factors, cellular trafficking, RNA replication and translation of viral proteins that either favor or restrict ZIKV replication (34, 57-60). The immune response capabilities of each cell line studied can also influence the replication rate or cytopathic effects (48, 61). Specific viral proteins can also interact with cellular components and induce metabolic disturbances in cells, which could lead to pathogenesis, decreased cell growth and ultimately cell death (33, 43, 50, 52, 62).

In addition, the difference in cytopathicity could have its origin in the extent of viral replication, which is the result of both cellular and viral factors. To approach viral replication after viral entry, we measured the intracellular accumulation of viral RNA. Our results show that genomic RNA levels of HS-2015-BA-01 are greater than that of PLCal_ZV in Vero and in HEK 293T cells at 24 h (Figure 3.3). In neuroblastoma SH-SY5Y cells, at each MOI tested, the viral RNA levels were similar between the two strains, indicating that the amount of viral RNA accumulation cannot

explain the increased cytopathicity of the Brazilian isolate in these cells. Previous studies that compared strains from the African and the Asian lineage have reported a higher replication rate and cytopathicity for the African lineage in different cell lines (63). Specifically, in a neuroblastoma cell line SK-N-SH (the precursor of SH-SY5Y), two African strains replicated faster than two Asian strains, but the viral RNA produced was not quantified (28). When qRT-PCR was performed to compare the American isolate from Puerto Rico to the African MR766 strain, a higher RNA production was found for the Puerto Rico strain in two endothelial cells but no neuronal cells were used in this study (54). Therefore, this is the first report that shows higher viral RNA accumulation and higher cytopathicity for a Brazilian isolate compared to an early Asian Thai strain in the endothelial monkey (Vero) and human (HEK 293T) cells, whereas in the neuroblastoma cells SH-SY5Y the cytopathicity of the Brazilian isolate is higher with similar intracellular RNA levels (Figures 3.2–3.4). These results suggest that some neuropathology may not be linked to higher viral RNA accumulation but rather to a specific activity of one or several viral proteins.

Previous studies have shown that aa polymorphism in the ZIKV polyprotein can alter cell tropism, virulence or the replication rate of viruses. For example, a substitution of five aa in ZIKV has contributed to the adaptation from mosquitoes to human and a single aa substitution in NS1 was associated with increased infectivity in mosquitoes (64-66). Here we found no further changes in the E and NS1 proteins between PLCal_ZV and HS-2015-BA-01 strains, suggesting that the increased cytopathicity and differences in viral RNA levels may be due to polymorphisms in other ZIKV proteins (Figure 3.1 and Table 3.1). We therefore compared the predicted secondary structure of each modified protein (Figure S3.2 summarized in Table 3.2). In the PrM protein,

S139N and S273R induced modifications that are predicted to cause several changes between β-strands and coil structures. A recent report comparing Americas' isolates to an early Asian strain from Cambodia identified S139N as a major mutation that contributes to fetal microcephaly in a mouse model (62). The prM protein is involved in virus maturation and secretion. The higher viral production despite similar RNA levels in SH-SY5Y for the HS-2015-BA-01 compared to PLCal_ZV strain suggests that S139N polymorphism in prM may contribute to increased viral egress and dissemination and consequently to cytopathicity and neuropathology. Additional polymorphisms of the ZIKV proteins were identified in NS2A, NS3 and NS5. The Y2086H polymorphism in NS3 protease and helicase occurred between ZIKV PLCal_ZV and THA/2014/SV0127-14, another Thai isolate (20, 30, 36, 67). It remains to be determined if this mutation has changed the proteolytic activity of NS3 in the subsequent isolates. NS5 acts as a methyl transferase in its N-terminus and as an RNA-dependent RNA polymerase in its C-terminus (68). Mutation M2634V in NS5 was identified in all Latin American viruses but not in French Polynesia isolates. Further studies will be required to determine if it had an incidence on NS5 activity in the Americas' isolates (30). Although the 5′ and 3′ RNA elements could also play critical roles in the viral replication cycle (20), our study focused on the aa sequence changes and their impacts on predicted secondary structures. Their consequences on increased cytopathicity may contribute to neuropathology. HS-2015-BA-01 has been used in vivo in a murine model and in a primate model (33, 61). The virus kills fetal mice neurons very efficiently (33), but adult monkeys show an efficient immune reaction against the virus with no major pathology (61). Further research will address the main determinants of placenta transmission, teratogenesis and neuropathology.

3.6 MATERIALS AND METHODS

3.6.1. Cell Culture

HEK 293T cells (69, 70) were maintained in Dulbecco's modified Eagle's medium (DMEM) with high glucose (Hyclone, Logan, UT, USA) supplemented with 10% fetal bovine serum (FBS) (Hyclone, Logan, UT, USA), 50 U/mL Penicillin and 50 µg/mL Streptomycin (Thermo Fisher Scientific, Burlington, ON, Canada). African green monkey epithelial Vero cells (48) were maintained in DMEM with high glucose, supplemented with 5% FBS, 1% non-essential amino acids, 1% L-glutamine, 50 U/mL Penicillin and 50 µg/mL Streptomycin (Wisent, St Bruno, QC, Canada). Neuroblastoma SH-SY5Y cells (71) were obtained from Dr. Marc Fabian (LDI and McGill University, Montréal, QC, Canada) and maintained in DMEM/Ham's F12 50/50 mix (Wisent, St Bruno, QC, Canada), supplemented with 10% FBS, 50 U/mL Penicillin and 50 µg/mL Streptomycin.

3.6.2. Zika Virus Strains

The Canadian imported Thai ZIKV strain PLCal_ZV (Genbank accession KF993678.1), passaged four times in Vero cells was previously described (36, 48). The Brazilian ZIKV strain HS-2015-BA-01 isolated in August 2015 in Salvador, Bahia was previously described (Genbank accession KX520666.1). It was passaged three times in *Aedes albopictus* C6/36 mosquito cells and once in Vero cells (33).

3.6.3. Zika Virus Amplification

ZIKV stocks were prepared by passaging in Vero cells. Briefly, 6.0×10^6 Vero cells were plated in a T182.5 flask. On day 1, the growth medium was removed and cells were washed with Phosphate Buffer Saline (PBS) (Wisent, St Bruno, QC, Canada). Cells were then infected at a

multiplicity of infection (MOI) of 0.5 in 10 mL of Eagle's minimal essential medium (EMEM) (Wisent, St Bruno, QC, Canada) and incubated (37 °C, 5% CO_2) for 2 h. The infection medium was then removed and replaced with ZIKV infection medium: DMEM supplemented with 2% FBS; 1% non-essential amino acids; 1% L-glutamine; 50 U/mL Penicillin and 50 µg/mL Streptomycin (Wisent, St Bruno, QC, Canada), and; 15 mM Hepes buffer (Sigma-Aldrich, Oakville, ON, Canada). At two days post-infection, the supernatant was filtered through a 0.45 µM membrane, viral stocks were tittered by plaque forming unit (PFU) assay, aliquoted and stored at −80 °C.

3.6.4. Live Cell Imaging of Zika Virus Infection

For this, 3.0×10^5 Vero, HEK 293T and SH-SY5Y cells were seeded in 12-well plates and incubated overnight. Growth medium was removed and cells were washed with PBS. Cells were infected at MOI of 0.1 in 1 mL of EMEM with either ZIKV PLCal_ZV or ZIKV HS-2015-BA-01 and incubated for 2 h. The infection medium was replaced with supplemented ZIKV infection medium in DMEM or DMEM/Ham's F12 50/50 mix. The infection was followed for 6, 12, 24 and 48 h to observe and visualize the cytopathic effects. Capture imaging of live cells was acquired with a ZOE cell imager (Bio-Rad, Mississauga, ON, Canada).

3.6.5. Plaque Forming Unit (PFU) Assay

At this stage, 6.0×10^5 Vero cells were seeded in six-well plates and incubated overnight. On day 1, eight serial dilutions (1 in 10) were performed with the supernatant filtrates in EMEM. The medium was removed, cells were washed with PBS and then incubated with the virus dilutions for 2 h. After incubation, the virus dilutions were removed and replaced with a mixture of: 1.2% carboxymethylcellulose (CMC) (Sigma-Aldrich), 2% FBS and 50 U/mL Penicillin and 50 µg/mL

Streptomycin in EMEM. Four days post-infection, the CMC medium was removed, and after two washes with PBS, cells were fixed with 2 mL of a 4% paraformaldehyde (PFA) solution, washed with ddH_2O and incubated at room temperature (RT) with a 0.1% crystal violet solution for 30 min to visualize plaques. Viral titers were calculated as follows:

$$\frac{\#\ of\ plaques}{dilution\ factor\ \times\ infection\ volume}$$

3.6.6. Quantitative Reverse Transcription Polymerase Chain Reaction (qRT-PCR)

RNA was extracted from Vero, HEK 293T and SH-SY5Y cell lines mock infected or infected with PLCal_ZV or HS-2015-BA-01 at MOI of 0.01, 0.1 and 0.5 for 24 h with Trizol reagent (Life Technologies, Burlington, ON, Canada) and further purified with RNeasy (QIAGEN, Hilden, Germany). RNase-Free DNase Set (QIAGEN) was loaded onto the RNeasy columns. cDNA was synthesized using 1000 ng of the extracted RNA using Superscript II according to the manufacturer's protocol (Invitrogen, Burlington, ON, Canada). qPCR was performed by diluting the cDNA (1:60) due to the comparison with the threshold cycle (Ct) values from the ZIKV standard curve. The standard curve was generated by serial dilution of pooled samples of infected cell lines with their respected viruses. BrightGreen qPCR MasterMix-Low ROX and a Bio-Rad CFX96 were used for performing the qPCR. Primers for TATA-box binding protein (TBP) and Peptidylprolyl isomerase A (PPIA) were used as internal controls as previously described (72). ZIKV primers were designed for this work with the following sequences: Forward 5′-CAAAAGGAGGCCCTGGTCAT-3′, Reverse 5′-ATGAAAGACGTCCACCCCAC-3′ (92 bp product). Samples were loaded in quadruplicates. qPCR conditions were as follows: 95 °C for 5 min followed by 50 cycles of 95 °C for 10 s, 62 °C for 15 s, 72 °C for 5 s. Finally, one cycle of 65 °C for 5 s and one of 95 °C for 5 s. Data analysis was performed using Bio-Rad CFX software

(http://www.bio-rad.com/en-ca/category/qpcr-analysis-software) and GraphPad Prism 5 (GraphPad Software, La Jolla, CA, USA).

3.6.7. Cell Viability

Cell viability was evaluated by the metabolism of the water-soluble tetrazolium salt 1 (WST-1) cell proliferation reagent (Roche, Indianapolis, IN, USA). Briefly, 2.5×10^4 Vero, HEK 293T, and Neuroblastoma SH-SY5Y cells were seeded in 96-well plates and incubated overnight. On day 1, the growth medium was removed and cells were washed with PBS. Cells were then infected with either PLCal_ZV or HS-2015-BA-01 ZIKV isolates at an MOI of 1, 0.5, 0.1, and 0.01 in 100 µL of EMEM. The cells were incubated with the virus dilutions for 2 h. Virus solutions were then removed and replaced with 100 µL of the respective growth media. 24 and 48 h post-infection, 50 µL of Dimethyl sulfoxide (DMSO) (Sigma-Aldrich, Oakville, ON, Canada) was added to four wells of each cell line as a control for cell death. After 15 min incubation at RT, 10 µL of WST-1 reagent was added to each well and cells were incubated for an additional 1.5 h at 37 °C. ZIKV was then neutralized for 20 min by the addition of 50 µL PBS with 4% NP40 (Sigma-Aldrich, Oakville, ON, Canada). The plate was then read on a Benchmark Plus microplate spectrophotometer (Bio-Rad, Mississauga, ON, Canada). Absorbance was measured at 450 nm (test wavelength) and 690 nm (reference wavelength) and the reference reading was subtracted from the test reading. The value of the uninfected cells was set as 100% viability. The viability of each condition was expressed as a percentage of the uninfected cells for each cell line. Each condition was performed in triplicates, and the percentage viability for each cell line at each MOI was calculated as follows:

$$\frac{OD_{infected}^{450\text{ nm}} - OD_{infected}^{690\text{ nm}}}{OD_{mock}^{450\text{ nm}} - OD_{mock}^{690\text{ nm}}} \times 100.$$

3.6.8. ZIKV Polyprotein Sequence Alignment and Secondary Structure Predictions

ZIKV DNA sequence from PLCal_ZV and HS-2015-BA-01 were aligned against the ancestor African strain MR766 to define the protein boundaries in Clustal W (Kyoto University Bioinformatics Center, Kyoto, Japan) and Molecular Evolutionary Genetics Analysis, MEGA 6 (The Pennsylvania State University, Pennsylvania, USA). This alignment helped us to define the ZIKV polyprotein sequences of PLCal_ZV and HS-2015-BA-01. Once we defined the precise boundaries of each ZIKV protein, we submitted the aa sequence of each mature protein to PSIPRED (http://bioinf.cs.ucl.ac.uk/psipred/) to predict the overall secondary structure (α-helix, β-strand and coil content).

Supplementary Materials: The following are available online at https://www.mdpi.com/1999-4915/10/2/53, Supplementary Material. Figure S1: Amino acids sequence comparison between the ZIKV Canadian-imported Thai strain PLCal_ZV and the Brazilian HS-2015-BA-01 strain. Figure S2: Protein secondary structure comparison between the ZIKV Canadian-imported Thai strain PLCal_ZV and the Brazilian HS-2015-BA-01 strain.

3.7 REFERENCES

1. Musso D, Gubler DJ. 2016. Zika Virus. Clin Microbiol Rev 29:487-524.
2. Dick GW, Kitchen SF, Haddow AJ. 1952. Zika virus. I. Isolations and serological specificity. Trans R Soc Trop Med Hyg 46:509-20.
3. Heinz FX, Stiasny K. 2017. The Antigenic Structure of Zika Virus and Its Relation to Other Flaviviruses: Implications for Infection and Immunoprophylaxis. Microbiol Mol Biol Rev 81:e00055-16.
4. Macnamara FN. 1954. Zika virus: a report on three cases of human infection during an epidemic of jaundice in Nigeria. Trans R Soc Trop Med Hyg 48:139-45.
5. Lanciotti RS, Kosoy OL, Laven JJ, Velez JO, Lambert AJ, Johnson AJ, Stanfield SM, Duffy MR. 2008. Genetic and serologic properties of Zika virus associated with an epidemic, Yap State, Micronesia, 2007. Emerg Infect Dis 14:1232-9.
6. Roth A, Mercier A, Lepers C, Hoy D, Duituturaga S, Benyon E, Guillaumot L, Souares Y. 2014. Concurrent outbreaks of dengue, chikungunya and Zika virus infections - an unprecedented epidemic wave of mosquito-borne viruses in the Pacific 2012-2014. Euro Surveill 19:20929.
7. Relich RF, Loeffelholz M. 2017. Zika Virus. Clin Lab Med 37:253-267.
8. Zanluca C, Melo VC, Mosimann AL, Santos GI, Santos CN, Luz K. 2015. First report of autochthonous transmission of Zika virus in Brazil. Mem Inst Oswaldo Cruz 110:569-72.
9. Duffy MR, Chen TH, Hancock WT, Powers AM, Kool JL, Lanciotti RS, Pretrick M, Marfel M, Holzbauer S, Dubray C, Guillaumot L, Griggs A, Bel M, Lambert AJ, Laven J, Kosoy O, Panella A, Biggerstaff BJ, Fischer M, Hayes EB. 2009. Zika virus outbreak on Yap Island, Federated States of Micronesia. N Engl J Med 360:2536-43.
10. Olson JG, Ksiazek TG, Suhandiman, Triwibowo. 1981. Zika virus, a cause of fever in Central Java, Indonesia. Trans R Soc Trop Med Hyg 75:389-93.
11. Brasil P, Pereira JP, Jr., Moreira ME, Ribeiro Nogueira RM, Damasceno L, Wakimoto M, Rabello RS, Valderramos SG, Halai UA, Salles TS, Zin AA, Horovitz D, Daltro P, Boechat M, Raja Gabaglia C, Carvalho de Sequeira P, Pilotto JH, Medialdea-Carrera R, Cotrim da Cunha D, Abreu de Carvalho LM, Pone M, Machado Siqueira A, Calvet GA, Rodrigues Baiao AE, Neves ES, Nassar de Carvalho PR, Hasue RH, Marschik PB, Einspieler C, Janzen C, et al. 2016. Zika Virus Infection in Pregnant Women in Rio de Janeiro. N Engl J Med 375:2321-2334.
12. do Rosario MS, de Jesus PA, Vasilakis N, Farias DS, Novaes MA, Rodrigues SG, Martins LC, Vasconcelos PF, Ko AI, Alcantara LC, de Siqueira IC. 2016. Guillain-Barre Syndrome After Zika Virus Infection in Brazil. Am J Trop Med Hyg 95:1157-1160.
13. Dos Santos T, Rodriguez A, Almiron M, Sanhueza A, Ramon P, de Oliveira WK, Coelho GE, Badaro R, Cortez J, Ospina M, Pimentel R, Masis R, Hernandez F, Lara B, Montoya R, Jubithana B, Melchor A, Alvarez A, Aldighieri S, Dye C, Espinal MA. 2016. Zika Virus and the Guillain-Barre Syndrome - Case Series from Seven Countries. N Engl J Med 375:1598-1601.
14. Mlakar J, Korva M, Tul N, Popovic M, Poljsak-Prijatelj M, Mraz J, Kolenc M, Resman Rus K, Vesnaver Vipotnik T, Fabjan Vodusek V, Vizjak A, Pizem J, Petrovec M, Avsic Zupanc T. 2016. Zika Virus Associated with Microcephaly. N Engl J Med 374:951-8.
15. Cao-Lormeau VM, Blake A, Mons S, Lastere S, Roche C, Vanhomwegen J, Dub T, Baudouin L, Teissier A, Larre P, Vial AL, Decam C, Choumet V, Halstead SK, Willison

HJ, Musset L, Manuguerra JC, Despres P, Fournier E, Mallet HP, Musso D, Fontanet A, Neil J, Ghawche F. 2016. Guillain-Barre Syndrome outbreak associated with Zika virus infection in French Polynesia: a case-control study. Lancet 387:1531-1539.
16. Cauchemez S, Besnard M, Bompard P, Dub T, Guillemette-Artur P, Eyrolle-Guignot D, Salje H, Van Kerkhove MD, Abadie V, Garel C, Fontanet A, Mallet HP. 2016. Association between Zika virus and microcephaly in French Polynesia, 2013-15: a retrospective study. Lancet 387:2125-2132.
17. Lim SK, Lim JK, Yoon IK. 2017. An Update on Zika Virus in Asia. Infect Chemother 49:91-100.
18. Ribeiro LS, Marques RE, Jesus AM, Almeida RP, Teixeira MM. 2016. Zika crisis in Brazil: challenges in research and development. Curr Opin Virol 18:76-81.
19. Shi Y, Gao GF. 2017. Structural Biology of the Zika Virus. Trends Biochem Sci 42:443-456.
20. Ye Q, Liu ZY, Han JF, Jiang T, Li XF, Qin CF. 2016. Genomic characterization and phylogenetic analysis of Zika virus circulating in the Americas. Infect Genet Evol 43:43-9.
21. Kostyuchenko VA, Lim EX, Zhang S, Fibriansah G, Ng TS, Ooi JS, Shi J, Lok SM. 2016. Structure of the thermally stable Zika virus. Nature 533:425-8.
22. Hamel R, Dejarnac O, Wichit S, Ekchariyawat P, Neyret A, Luplertlop N, Perera-Lecoin M, Surasombatpattana P, Talignani L, Thomas F, Cao-Lormeau VM, Choumet V, Briant L, Despres P, Amara A, Yssel H, Misse D. 2015. Biology of Zika Virus Infection in Human Skin Cells. J Virol 89:8880-96.
23. Meertens L, Labeau A, Dejarnac O, Cipriani S, Sinigaglia L, Bonnet-Madin L, Le Charpentier T, Hafirassou ML, Zamborlini A, Cao-Lormeau VM, Coulpier M, Misse D, Jouvenet N, Tabibiazar R, Gressens P, Schwartz O, Amara A. 2017. Axl Mediates ZIKA Virus Entry in Human Glial Cells and Modulates Innate Immune Responses. Cell Rep 18:324-333.
24. Olagnier D, Muscolini M, Coyne CB, Diamond MS, Hiscott J. 2016. Mechanisms of Zika Virus Infection and Neuropathogenesis. DNA Cell Biol 35:367-72.
25. Richard AS, Shim BS, Kwon YC, Zhang R, Otsuka Y, Schmitt K, Berri F, Diamond MS, Choe H. 2017. AXL-dependent infection of human fetal endothelial cells distinguishes Zika virus from other pathogenic flaviviruses. Proc Natl Acad Sci U S A 114:2024-2029.
26. Rajah MM, Pardy RD, Condotta SA, Richer MJ, Sagan SM. 2016. Zika Virus: Emergence, Phylogenetics, Challenges, and Opportunities. ACS Infect Dis 2:763-772.
27. Wang L, Valderramos SG, Wu A, Ouyang S, Li C, Brasil P, Bonaldo M, Coates T, Nielsen-Saines K, Jiang T, Aliyari R, Cheng G. 2016. From Mosquitos to Humans: Genetic Evolution of Zika Virus. Cell Host Microbe 19:561-5.
28. Anfasa F, Siegers JY, van der Kroeg M, Mumtaz N, Stalin Raj V, de Vrij FMS, Widagdo W, Gabriel G, Salinas S, Simonin Y, Reusken C, Kushner SA, Koopmans MPG, Haagmans B, Martina BEE, van Riel D. 2017. Phenotypic Differences between Asian and African Lineage Zika Viruses in Human Neural Progenitor Cells. mSphere 2:e00292-17.
29. Lanciotti RS, Lambert AJ, Holodniy M, Saavedra S, Signor Ldel C. 2016. Phylogeny of Zika Virus in Western Hemisphere, 2015. Emerg Infect Dis 22:933-5.

30. Pettersson JH, Eldholm V, Seligman SJ, Lundkvist A, Falconar AK, Gaunt MW, Musso D, Nougairede A, Charrel R, Gould EA, de Lamballerie X. 2016. How Did Zika Virus Emerge in the Pacific Islands and Latin America? MBio 7:e01239-16.
31. Shi W, Zhang Z, Ling C, Carr MJ, Tong Y, Gao GF. 2016. Increasing genetic diversity of Zika virus in the Latin American outbreak. Emerg Microbes Infect 5:e68.
32. Naccache SN, Theze J, Sardi SI, Somasekar S, Greninger AL, Bandeira AC, Campos GS, Tauro LB, Faria NR, Pybus OG, Chiu CY. 2016. Distinct Zika Virus Lineage in Salvador, Bahia, Brazil. Emerg Infect Dis 22:1788-92.
33. Costa VV, Del Sarto JL, Rocha RF, Silva FR, Doria JG, Olmo IG, Marques RE, Queiroz-Junior CM, Foureaux G, Araujo JMS, Cramer A, Real A, Ribeiro LS, Sardi SI, Ferreira AJ, Machado FS, de Oliveira AC, Teixeira AL, Nakaya HI, Souza DG, Ribeiro FM, Teixeira MM. 2017. N-Methyl-d-Aspartate (NMDA) Receptor Blockade Prevents Neuronal Death Induced by Zika Virus Infection. MBio 8:e00350-17.
34. Hou W, Armstrong N, Obwolo LA, Thomas M, Pang X, Jones KS, Tang Q. 2017. Determination of the Cell Permissiveness Spectrum, Mode of RNA Replication, and RNA-Protein Interaction of Zika Virus. BMC Infect Dis 17:239.
35. Oh Y, Zhang F, Wang Y, Lee EM, Choi IY, Lim H, Mirakhori F, Li R, Huang L, Xu T, Wu H, Li C, Qin CF, Wen Z, Wu QF, Tang H, Xu Z, Jin P, Song H, Ming GL, Lee G. 2017. Zika virus directly infects peripheral neurons and induces cell death. Nat Neurosci 20:1209-1212.
36. Fonseca K, Meatherall B, Zarra D, Drebot M, MacDonald J, Pabbaraju K, Wong S, Webster P, Lindsay R, Tellier R. 2014. First case of Zika virus infection in a returning Canadian traveler. Am J Trop Med Hyg 91:1035-8.
37. Malone RW, Homan J, Callahan MV, Glasspool-Malone J, Damodaran L, Schneider Ade B, Zimler R, Talton J, Cobb RR, Ruzic I, Smith-Gagen J, Janies D, Wilson J. 2016. Zika Virus: Medical Countermeasure Development Challenges. PLoS Negl Trop Dis 10:e0004530.
38. Miner JJ, Diamond MS. 2017. Zika Virus Pathogenesis and Tissue Tropism. Cell Host Microbe 21:134-142.
39. Foo SS, Chen W, Chan Y, Bowman JW, Chang LC, Choi Y, Yoo JS, Ge J, Cheng G, Bonnin A, Nielsen-Saines K, Brasil P, Jung JU. 2017. Asian Zika virus strains target CD14+ blood monocytes and induce M2-skewed immunosuppression during pregnancy. Nat Microbiol 2:1558-1570.
40. Michlmayr D, Andrade P, Gonzalez K, Balmaseda A, Harris E. 2017. CD14+CD16+ monocytes are the main target of Zika virus infection in peripheral blood mononuclear cells in a paediatric study in Nicaragua. Nat Microbiol 2:1462-1470.
41. Salinas S, Erkilic N, Damodar K, Moles JP, Fournier-Wirth C, Van de Perre P, Kalatzis V, Simonin Y. 2017. Zika Virus Efficiently Replicates in Human Retinal Epithelium and Disturbs Its Permeability. J Virol 91:e02144-16.
42. Retallack H, Di Lullo E, Arias C, Knopp KA, Laurie MT, Sandoval-Espinosa C, Mancia Leon WR, Krencik R, Ullian EM, Spatazza J, Pollen AA, Mandel-Brehm C, Nowakowski TJ, Kriegstein AR, DeRisi JL. 2016. Zika virus cell tropism in the developing human brain and inhibition by azithromycin. Proc Natl Acad Sci U S A 113:14408-14413.

43. Tang H, Hammack C, Ogden SC, Wen Z, Qian X, Li Y, Yao B, Shin J, Zhang F, Lee EM, Christian KM, Didier RA, Jin P, Song H, Ming GL. 2016. Zika Virus Infects Human Cortical Neural Progenitors and Attenuates Their Growth. Cell Stem Cell 18:587-90.
44. Chen JC, Wang Z, Huang H, Weitz SH, Wang A, Qiu X, Baumeister MA, Uzgiris A. 2016. Infection of human uterine fibroblasts by Zika virus in vitro: implications for viral transmission in women. Int J Infect Dis 51:139-140.
45. Tabata T, Petitt M, Puerta-Guardo H, Michlmayr D, Wang C, Fang-Hoover J, Harris E, Pereira L. 2016. Zika Virus Targets Different Primary Human Placental Cells, Suggesting Two Routes for Vertical Transmission. Cell Host Microbe 20:155-66.
46. Griffin BD, Muthumani K, Warner BM, Majer A, Hagan M, Audet J, Stein DR, Ranadheera C, Racine T, De La Vega MA, Piret J, Kucas S, Tran KN, Frost KL, De Graff C, Soule G, Scharikow L, Scott J, McTavish G, Smid V, Park YK, Maslow JN, Sardesai NY, Kim JJ, Yao XJ, Bello A, Lindsay R, Boivin G, Booth SA, Kobasa D, et al. 2017. DNA vaccination protects mice against Zika virus-induced damage to the testes. Nat Commun 8:15743.
47. Siemann DN, Strange DP, Maharaj PN, Shi PY, Verma S. 2017. Zika Virus Infects Human Sertoli Cells and Modulates the Integrity of the In Vitro Blood-Testis Barrier Model. J Virol 91:e00623-17.
48. Pardy RD, Rajah MM, Condotta SA, Taylor NG, Sagan SM, Richer MJ. 2017. Analysis of the T Cell Response to Zika Virus and Identification of a Novel CD8+ T Cell Epitope in Immunocompetent Mice. PLoS Pathog 13:e1006184.
49. Sacramento CQ, de Melo GR, de Freitas CS, Rocha N, Hoelz LV, Miranda M, Fintelman-Rodrigues N, Marttorelli A, Ferreira AC, Barbosa-Lima G, Abrantes JL, Vieira YR, Bastos MM, de Mello Volotao E, Nunes EP, Tschoeke DA, Leomil L, Loiola EC, Trindade P, Rehen SK, Bozza FA, Bozza PT, Boechat N, Thompson FL, de Filippis AM, Bruning K, Souza TM. 2017. The clinically approved antiviral drug sofosbuvir inhibits Zika virus replication. Sci Rep 7:40920.
50. Cortese M, Goellner S, Acosta EG, Neufeldt CJ, Oleksiuk O, Lampe M, Haselmann U, Funaya C, Schieber N, Ronchi P, Schorb M, Pruunsild P, Schwab Y, Chatel-Chaix L, Ruggieri A, Bartenschlager R. 2017. Ultrastructural Characterization of Zika Virus Replication Factories. Cell Rep 18:2113-2123.
51. Frumence E, Roche M, Krejbich-Trotot P, El-Kalamouni C, Nativel B, Rondeau P, Misse D, Gadea G, Viranaicken W, Despres P. 2016. The South Pacific epidemic strain of Zika virus replicates efficiently in human epithelial A549 cells leading to IFN-beta production and apoptosis induction. Virology 493:217-26.
52. Offerdahl DK, Dorward DW, Hansen BT, Bloom ME. 2017. Cytoarchitecture of Zika virus infection in human neuroblastoma and Aedes albopictus cell lines. Virology 501:54-62.
53. Oehler E, Watrin L, Larre P, Leparc-Goffart I, Lastere S, Valour F, Baudouin L, Mallet H, Musso D, Ghawche F. 2014. Zika virus infection complicated by Guillain-Barre syndrome--case report, French Polynesia, December 2013. Euro Surveill 19:20720.
54. Liu S, DeLalio LJ, Isakson BE, Wang TT. 2016. AXL-Mediated Productive Infection of Human Endothelial Cells by Zika Virus. Circ Res 119:1183-1189.
55. Savidis G, McDougall WM, Meraner P, Perreira JM, Portmann JM, Trincucci G, John SP, Aker AM, Renzette N, Robbins DR, Guo Z, Green S, Kowalik TF, Brass AL. 2016.

Identification of Zika Virus and Dengue Virus Dependency Factors using Functional Genomics. Cell Rep 16:232-246.
56. Wells MF, Salick MR, Wiskow O, Ho DJ, Worringer KA, Ihry RJ, Kommineni S, Bilican B, Klim JR, Hill EJ, Kane LT, Ye C, Kaykas A, Eggan K. 2016. Genetic Ablation of AXL Does Not Protect Human Neural Progenitor Cells and Cerebral Organoids from Zika Virus Infection. Cell Stem Cell 19:703-708.
57. Amorim R, Temzi A, Griffin BD, Mouland AJ. 2017. Zika virus inhibits eIF2alpha-dependent stress granule assembly. PLoS Negl Trop Dis 11:e0005775.
58. Hou S, Kumar A, Xu Z, Airo AM, Stryapunina I, Wong CP, Branton W, Tchesnokov E, Gotte M, Power C, Hobman TC. 2017. Zika virus hijacks stress granule proteins and modulates the host stress response. J Virol doi:10.1128/JVI.00474-17.
59. Valadao AL, Aguiar RS, de Arruda LB. 2016. Interplay between Inflammation and Cellular Stress Triggered by Flaviviridae Viruses. Front Microbiol 7:1233.
60. Xin QL, Deng CL, Chen X, Wang J, Wang SB, Wang W, Deng F, Zhang B, Xiao G, Zhang LK. 2017. Quantitative Proteomic Analysis of Mosquito C6/36 Cells Reveals Host Proteins Involved in Zika Virus Infection. J Virol 91:e00554-17.
61. Silveira ELV, Rogers KA, Gumber S, Amancha P, Xiao P, Woollard SM, Byrareddy SN, Teixeira MM, Villinger F. 2017. Immune Cell Dynamics in Rhesus Macaques Infected with a Brazilian Strain of Zika Virus. J Immunol 199:1003-1011.
62. Yuan L, Huang XY, Liu ZY, Zhang F, Zhu XL, Yu JY, Ji X, Xu YP, Li G, Li C, Wang HJ, Deng YQ, Wu M, Cheng ML, Ye Q, Xie DY, Li XF, Wang X, Shi W, Hu B, Shi PY, Xu Z, Qin CF. 2017. A single mutation in the prM protein of Zika virus contributes to fetal microcephaly. Science 358:933-936.
63. Simonin Y, van Riel D, Van de Perre P, Rockx B, Salinas S. 2017. Differential virulence between Asian and African lineages of Zika virus. PLoS Negl Trop Dis 11:e0005821.
64. Liu Y, Liu J, Du S, Shan C, Nie K, Zhang R, Li XF, Zhang R, Wang T, Qin CF, Wang P, Shi PY, Cheng G. 2017. Evolutionary enhancement of Zika virus infectivity in Aedes aegypti mosquitoes. Nature 545:482-486.
65. Ramaiah A, Dai L, Contreras D, Sinha S, Sun R, Arumugaswami V. 2017. Comparative analysis of protein evolution in the genome of pre-epidemic and epidemic Zika virus. Infect Genet Evol 51:74-85.
66. Sirohi D, Chen Z, Sun L, Klose T, Pierson TC, Rossmann MG, Kuhn RJ. 2016. The 3.8 A resolution cryo-EM structure of Zika virus. Science 352:467-70.
67. Ellison DW, Ladner JT, Buathong R, Alera MT, Wiley MR, Hermann L, Rutvisuttinunt W, Klungthong C, Chinnawirotpisan P, Manasatienkij W, Melendrez MC, Maljkovic Berry I, Thaisomboonsuk B, Ong-Ajchaowlerd P, Kaneechit W, Velasco JM, Tac-An IA, Villa D, Lago CB, Roque VG, Jr., Plipat T, Nisalak A, Srikiatkhachorn A, Fernandez S, Yoon IK, Haddow AD, Palacios GF, Jarman RG, Macareo LR. 2016. Complete Genome Sequences of Zika Virus Strains Isolated from the Blood of Patients in Thailand in 2014 and the Philippines in 2012. Genome Announc 4.
68. Zhao B, Yi G, Du F, Chuang YC, Vaughan RC, Sankaran B, Kao CC, Li P. 2017. Structure and function of the Zika virus full-length NS5 protein. Nat Commun 8:14762.
69. Clerzius G, Shaw E, Daher A, Burugu S, Gelinas JF, Ear T, Sinck L, Routy JP, Mouland AJ, Patel RC, Gatignol A. 2013. The PKR activator, PACT, becomes a PKR inhibitor during HIV-1 replication. Retrovirology 10:96.

70. Scarborough RJ, Levesque MV, Boudrias-Dalle E, Chute IC, Daniels SM, Ouellette RJ, Perreault JP, Gatignol A. 2014. A Conserved Target Site in HIV-1 Gag RNA is Accessible to Inhibition by Both an HDV Ribozyme and a Short Hairpin RNA. Mol Ther Nucleic Acids 3:e178.
71. Ciccarone V, Spengler BA, Meyers MB, Biedler JL, Ross RA. 1989. Phenotypic diversification in human neuroblastoma cells: expression of distinct neural crest lineages. Cancer Res 49:219-25.
72. Li T, Diao H, Zhao L, Xing Y, Zhang J, Liu N, Yan Y, Tian X, Sun W, Liu B. 2017. Identification of suitable reference genes for real-time quantitative PCR analysis of hydrogen peroxide-treated human umbilical vein endothelial cells. BMC Mol Biol 18:10.

CHAPTER IV

Downregulation of nuclear transcription factor NPAS4 and NR4A family correlates with the death of fetal mice neurons infected with ZIKV.

This chapter is adapted from the following manuscript:

Alpuche-Lazcano SP, Saliba J, Costa VV, Ribeiro LS, Blank V, Mouland AJ, Teixeira MM, and Gatignol A. 2020. “Downregulation of nuclear transcription factor NPAS4 and NR4A family correlates with the death of fetal mice neurons infected with ZIKV”. Submitted manuscript.

4.1 PREFACE

ZIKV infection triggers cytopathic effects in different cell types. We therefore hypothesize that these effects must be tightly related to changes in the transcriptome, which is regulated by changes in the RNAi pathway. In this chapter, we used different bioinformatic analyses to integrate changes in the transcriptome of fetal murine neurons infected with ZIKV to the dysregulated miRNAs produced by the infection.

4.2 ABSTRACT

Zika virus (ZIKV) infection in neurons is correlated to neurological complications and congenital malformations. To date, ZIKV tropism and pathogenesis are not entirely understood. MicroRNAs (miRNAs) are post-transcriptional regulators of cellular pathways and they contribute to cell development, disease and death. Very few researchers have reported an integrative analysis of mRNAs and miRNAs during ZIKV infection. In this study, we used microarrays to analyze gene expression levels following ZIKV infection of fetal murine neurons. We observed that the expression of transcription factors like neural PAS domain protein 4 (Npas4) and members of the orphan nuclear receptor 4 (Nr4as) was decreased after viral infection, likely affecting cellular pathways such as RNA metabolism and transcription. We next examined the expression of 3195 miRNAs in infected murine primary neurons and found that 19 miRNAs were highly dysregulated upon ZIKV infection. An integrative analysis of the differentially expressed miRNAs indicates that Npas4 and Nr4a3 could be modulated by the miRNA response. Our data identified profound abnormal regulation of novel transcriptional factors and miRNAs during ZIKV infection of fetal murine neurons.

Keywords: ZIKV, mRNAs, miRNAs, Npas4, Nr4as.

4.3 INTRODUCTION

Zika virus (ZIKV) is an emerging flavivirus transmitted by mosquitoes *Aedes aegypti*, *Aedes albopictus,* and potentially *Culex quinquefasciatus* (1). ZIKV was first isolated from sentinel rhesus monkeys in Ziika forest of Uganda in 1947 (2). By 1966, it reached Asia and remained in quietness for decades until 2013 when it was found in French Polynesia and shortly after reached Brazil, Latin America and the US (3-5). ZIKV infection triggers mild symptoms in adults such as fever, headache, rash, conjunctivitis and arthralgia (6, 7). ZIKV is also associated with neurological complications like Guillain-Barré syndrome and congenital brain abnormalities like microcephaly in neonates (8-11). To date, neither a vaccine nor a treatment is available to prevent or treat the infection (12).

ZIKV belongs to the Flaviviridae family with a single monocistronic transcript of 11kb positive RNA, which is translated into a single polyprotein. The polyprotein contains structural domains (C, prM and E) and non-structural domains (NS1, NS2A, NS2B, NS3, NS4A, NS4B and NS5) that are cleaved by the viral NS2B-NS3 protease and cellular peptidases including furin (13-16). ZIKV structural and non-structural proteins have functions similar to other flavivirus enzymes, including the RNA-dependent RNA polymerase (RdRp) and protease, but specific characteristics are involved in virus-host interactions and interfere with cell functions (17-21). The E protein of ZIKV mediates its attachment to cellular receptors like Ax1, Tim-1, Tyro3 and DC-SIGN present on the surface of various cell types, including epidermal, immune, retinal cells and neurons (22-33). This binding triggers clathrin-mediated endocytosis followed by the replication cycle in the endoplasmic reticulum (ER) presumably similar to other flaviviruses (6, 31, 34-37). To date, the interaction of ZIKV with cellular pathways like the RNA interference (RNAi) pathway is not completely explored.

The RNAi pathway is a cellular mechanism that represses messenger RNA (mRNA) expression or mediates its decay through small RNA transcripts of 22 nucleotides called micro RNA (miRNAs). In humans, more than 60% of protein-coding genes are regulated through the silencing of mRNAs by RNAi (38). MiRNAs modulate mRNAs at all times and regardless of the cell condition, from development to genetic diseases, cancer or during infections (39-44).

Few studies have explored the mRNA and miRNA expression in ZIKV infected cells (45-47) and the relationship between cellular RNA pathways and ZIKV has not been explored. Experiments on infected astrocytes revealed an upregulation of miRNAs with antiviral properties, whereas some other miRNAs were implicated in the regulation of the unfolded protein response pathway, essential for protein folding in the ER and critical for flaviviruses (45). MRNA and miRNA screening in primary murine neurons during ZIKV infection found a significant downregulation of genes involved in inflammatory responses (46). Recently, Ago2-CLIP sequencing analysis in infected human neuroprogenitor cells (NPCs) revealed miRNA-mediated repression of genes involved in neurogenesis, metabolism and stem cell maintenance (47). We and others showed that a Brazilian ZIKV isolate HS-2015-BA-01 was more cytopathic than an early Asian ZIKV strain (48, 49). Here, we infected primary murine fetal neurons with the ZIKV Brazilian strain and extracted total RNA from these neurons to determine the mRNA and miRNA profiles at 6 and 24 h of infection. We identified that Npas4 and Nr4a3 transcription factors are profoundly modulated upon ZIKV infection with a concomitant increase of miRNAs that target them.

4.4 RESULTS

4.4.1 ZIKV HS-2015-BA-01 infection induces cell death of fetal murine neurons at 24 h

We previously showed that ZIKV HS-2015-BA-01 infects around 99 % of fetal mice neurons (50). Therefore, we cultured fetal mouse neurons from the corticostriatal brain region. We performed IFs and observed that around 99% of the cultured cells were positive to NeuN, an integral marker of neurons (50, 51). We then infected or mock-infected neurons with ZIKV Brazilian isolate HS-2015-BA-01 at MOI of 1 for 6 h or 24 h. After each infection time, we carried out IFs using NeuN and 4G2 antibody (Ab), which recognizes ZIKV protein E (Fig 4.1). Experiments at 6 hpi showed a high density of neurons (NeuN, 6 h) where ~16% of cells were expressing ZIKV E protein (Fig 4.1, top panels). At 24 hpi, a considerable number of cells was decreased (≥ 50%) concomitantly with a high percentage of infection (~59 %) in the surviving cells (Fig 4.1, bottom panels).

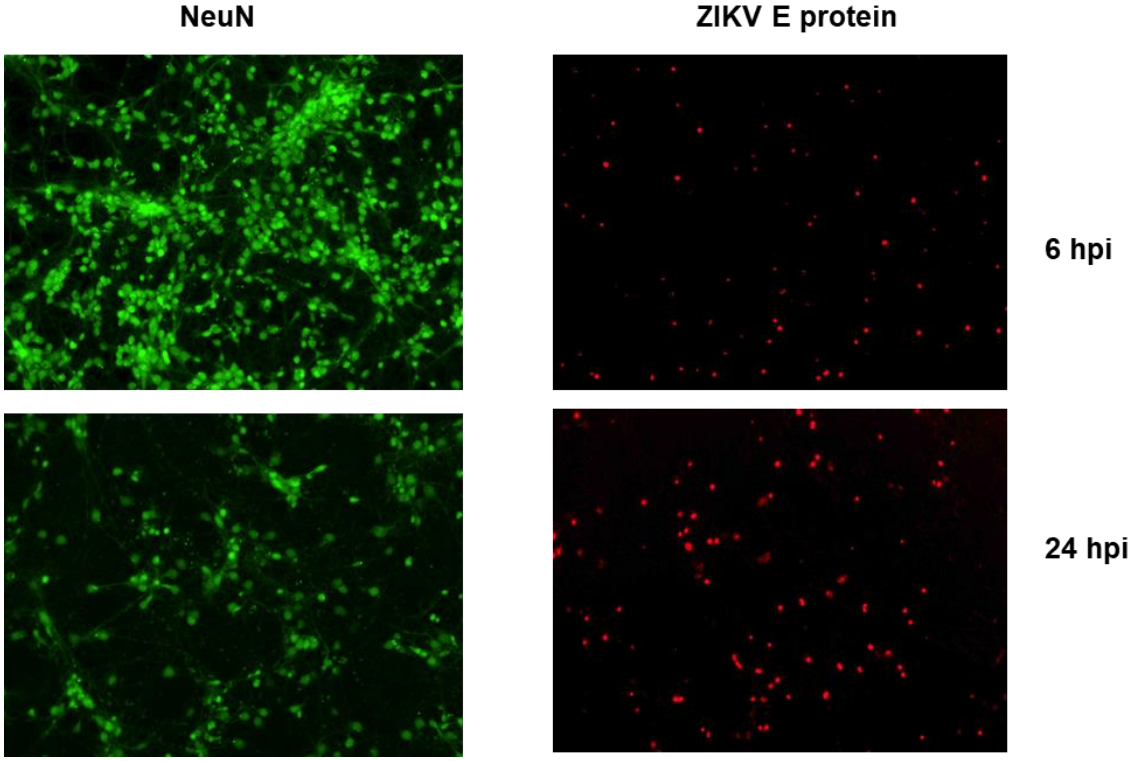

Figure 4. 1 Embryonic neurons death by ZIKV is exacerbated through the time.

Embryonic mice neurons were infected with ZIKV HS-2015-BA-01 at MOI of 1 for 6 and 24 h. After each infection time, cells were fixed and stained with the neuronal marker NeuN (green) and ZIKV E protein (red). Top panels show the infection at 6 h (~16% expressed E protein), whereas the bottom lane shows the results at 24 h (~59% expressed E protein).

4.4.2 ZIKV infection of fetal murine neurons induces downregulation of transcription factors genes

To further understand the consequences of ZIKV infection, we analyzed the transcriptome of mock-infected and infected fetal neurons. After 6 and 24 hpi at MOI of 1, we extracted RNA and performed microarrays using Affymetrix technology. We analyzed a total of 34472 genes using TAC 3.0 with a ± 2 fold cutoff and a $p \leq 0.05$ criteria to screen dysregulated genes (Fig 4.2A, B). At 6 hpi, we found that mitochondrially encoded tRNA glutamine (mt-Tq), an unannotated gene and small nucleolar RNA, H/ACA box 2B (Snora2b) were upregulated (Fig 4.2A, C, Table 1). Vomeronasal 1 receptor 14 (Vmn1r14) was the only downregulated gene at 6 hpi. In contrast, the proportion of downregulated genes at 24 hpi was higher than the upregulated genes. We observed 21 genes negatively regulated and 13 genes that were overexpressed (Fig 4.2B, C, Table 2). We noticed that the most downregulated genes were coding for transcription factors such as Npas4 and Nr4a family (Nr4a1, Nr4a2, Nr4a3) (52, 53). We also observed that the subtilisin-like protease Pcsk1 and the non-coding (nc) RNA 1700016P03Rik were downregulated at 24 hpi. Among the overexpressed genes at 24 h, we detected cyclin-dependent kinase 6 (Cdk6), heat shock protein beta-8 (Hspb8), the transcription factor (Hes5) and the Glial fibrillary acidic protein (Gfap) that were increased up to 2.4 folds in the presence of the virus (Fig 4.2D, Table 2). To determine whether the abnormal regulation of Npas4 and Nr4a family was strongly decreased at 24 hpi, we validated these genes through qRT-PCR. Our results confirmed that Npas4, Nr4a1, Nr4a2 and

Nr4a3 transcripts were profoundly affected by ZIKV infection after 24 h (Fig 4.3). Likewise, qRT-PCR results showed that Npas4 transcripts were the most affected genes after 24 hpi (Fig 4.3). Overall, our collected data demonstrate that ZIKV modifies cellular factors at 6 hpi and more substantially at 24 hpi.

A)

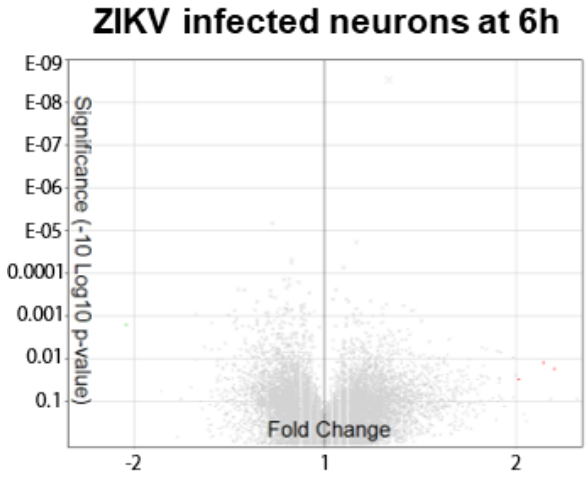

B)

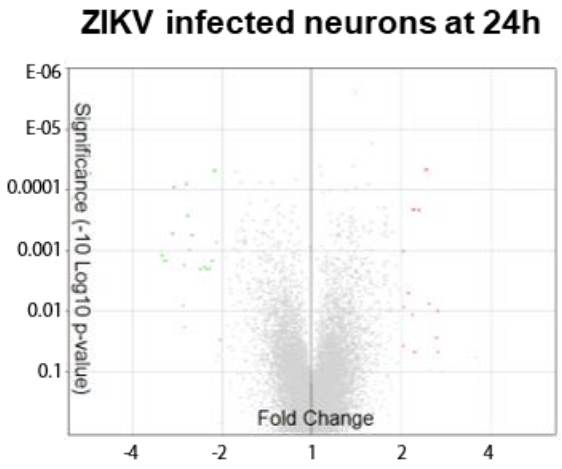

C)

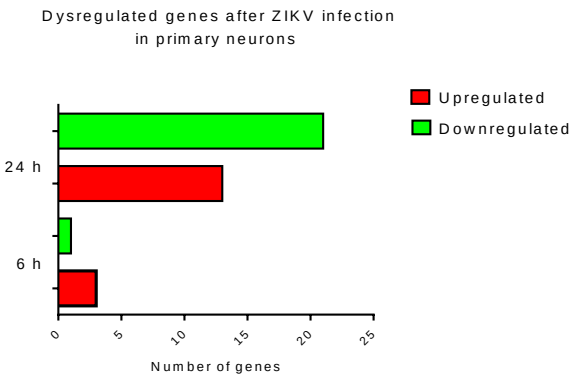

D)

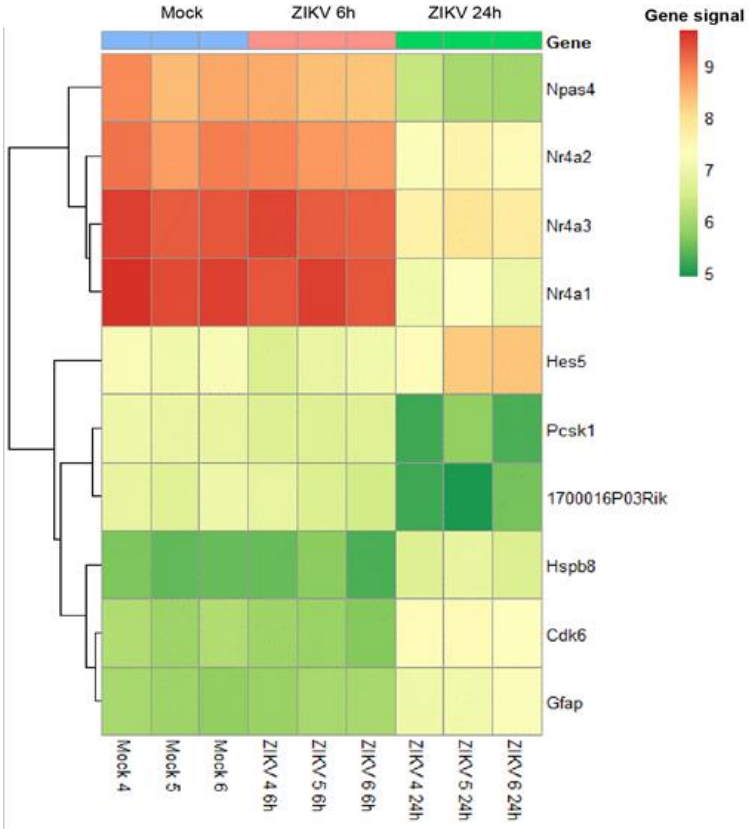

Figure 4. 2 Transcriptome analysis of ZIKV infected neurons.

Total RNA was collected after 6 or 24 h infection, and mRNA variations were analyzed by microarrays. (A and B) Volcano plot of differentially expressed genes after ZIKV infection at 6 h (A) and 24 h (B). Green (downregulated) and red (upregulated) dots represent differentially expressed genes with ≥ 2 fold. (C) The number of dysregulated genes ≥ 2 fold change and $p<0.05$. (D) Clustered heat map with the top 10 dysregulated genes at 24 h and its comparison at 6 h. The scale located next to the heatmap represents the gene signal.

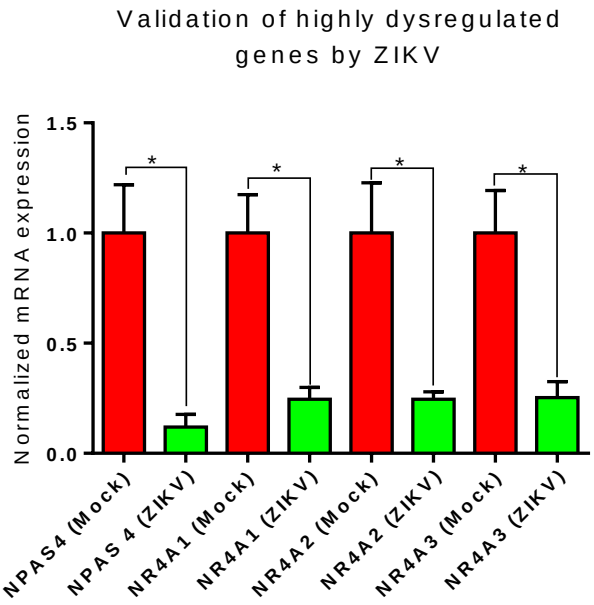

Figure 4. 3 QRT-PCR validation for Npas4 and Nr4a family.

QRT-PCR was compared to microarray readouts for Npas4, Nr4a1, Nr4a2 and Nr4a3 at 24 hpi in fetal murine neurons. Error bars represent the standard deviation of three independent experiments. Ordinary one-way ANOVA was used to assess significance where * represents a $p < 0.05$.

Table 4. 1 Dysregulated host genes (≥2 fold change) found in primary neurons infected with ZIKV 6 hpi.

Gene Symbol	Fold Change	p-value
Mt-tq	2.3	0.017035
(Not annotated gene)	2.21	0.012189
Snora2b*	2.02	0.029254
Vmn1r14	-2.06	0.001573

* We found miRNAs or other non-coding RNAs in Affymetrix MoGene 2.0 array, however, the array is not optimized for miRNA and ncRNAs and the results must be taken cautiously.

Table 4. 2 Dysregulated host genes (≥2 fold change) found in primary neurons infected with ZIKV 24 hpi.

Gene Symbol	Fold Change	p-value
Gm22973	2.65	0.047978
(Not annotated gene)	2.64	0.009879
Gm22149	2.63	0.027418
Gm10115	2.47	0.007535
Cdk6	2.42	0.000046
Hspb8	2.28	0.000214
Hes5	2.21	0.047549
Gfap	2.19	0.000211
Mir3962*	2.17	0.01149
Far2	2.11	0.004998
Sphkap	2.03	0.008542
Rgs6	2.03	0.001037

Cyp2d40	2.02	0.037422
Gm5373	-2.03	0.029575
Fosl2	-2.09	0.000727
Prdm10	-2.12	0.000048
Capn6	-2.16	0.001462
Trib1	-2.2	0.001976
Vtn	-2.24	0.002113
Ccdc184	-2.28	0.001893
Rem2	-2.36	0.002004
Per1	-2.52	0.00056
Rgs4	-2.57	0.000977
Rel	-2.61	0.000268
N-r5s54	-2.63	0.00008
Mir186*	-2.67	0.018179
Rgs2	-2.68	0.001718
(not annotated gene)	-2.69	0.008003
Nr4a3	-2.9	0.000091
Nr4a2	-2.93	0.000525
1700016p03rik*	-3.1	0.001467
Pcsk1	-3.18	0.001203
Nr4a1	-5.55	0.000054
Npas4	-6.32	0.00014

* We found miRNAs or other ncRNAs in Affymetrix MoGene 2.0 array, however, the array is not optimized for miRNA and ncRNAs and the results must be taken cautiously.

4.4.3. The neuronal system pathway and the metabolism-transcription of RNA pathway are disturbed upon ZIKV infection in murine primary neurons.

To investigate the correlation between the atypical regulated genes by ZIKV with the possible impact within the infected cell, we performed GSEA from 34472 genes. GSEA uses a set of genes and correlates those genes with possible cellular pathways. We identified that the ranked genes at 6 hpi were related to the neuronal system and metabolism of RNA pathways (Fig 4.4). The neuronal system pathway embraces events of transmission across electrical synapses, transmission across chemical synapses, potassium channels and protein-protein interactions at synapses that are affected (54). Metabolism of RNA had the highest ratio of genes; this pathway encompasses the mRNA processing and export from the nucleus to the cytoplasm (55).

Furthermore, GSEA at 24 hpi identified that neuronal system and metabolism of RNA were still affected (Fig 4.5A, B, C, E). Additionally, GSEA correlated a cluster to the gene expression pathway within transcriptional events (Fig 4.5A, D, E) (56). This pathway displayed 15 new genes that were not modified at 6 h, especially the NR4A family that was drastically downregulated at 24 h (Fig 4.5E, Table 2). Therefore, GSEA showed that the neuronal system and metabolism of RNA are perturbed at early and late phases of infection. The gene transcription pathway is largely affected at 24 hpi and our data suggest that the downregulation of neuronal transcriptional factors like the Nr4a might play a significant role in the cytopathic effects of the infection.

A)

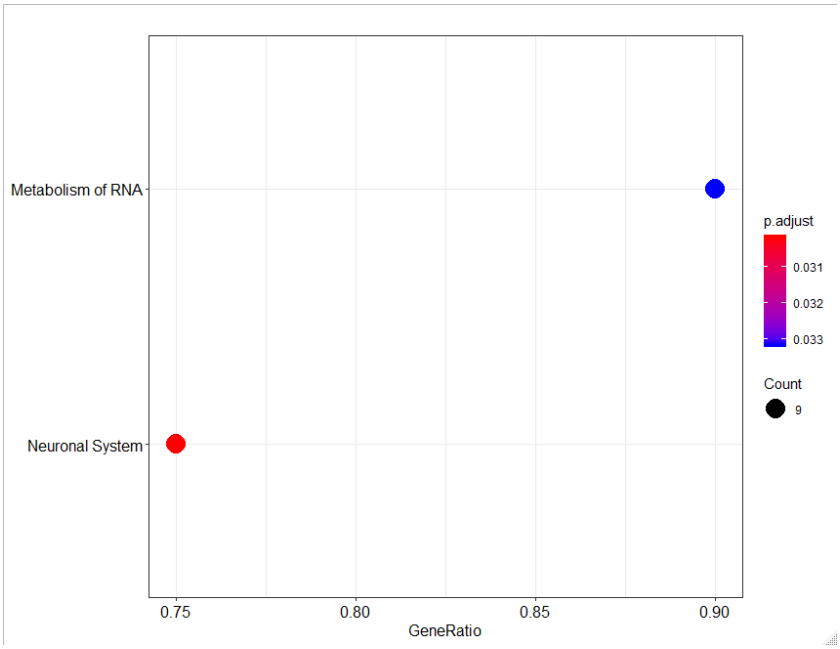
Metabolism of RNA
Neuronal System
0.75
0.80
0.85
0.90
GeneRatio
p.adjust
0.031
0.032
0.033
Count
9

B)

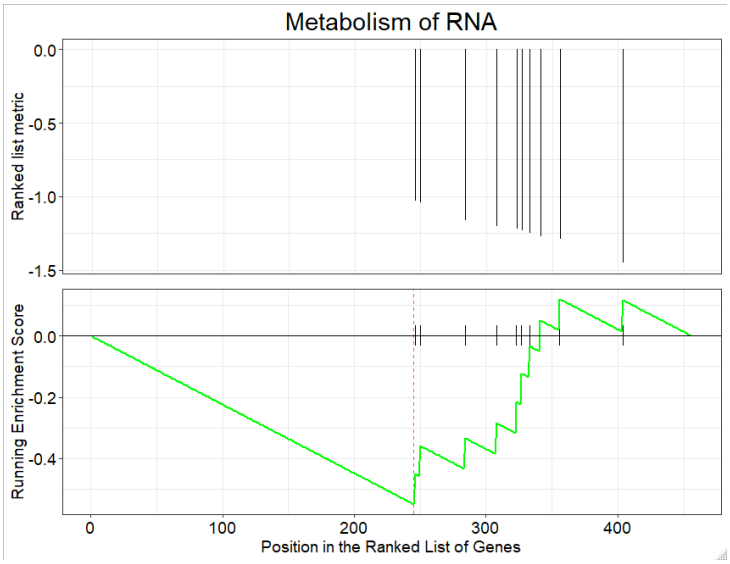
Metabolism of RNA
Ranked list metric
0.0
-0.5
-1.0
-1.5
Running Enrichment Score
0.0
-0.2
-0.4
0
100
200
300
400
Position in the Ranked List of Genes

C)

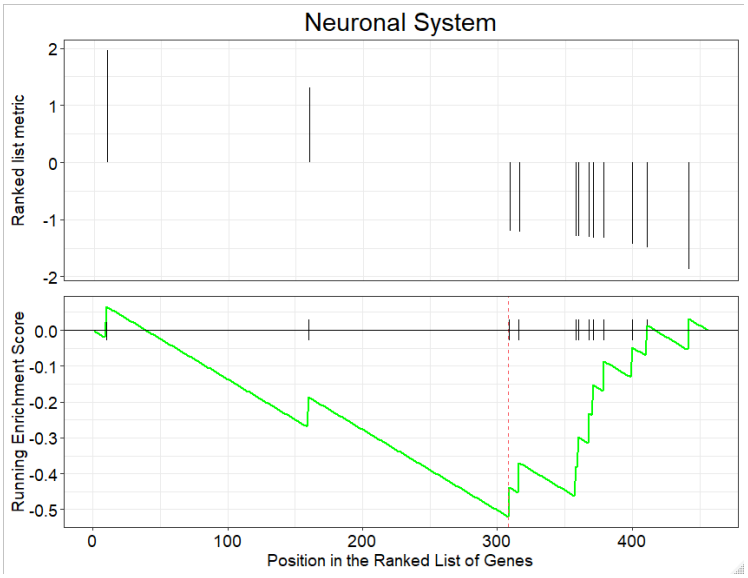

D)

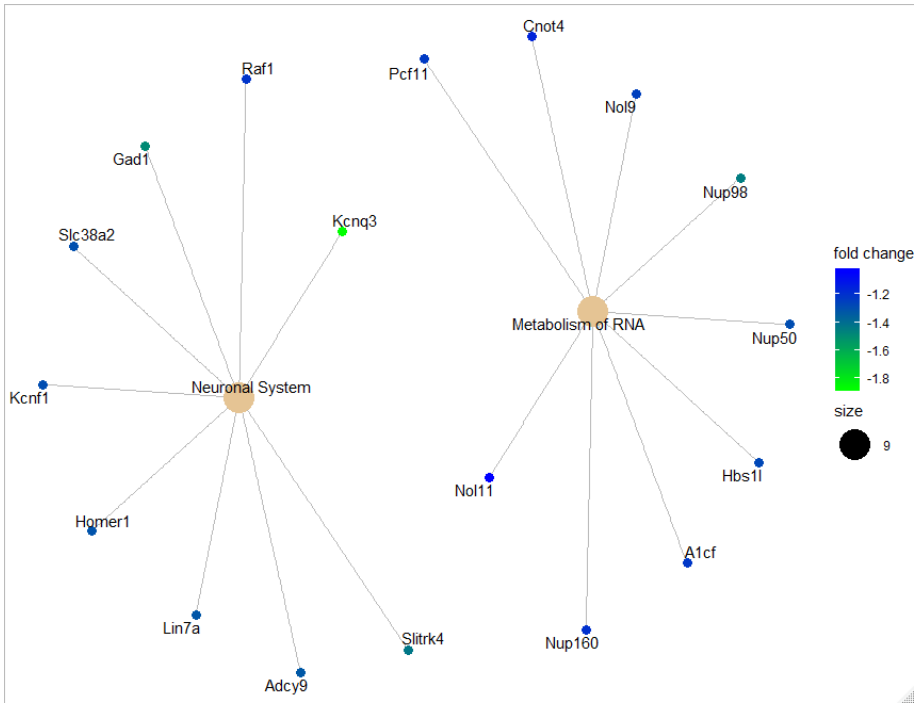

Figure 4. 4 GSEA of putative mRNAs at 6 hpi with ZIKV.

(A) Dotplot of inferred pathways at 6 hpi. The size of the circles represents the number of dysregulated genes and the color represents the p-value. The y-axis displays the pathways by the dysregulated gene expression, whereas the x-axis shows the fold enrichment. (B and C) GSEA plot analysis of ranked genes in the metabolism of RNA and neuronal system. The top graph represents cluster of genes into the chosen pathway whereas the bottom panel reflects up and

downregulated genes. (D) Gene-Concept Network depicting the linkages of genes and biological concepts (metabolism of RNA and neuronal system) as a network. Only core enriched genes are displayed.

A)

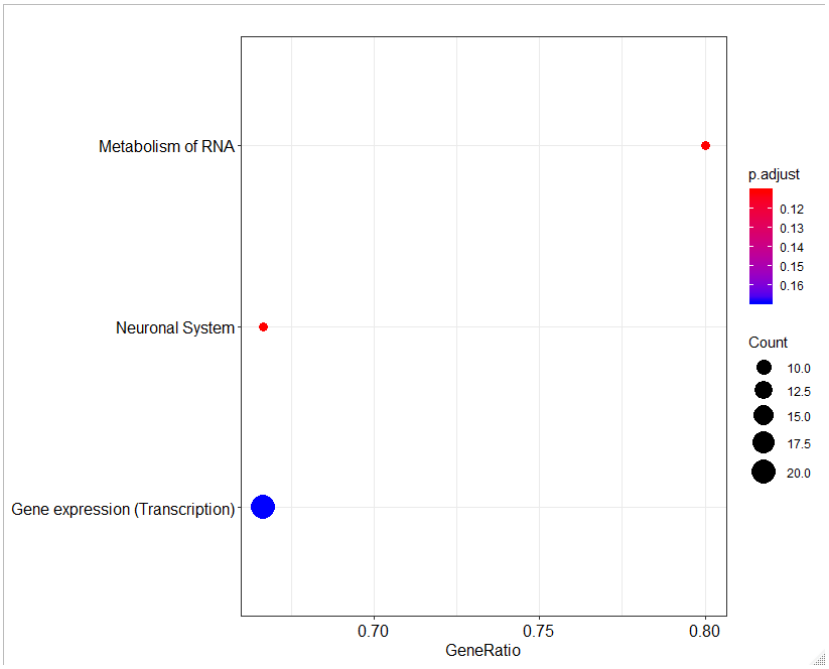

B)

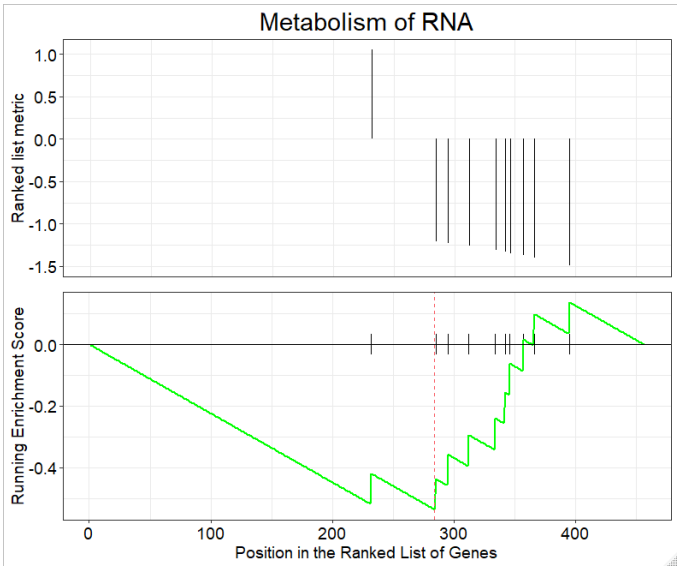

C)

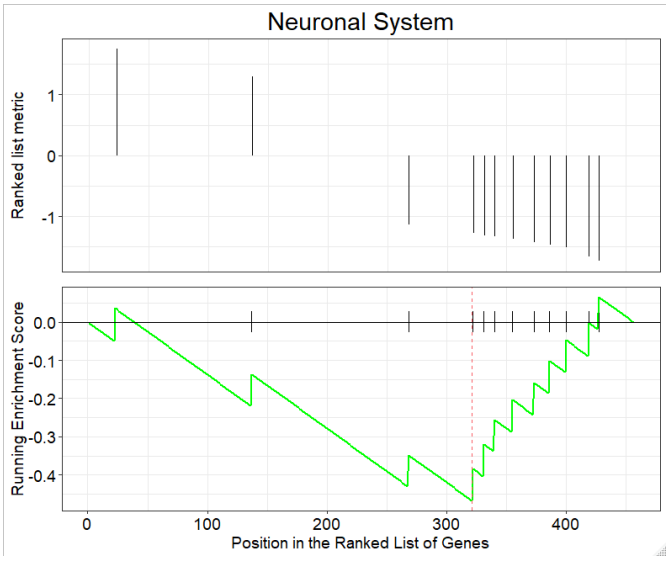

D)

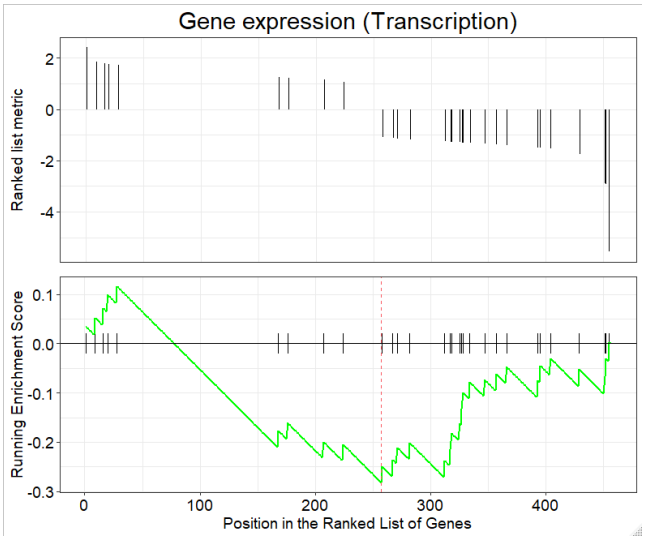

E)

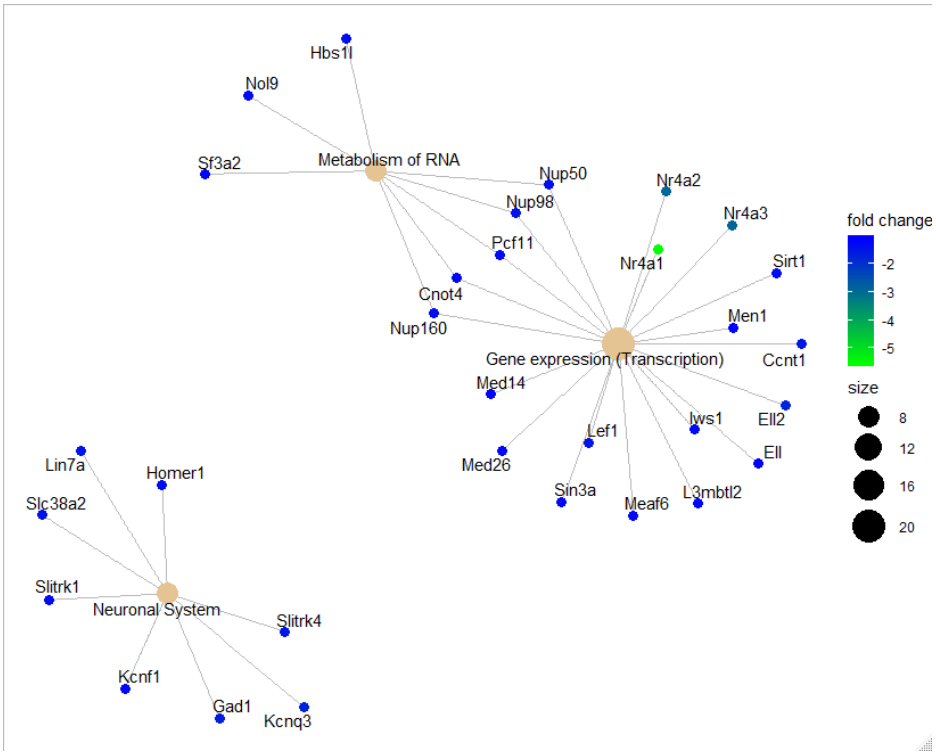

Figure 4. 5 GSEA of putative mRNAs at 24 hpi with ZIKV.

(A) Dotplot of inferred pathways at 24 hpi. The size of the circles represents the number of dysregulated genes and the color represents the p-value. The y-axis displays the pathways by the

dysregulated gene expression, whereas the x-axis shows the fold enrichment. (B, C and D) GSEA plot analysis of ranked genes in the metabolism of RNA, neuronal system and gene expression. The top graph represents cluster of genes into the chosen pathway whereas the bottom panel reflects up and downregulated genes. (E) Gene-Concept Network depicting the linkages of genes and biological concepts (metabolism of RNA, neuronal system and transcription) as a network. Only core enriched genes are displayed.

4.4.4. Infected fetal murine neurons with ZIKV show dysregulation of specific miRNAs

We then wanted to determine whether miRNAs could contribute to the disruption of gene expression in the infected neurons. Using Affymetrix GeneChip miRNA 4.0 and TAC 3.0, we analyzed a total of 3195 miRNAs and filtered those with more or less than 2 fold change and a $p \leq 0.05$. After six hours of infection, we found that three miRNAs were differentially expressed. MiR-Let-7b-3p was upregulated, whereas miR-670-3p and miR3068-5p had lower expression than mock (Fig 4.6A, C, D Table 4.3).

Conversely, after 24 h of infection, nine miRNAs were upregulated and seven were downregulated (Fig 4.6B, C, D, Table 4.4). This information allowed us to explore the correlation between miRNAs and the changes in the transcriptome at similar times. We first sought to identify the predicted targets of the dysregulated miRNAs (Supplementary S1) at 6 and 24 hpi using miRDB, Target Scan and Affymetrix TAC 3.0. MiR-Let-7b-3p at 6h had 1380 predicted targets, whereas the two downregulated miRNAs could target a total of 1137 genes, but no gene correlation was found at 6 hpi. We then analyzed the targets of 9 upregulated and 7 downregulated miRNAs at 24 h. From a total 4071 predicted targets from the upregulated miRNAs, we identified a correlation between Npas4, Nr4a3, Rgs2 and Capn6 with the expression of miR-1945, miR-7116-5p, miR-7013-5p, miR-Let-7d-3p and miR-493-3p (Table 4.5). Interestingly, we noticed that two different

miRNAs, miR-7116-5p, miR-7013-5p target Nr4a3. This result suggests a possible transcriptional regulation of Nr4a3 by miRNAs. We followed our analysis with the 7 downregulated miRNAs, which generated a total of 2005 potential targets (Supplementary S1). Among them, Cdk6 and Rgs6 (Table 4.2) could be modulated by miR-3084-3p and miR-7111, respectively (Table 4.5).

A)

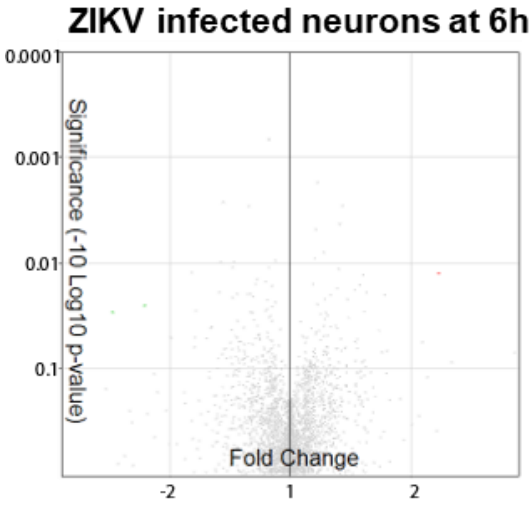

B)

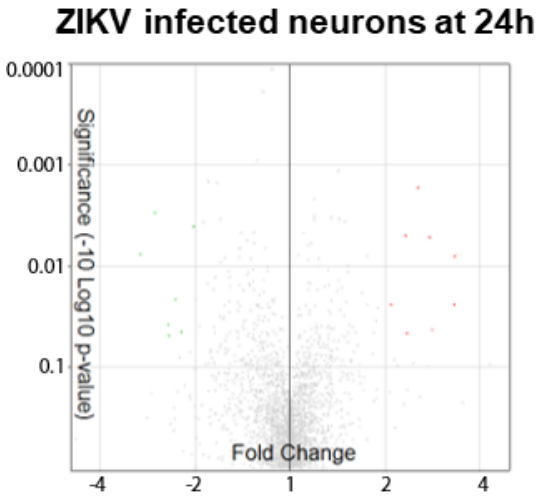

C)

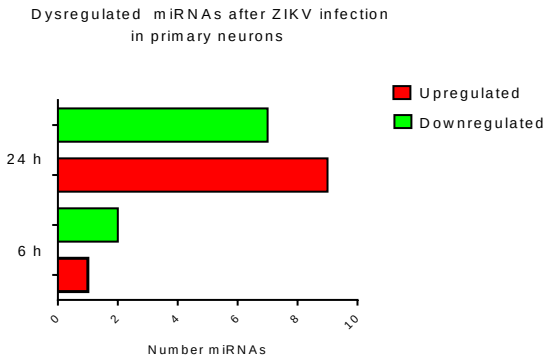

D)

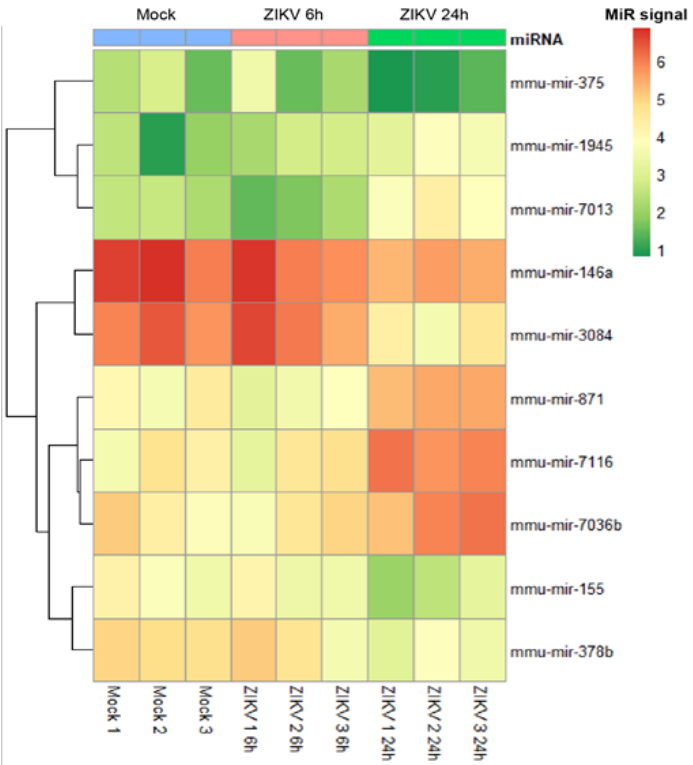

Figure 4. 6 miRNA analysis of ZIKV infected neurons.

Total RNA was collected after the infection time points and the miRNA expression was analyzed by microarrays. (A and B) Volcano plot of differentially expressed miRNAs after ZIKV infection at 6 h (A) and 24 h (B). Green (downregulated) and red (upregulated) represent differentially expressed miRNAs with ≥2 fold change in the expression. (C) Dysregulated genes with ≥2 fold change and $p<0.05$, green represents downregulated miRNAs and red the upregulated miRNAs. (D) Clustered heat map with the top 10 dysregulated miRNAs at 24 h and its comparison at 6 h.

Table 4. 3 Dysregulated miRNAs (≥2 fold change) found in primary neurons infected with ZIKV 6 hpi.

miRNA	Fold Change	p-value
miR-Let-7b-3p	2.35	0.012478
mR-670-3p	-2.31	0.025462
miR-3068-5p	-2.78	0.029233

Table 4. 4 Dysregulated miRNAs (≥2 fold change) found in primary neurons infected with ZIKV 24 hpi.

miRNA	Fold Change	p-value
miR-7116-5p	3.32	0.008014
miR-1945	3.31	0.024117
miR-7036b-5p	2.82	0.04231
miR-871-5p	2.77	0.005192
miR-7013-5p	2.54	0.001682
miR-493-3p	2.35	0.046602
miR-465c-1	2.32	0.005
miR-465c-2	2.32	0.005
miR-Let-7d-3p	2.09	0.024243
miR-711	-2.02	0.004064

miR-7083-5p	-2.21	0.044813
miR-146a-5p	-2.31	0.021464
miR-375-3p	-2.42	0.048949
miR-155-5p	-2.43	0.037988
miR-378b	-2.67	0.002953
miR-3084-3p	-2.99	0.007623

Table 4. 5 miRNA predicted dysregulated targets

Upregulated miRNAs at 24h	MiRNA fold change	Downregulated target	Target fold change
miR-1945	3.31	Npas4	-6.32
miR-7116-5p	3.32	Nr4a3	-2.9
miR-7013-5p	2.54	Nr4a3	-2.9
miR-Let-7d-3p	2.09	Rgs2	-2.68
miR-493-3p	2.35	Capn6	-2.16
Downregulated miRNAs at 24h	MiRNA fold change	Upregulated target	Target fold change
miR-3084-3p	-2.99	Cdk6	2.42
miR-711	-2.02	Rgs6	2.03

4.5 DISCUSSION

To investigate the consequences of ZIKV infection with an early Brazilian strain during neurogenesis, we infected mice embryonic neurons with HS-2015-BA-01 and extracted total RNA at 6 and 24 h to evaluate the changes in the transcriptome and the miRNA profile (Fig 4.1). Our first observation in the transcriptome at 6 hpi demonstrated the influence of ZIKV in few genes (Fig 4.2A, C). In contrast, the number of genes that had a change in their mRNA expression was considerably heightened at 24 hpi (Fig 4.2B, C). Among these genes, we observed that

transcription factors from the Npas and the Nr4a family were strongly downregulated (Fig 4.2D, Table 4.2).

Npas4 and Nr4as belong to immediate-early genes (IEG), which can be stimulated in different regions of the brain in response to physiological stimuli (calcium influx, nerve growth factors) or pathological stimuli (inflammatory agents like TNF-α, or lipopolysaccharide LPS) (52, 53). Npas4 is only transcribed into neurons and it regulates the response of neuronal excitation through the balance of inhibitory and excitatory synapses (57). The disruption of this balance is related to neurological disorders like schizophrenia, autism, anxiety and depression (58, 59). Npas4 plays a key role during neuronal development and differentiation in embryonic and postnatal growth (60-62). The expression of Npas4 influences around 300 genes, among which more than half are linked to neurological activity (57). In our studies, the infection of neurons with ZIKV downregulated the transcription of Npas4 by ~6 fold change, which suggests a profound dysregulation in neuronal functions (Fig 4.2D, Table 4.2).

The IEGs, Nr4as (Nr4a1, Nr4a2 and Nr4a3) like Npas4 play an essential role in the homeostasis and response due to external stimuli (52, 53). Each member behaves differently in distinct tissues. For instance, Nr4a1 or Nur77 induces apoptosis in T-cells and macrophages (53, 63, 64) but also mediates the neuroprotector cAMP response element-binding protein (CREB) and promotes the synaptic remodeling in neurons (53, 65-67). Nr4a2 (Nurr1) plays an essential role as neuroprotector and mutations or absence of the gene are associated with dysfunction in neuronal development and chronic pathologies like Parkinson's disease (68, 69). Similarly, Nr4a3 (NOR-1) is abundant, but its reduction significantly affects neuronal survival and axon guidance (70). Thus, we showed that the infection of ZIKV was pivotal for the decrease of Nr4as transcript levels or stability (Fig 4.2D, Table 4.2).

Due to the relevance of these genes in neurons in different contexts, we performed qRT-PCR assays to validate them (Fig 4.3). QRT-PCR demonstrated similar results than using microarrays, showing a deep decrease in Npas4 and Nr4as. Notably, Npas4 was the most downregulated gene in both techniques (Fig 4.2D and 4.3). Overall, using two different approaches we confirmed that Npas4 and Nr4a genes were profoundly affected at 24 hpi with ZIKV.

To understand the influence of the dysregulated genes by ZIKV, we performed GSEA using the 34472 genes contained in Mouse Gene ST 2.0 array. We consistently observed the neuronal system and metabolism of RNA pathways being affected at both time points and the transcription pathway only at 24 hpi (Fig 4.4 and 4.5). The strong downregulation of Nr4as at 24h could influence the transcription pathway, which likely affects hundreds of genes (Fig 4.4E). Of note, Npas4 was not present in any of the cellular pathway databases we assessed.

Multiple factors can influence the abnormal regulation of genes after viral infection. MiRNAs are master regulators of posttranscriptional gene activity and their activity modifies cell development, disease and survival (71-74). In neurons, miRNA activity is critical by its contribution to the modulation of different processes like synapse development, axon guidance, neurogenesis and aging (75-78). We analyzed expression levels of a total of 3195 miRNAs and we identified significant changes during ZIKV infection. Our analysis at 6 hpi showed an upregulation of miR-Let-7b-3p (Table 3). Netrin-1 (Ntn1) is an axon guidance factor that governs the neuronal migration and increased levels of this protein are linked to cell survival and axon regeneration (79, 80). Another report found miR-Let7 negatively regulates Ntn1, causing a decrease in the axon outgrowth (78). Therefore, the early overexpression of Let-7b and the inhibition of axon spread might contribute to the ZIKV pathogenesis and cell death.

Few studies have profiled an integrative analysis of mRNAs and miRNAs in infected ZIKV embryonic neurons or human neuronal stem cells (NSC) (46, 47). The integrative study from previous works demonstrated that the inflammatory, apoptotic, cell cycle, neurogenesis, stem cell maintenance, and metabolism are potentially affected by miRNAs due to ZIKV infection from 12 h to 3 days post-infection (46, 47). Interestingly, the integrative networks of the ZIKV-modulated mRNAs by miRNAs had upregulated factors such as TP53 or Cdk6 that can be downregulated by multiple miRNAs (47). Our miRNA data at 24 h showed a significant number of differences between control and infected cells (Fig 4.6B, C, D). Among the miRNAs with more than two-fold change, we came across miR-3084-3p that had a reduced expression (Fig 4.6D, Table 4.4). Our integrative analysis correlated miR-3084-3p with augmented levels of Cdk6 (Supplementary S1 and Table 4.5). Moreover, our integrative study demonstrated that the 2.9 fold downregulation of Nr4a3 could be attributed to the increased expression of miR-7116-5p and miR-7013-5p (Fig 4.2D, 4.6D, Table 4.5). On the other hand, the overexpression of miR-1945 might contribute to the 6.3 fold decrease of Npas4, but certainly, additional factors could be involved (Fig 4.2D, 4.6D, Table 4.5).

In conclusion, we discovered novel potential factors that influence the pathogenesis of ZIKV in murine fetal neurons. Our results indicate that the downregulation of transcriptional factors like Npas4 and Nr4a family could affect the RNA transcriptional pathway where some of its components may interrelate with miRNAs.

4.6 MATERIALS AND METHODS

4.6.1.Neuronal cell cultures

C57BL/6 mice (25-30g were housed at 23°C on a 12 hours (h) light/12 h dark cycle following the recommendations of the Brazilian Government (law 11794/2008a) and approved by the Committee on Animal Ethics of the UFMG (CEUA/UFMG, permit protocol no. 242/2016). Mice embryos on day 15 were dissected to prepare cerebral cortex and striatal region. After tissue digestion and dissociation, neurons were plated on previously polyL-ornithine-coated dishes with Neurobasal® medium supplemented with N2 and B27, 2 mM GlutaMAX, penicillin-streptomycin (50 µg/mL each), for five days as previously described (50, 81).

4.6.2. ZIKV strain and virus infection

ZIKV strain HS-2015-BA-01 was passaged in *Aedes albopictus* C6/35 mosquito cell lines and titrated as described (48, 81, 82). Embryonic mice neurons were infected at MOI of 1 with HS-2015-BA-01 or mock-infected. After 1 h, the infection medium was removed and replaced with fresh supplemented neurobasal medium (Thermo Fisher Scientific). Mock and infected cells were maintained for 6 h and 24 h (50).

4.6.3. Immunofluorescence (IF) and imaging

IFs and imaging have been described elsewhere (50). Briefly, mock and infected embryonic neurons at 6 h and 24 h were fixed with 4% formaldehyde for 30 min, washed with PBS and permeabilized with Triton-X (0.3%). Mouse anti-4G2 (1:300) and mouse anti-NeuN (1:500) were added to coverslips and incubated overnight at 4°C according to (50). Cells were washed with PBS and incubated with goat anti-mouse (Alexa 546) for 1h. NucBlue™ was used to label nuclei with DAPI. Zeiss LSM 880

confocal microscope equipped with a 40×/1.30 oil DIC M27 objective was used for imaging acquisition.

4.6.4. RNA extraction

RNA was extracted from primary neurons, mock and infected cells with HS-2015-BA-01 at 6 h and 24 h in triplicates. The RNA extraction was performed using TRIzol reagent (Invitrogen) and precipitated with anhydrous ethanol as described (48). Total RNA was centrifuged and resuspended in Ultrapure DNase/RNase-free distilled water (Invitrogen) followed by purification through miRNeasy mini kit columns (QIAGEN). RNase-free DNase set (QIAGEN) was added onto the columns to eliminate any trace of DNA. Total RNA was collected from the column using 50 µl of ultrapure distilled water. The collected RNA was precipitated using 50 µl of ammonium acetate, 5 µl of glycogen molecular grade (Thermo Fisher Scientific) and 700 µl of anhydrous ethanol at -80°C for one hour followed by 30 min of centrifugation at 13,200 rpm. We washed the pellet once with ice-cold ethanol 70%, dried and diluted in ultrapure distilled water to reach a 3 µg/25 µl concentration required by Genome Quebec for microarray analysis. The RNA concentration was measured with a Spectrophotometer/Fluorometer (DeNovix, DS-11 FX+).

4.6.5. Affymetrix microarray chips, Expression Console (EC) and Transcription Analysis Console (TAC) analysis

RNA samples at 3 µg/25 µl were analyzed by Genome Quebec, Montreal, Canada. Mouse Gene ST 2.0 arrays from Affymetrix were used for mRNA and GeneChip miRNA 4.0 (Affymetrix) Array (Mouse) for miRNAs. Our readouts were downloaded from Genome Quebec server and analyzed with Expression Console (EC) software (Affymetrix) to assess the quality metrics such as absolute deviation residuals, relative log expression and pos_neg_AUC to estimate the correct positive rate.

After a quality assessment, samples were analyzed with the Transcriptome Analysis Console (TAC 3.0, Affymetrix). We adjusted a ± 2 fold cutoff with a $p \leq 0.05$ (ANOVA) to filter all genes and miRNAs in mock, ZIKV 6 h and 24 h samples.

4.6.6. Quantitative Reverse Transcription Polymerase Chain Reaction (qRT-PCR)

After RNA extraction from fetal murine cells infected or mock-infected with HS-2015-BA-01 at 24 h, a 1000 ng were utilized to synthesize complementary DNA (cDNA) using Superscript II (Invitrogen) according to the manufacturer's protocol. qPCR was carried out by diluting cDNA from mock or infected cells (1:60) due to the comparison with the quantification cycle (Cq) values from the standard curve of Npas4 and Nr4as genes. BrightGreen 2X qPCR MasterMix (ABM) and CFX96 thermocycler (Bio-Rad) were used to perform the qPCR assay. Npas4, Nr4a1, Nr4a2 and Nr4a3 primers were designed for this work. Npas4 Forward (F) 5'ACCTAGCCCTACTGGACGTT 3', Reverse (R) 5' CGGGGTGTAGCAGTCCATAC3' (99 bp product length). Nr4a1 F5'CGGCCCATTAGATGAGACCC3', R 5' GTTGGGTGTAGATGGCGAGG3' (85 bp product length). Nr4a2 F 5'TGGTTCGCACGGACAGTTTA3', R 5'GGGCACTGATCAGACTCACC3' (108 bp product length). Nr4a3 F 5'AGGGCTTCTTCAAGAGAACGG3', R 5' TACTGACATCGGTTTCGGCG3' (100 bp product length). Primers for TATA-box binding protein (Tbp) and eukaryotic translation elongation factor 2 (Eef2) were used as internal controls as previously described (83, 84). qPCR conditions were as follows: 95 ℃ for 5 min followed by 49 cycles of 95 ℃ for 10 s, 60 ℃ for 15 s, 72 ℃ for 5 s. Finally, one cycle of 65 ℃ for 5 s and one of 95 ℃ for 50 s. Data analysis was performed using Bio-Rad CFX maestro (Bio-Rad) and GraphPad Prism 6 (GraphPad Software).

4.6.7. Gene set enrichment analysis (GSEA)

GSEA was performed using normalized expression files (EC and TAC 3.0) from Affymetrix Mouse Gene ST 2.0 arrays and R packages ReactomePA (85) and clusterProfiler (86) with default settings.

4.6.8.Targetome analysis

Differentially expressed miRNAs at 6 and 24 h post-infection (pi) were analyzed with three databases of predicted targets to correlate dysregulated genes of infected ZIKV neurons found in Mouse Gene ST 2.0. We used miRDB (87), Target scan (38, 88-91) and Affymetrix TAC 3.0 to generate targets at 6 and 24 hpi to identify identical genes present into the gene array files.

4.7 REFERENCES

1. Guedes DR, Paiva MH, Donato MM, Barbosa PP, Krokovsky L, Rocha S, Saraiva K, Crespo MM, Rezende TM, Wallau GL, Barbosa RM, Oliveira CM, Melo-Santos MA, Pena L, Cordeiro MT, Franca RFO, Oliveira AL, Peixoto CA, Leal WS, Ayres CF. 2017. Zika virus replication in the mosquito Culex quinquefasciatus in Brazil. Emerg Microbes Infect 6:e69.
2. Dick GW, Kitchen SF, Haddow AJ. 1952. Zika virus. I. Isolations and serological specificity. Trans R Soc Trop Med Hyg 46:509-20.
3. Hancock WT, Marfel M, Bel M. 2014. Zika virus, French Polynesia, South Pacific, 2013. Emerg Infect Dis 20:1960.
4. Liu ZY, Shi WF, Qin CF. 2019. The evolution of Zika virus from Asia to the Americas. Nat Rev Microbiol 17:131-139.
5. Massad E, Burattini MN, Khan K, Struchiner CJ, Coutinho FAB, Wilder-Smith A. 2017. On the origin and timing of Zika virus introduction in Brazil. Epidemiol Infect 145:2303-2312.
6. Relich RF, Loeffelholz M. 2017. Zika Virus. Clin Lab Med 37:253-267.
7. Zanluca C, Melo VC, Mosimann AL, Santos GI, Santos CN, Luz K. 2015. First report of autochthonous transmission of Zika virus in Brazil. Mem Inst Oswaldo Cruz 110:569-72.
8. Faizan MI, Abdullah M, Ali S, Naqvi IH, Ahmed A, Parveen S. 2016. Zika Virus-Induced Microcephaly and Its Possible Molecular Mechanism. Intervirology 59:152-158.
9. Brasil P, Pereira JP, Jr., Moreira ME, Ribeiro Nogueira RM, Damasceno L, Wakimoto M, Rabello RS, Valderramos SG, Halai UA, Salles TS, Zin AA, Horovitz D, Daltro P, Boechat M, Raja Gabaglia C, Carvalho de Sequeira P, Pilotto JH, Medialdea-Carrera R, Cotrim da Cunha D, Abreu de Carvalho LM, Pone M, Machado Siqueira A, Calvet GA, Rodrigues Baiao AE, Neves ES, Nassar de Carvalho PR, Hasue RH, Marschik PB, Einspieler C, Janzen C, et al. 2016. Zika Virus Infection in Pregnant Women in Rio de Janeiro. N Engl J Med 375:2321-2334.
10. Adebanjo T, Godfred-Cato S, Viens L, Fischer M, Staples JE, Kuhnert-Tallman W, Walke H, Oduyebo T, Polen K, Peacock G, Meaney-Delman D, Honein MA, Rasmussen SA, Moore CA. 2017. Update: Interim Guidance for the Diagnosis, Evaluation, and Management of Infants with Possible Congenital Zika Virus Infection - United States, October 2017. MMWR Morb Mortal Wkly Rep 66:1089-1099.
11. Dos Santos T, Rodriguez A, Almiron M, Sanhueza A, Ramon P, de Oliveira WK, Coelho GE, Badaro R, Cortez J, Ospina M, Pimentel R, Masis R, Hernandez F, Lara B, Montoya R, Jubithana B, Melchor A, Alvarez A, Aldighieri S, Dye C, Espinal MA. 2016. Zika Virus and the Guillain-Barre Syndrome - Case Series from Seven Countries. N Engl J Med 375:1598-1601.
12. Zou J, Shi PY. 2019. Strategies for Zika drug discovery. Curr Opin Virol 35:19-26.
13. Shi Y, Gao GF. 2017. Structural Biology of the Zika Virus. Trends Biochem Sci 42:443-456.
14. Ye Q, Liu ZY, Han JF, Jiang T, Li XF, Qin CF. 2016. Genomic characterization and phylogenetic analysis of Zika virus circulating in the Americas. Infect Genet Evol 43:43-9.
15. Pierson TC, Diamond MS. 2012. Degrees of maturity: the complex structure and biology of flaviviruses. Curr Opin Virol 2:168-75.

16. Barrows NJ, Campos RK, Liao KC, Prasanth KR, Soto-Acosta R, Yeh SC, Schott-Lerner G, Pompon J, Sessions OM, Bradrick SS, Garcia-Blanco MA. 2018. Biochemistry and Molecular Biology of Flaviviruses. Chem Rev 118:4448-4482.
17. Lee JK, Shin OS. 2019. Advances in Zika Virus(-)Host Cell Interaction: Current Knowledge and Future Perspectives. Int J Mol Sci 20:E1101.
18. Chung KM, Liszewski MK, Nybakken G, Davis AE, Townsend RR, Fremont DH, Atkinson JP, Diamond MS. 2006. West Nile virus nonstructural protein NS1 inhibits complement activation by binding the regulatory protein factor H. Proc Natl Acad Sci U S A 103:19111-6.
19. Amorim JH, Alves RP, Boscardin SB, Ferreira LC. 2014. The dengue virus non-structural 1 protein: risks and benefits. Virus Res 181:53-60.
20. Phoo WW, Li Y, Zhang Z, Lee MY, Loh YR, Tan YB, Ng EY, Lescar J, Kang C, Luo D. 2016. Structure of the NS2B-NS3 protease from Zika virus after self-cleavage. Nat Commun 7:13410.
21. Heinz FX, Stiasny K. 2017. The Antigenic Structure of Zika Virus and Its Relation to Other Flaviviruses: Implications for Infection and Immunoprophylaxis. Microbiol Mol Biol Rev 81:e00055-16.
22. Hamel R, Dejarnac O, Wichit S, Ekchariyawat P, Neyret A, Luplertlop N, Perera-Lecoin M, Surasombatpattana P, Talignani L, Thomas F, Cao-Lormeau VM, Choumet V, Briant L, Despres P, Amara A, Yssel H, Misse D. 2015. Biology of Zika Virus Infection in Human Skin Cells. J Virol 89:8880-96.
23. Kim JA, Seong RK, Son SW, Shin OS. 2019. Insights into ZIKV-Mediated Innate Immune Responses in Human Dermal Fibroblasts and Epidermal Keratinocytes. J Invest Dermatol 139:391-399.
24. Sun X, Hua S, Chen HR, Ouyang Z, Einkauf K, Tse S, Ard K, Ciaranello A, Yawetz S, Sax P, Rosenberg ES, Lichterfeld M, Yu XG. 2017. Transcriptional Changes during Naturally Acquired Zika Virus Infection Render Dendritic Cells Highly Conducive to Viral Replication. Cell Rep 21:3471-3482.
25. Foo SS, Chen W, Chan Y, Bowman JW, Chang LC, Choi Y, Yoo JS, Ge J, Cheng G, Bonnin A, Nielsen-Saines K, Brasil P, Jung JU. 2017. Asian Zika virus strains target CD14(+) blood monocytes and induce M2-skewed immunosuppression during pregnancy. Nat Microbiol 2:1558-1570.
26. Michlmayr D, Andrade P, Gonzalez K, Balmaseda A, Harris E. 2017. CD14(+)CD16(+) monocytes are the main target of Zika virus infection in peripheral blood mononuclear cells in a paediatric study in Nicaragua. Nat Microbiol 2:1462-1470.
27. Rosenberg AZ, Yu W, Hill DA, Reyes CA, Schwartz DA. 2017. Placental Pathology of Zika Virus: Viral Infection of the Placenta Induces Villous Stromal Macrophage (Hofbauer Cell) Proliferation and Hyperplasia. Arch Pathol Lab Med 141:43-48.
28. Bayer A, Lennemann NJ, Ouyang Y, Bramley JC, Morosky S, Marques ET, Jr., Cherry S, Sadovsky Y, Coyne CB. 2016. Type III Interferons Produced by Human Placental Trophoblasts Confer Protection against Zika Virus Infection. Cell Host Microbe 19:705-12.
29. Cheng F, Ramos da Silva S, Huang IC, Jung JU, Gao SJ. 2018. Suppression of Zika Virus Infection and Replication in Endothelial Cells and Astrocytes by PKA Inhibitor PKI 14-22. J Virol 92:e02019-17.

30. Nowakowski TJ, Pollen AA, Di Lullo E, Sandoval-Espinosa C, Bershteyn M, Kriegstein AR. 2016. Expression Analysis Highlights AXL as a Candidate Zika Virus Entry Receptor in Neural Stem Cells. Cell Stem Cell 18:591-6.
31. Meertens L, Labeau A, Dejarnac O, Cipriani S, Sinigaglia L, Bonnet-Madin L, Le Charpentier T, Hafirassou ML, Zamborlini A, Cao-Lormeau VM, Coulpier M, Misse D, Jouvenet N, Tabibiazar R, Gressens P, Schwartz O, Amara A. 2017. Axl Mediates ZIKA Virus Entry in Human Glial Cells and Modulates Innate Immune Responses. Cell Rep 18:324-333.
32. Roach T, Alcendor DJ. 2017. Zika virus infection of cellular components of the blood-retinal barriers: implications for viral associated congenital ocular disease. J Neuroinflammation 14:43.
33. Bagasra O, Addanki KC, Goodwin GR, Hughes BW, Pandey P, McLean E. 2017. Cellular Targets and Receptor of Sexual Transmission of Zika Virus. Appl Immunohistochem Mol Morphol 25:679-686.
34. Wang A, Thurmond S, Islas L, Hui K, Hai R. 2017. Zika virus genome biology and molecular pathogenesis. Emerg Microbes Infect 6:e13.
35. Olagnier D, Muscolini M, Coyne CB, Diamond MS, Hiscott J. 2016. Mechanisms of Zika Virus Infection and Neuropathogenesis. DNA Cell Biol 35:367-72.
36. Richard AS, Shim BS, Kwon YC, Zhang R, Otsuka Y, Schmitt K, Berri F, Diamond MS, Choe H. 2017. AXL-dependent infection of human fetal endothelial cells distinguishes Zika virus from other pathogenic flaviviruses. Proc Natl Acad Sci U S A 114:2024-2029.
37. Agrelli A, de Moura RR, Crovella S, Brandao LAC. 2019. ZIKA virus entry mechanisms in human cells. Infect Genet Evol 69:22-29.
38. Friedman RC, Farh KK, Burge CB, Bartel DP. 2009. Most mammalian mRNAs are conserved targets of microRNAs. Genome Res 19:92-105.
39. Gartel AL, Kandel ES. 2006. RNA interference in cancer. Biomol Eng 23:17-34.
40. Mansoori B, Sandoghchian Shotorbani S, Baradaran B. 2014. RNA interference and its role in cancer therapy. Adv Pharm Bull 4:313-21.
41. Cullen BR. 2014. Viruses and RNA interference: issues and controversies. J Virol 88:12934-6.
42. Vienberg S, Geiger J, Madsen S, Dalgaard LT. 2017. MicroRNAs in metabolism. Acta Physiol (Oxf) 219:346-361.
43. Bruscella P, Bottini S, Baudesson C, Pawlotsky JM, Feray C, Trabucchi M. 2017. Viruses and miRNAs: More Friends than Foes. Front Microbiol 8:824.
44. Meola N, Gennarino VA, Banfi S. 2009. microRNAs and genetic diseases. Pathogenetics 2:7.
45. Kozak RA, Majer A, Biondi MJ, Medina SJ, Goneau LW, Sajesh BV, Slota JA, Zubach V, Severini A, Safronetz D, Hiebert SL, Beniac DR, Booth TF, Booth SA, Kobinger GP. 2017. MicroRNA and mRNA Dysregulation in Astrocytes Infected with Zika Virus. Viruses 9:297.
46. Azouz F, Arora K, Krause K, Nerurkar VR, Kumar M. 2019. Integrated MicroRNA and mRNA Profiling in Zika Virus-Infected Neurons. Viruses 11:162.
47. Dang JW, Tiwari SK, Qin Y, Rana TM. 2019. Genome-wide Integrative Analysis of Zika-Virus-Infected Neuronal Stem Cells Reveals Roles for MicroRNAs in Cell Cycle and Stemness. Cell Rep 27:3618-3628.e5.

48. Alpuche-Lazcano SP, McCullogh CR, Del Corpo O, Rance E, Scarborough RJ, Mouland AJ, Sagan SM, Teixeira MM, Gatignol A. 2018. Higher Cytopathic Effects of a Zika Virus Brazilian Isolate from Bahia Compared to a Canadian-Imported Thai Strain. Viruses 10:53.
49. Barnard TR, Rajah MM, Sagan SM. 2018. Contemporary Zika Virus Isolates Induce More dsRNA and Produce More Negative-Strand Intermediate in Human Astrocytoma Cells. Viruses 10:728.
50. Olmo IG, Carvalho TG, Costa VV, Alves-Silva J, Ferrari CZ, Izidoro-Toledo TC, da Silva JF, Teixeira AL, Souza DG, Marques JT, Teixeira MM, Vieira LB, Ribeiro FM. 2017. Zika Virus Promotes Neuronal Cell Death in a Non-Cell Autonomous Manner by Triggering the Release of Neurotoxic Factors. Front Immunol 8:1016.
51. Wolf HK, Buslei R, Schmidt-Kastner R, Schmidt-Kastner PK, Pietsch T, Wiestler OD, Blumcke I. 1996. NeuN: a useful neuronal marker for diagnostic histopathology. J Histochem Cytochem 44:1167-71.
52. Sun X, Lin Y. 2016. Npas4: Linking Neuronal Activity to Memory. Trends Neurosci 39:264-275.
53. Safe S, Jin UH, Morpurgo B, Abudayyeh A, Singh M, Tjalkens RB. 2016. Nuclear receptor 4A (NR4A) family - orphans no more. J Steroid Biochem Mol Biol 157:48-60.
54. Reactome. 2003. Neuronal System. http://reactome.org/content/detail/R-HSA-112316. Accessed
55. Hocine S, Singer RH, Grunwald D. 2010. RNA processing and export. Cold Spring Harb Perspect Biol 2:a000752.
56. Reactome. 2019. Gene expression (Transcription). https://reactome.org/content/detail/R-HSA-74160. Accessed
57. Lin Y, Bloodgood BL, Hauser JL, Lapan AD, Koon AC, Kim TK, Hu LS, Malik AN, Greenberg ME. 2008. Activity-dependent regulation of inhibitory synapse development by Npas4. Nature 455:1198-204.
58. Gao R, Penzes P. 2015. Common mechanisms of excitatory and inhibitory imbalance in schizophrenia and autism spectrum disorders. Curr Mol Med 15:146-67.
59. Jaehne EJ, Klaric TS, Koblar SA, Baune BT, Lewis MD. 2015. Effects of Npas4 deficiency on anxiety, depression-like, cognition and sociability behaviour. Behav Brain Res 281:276-82.
60. Damborsky JC, Slaton GS, Winzer-Serhan UH. 2015. Expression of Npas4 mRNA in Telencephalic Areas of Adult and Postnatal Mouse Brain. Front Neuroanat 9:145.
61. Klaric TS, Thomas PQ, Dottori M, Leong WK, Koblar SA, Lewis MD. 2014. A reduction in Npas4 expression results in delayed neural differentiation of mouse embryonic stem cells. Stem Cell Res Ther 5:64.
62. Heslin K, Coutellier L. 2018. Npas4 deficiency and prenatal stress interact to affect social recognition in mice. Genes Brain Behav 17:e12448.
63. McMorrow JP, Murphy EP. 2011. Inflammation: a role for NR4A orphan nuclear receptors? Biochem Soc Trans 39:688-93.
64. Kim SO, Ono K, Tobias PS, Han J. 2003. Orphan nuclear receptor Nur77 is involved in caspase-independent macrophage cell death. J Exp Med 197:1441-52.
65. Volakakis N, Kadkhodaei B, Joodmardi E, Wallis K, Panman L, Silvaggi J, Spiegelman BM, Perlmann T. 2010. NR4A orphan nuclear receptors as mediators of CREB-dependent neuroprotection. Proc Natl Acad Sci U S A 107:12317-22.

66. Mount MP, Zhang Y, Amini M, Callaghan S, Kulczycki J, Mao Z, Slack RS, Anisman H, Park DS. 2013. Perturbation of transcription factor Nur77 expression mediated by myocyte enhancer factor 2D (MEF2D) regulates dopaminergic neuron loss in response to 1-methyl-4-phenyl-1,2,3,6-tetrahydropyridine (MPTP). J Biol Chem 288:14362-71.
67. Levesque D, Rouillard C. 2007. Nur77 and retinoid X receptors: crucial factors in dopamine-related neuroadaptation. Trends Neurosci 30:22-30.
68. Le WD, Xu P, Jankovic J, Jiang H, Appel SH, Smith RG, Vassilatis DK. 2003. Mutations in NR4A2 associated with familial Parkinson disease. Nat Genet 33:85-9.
69. Zetterstrom RH, Solomin L, Jansson L, Hoffer BJ, Olson L, Perlmann T. 1997. Dopamine neuron agenesis in Nurr1-deficient mice. Science 276:248-50.
70. Ponnio T, Conneely OM. 2004. nor-1 regulates hippocampal axon guidance, pyramidal cell survival, and seizure susceptibility. Mol Cell Biol 24:9070-8.
71. Song L, Tuan RS. 2006. MicroRNAs and cell differentiation in mammalian development. Birth Defects Res C Embryo Today 78:140-9.
72. Hwang HW, Mendell JT. 2006. MicroRNAs in cell proliferation, cell death, and tumorigenesis. Br J Cancer 94:776-80.
73. Ardekani AM, Naeini MM. 2010. The Role of MicroRNAs in Human Diseases. Avicenna J Med Biotechnol 2:161-79.
74. Mattick JS, Makunin IV. 2005. Small regulatory RNAs in mammals. Hum Mol Genet 14 Spec No 1:R121-32.
75. Hu Z, Li Z. 2017. miRNAs in synapse development and synaptic plasticity. Curr Opin Neurobiol 45:24-31.
76. Danka Mohammed CP, Park JS, Nam HG, Kim K. 2017. MicroRNAs in brain aging. Mech Ageing Dev 168:3-9.
77. Rajman M, Schratt G. 2017. MicroRNAs in neural development: from master regulators to fine-tuners. Development 144:2310-2322.
78. Wang X, Chen Q, Yi S, Liu Q, Zhang R, Wang P, Qian T, Li S. 2019. The microRNAs let-7 and miR-9 down-regulate the axon-guidance genes Ntn1 and Dcc during peripheral nerve regeneration. J Biol Chem 294:3489-3500.
79. Wang X, Xu J, Gong J, Shen H, Wang X. 2013. Expression of netrin-1 and its receptors, deleted in colorectal cancer and uncoordinated locomotion-5 homolog B, in rat brain following focal cerebral ischemia reperfusion injury. Neural Regen Res 8:64-9.
80. Moon C, Kim H, Ahn M, Jin JK, Wang H, Matsumoto Y, Shin T. 2006. Enhanced expression of netrin-1 protein in the sciatic nerves of Lewis rats with experimental autoimmune neuritis: possible role of the netrin-1/DCC binding pathway in an autoimmune PNS disorder. J Neuroimmunol 172:66-72.
81. Costa VV, Del Sarto JL, Rocha RF, Silva FR, Doria JG, Olmo IG, Marques RE, Queiroz-Junior CM, Foureaux G, Araujo JMS, Cramer A, Real A, Ribeiro LS, Sardi SI, Ferreira AJ, Machado FS, de Oliveira AC, Teixeira AL, Nakaya HI, Souza DG, Ribeiro FM, Teixeira MM. 2017. N-Methyl-d-Aspartate (NMDA) Receptor Blockade Prevents Neuronal Death Induced by Zika Virus Infection. MBio 8:e00350-17.
82. Costa VV, Fagundes CT, Valadao DF, Avila TV, Cisalpino D, Rocha RF, Ribeiro LS, Ascencao FR, Kangussu LM, Celso MQ, Jr., Astigarraga RG, Gouveia FL, Silva TA, Bonaventura D, Sampaio Dde A, Leite AC, Teixeira MM, Souza DG. 2014. Subversion of early innate antiviral responses during antibody-dependent enhancement of Dengue

virus infection induces severe disease in immunocompetent mice. Med Microbiol Immunol 203:231-50.
83. Presutti D, Ceccarelli M, Micheli L, Papoff G, Santini S, Samperna S, Lalli C, Zentilin L, Ruberti G, Tirone F. 2018. Tis21-gene therapy inhibits medulloblastoma growth in a murine allograft model. PLoS One 13:e0194206.
84. Eissa N, Hussein H, Wang H, Rabbi MF, Bernstein CN, Ghia JE. 2016. Stability of Reference Genes for Messenger RNA Quantification by Real-Time PCR in Mouse Dextran Sodium Sulfate Experimental Colitis. PLoS One 11:e0156289.
85. Yu G, He QY. 2016. ReactomePA: an R/Bioconductor package for reactome pathway analysis and visualization. Mol Biosyst 12:477-9.
86. Yu G, Wang LG, Han Y, He QY. 2012. clusterProfiler: an R package for comparing biological themes among gene clusters. Omics 16:284-7.
87. Wong N, Wang X. 2015. miRDB: an online resource for microRNA target prediction and functional annotations. Nucleic Acids Res 43:D146-52.
88. Agarwal V, Bell GW, Nam JW, Bartel DP. 2015. Predicting effective microRNA target sites in mammalian mRNAs. Elife 4:05005.
89. Garcia DM, Baek D, Shin C, Bell GW, Grimson A, Bartel DP. 2011. Weak seed-pairing stability and high target-site abundance decrease the proficiency of lsy-6 and other microRNAs. Nat Struct Mol Biol 18:1139-46.
90. Grimson A, Farh KK, Johnston WK, Garrett-Engele P, Lim LP, Bartel DP. 2007. MicroRNA targeting specificity in mammals: determinants beyond seed pairing. Mol Cell 27:91-105.
91. Lewis BP, Burge CB, Bartel DP. 2005. Conserved seed pairing, often flanked by adenosines, indicates that thousands of human genes are microRNA targets. Cell 120:15-20.

CHAPTER V

DISCUSSION

5.1 MiRNAs friends or foes? MiRNAs during HIV-1 and ZIKV infection.

To date, the exact role that miRNAs play during viral infections in mammalian cells at multiple levels is not fully elucidated. Infected cells with HIV-1 can produce miRNAs that can impair or enhance the virus replication. MiR29a hybridizes with a high affinity to Nef sequence and degrades HIV-1 transcripts within P-bodies (1-3). Monocytes and resting $CD4^+$ T cells express high levels of miR-198 and miR27b that negatively regulates CycT1, which is part of p-TEFb, an essential factor for virus transactivation (4, 5). Conversely, miRLet-7c, compensates the negative regulation over p-TEFb degrading P21, which blocks transcriptional elongation (6). Our research did not focus on new miRNAs that were down or overproduced in the presence of the HIV-1 Gag. Instead, we discovered that Gag binds Dicer and changes the loading concentration of miRNAs that were already produced. This result raises the question of whether the cell produces miRNAs that can be functionally influenced by HIV-1 proteins with the consequence of an altered function for these miRNAs. To discriminate whether miRNAs in Dicer/Gag are sequestered with a decreased activity or loaded faster for an increased activity, it will be necessary to select a specific miRNA, overproduce it and observe the silencing on one or two targets. These experiments will be carried out in the absence and in the presence of Gag. The hypothesis of Dicer/Gag sequestering the specific miRNA should show more protein expression, whereas more loading and activity would lead to less protein expression.

Dicer activity and processing are complemented by partner proteins TRBP, PACT and Ago2 (7) and other proteins can modify Dicer's activity as shown by several examples (8): 1) viral suppressors like HCV viral core protein can interact with Dicer and antagonizes the gene silencing (9); 2) ADAR-1 that transiently interact with Dicer, facilitates the cleavage rate and the miRNA

loading on Ago2 (10); 3) Some proteins influence Dicer localization and regulation. For instance, NUP 153 or cytoskeleton-linking endoplasmic reticulum membrane protein of 63 kD (CLIMP-63) can re-localize and regulate Dicer's function (11, 12). Therefore, we suggest that Gag might obey to one of these categories affecting the miRNA functionality.

ZIKV infection also modifies the global landscape of cellular miRNAs. In contrast to HIV-1 infection, many miRNAs that are dysregulated upon ZIKV entry may be linked to the innate immunity against the virus. The increased production of miRNAs during ZIKV infection, the augmented titers of the virus in the absence of Dicer or Ago2 and the elimination of ZIKV linked to a boosted RNAi response, all support the idea that RNAi is disadvantageous for ZIKV replication (13, 14). MiRNA and mRNA profiles of ZIKV infected neurons showed increased levels of miR-155, miR-203 and miR-29a, which are known to possess antiviral activity (15). To control the viral spread, primary neurons infected with ZIKV have shown to increase miR-9, which downregulates the glial cell-derived neurotrophic factor (GDNF) and consequently triggers apoptotic processes (16). In Chapter IV, we and others demonstrated that an infected cell with ZIKV increases the production of Cdk6 and changes the concentration of miRNAs that regulate it, including miR3084-3p (17). The disruption of RNAi in infected cells has been documented by different experiments. ZIKV stimulates the production of miR148a in different cell types whose target is *DICER1* gene, which consequently impairs RNAi and the modulation of hundreds of genes (18, 19). ZIKV also upregulates miR125a 3p and 5p, which probably trigger a reduction of mitochondrial antiviral-signaling (MAVS) (20). MAVS plays an essential role in the signaling of the innate immune response over key elements like RIG-I and IFN (17). A significant physiological consequence triggered by the ZIKV miRNA dysregulation has been observed with the upregulation of miR124-3p. Augmented levels of miR124-3p downregulate the transferrin

receptor TFR that mediates iron uptake, cell cycle and metabolism regulation and these changes contribute to CZVS (17, 21). In chapter IV we also describe a possible interplay between upregulated miRNAs and downregulated genes, which have essential roles in neurogenesis and early gene transcription. Among them, the nuclear receptor NR4A3 showed decreased levels upon ZIKV infection. Interestingly, this gene could be modulated by miR7116-5p and miR7013-5p that were heightened in our experimental results (Table 4.5).

5.2 Dysregulated miRNAs and effects on their respective target genes.

The outcome of disrupting RNAi is the dysregulation of many genes. Our findings in chapters II and IV allowed us to pinpoint different genes that could change HIV-1 and ZIKV replication and pathogenesis. Dicer/Gag interaction resulted in higher amounts of specific miRNAs bound to Dicer compared to Dicer alone. Among those miRNA, miR642a-3p might be implicated in HIV-1 replication because it is predicted to target the mRNA of AFF4, a protein that belongs to the super elongation complex (SEC) of transcription. Indeed, this complex assists RNA Pol II processivity during transcription and elongation. SEC is composed of p-TEFb (Cdk9 and CycT1), the elongation factor for RNA polymerase II 2 (ELL2), the transcription factor/coactivator ENL/AF9 and the scaffold proteins AFF1 and AFF4 (22). To transactivate HIV-1 RNA, Tat recruits SEC by binding directly to CycT1 and to AFF4 indirectly (23, 24). Crystal structures and biophysical data unveiled that AFF4 stabilizes CycT1 and Tat during their conformational change produced by the interaction with TAR (23). Therefore, in the presence of AFF4, CycT1 and Tat increase their affinity to TAR by 50 fold (23). AFF4 can be targeted by miR642a-3p, which was found in our Dicer/Gag readouts as one of the most bound miRNA into this complex. To confirm the effects of Dicer/Gag-miR642a-3p, we propose to use miRNA mimics (ThermoFisher) and confirm the

knockdown of AFF4. After having verified that miR642-3p downregulates the expression of AFF4, we will co-transfect Gag and miR642-3p mimic to determine if AFF4 concentration is decreased or increased compared to controls. A decreased AFF4 with Gag would mean that Gag increases miR642-3p activity by enhancing its accessibility to Dicer. If AFF4 expression is increased, Gag would sequester miR642-3p in a Dicer/Gag complex to block miRNA action. The consequences of either a decrease or an increased in AFF4 expression should be reflected respectively by corresponding changes in HIV-1 transactivation.

Other miRNAs that interacted more with Dicer/Gag complexes than to Dicer alone were miR766-5p, which had seven predicted targets and miR766-3p with three predicted targets that might be related to HIV-1 infection (Chapter II). However, these targets have not been explored and we have little data about their relationships with HIV-1. It would be interesting to overexpressed miR766-5p and 3p separately and observe if there are changes in the virus replication rate.

Different teams have documented dysregulated miRNAs and the effects on some targets during ZIKV infection (15, 17, 25). The miRNA profile upon ZIKV entry has been linked to the dysregulation of different mRNAs and pathways such as inflammation, neurogenesis, metabolism, stem cell maintenance, protein folding in the ER and apoptosis (15-17, 25). In Chapter IV, we describe that the NR4A family and NPAS4 were highly downregulated. Our integrative analysis with mRNAs also demonstrated a possible association with dysregulated miRNAs. Interestingly, one member of the NR4A family was downregulated, whereas two miRNAs that target it were increased in infected neurons. NR4A3 is a nuclear receptor transcription factor that is constitutively active and does not need ligand modulation. Furthermore, NR4A3 and its receptor family are immediate-early genes that can be triggered by external agents (26). The lack of NR4A3

in neurons can lead to defective axonal growth and cell death (26). In other cell types like monocytes and macrophages, NR4A3 has anti-inflammatory properties (27). Distinct experiments demonstrated that the overexpression of NR4A3 in monocytes shuts off the inflammation process, whereas downregulation of this molecule in macrophages augments proinflammatory cytokines and chemokines (28). Our short-term goal will be to investigate whether overexpressed levels of NR4A3 could impair ZIKV replication, reduce neuronal death and restore normal neuron function. We next like to corroborate the downregulation of NR4A3 by miR7116-5p and miR7013-5p and show that they can target NR4A3 transcripts in infected neurons. Inhibiting miR7116-5p and miR7013-5p would be a mean to increase NR4A3 protein levels.

5.3. HIV-1 and ZIKV modulate other ncRNAs

Dicer is an endonuclease that participates in the regulation of miRNAs but also binds different ncRNA like snoRNAs, sdRNAs, psnoRNAs, LINE-1 and even viral components like HIV-1 TAR and flaviviral sfRNAs (29-39). Our results show that it is also the case in the context of HIV-1 and ZIKV infection. RIP-seq results of Dicer/Gag interaction (Chapter II) demonstrated that for some miRNAs, the loading or retention on Dicer changes in the presence of Gag (40). During this process, we identified other RNAs that are also affected by this interaction (Appendix I). Among them, small nucleolar RNA, C/D box (SNORD) 104 was less concentrated in Dicer/Gag IPs while SNORD6, SNORD101, SNORD5, SNORD12C, SNORD13 and SNORD118 were more concentrated (Table 6.1). Box C/D snoRNAs are conserved RNA sequences in the nucleolus of 70-90 nt length generated by Pol II or derived from intronic sequences (41). Commonly, they participate in the generation of ribosomal RNA (rRNA) (42). Nonetheless, almost half of the SNORDs are considered “orphan” because they do not participate in methylation or recruitment

of enzymes involved in the maturation of rRNA (43, 44). Among non-canonical functions, SNORDs are functional in alternative splicing (45, 46), mRNA polyadenylation (47), PKR activation (48) and Dicer substrates for miRNA's generation (29-31). Some studies have explored how viruses co-opt SNORDs and what could be their function. Screening experiments in twelve different viruses showed that 83 SNORDs are necessary for a succesful infection (49). HIV-1 Rev protein can bind nucleophosmin 1 (NPM1) which allows Rev to relocalize to the nucleolus (50). Surprisingly, under certain conditions, Gag is imported to the nucleus and accumulates into the nucleolus (51). Our PLA experiments showed partial re-localization of Dicer/Gag to the nucleus. A correlation with our RIP-seq results anticipates that it could be possibly relocated to the nucleolus because of the interaction with SNORDs (Fig 2.5, Table 6.1). Two options fit with these results. In certain conditions, the RBD domain in Dicer behaves as an NLS interacting with importins β, 7, 8 and allowing its access to the nucleus (52). Alternatively Gag through NC domain could help Dicer be imported to the nucleus and nucleolus (51). Currently, we do not know why SNORDs are more concentrated in Dicer/Gag IP than in Dicer IP and what possible roles it could play during the infection. Our short term goal is to validate a few SNORDs in Dicer and Dicer/Gag complexes as well as to know whether these SNORDs are subjected to Dicer catalytic activity. An overexpression of SNORDs during HIV-1 replication could also indicate if it helps or inhibit viral replication.

RIP-seq analysis also demonstrated that other ncRNAs besides SNORDs interact more with Dicer/Gag than Dicer alone. Our interest was sparked by the observation of 7SK RNA in our list (Table 6.1). 7SK is a highly abundant 331 nt ncRNA that negatively regulates p-TEFb through the interaction with HEXamethylene-bis-acetamide-Inducible protein in vascular smooth muscle cells (HEXIM1) (53, 54). After Tat translation and import to the cell nucleus, it competes with HEXIM1

and removes p-TEFb away from 7SK structure to recruit it to the nascent TAR element where transactivation events take place enhancing viral production by several hundred-fold (55). A follow-up experiment from our results on 7SK corroborated the higher abundance of 7SK, specifically on Dicer/Gag complexes and not in total RNA levels (Fig 6.1). We confirmed that 7SK binds to Dicer and Gag individually which probably could explain the higher abundance. Our preliminary results suggest that Dicer influences the transactivation process. It remains to be determined if this is due to either TAR RNA cleavage shown by others (36, 38), or to increased binding to the Dicer/Gag complex. Further research should test any catalytic activity on 7SK by Dicer and if HIV-1 Gag influences it.

ZIKV also influences the expression or function of different ncRNAs. LncRNAs are usually generated from intronic or intergenic regions (56). LncRNAs are more than 200 nt that can be capped and polyadenylated; they play regulatory functions in proliferation, differentiation, development and are localized in the nucleus or cytoplasm (57-59). Recent ncRNA screening found 149 differentially expressed lncRNAs upon ZIKV infection in NPC linked to the modulation of different cell processes like cell cycle, apoptosis and immune response (60). A novel characterized cytoplasmic lncRNA called lncATV inhibits the activity of retinoic acid-inducible gene I (RIG-I). Upon ZIKV infection, basal levels of lncATV are increased and impair RIG-I function, thus allowing virus production (61). Our readouts in Chapter IV demonstrated a 3.1 fold decrease of the uncharacterized lncRNA 1700016P03Rik (Table 4.2). Future experiments must be carried out to elucidate the role of 1700016P03Rik and the next step is to study how ZIKV replication might be affected through the rescue of 1700016P03Rik.

5.4 Perspectives on dysregulated miRNAs during HIV-1 and ZIKV infections.

The results described in Chapters II and IV could be used for future strategies to cure HIV-1 and ZIKV infections. In Chapter II, we observed that the interaction between Dicer and Gag recruits more miR642a-3p, which is predicted to target AFF4, an essential factor for HIV-1 replication (62, 63). After the target confirmation, we could investigate miR642a-3p with different strategies toward a model to cure HIV-1. The knowledge obtained from other miRNAs could help us to elaborate on such strategies. MiR29a targets HIV-1 Nef sequence (2, 64) which is next to the 3'LTR. MiR29a can bind long viral transcripts and take them to P-bodies where they are degraded (2). Basal levels of miR29a are insufficient to control the virus, thereby transfection and overexpression or endogenous stimulation of this miRNA reduce HIV-1 replication (3, 65, 66). These characteristics of miR29a can be further explored in potential clinical applications. The "shock and kill" strategy seeks the reactivation of HIV-1 within viral reservoirs in patients under ART. The complete inhibition of miR29a alone or combined with LRAs could be used to stimulate a more significant viral reactivation, which activates the immune system that destroys the infected cell (1). Alternatively, deep latency using the "block and lock" strategy might be used. A constant overexpression of miR29a using a lentiviral vector might control the HIV-1 replication. Nonetheless, because of the nature of miR29a and the close relationship in its dysregulation with cancer, it is necessary to investigate agonists that can modulate miR29a before incorporating this strategy into patients (1, 67).

Other miRNAs involved in the regulation of viral replication or latency could also be used in similar strategies. For example, miR-125b-5p, miR-150-5p, miR133b, miR-138-5p, miR-28 and miR382 can promote latency whereas miR-155-5p, miR-92a-3p, miR-149-5p and miR-423-3p

impair HIV-1 replication (62). Targeting HIV-1 HDF is feasible, miR29b, miR150, miR223 and miR27b are negative regulators of CycT1 expression and miRNA mimics could be used to maintain the virus in a latent stage, whereas anti-miRNAs could reactivate it. The understanding of dysregulated miRNA and potential cure strategies using RNAi are not limited to HIV-1. Computational approaches have unveiled different cellular miRNAs with complementary sequences to ZIKV transcripts, which might affect its replication (68). In addition, a comprehensive bioinformatic analysis has determined siRNAs that have a high potential to target most of ZIKV strains and other flaviviruses (69). Future strategies to cure ZIKV infection using RNAi not only embraces direct control over viral transcripts but also indirect mechanisms. For example, an integrative analysis performed in Ago2-CLIP-seq of miRNA-mRNA during ZIKV infection showed that miR124-3p is upregulated (17). MiR124-3p regulates transferrin receptors (*TFRC*), which modulate iron uptake, metabolism and stem cell renewal (21, 70, 71). Iron regulation is involved in cell cycle and neuronal development. Its deregulation likely contributes to neuronal damage by the recent ZIKV strains.

Our integrative analysis of miRNA-mRNA during ZIKV infection showed an upregulation in Cdk6 and a downregulation of a possible miRNA regulator, miR3084-3p. Cdk6 function is part of the cell cycle regulation, allowing the cell to enter into the S-phase. Mutations in Cdk6 result in longer S-phase, shorter G1 intervals and abnormalities in centrosomes that provoke an improper organization of the nucleus and microtubules (72). Therefore, disturbances in Cdk6 are linked to a failure in neurogenesis (72). The upregulation of Cdk6, alongside the downregulation of NR4A3 and NPAS4 also involved in neurogenesis, could be part of an approach to restore normal neuronal functions. The first step will be to determine whether the miRNAs found during our analysis indeed participate to the regulation of Cdk6, NR4A3 and NPAS4. Second, we need to study if any of

those cellular factors play an essential role during ZIKV infection. Finally, we could regulate these factors through the use of miRNA mimics to decrease Cdk6 expression or antagomirs that sequester miRNAs to increase the levels of NPAS4 or NR4A3.

5.5 Conclusions

The infection by viruses triggers different mechanisms that result in RNAi disturbances. We explored how two different viruses induce modifications of RNAi in different ways. Extensive research on RNAi and HIV-1 has been carried out for years and still, definite conclusions have not been drawn. Many authors have explored different miRNAs produced by the cell upon HIV-1 infection. However, all of these changes do not seem to be final for HIV-1 replication and only the overexpression or the lack of specific RNAi elements could influence the infection. Our research brought another perspective, based on our initial evidence, also corroborated by other investigators, that RNAi is still functional in HIV-1 replicating cells. In addition, we demonstrated that an interaction between Dicer and HIV-1 Gag could influence the direction of the infection without altering the miRNA production but affecting the miRNA functionality. We identified for the first time that miR642a 3p, miR755 5p and 3p are recruited more to Dicer/Gag than to Dicer in the absence of Gag. Specifically, miR642a 3p is predicted to target AFF4 a crucial factor in the transcriptional elongation complex essential for the virus transcription. The characterization of miR642a 3p and AFF4 might lead to significant developments in HIV-1 functional cures, specifically in approaches of “block and lock” or “shock and kill”.

Dicer interaction is not limited to pre-miRNAs. We found that Dicer interacts with substrates different than miRNAs whose binding was changed in the presence of HIV-1 Gag. During RIP-seq analysis described in chapter II, we discovered that snoRNAs and lncRNA could bind Dicer,

but more interestingly, we found that the presence of Gag increases and in some cases, decreases such interaction. Particularly 7SK, an RNA involved in the transactivation of HIV-1, was more bound to Dicer/Gag than to Dicer alone. Further investigation is needed to elucidate what is the outcome of the cell and the infection.

Regarding ZIKV, we first demonstrated how distinct strains impair the cell differently. In this research, we found that a Brazilian strain causes more cell death than an early Asian one. Further analysis of the Brazilian strain allowed us to describe the disturbances within neurons by analyzing their transcriptome. We then integrated the transcriptomics with miRNA screening results and showed that dysregulated miRNAs might affect their targets found in the transcriptome. Among the genes, we found that the most affected genes are involved in neurogenesis, like NPAS4, NR4A3 and Cdk6, and we also identified miRNAs that could regulate them. This information will be useful to researchers who pursue the understanding of the virus behavior during neuronal development and its implications on CZVS cases.

The final comment of this thesis is that the relationship between RNAi and viruses are different depending on the virus. For ZIKV, it is likely that RNAi might help to clear out the infection. Our results show a profound modification of the transcriptome and the ncRNA profile upon ZIKV infection, which likely participates in the pathogenesis. For HIV-1, whereas other studies have shown many alterations of miRNA expression during the virus replication or latency, we have shown that the function of specific miRNAs could change due to their increased availability or sequestration by Dicer/Gag complex. Overall, our results have contributed to a better understanding of the relationship between viruses and the RNAi pathway.

REFERENCES

1. Frattari G, Aagaard L, Denton PW. 2017. The role of miR-29a in HIV-1 replication and latency. J Virus Erad 3:185-191.
2. Nathans R, Chu CY, Serquina AK, Lu CC, Cao H, Rana TM. 2009. Cellular microRNA and P bodies modulate host-HIV-1 interactions. Mol Cell 34:696-709.
3. Patel P, Ansari MY, Bapat S, Thakar M, Gangakhedkar R, Jameel S. 2014. The microRNA miR-29a is associated with human immunodeficiency virus latency. Retrovirology 11:108.
4. Sung TL, Rice AP. 2009. miR-198 inhibits HIV-1 gene expression and replication in monocytes and its mechanism of action appears to involve repression of cyclin T1. PLoS Pathog 5:e1000263.
5. Chiang K, Sung TL, Rice AP. 2012. Regulation of cyclin T1 and HIV-1 Replication by microRNAs in resting CD4+ T lymphocytes. J Virol 86:3244-52.
6. Farberov L, Herzig E, Modai S, Isakov O, Hizi A, Shomron N. 2015. MicroRNA-mediated regulation of p21 and TASK1 cellular restriction factors enhances HIV-1 infection. J Cell Sci 128:1607-16.
7. Koscianska E, Starega-Roslan J, Krzyzosiak WJ. 2011. The role of Dicer protein partners in the processing of microRNA precursors. PLoS One 6:e28548.
8. Kurzynska-Kokorniak A, Koralewska N, Pokornowska M, Urbanowicz A, Tworak A, Mickiewicz A, Figlerowicz M. 2015. The many faces of Dicer: the complexity of the mechanisms regulating Dicer gene expression and enzyme activities. Nucleic Acids Res 43:4365-80.
9. Chen W, Zhang Z, Chen J, Zhang J, Zhang J, Wu Y, Huang Y, Cai X, Huang A. 2008. HCV core protein interacts with Dicer to antagonize RNA silencing. Virus Res 133:250-8.
10. Ota H, Sakurai M, Gupta R, Valente L, Wulff BE, Ariyoshi K, Iizasa H, Davuluri RV, Nishikura K. 2013. ADAR1 forms a complex with Dicer to promote microRNA processing and RNA-induced gene silencing. Cell 153:575-89.
11. Ando Y, Tomaru Y, Morinaga A, Burroughs AM, Kawaji H, Kubosaki A, Kimura R, Tagata M, Ino Y, Hirano H, Chiba J, Suzuki H, Carninci P, Hayashizaki Y. 2011. Nuclear pore complex protein mediated nuclear localization of dicer protein in human cells. PLoS One 6:e23385.
12. Pepin G, Perron MP, Provost P. 2012. Regulation of human Dicer by the resident ER membrane protein CLIMP-63. Nucleic Acids Res 40:11603-17.
13. Xie X, Shi PY. 2019. Anti-Zika virus RNAi in neural progenitor cells. Cell Res 29:261-262.
14. Xu YP, Qiu Y, Zhang B, Chen G, Chen Q, Wang M, Mo F, Xu J, Wu J, Zhang RR, Cheng ML, Zhang NN, Lyu B, Zhu WL, Wu MH, Ye Q, Zhang D, Man JH, Li XF, Cui J, Xu Z, Hu B, Zhou X, Qin CF. 2019. Zika virus infection induces RNAi-mediated antiviral immunity in human neural progenitors and brain organoids. Cell Res 29:265-273.
15. Azouz F, Arora K, Krause K, Nerurkar VR, Kumar M. 2019. Integrated MicroRNA and mRNA Profiling in Zika Virus-Infected Neurons. Viruses 11:162.

16. Zhang H, Chang Y, Zhang L, Kim SN, Otaegi G, Zhang Z, Nie Y, Mubarak T, Li C, Qin CF, Xu Z, Sun T. 2019. Upregulation of MicroRNA miR-9 Is Associated with Microcephaly and Zika Virus Infection in Mice. Mol Neurobiol 56:4072-4085.
17. Dang JW, Tiwari SK, Qin Y, Rana TM. 2019. Genome-wide Integrative Analysis of Zika-Virus-Infected Neuronal Stem Cells Reveals Roles for MicroRNAs in Cell Cycle and Stemness. Cell Rep 27:3618-3628.e5.
18. Castro FL, Geddes VEV, Monteiro FLL, Goncalves R, Campanati L, Pezzuto P, Paquin-Proulx D, Schamber-Reis BL, Azevedo GS, Goncalves AL, Cunha DP, Moreira MEL, Vasconcelos ZFM, Chimeli L, Melo A, Tanuri A, Nixon DF, Ribeiro-Alves M, Aguiar RS. 2019. MicroRNAs 145 and 148a Are Upregulated During Congenital Zika Virus Infection. ASN Neuro 11:1759091419850983.
19. Ferreira RN, Holanda GM, Pinto Silva EV, Casseb SMM, Melo KFL, Carvalho CAM, Lima JA, Vasconcelos PFC, Cruz ACR. 2018. Zika Virus Alters the Expression Profile of microRNA-Related Genes in Liver, Lung, and Kidney Cell Lineages. Viral Immunol 31:583-588.
20. Hsu AC, Dua K, Starkey MR, Haw TJ, Nair PM, Nichol K, Zammit N, Grey ST, Baines KJ, Foster PS, Hansbro PM, Wark PA. 2017. MicroRNA-125a and -b inhibit A20 and MAVS to promote inflammation and impair antiviral response in COPD. JCI Insight 2:e90443.
21. Silvestroff L, Franco PG, Pasquini JM. 2013. Neural and oligodendrocyte progenitor cells: transferrin effects on cell proliferation. ASN Neuro 5:e00107.
22. He N, Chan CK, Sobhian B, Chou S, Xue Y, Liu M, Alber T, Benkirane M, Zhou Q. 2011. Human Polymerase-Associated Factor complex (PAFc) connects the Super Elongation Complex (SEC) to RNA polymerase II on chromatin. Proc Natl Acad Sci U S A 108:E636-45.
23. Schulze-Gahmen U, Echeverria I, Stjepanovic G, Bai Y, Lu H, Schneidman-Duhovny D, Doudna JA, Zhou Q, Sali A, Hurley JH. 2016. Insights into HIV-1 proviral transcription from integrative structure and dynamics of the Tat:AFF4:P-TEFb:TAR complex. Elife 5.
24. Gu J, Babayeva ND, Suwa Y, Baranovskiy AG, Price DH, Tahirov TH. 2014. Crystal structure of HIV-1 Tat complexed with human P-TEFb and AFF4. Cell Cycle 13:1788-97.
25. Kozak RA, Majer A, Biondi MJ, Medina SJ, Goneau LW, Sajesh BV, Slota JA, Zubach V, Severini A, Safronetz D, Hiebert SL, Beniac DR, Booth TF, Booth SA, Kobinger GP. 2017. MicroRNA and mRNA Dysregulation in Astrocytes Infected with Zika Virus. Viruses 9:297.
26. Ponnio T, Conneely OM. 2004. nor-1 regulates hippocampal axon guidance, pyramidal cell survival, and seizure susceptibility. Mol Cell Biol 24:9070-8.
27. Rodriguez-Calvo R, Tajes M, Vazquez-Carrera M. 2017. The NR4A subfamily of nuclear receptors: potential new therapeutic targets for the treatment of inflammatory diseases. Expert Opin Ther Targets 21:291-304.
28. Bonta PI, van Tiel CM, Vos M, Pols TW, van Thienen JV, Ferreira V, Arkenbout EK, Seppen J, Spek CA, van der Poll T, Pannekoek H, de Vries CJ. 2006. Nuclear receptors Nur77, Nurr1, and NOR-1 expressed in atherosclerotic lesion macrophages reduce lipid loading and inflammatory responses. Arterioscler Thromb Vasc Biol 26:2288-94.

29. Kawaji H, Nakamura M, Takahashi Y, Sandelin A, Katayama S, Fukuda S, Daub CO, Kai C, Kawai J, Yasuda J, Carninci P, Hayashizaki Y. 2008. Hidden layers of human small RNAs. BMC Genomics 9:157.
30. Falaleeva M, Stamm S. 2013. Processing of snoRNAs as a new source of regulatory non-coding RNAs: snoRNA fragments form a new class of functional RNAs. Bioessays 35:46-54.
31. Brameier M, Herwig A, Reinhardt R, Walter L, Gruber J. 2011. Human box C/D snoRNAs with miRNA like functions: expanding the range of regulatory RNAs. Nucleic Acids Res 39:675-86.
32. Ender C, Krek A, Friedlander MR, Beitzinger M, Weinmann L, Chen W, Pfeffer S, Rajewsky N, Meister G. 2008. A human snoRNA with microRNA-like functions. Mol Cell 32:519-28.
33. Heras SR, Macias S, Plass M, Fernandez N, Cano D, Eyras E, Garcia-Perez JL, Caceres JF. 2013. The Microprocessor controls the activity of mammalian retrotransposons. Nat Struct Mol Biol 20:1173-81.
34. Yang N, Kazazian HH, Jr. 2006. L1 retrotransposition is suppressed by endogenously encoded small interfering RNAs in human cultured cells. Nat Struct Mol Biol 13:763-71.
35. Hellwig S, Bass BL. 2008. A starvation-induced noncoding RNA modulates expression of Dicer-regulated genes. Proc Natl Acad Sci U S A 105:12897-902.
36. Ouellet DL, Plante I, Landry P, Barat C, Janelle ME, Flamand L, Tremblay MJ, Provost P. 2008. Identification of functional microRNAs released through asymmetrical processing of HIV-1 TAR element. Nucleic Acids Res 36:2353-65.
37. Omoto S, Ito M, Tsutsumi Y, Ichikawa Y, Okuyama H, Brisibe EA, Saksena NK, Fujii YR. 2004. HIV-1 nef suppression by virally encoded microRNA. Retrovirology 1:44.
38. Klase Z, Kale P, Winograd R, Gupta MV, Heydarian M, Berro R, McCaffrey T, Kashanchi F. 2007. HIV-1 TAR element is processed by Dicer to yield a viral micro-RNA involved in chromatin remodeling of the viral LTR. BMC Mol Biol 8:63.
39. Moon SL, Dodd BJ, Brackney DE, Wilusz CJ, Ebel GD, Wilusz J. 2015. Flavivirus sfRNA suppresses antiviral RNA interference in cultured cells and mosquitoes and directly interacts with the RNAi machinery. Virology 485:322-9.
40. Alpuche-Lazcano SP, Scarborough RJ, Daniels SM, Rance E, Mouland AJ, Gatignol A. 2020. HIV-1 Gag interacts with Dicer and increases its binding to specific microRNAs. submitted.
41. Filipowicz W, Pelczar P, Pogacic V, Dragon F. 1999. Structure and biogenesis of small nucleolar RNAs acting as guides for ribosomal RNA modification. Acta Biochim Pol 46:377-89.
42. Tycowski KT, You ZH, Graham PJ, Steitz JA. 1998. Modification of U6 spliceosomal RNA is guided by other small RNAs. Mol Cell 2:629-38.
43. Deschamps-Francoeur G, Garneau D, Dupuis-Sandoval F, Roy A, Frappier M, Catala M, Couture S, Barbe-Marcoux M, Abou-Elela S, Scott MS. 2014. Identification of discrete classes of small nucleolar RNA featuring different ends and RNA binding protein dependency. Nucleic Acids Res 42:10073-85.
44. Smith CM, Steitz JA. 1997. Sno storm in the nucleolus: new roles for myriad small RNPs. Cell 89:669-72.
45. Falaleeva M, Pages A, Matuszek Z, Hidmi S, Agranat-Tamir L, Korotkov K, Nevo Y, Eyras E, Sperling R, Stamm S. 2016. Dual function of C/D box small nucleolar RNAs in

rRNA modification and alternative pre-mRNA splicing. Proc Natl Acad Sci U S A 113:E1625-34.
46. Scott MS, Ono M, Yamada K, Endo A, Barton GJ, Lamond AI. 2012. Human box C/D snoRNA processing conservation across multiple cell types. Nucleic Acids Res 40:3676-88.
47. Huang C, Shi J, Guo Y, Huang W, Huang S, Ming S, Wu X, Zhang R, Ding J, Zhao W, Jia J, Huang X, Xiang AP, Shi Y, Yao C. 2017. A snoRNA modulates mRNA 3' end processing and regulates the expression of a subset of mRNAs. Nucleic Acids Res 45:8647-8660.
48. Youssef OA, Safran SA, Nakamura T, Nix DA, Hotamisligil GS, Bass BL. 2015. Potential role for snoRNAs in PKR activation during metabolic stress. Proc Natl Acad Sci U S A 112:5023-8.
49. Murray JL, Sheng J, Rubin DH. 2014. A role for H/ACA and C/D small nucleolar RNAs in viral replication. Mol Biotechnol 56:429-37.
50. Fankhauser C, Izaurralde E, Adachi Y, Wingfield P, Laemmli UK. 1991. Specific complex of human immunodeficiency virus type 1 rev and nucleolar B23 proteins: dissociation by the Rev response element. Mol Cell Biol 11:2567-75.
51. Lochmann TL, Bann DV, Ryan EP, Beyer AR, Mao A, Cochrane A, Parent LJ. 2013. NC-mediated nucleolar localization of retroviral gag proteins. Virus Res 171:304-18.
52. Doyle M, Badertscher L, Jaskiewicz L, Guttinger S, Jurado S, Hugenschmidt T, Kutay U, Filipowicz W. 2013. The double-stranded RNA binding domain of human Dicer functions as a nuclear localization signal. Rna 19:1238-52.
53. Barrandon C, Bonnet F, Nguyen VT, Labas V, Bensaude O. 2007. The transcription-dependent dissociation of P-TEFb-HEXIM1-7SK RNA relies upon formation of hnRNP-7SK RNA complexes. Mol Cell Biol 27:6996-7006.
54. Egloff S, Studniarek C, Kiss T. 2018. 7SK small nuclear RNA, a multifunctional transcriptional regulatory RNA with gene-specific features. Transcription 9:95-101.
55. Pham VV, Salguero C, Khan SN, Meagher JL, Brown WC, Humbert N, de Rocquigny H, Smith JL, D'Souza VM. 2018. HIV-1 Tat interactions with cellular 7SK and viral TAR RNAs identifies dual structural mimicry. Nat Commun 9:4266.
56. Deveson IW, Hardwick SA, Mercer TR, Mattick JS. 2017. The Dimensions, Dynamics, and Relevance of the Mammalian Noncoding Transcriptome. Trends Genet 33:464-478.
57. Ahmed W, Liu ZF. 2018. Long Non-Coding RNAs: Novel Players in Regulation of Immune Response Upon Herpesvirus Infection. Front Immunol 9:761.
58. Dahariya S, Paddibhatla I, Kumar S, Raghuwanshi S, Pallepati A, Gutti RK. 2019. Long non-coding RNA: Classification, biogenesis and functions in blood cells. Mol Immunol 112:82-92.
59. Long Y, Wang X, Youmans DT, Cech TR. 2017. How do lncRNAs regulate transcription? Sci Adv 3:eaao2110.
60. Hu B, Huo Y, Yang L, Chen G, Luo M, Yang J, Zhou J. 2017. ZIKV infection effects changes in gene splicing, isoform composition and lncRNA expression in human neural progenitor cells. Virol J 14:217.
61. Fan J, Cheng M, Chi X, Liu X, Yang W. 2019. A Human Long Non-coding RNA LncATV Promotes Virus Replication Through Restricting RIG-I-Mediated Innate Immunity. Front Immunol 10:1711.

62. Delannoy A, Poirier M, Bell B. 2019. Cat and Mouse: HIV Transcription in Latency, Immune Evasion and Cure/Remission Strategies. Viruses 11.
63. Krasnopolsky S, Marom L, Victor RA, Kuzmina A, Schwartz JC, Fujinaga K, Taube R. 2019. Fused in sarcoma silences HIV gene transcription and maintains viral latency through suppressing AFF4 gene activation. Retrovirology 16:16.
64. Hariharan M, Scaria V, Pillai B, Brahmachari SK. 2005. Targets for human encoded microRNAs in HIV genes. Biochem Biophys Res Commun 337:1214-8.
65. Sun G, Li H, Wu X, Covarrubias M, Scherer L, Meinking K, Luk B, Chomchan P, Alluin J, Gombart AF, Rossi JJ. 2012. Interplay between HIV-1 infection and host microRNAs. Nucleic Acids Res 40:2181-96.
66. Adoro S, Cubillos-Ruiz JR, Chen X, Deruaz M, Vrbanac VD, Song M, Park S, Murooka TT, Dudek TE, Luster AD, Tager AM, Streeck H, Bowman B, Walker BD, Kwon DS, Lazarevic V, Glimcher LH. 2015. IL-21 induces antiviral microRNA-29 in CD4 T cells to limit HIV-1 infection. Nat Commun 6:7562.
67. Jiang H, Zhang G, Wu JH, Jiang CP. 2014. Diverse roles of miR-29 in cancer (review). Oncol Rep 31:1509-16.
68. Pylro VS, Oliveira FS, Morais DK, Cuadros-Orellana S, Pais FS, Medeiros JD, Geraldo JA, Gilbert J, Volpini AC, Fernandes GR. 2016. ZIKV - CDB: A Collaborative Database to Guide Research Linking SncRNAs and ZIKA Virus Disease Symptoms. PLoS Negl Trop Dis 10:e0004817.
69. Giulietti M, Righetti A, Cianfruglia L, Sabanovic B, Armeni T, Principato G, Piva F. 2018. To accelerate the Zika beat: Candidate design for RNA interference-based therapy. Virus Res 255:133-140.
70. Sanchez M, Galy B, Dandekar T, Bengert P, Vainshtein Y, Stolte J, Muckenthaler MU, Hentze MW. 2006. Iron regulation and the cell cycle: identification of an iron-responsive element in the 3'-untranslated region of human cell division cycle 14A mRNA by a refined microarray-based screening strategy. J Biol Chem 281:22865-74.
71. Schonberg DL, Miller TE, Wu Q, Flavahan WA, Das NK, Hale JS, Hubert CG, Mack SC, Jarrar AM, Karl RT, Rosager AM, Nixon AM, Tesar PJ, Hamerlik P, Kristensen BW, Horbinski C, Connor JR, Fox PL, Lathia JD, Rich JN. 2015. Preferential Iron Trafficking Characterizes Glioblastoma Stem-like Cells. Cancer Cell 28:441-455.
72. Hussain MS, Baig SM, Neumann S, Peche VS, Szczepanski S, Nurnberg G, Tariq M, Jameel M, Khan TN, Fatima A, Malik NA, Ahmad I, Altmuller J, Frommolt P, Thiele H, Hohne W, Yigit G, Wollnik B, Neubauer BA, Nurnberg P, Noegel AA. 2013. CDK6 associates with the centrosome during mitosis and is mutated in a large Pakistani family with primary microcephaly. Hum Mol Genet 22:5199-214.

CHAPTER VI

APPENDIX I

LONG NON-CODING RNAs BINDING TO DICER/GAG

6.1 INTRODUCTION

HIV-1 replication cycle is a highly regulated process that requires different viral and cellular proteins. After the provirus integration to the host genome, a small amount of viral RNA is produced, doubly spliced and exported to the cytoplasm to produce viral proteins Tat, Rev and Nef. Tat goes to the nucleus and generates significant concentrations of viral RNA by a mechanism named transactivation. During this process, Tat binds to p-TEFb and brings it to the TAR RNA. P-TEFb hyperphosphorylates RNA Pol II at the HIV-1 promoter, augmenting the number of transcripts several times (1-4). In the absence of Tat, p-TEFb is sequestered by the 7SK RNA complex (5-7). 7SK is a conserved and abundant ncRNA of 332 nt that mainly remains within the cell nucleus with some pools throughout the cytoplasm (8). Cellular proteins associated with 7SK, such as La-related protein 7 (LaRP7) and methylphosphate capping enzyme (MePCE) stabilizes the RNA whereas HEXM1/2, control p-TEFb through the inhibition of the ATP pocket in Cdk9 (9-11).

Once a large number of viral transcripts are produced, the unspliced and singly spliced products are exported from the nucleus to the cytoplasm in an assisted process by Rev and the viral sequence RRE along with the host factors CRM1 and RanGTP (12-14). During the late phase of the replication cycle, unspliced RNAs will code for Gag and Gag-Pol. Gag contains different domains: MA, CA, NC, P6 and two spacer peptides flanking NC, SP1 and SP2 (15). Gag is the major structural protein in HIV-1 and Gag alone is sufficient to assemble virus-like particles (VLP) (16).

Currently, ncRNAs like 7SK are further explored to determine their functions. Proteins of the RNAi pathway can interact with these ncRNAs types (17, 18). Usually, Dicer recognizes dsRNA and generates products of ~22nt. Dicer L shape facilitates the dsRNA recognition through the PAZ domain (19, 20). The RNase, the platform and the PAZ domain are rigid structures but behave like

hinges that make Dicer bind and bend virtually any dsRNA (21, 22). Indeed, Dicer interacts with tRNA, snoRNA and lncRNAs (23-26). We previously showed that Dicer interacts with Gag, which makes specific miRNAs interact better with this complex rather than to Dicer alone (27). In the present study, we observed that Dicer interacts with ncRNAs like snoRNAs and lncRNAs. We specifically confirm a higher concentration of 7SK bound to Dicer/Gag rather than Dicer alone.

6.2 RESULTS

6.2.1 Dicer and Dicer/Gag bind snoRNAs and lncRNAs.

Our previous work described that Dicer/Gag complexes recruit a higher concentration of specific miRNAs compared to Dicer alone and that these complexes can be localized within the cell nucleus and cytoplasm (27). To further analyze our RIP-seq results of Dicer and Dicer/Gag (Chapter II, section 2.4.7), we used a different bioinformatic approach after the peak calling using DiffBind and edgeR software. This approach can reveal Dicer interaction with double-stranded ncRNAs, and not limited to miRNAs. We found that Dicer binds snoRNAs and other ncRNAs. More interestingly, we found that Dicer had more or less concentration of ncRNAs in the presence of Gag as it does with miRNAs. The majority of RNAs in our list do not have an annotation, but few of them were annotated as snoRNAs and lncRNAs (Table 6.1).

Among the ncRNAs, our interest was sparked by the increased presence of 7SK RNA, an essential regulator of HIV-1 transactivation, which sequesters p-TEFb complex and prevents its activity on transcriptional elongation (5). The 7SK RNA bound to Dicer in the presence of Gag reached an 8.94 fold increase compared to Dicer with a false discovery rate (FDR) of 0.0004. We also noticed that the transcript length into Dicer or Dicer/Gag is 102 nt instead of 332 nt, the expected length of 7SK. We looked at this particular result in IGV using the BAM files and found that the entire

transcript is there. However, most of the reads during the sequencing were aligned to the M7 region on 7SK (Fig 6.1A).

Table 6. 1 Fold change table of ncRNAs detected on RIP-seq of Dicer and Dicer/Gag.

Transcript length	Dicer (fold change)	Dicer/Gag (fold change)	p.value	FDR	Gene
21	12.69	0	9.56E-06	0.0039	
115	10.8	0	1.18E-07	0.000128	
389	9.99	0	2.58E-07	0.000187	
19	9.87	0	3.65E-05	0.0112	
44	9.43	0	4.67E-05	0.0121	
83	9.38	0	4.81E-05	0.0121	
21	9.07	0	2.45E-06	0.0013	
57	9.06	0	5.82E-05	0.0131	SNORD104
89	9.01	0	2.27E-17	1.48E-13	
23	8.15	0	0.000105	0.0214	
108	7.36	0	0.000185	0.0326	
141	7.13	0	0.00022	0.0378	
69	7	0	7.13E-06	0.00311	
35	6.88	0	0.000269	0.0437	
69	6.83	0	0.00028	0.0437	
52	5.84	0	0.000281	0.0437	
49	0	13.85	1.25E-08	2.72E-05	
64	0	11.8	6.57E-08	8.58E-05	
63	0	11.57	1.55E-05	0.00596	
40	0	10.43	1.54E-07	0.000144	SNORD6
49	0	10.43	2.69E-05	0.0088	
51	0	9.8	3.78E-05	0.0112	SNORD101
56	0	9.54	4.39E-05	0.012	
261	0	9.25	5.20E-05	0.0122	
53	0	9.25	5.21E-05	0.0122	LINC01962
42	0	9.18	1.91E-06	0.00114	SNORD5
102	0	8.94	6.13E-07	4.00E-04	RN7SK
52	0	8.81	6.80E-05	0.0148	
31	0	8.7	1.57E-13	5.12E-10	
179	0	8.34	9.18E-05	0.0193	
44	0	8.15	4.01E-06	0.00187	
30	0	7.82	0.000131	0.026	
22	0	7.7	0.000144	0.0276	
60	0	7.59	2.59E-06	0.0013	SNORD12C
53	0	7.53	0.000163	0.0303	NUFIP1
91	0	7.47	0.00017	0.0309	SNORD13
342	0	7.29	2.11E-07	0.000172	
96	0	7.08	1.89E-05	0.00685	SNORD118
151	0	6.97	0.000249	0.0417	
238	0	6.06	4.25E-05	0.012	
61	0	6.03	2.15E-05	0.00738	
508	0	5.72	2.34E-08	3.82E-05	

FDR=False discovery rate

6.2.2 RIP-qRT-PCR and reverse RIP-qRT-PCR of Dicer/Gag complexes concentrate 7SK

To confirm RIP-seq results of 7SK RNA into Dicer and Dicer/Gag complexes, we transfected HEK 293T cells with HA-Dicer/Flag or HA-Dicer/Flag-Gag. 48h after transfection, we immunoprecipitated HA or Flag (Reverse IP), followed by qRT-PCR (Material and Methods). We then compared the collected RNA from the IPs to the input. Because we found an increased amount of 7SK-M7 regions in the RIP-seq readouts, we used two different primers to analyze 7SK in the IPs (Fig 6.1). The first set of primers was designed to amplify from the 106 bp (from 7-112 nt) bars, which is not located in M7 (aqua-green bars). The second set of primers encompasses a small section of 207-306 nt (100 bp) in the M7 (red bars) found in the RIP-seq results.

Our analysis shows that the basal levels of 7SK (input) do not change in the presence of Gag (Fig 6.1B). In contrast, IP-Dicer readouts validated the RIP-seq results where Dicer/Gag complexes had more 7SK bound than Dicer regardless of the 7SK region (Fig 6.1C). We followed our analysis and investigated if we might observe similar changes by reverse IP (IP-Flag). The IP of Gag or Dicer/Gag showed that Gag could bind 7SK transcripts too, albeit Dicer/Gag complexes had higher amounts of 7SK regardless of the region (Fig 6.1D). However, the smaller amount of bound 7SK to Gag and the large variations renders these results less significant, suggesting that Gag binds 7SK with less affinity than Dicer.

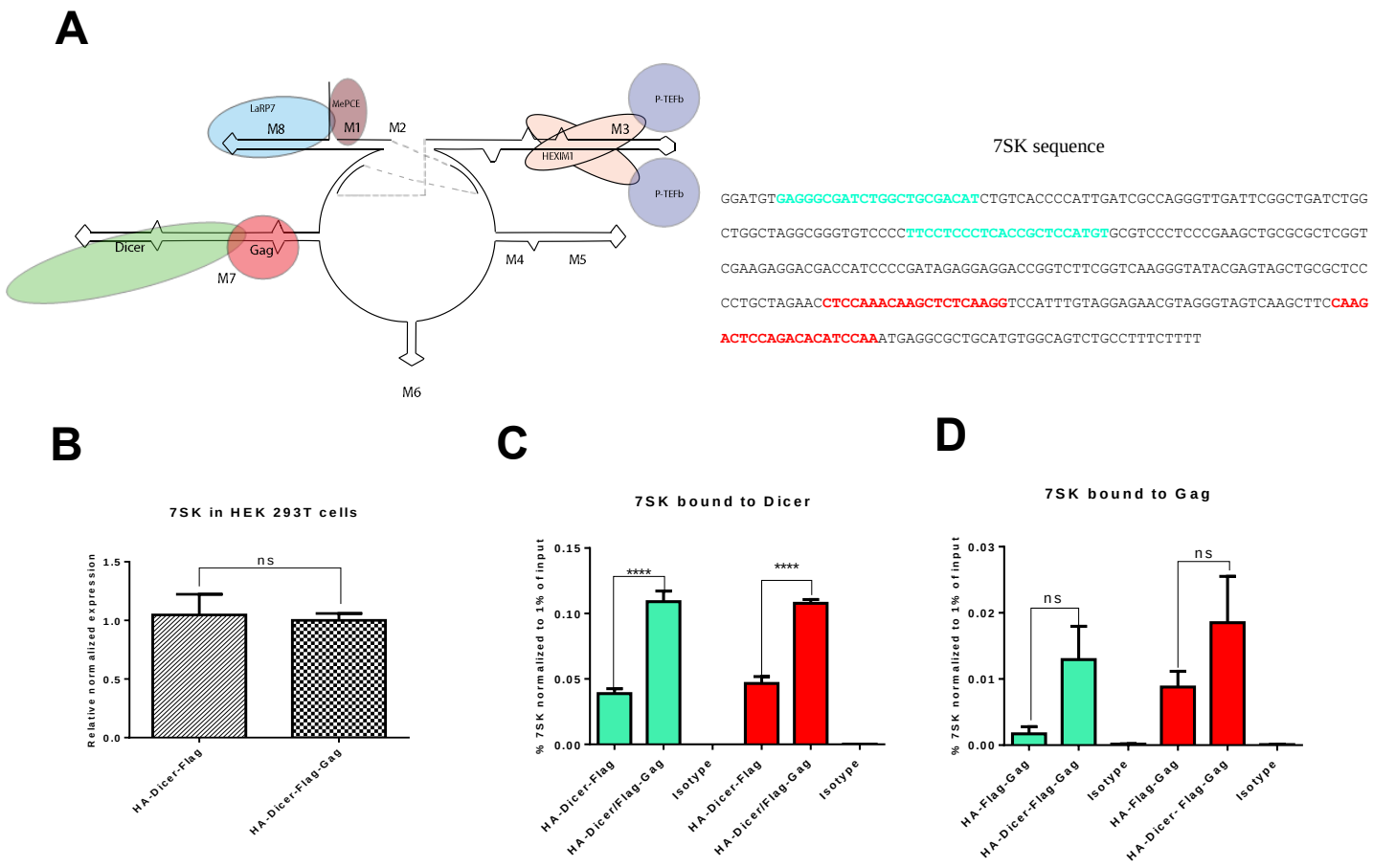

Figure 6. 1 RIP-qRT-PCR of 7SK in Dicer/Gag.

A) Representation of 7SK complex. 7SK M1 region harbors MePCE, M3 shows a dimer of HEXIM1 along with a dimer of p-TEFb, Dicer or Dicer/Gag was found to interact mainly with M7 and M8 with LaRP7. On the right side, the 7SK sequence highlighting the primers for validation, from 7-112 nt in aqua-green and from 207-306 nt in red. B) 7SK $\Delta\Delta Cq$ of HEK 293T cells co-transfected with Dicer or Dicer/Gag (inputs). C) Dicer immunoprecipitation and qRT-PCR of 7SK. The x-axis shows the IP-HA conditions plus isotype control. Aqua-green bars display an amplicon of 106 bp (from 7-112 nt), $p<0.0001$. Red bars represent the amplification of 100 bp (207-306 nt) in the M7 region (red), $p<0.0001$. D) Gag IP and qRT-PCR of 7SK. The x-axis shows the IP-Flag conditions plus isotype control. Aqua-green bars display an amplicon of 106 bp , $p<0.0001$. Red bars represent the amplification of 100 bp in red, $p<0.0001$.

6.2.3 HIV-1 infected Sup-T1 cells do not display differences in 7SK basal levels.

To further determine if 7SK increase in Dicer binding could be attributed to a difference in its production by viral products proteins, we infected T-cell lines Sup-T1 with HIV-1 and tracked the infection up to 9 to 12 days (Fig 6.2A) in three independent experiments. We chose two different time points during the infection to verify the amount of 7SK. Day five represents HIV-1 passing the threshold of small quantification of RT activity and day 9 or 12 when the virus has a high replication rate. We then performed qRT-PCR for 7SK using 7SK1 primers. Our results indicate that 7SK levels are similar in infected and mock-infected cells (Fig 6.2B). Therefore, the increased amount of 7SK observed in Dicer and Dicer/Gag complexes cannot be attributed to an increased production by Gag expression or HIV-1 infection.

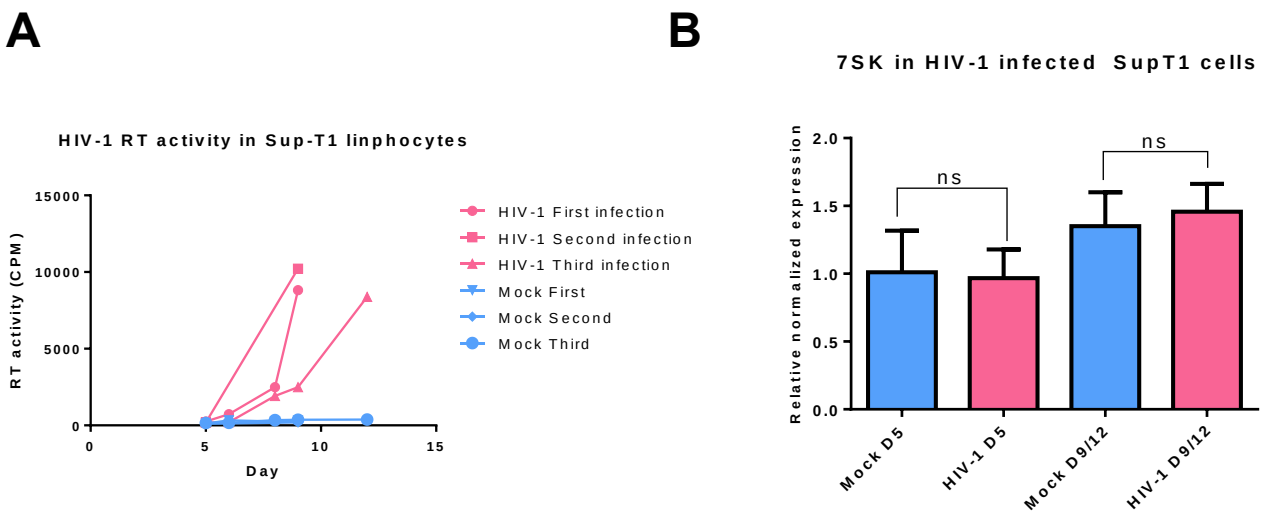

Figure 6. 2 7SK expression on infected Sup-T1 with HIV-1.

A) HIV-1 RT activity tracked and detected with α^{32}P CTP at days 5, 6, 8, 9 or 12 of infection. Y-axis displays the counts per minute (CPM) and X-axis the days of infection. B) Relative normalized expression of 7SK in infected and mock-infected SupT1 with HIV-1 at day 5 and 9 or 12 (as shown in A).

6.3 DISCUSSION

Our previous work demonstrated how Dicer/Gag interaction can influence the loading of different miRNAs. In this preliminary work, we modified specific bioinformatic parameters and discovered that not only miRNAs could bind to Dicer and Dicer/Gag but also lncRNAs, snoRNAs and other ncRNAs where no annotation exists. Using a differential binding (Diffbind) analysis and a statistical approach with edgeR, we identified that Dicer bound 16 sequences at a higher concentration than Dicer/Gag with a significant FDR value. Among those, SNORD104 was the only annotated gene for Dicer. The analysis of samples from Dicer/Gag IPs showed 26 more concentrated RNA sequences than with Dicer alone. Among them, 9 sequences are known. The majority of these sequences belong to Box C/D snoRNAs that do not participate to the generation of rRNA. Instead, these snoRNAs might participate in splicing, polyadenylation, or being Dicer substrates to form miRNAs (24, 25, 28-31). Our readouts also detected the long intergenic non-protein coding RNA 1962 (LINC01962) an 863 nt RNA, which was found more frequently bound to Dicer/Gag complexes than to Dicer alone.

The negative p-TEFb regulator 7SK is another lncRNA that binds preferentially to Dicer/Gag (Table 6.1). 7SK has high relevance to HIV-1 replication because 7SK sequesters p-TEFb, which can be recruited by Tat for viral transactivation. Our bioinformatic analysis using DiffBind and statistical analysis with edgeR only recognized a fragment of 102 nt from 332 nt in 7SK. To elucidate this information, we looked at the BAM files that contain the reads aligned to the human genome and found that the entire 7SK sequence was bound to Dicer in the presence or absence of Gag. Interestingly, a 7SK fragment of 102 nt corresponding to the M7 stem loop in 7SK was more concentrated. Previous work with another member of the 7S family (7SL) (32), identified that Dicer binds and cleaves 7SL into fragments of different lengths (33). We designed two different

sets of primers and we confirmed our RIP-seq results by IP-HA-Dicer-qRT-PCR. The first set of primers (7SK1) was designed to amplify the first nucleotides of 7SK but not M7 and the second set (7SK2) to detect M7. We corroborated that Dicer/Gag contains more 7SK ($p<0.0001$) with no changes in the input (Fig 6.1A, B). Surprisingly, we did not notice any difference of 7SK using the two different primers.

We then carried out reverse IPs and precipitated Gag in the presence or absence of Dicer. We noticed that Gag could bind 7SK without Dicer, although the concentration of 7SK was increased in its presence (Fig 6.1C). Gag is the primary structural protein of HIV-1 that interacts with the genomic RNA and packages it into the nascent viral particles. But its binding is not limited to viral RNA (34). NC domain interacts and unwinds $tRNA^{Lys3}$ followed by annealing an 18 nt sequence to the viral RNA that is used as a primer for cDNA synthesis (35). Another example is 7SL, a cytoplasmic lncRNA that is part of the signal recognition particle complex that mediates the translocation of proteins into the ER lumen (36). 7SL interacts with Gag and is incorporated into viral particles (37, 38). Recent data suggest that one virion possesses 14 copies of 7SL but its function in the context of HIV-1 is unknown (39).

To confirm that 7SK expression is not affected by Gag or any other HIV-1 component, we infected Sup-T1 cells with HIV-1 up to 9 to 12 days. After confirming the peaks of infection at day 9 or 12 by RT activity assay, we measure the 7SK expression of mock and infected cells at day 5 and day 9 or 12. Our readouts on 7SK verified that its transcription is not affected by HIV-1 (Fig 6.2). Therefore, our results suggest that the differences in 7SK concentration between Dicer and Dicer/Gag observed after IPs are governed only by the binding. In summary, HIV-1 Gag changes the concentration of ncRNAs bound to Dicer.

We confirmed that 7SK binds to Dicer and Gag together and individually but the affinity with Gag seems to be lower as indicated by the normalized percent of input (Fig 6.1C compared to D). A follow-up investigation should address whether Dicer can cleave 7SK and the consequences in the viral transactivation.

6.4 MATERIALS AND METHODS

6.4.1. RNA immunoprecipitation sequencing (RIP-seq) and analysis for ncRNAs

We previously described the RIP-sec protocol in chapter II. Briefly, HEK 293T cells were transfected with HA-Dicer/pFlag (Dicer), HA-Dicer/Flag-Gag (Dicer/Gag), HA/Flag-Gag (negative control). 48 h after transfection we lysed the cells with the RNA extraction buffer [150 mM NaCl, 50 mM Tris, pH 7.5, 5 mM EDTA, 0.5% Nonidet P-40, 0.5% of RNaseOUT (Invitrogen), 0.2% of Vanadyl (NEB), 100 mM of DTT (Invitrogen) protease and phosphatase inhibitor cocktail (Roche)]. The supernatant was preserved and incubated with 50 µl of 1% BSA blocked Pierce anti-HA magnetic beads (Thermo Fisher) or 1% BSA blocked Pierce NHS-activated magnetic beads (Thermo Fisher) with mouse monoclonal IgG1 isotype antibody overnight at 4°C with agitation. After this time, the supernatant was discarded and the beads were washed with RNA extraction buffer three times. 30 µl of Laemmli sample buffer was added to the beads and heated 5 min at 95°C for protein analysis. RNA extraction was performed by using Trizol reagent and purified with miRNeasy mini kit (QIAGEN) and DNase set (QIAGEN). Library preparation was performed with 300 ng of total RNA using New England BioLabs NEBNext® Small RNA Library Prep Set for Illumina® and run in Illumina HiSeq2500, SR50 at Genome Quebec, Canada.

Sequencing analysis was performed at Genome Quebec with the following setting: trimming and clipping were performed using Trimmomatic (40). The filtered reads were aligned to GRCh37 of

Homo_Sapiens using STAR (41). The generated BAM files were merged using Picard (42). Control samples (HA/Flag-Gag and the isotype antibody sample) were merged into a single file as well to use with the peak-calling software. We use MACSv2 for the peak calling, adjusting the nmodel and extsize parameters to reflect a better condition for the experiment (43). All called peaksets were annotated using annotatePeaks.pl from Homer (44).

To determine the statistical differences between peaks from both experimental conditions (Dicer vs Dicer/Gag), a Differential Binding Analysis was carried out using the R package DiffBind (45). The main idea of this package is to find overlapping peaks between the samples, merging the peak sets and then counting reads in the overlapping intervals of the peak sets. Differentially bound sites are identified based on evidence of binding affinity. The statistical analysis was carried out using edgeR (46, 47).

6.4.2 RIP- qRT-PCR

RIP qRT-PCR protocol is described in detail in chapter II (2.6.10). In brief, 2.6 x10^6 HEK-293T cells were co-transfected with a total of 9 µg of HA-Dicer and Flag-Gag. 48 h post-transfection cells were washed with PBS, lysed with RNA extraction buffer and centrifuged. The supernatant was kept, and 2.2 mg of protein was used for the IP and from it, 1% was used as input. Supernatants were cleared using 30 µl of agarose protein A beads (Millipore) in constant agitation for 1.5 h at 4°C. The sample was centrifuged at 8000 rpm for 1 min, and the supernatant was kept and incubated with 2 µl of the HA antibody (H6908, Sigma-Aldrich) or 2 µl of the Flag (Anti-Flag M2, Sigma-Aldrich) antibody or 1 µl of control rabbit serum overnight. 50 µl of pre-blocked Dynabeads protein A were added for 3 h at 4°C. The supernatant was discarded, and the beads were washed 3 times with an RNA extraction buffer for 5 min with a magnetic stand.

After the final wash, RNA was extracted using TRIzol-chloroform. Further purification was performed with miRNeasy mini kit and RNase-free DNase set. 300 ng of total RNA was used to synthesize cDNA. The protocol to detect 7SK was based on (48). Table 6.2 shows two different primers for 7SK. Data Cq acquisition and analysis were performed using Bio-Rad CFX96 and CFX maestro software respectively. Actin was used to calculate $\Delta\Delta Cq$ and percent input method [100*2^ (Adjusted input - Ct (IP)] for the abundance of 7SK in IPs. T-test was applied for statistical analysis using Graph-Pad Prism V6.

Table 6. 2. 7SK primers

Name	Sense	Sequence
7SK1	Fwd	GAGGGCGATCTGGCTGCGACAT
	Rev	ACATGGAGCGGTGAGGGAGGAA
7SK2	Fwd	CTCCCCTGCTAGAACCTCCAAA
	Rev	GCGCCTCATTTGGATGTGTC

6.4.3 Sup-T1 infection by HIV-1 and qRT-PCR

In biosafety level 3 (BL3) facilities, 2.4 x 10^6 Sup-T1 cells were plated. Twelve hours later, the cells were infected with 5 x 10^5 cpm of HIV-1 in 3 ml RPMI (Hyclone) and incubated for 2 h at 37 ℃. After this time, 2 ml of supplemented RPMI with 10% FBS were added in a T25 flask and incubated at 37 ℃ overnight. Next, 3 ml of fresh supplemented RPMI were added and re-incubated at 37 ℃. On day two, Sup-T1 cells were centrifuged at 1200 rpm for 5 min at room temperature and 4 ml of the supernatant were replaced by 4 ml of fresh media. On day 5, 1 ml of resuspended Sup-T1 was saved for RNA extraction. Sup-T1 cells were centrifuged at 1200 rpm for 5 min at room temperature and 200 µl of the supernatant were taken and added to a 96 well plate, which was stored at -20℃ for RT-activity assay. 4 ml of supernatant was removed and replaced by fresh

media and cells were re-incubated at 37 ℃. The process was repeated at days 6,8,9 or 12. HIV-1 RT activity protocol is described elsewhere (49).

In BL3 facilities, 1ml aliquots of infected cells at day 5,6,8,9 or 12 were centrifuged at 1200 rpm for 5 min at room temperature, the supernatant was discarded and 700 µl of TRIzol reagent with 140 µl of chloroform were added. RNA extraction, purification, and qRT-PCR were followed as indicated in (48) with 7SK1 primers (Table 6.2). Data Cq acquisition and analysis were performed using Bio-Rad CFX96 and CFX maestro software respectively. Actin was used to calculate $\Delta\Delta Cq$ of 7SK. T-test was applied for statistical analysis using Graph-Pad Prism V6.

6.5 REFERENCES

1. Cary DC, Fujinaga K, Peterlin BM. 2016. Molecular mechanisms of HIV latency. J Clin Invest 126:448-54.
2. Kao SY, Calman AF, Luciw PA, Peterlin BM. 1987. Anti-termination of transcription within the long terminal repeat of HIV-1 by tat gene product. Nature 330:489-93.
3. Garber ME, Wei P, KewalRamani VN, Mayall TP, Herrmann CH, Rice AP, Littman DR, Jones KA. 1998. The interaction between HIV-1 Tat and human cyclin T1 requires zinc and a critical cysteine residue that is not conserved in the murine CycT1 protein. Genes Dev 12:3512-27.
4. Wei P, Garber ME, Fang SM, Fischer WH, Jones KA. 1998. A novel CDK9-associated C-type cyclin interacts directly with HIV-1 Tat and mediates its high-affinity, loop-specific binding to TAR RNA. Cell 92:451-62.
5. Pham VV, Salguero C, Khan SN, Meagher JL, Brown WC, Humbert N, de Rocquigny H, Smith JL, D'Souza VM. 2018. HIV-1 Tat interactions with cellular 7SK and viral TAR RNAs identifies dual structural mimicry. Nat Commun 9:4266.
6. Delannoy A, Poirier M, Bell B. 2019. Cat and Mouse: HIV Transcription in Latency, Immune Evasion and Cure/Remission Strategies. Viruses 11.
7. Gatignol A. 2007. Transcription of HIV: Tat and cellular chromatin. Adv Pharmacol 55:137-59.
8. Faust TB, Li Y, Bacon CW, Jang GM, Weiss A, Jayaraman B, Newton BW, Krogan NJ, D'Orso I, Frankel AD. 2018. The HIV-1 Tat protein recruits a ubiquitin ligase to reorganize the 7SK snRNP for transcriptional activation. Elife 7:e31879.
9. Markert A, Grimm M, Martinez J, Wiesner J, Meyerhans A, Meyuhas O, Sickmann A, Fischer U. 2008. The La-related protein LARP7 is a component of the 7SK

ribonucleoprotein and affects transcription of cellular and viral polymerase II genes. EMBO Rep 9:569-75.
10. Jeronimo C, Forget D, Bouchard A, Li Q, Chua G, Poitras C, Therien C, Bergeron D, Bourassa S, Greenblatt J, Chabot B, Poirier GG, Hughes TR, Blanchette M, Price DH, Coulombe B. 2007. Systematic analysis of the protein interaction network for the human transcription machinery reveals the identity of the 7SK capping enzyme. Mol Cell 27:262-74.
11. Russo AA, Tong L, Lee JO, Jeffrey PD, Pavletich NP. 1998. Structural basis for inhibition of the cyclin-dependent kinase Cdk6 by the tumour suppressor p16INK4a. Nature 395:237-43.
12. Malim MH, Hauber J, Le SY, Maizel JV, Cullen BR. 1989. The HIV-1 rev trans-activator acts through a structured target sequence to activate nuclear export of unspliced viral mRNA. Nature 338:254-7.
13. Daly TJ, Cook KS, Gray GS, Maione TE, Rusche JR. 1989. Specific binding of HIV-1 recombinant Rev protein to the Rev-responsive element in vitro. Nature 342:816-9.
14. Fornerod M, Ohno M, Yoshida M, Mattaj IW. 1997. CRM1 is an export receptor for leucine-rich nuclear export signals. Cell 90:1051-60.
15. Freed EO. 2015. HIV-1 assembly, release and maturation. Nat Rev Microbiol 13:484-96.
16. Morikawa Y, Goto T, Sano K. 1999. In vitro assembly of human immunodeficiency virus type 1 Gag protein. J Biol Chem 274:27997-8002.
17. Pong SK, Gullerova M. 2018. Noncanonical functions of microRNA pathway enzymes - Drosha, DGCR8, Dicer and Ago proteins. FEBS Lett 592:2973-2986.
18. Li JH, Liu S, Zheng LL, Wu J, Sun WJ, Wang ZL, Zhou H, Qu LH, Yang JH. 2014. Discovery of Protein-lncRNA Interactions by Integrating Large-Scale CLIP-Seq and RNA-Seq Datasets. Front Bioeng Biotechnol 2:88.
19. Lau PW, Guiley KZ, De N, Potter CS, Carragher B, MacRae IJ. 2012. The molecular architecture of human Dicer. Nat Struct Mol Biol 19:436-40.
20. Liu Z, Wang J, Cheng H, Ke X, Sun L, Zhang QC, Wang HW. 2018. Cryo-EM Structure of Human Dicer and Its Complexes with a Pre-miRNA Substrate. Cell 173:1191-1203.e12.
21. Macrae IJ, Li F, Zhou K, Cande WZ, Doudna JA. 2006. Structure of Dicer and mechanistic implications for RNAi. Cold Spring Harb Symp Quant Biol 71:73-80.
22. Hutvagner G, McLachlan J, Pasquinelli AE, Balint E, Tuschl T, Zamore PD. 2001. A cellular function for the RNA-interference enzyme Dicer in the maturation of the let-7 small temporal RNA. Science 293:834-8.
23. Cole C, Sobala A, Lu C, Thatcher SR, Bowman A, Brown JW, Green PJ, Barton GJ, Hutvagner G. 2009. Filtering of deep sequencing data reveals the existence of abundant Dicer-dependent small RNAs derived from tRNAs. Rna 15:2147-60.
24. Kawaji H, Nakamura M, Takahashi Y, Sandelin A, Katayama S, Fukuda S, Daub CO, Kai C, Kawai J, Yasuda J, Carninci P, Hayashizaki Y. 2008. Hidden layers of human small RNAs. BMC Genomics 9:157.
25. Falaleeva M, Stamm S. 2013. Processing of snoRNAs as a new source of regulatory non-coding RNAs: snoRNA fragments form a new class of functional RNAs. Bioessays 35:46-54.
26. Faulkner GJ. 2013. Retrotransposon silencing during embryogenesis: dicer cuts in LINE. PLoS Genet 9:e1003944.

27. Alpuche-Lazcano SP, Scarborough RJ, Daniels SM, Rance E, Mouland AJ, Gatignol A. 2020. HIV-1 Gag interacts with Dicer and increases its binding to specific microRNAs. submitted.
28. Brameier M, Herwig A, Reinhardt R, Walter L, Gruber J. 2011. Human box C/D snoRNAs with miRNA like functions: expanding the range of regulatory RNAs. Nucleic Acids Res 39:675-86.
29. Yang N, Kazazian HH, Jr. 2006. L1 retrotransposition is suppressed by endogenously encoded small interfering RNAs in human cultured cells. Nat Struct Mol Biol 13:763-71.
30. Hellwig S, Bass BL. 2008. A starvation-induced noncoding RNA modulates expression of Dicer-regulated genes. Proc Natl Acad Sci U S A 105:12897-902.
31. Ouellet DL, Plante I, Landry P, Barat C, Janelle ME, Flamand L, Tremblay MJ, Provost P. 2008. Identification of functional microRNAs released through asymmetrical processing of HIV-1 TAR element. Nucleic Acids Res 36:2353-65.
32. Suh D, Yuan Y, Henning D, Reddy R. 1989. Secondary structure of 7SK and 7-2 small RNAs. Possible origin of some 7SK pseudogenes from cDNA formed through self-priming by 7SK RNA. Eur J Biochem 186:221-6.
33. Ren YF, Li G, Wu J, Xue YF, Song YJ, Lv L, Zhang XJ, Tang KF. 2012. Dicer-dependent biogenesis of small RNAs derived from 7SL RNA. PLoS One 7:e40705.
34. Rulli SJ, Jr., Hibbert CS, Mirro J, Pederson T, Biswal S, Rein A. 2007. Selective and nonselective packaging of cellular RNAs in retrovirus particles. J Virol 81:6623-31.
35. Rein A. 2010. Nucleic acid chaperone activity of retroviral Gag proteins. RNA Biol 7:700-5.
36. Egea PF, Stroud RM, Walter P. 2005. Targeting proteins to membranes: structure of the signal recognition particle. Curr Opin Struct Biol 15:213-20.
37. Itano MS, Arnion H, Wolin SL, Simon SM. 2018. Recruitment of 7SL RNA to assembling HIV-1 virus-like particles. Traffic 19:36-43.
38. Keene SE, King SR, Telesnitsky A. 2010. 7SL RNA is retained in HIV-1 minimal virus-like particles as an S-domain fragment. J Virol 84:9070-7.
39. Simonova A, Svojanovska B, Trylcova J, Hubalek M, Moravcik O, Zavrel M, Pavova M, Hodek J, Weber J, Cvacka J, Paces J, Cahova H. 2019. LC/MS analysis and deep sequencing reveal the accurate RNA composition in the HIV-1 virion. Sci Rep 9:8697.
40. Bolger AM, Lohse M, Usadel B. 2014. Trimmomatic: a flexible trimmer for Illumina sequence data. Bioinformatics 30:2114-20.
41. Dobin A, Davis CA, Schlesinger F, Drenkow J, Zaleski C, Jha S, Batut P, Chaisson M, Gingeras TR. 2013. STAR: ultrafast universal RNA-seq aligner. Bioinformatics 29:15-21.
42. passing Pb. 2019. Picard. https://broadinstitute.github.io/picard/. Accessed Mar, 2018.
43. Zhang Y, Liu T, Meyer CA, Eeckhoute J, Johnson DS, Bernstein BE, Nusbaum C, Myers RM, Brown M, Li W, Liu XS. 2008. Model-based analysis of ChIP-Seq (MACS). Genome Biol 9:R137.
44. Heinz S, Benner C, Spann N, Bertolino E, Lin YC, Laslo P, Cheng JX, Murre C, Singh H, Glass CK. 2010. Simple combinations of lineage-determining transcription factors prime cis-regulatory elements required for macrophage and B cell identities. Mol Cell 38:576-89.
45. Ross-Innes CS, Stark R, Teschendorff AE, Holmes KA, Ali HR, Dunning MJ, Brown GD, Gojis O, Ellis IO, Green AR, Ali S, Chin SF, Palmieri C, Caldas C, Carroll JS. 2012.

Differential oestrogen receptor binding is associated with clinical outcome in breast cancer. Nature 481:389-93.
46. Robinson MD, McCarthy DJ, Smyth GK. 2010. edgeR: a Bioconductor package for differential expression analysis of digital gene expression data. Bioinformatics 26:139-40.
47. McCarthy DJ, Chen Y, Smyth GK. 2012. Differential expression analysis of multifactor RNA-Seq experiments with respect to biological variation. Nucleic Acids Res 40:4288-97.
48. Alpuche-Lazcano SP, McCullogh CR, Del Corpo O, Rance E, Scarborough RJ, Mouland AJ, Sagan SM, Teixeira MM, Gatignol A. 2018. Higher Cytopathic Effects of a Zika Virus Brazilian Isolate from Bahia Compared to a Canadian-Imported Thai Strain. Viruses 10:53.
49. Scarborough RJ, Levesque MV, Perreault JP, Gatignol A. 2014. Design and evaluation of clinically relevant SOFA-HDV ribozymes targeting HIV RNA. Methods Mol Biol 1103:31-43.

APPENDIX II

KNOCK OUT OF TRBP USING CRISPR-CAS9

6.6 INTRODUCTION

MiRNA processing and targeting are carried out by the RISC-loading complex in the cytoplasm, which is composed of Dicer, TRBP and Ago2 (1). Dicer binds pre-miRNAs that were exported from the nucleus and edits them into ds-miRNAs (2, 3). After strand separation, the guide strand of the ds-miRNAs bound to Ago2 reaches the closest target and anneal the miRNA to the mRNA for later repression and degradation (4-7).

TRBP was originally discovered as a host protein that binds HIV-1 TAR RNA enhancing its replication and since then, different functions have been identified (8-11). In the context of RNAi, TRBP provides accuracy and steadiness to Dicer cleavage by placing the pre-miRNA into the right position, which enhances the processing kinetics (12-15). In the context of RNAi, the absence of TRBP compromises Dicer's cleavage, producing isomiRNAs that impair many mRNAs and, consequently, cell functions (16-18). TRBP knock out in mice induces a decrease in growth rate and defect in spermatogenesis in males. Premature death generally occurs at weaning, which confirms the importance of TRBP during development (19).

Gene editing technology began in 1971 with the production of the first restriction endonucleases (20) and to date, we use the recombination technology to produce changes within the genome (21). Three different technologies are currently available to knock out (KO) genes with programable nucleases, which create double-strand breaks (DSB). First, edition by zinc finger nucleases (ZFN) is based on the recombination with FokI (restriction enzyme) that detects and edits sequences of 18 nt (22). Another technology uses transcription activator-like effector nuclease (TALEN), which combines the activity of FokI and the bacterial type III secretion protein TALE (22). Finally, Clustered Regularly Interspaced Short Palindromic Repeats (CRISPR)-Cas9 is a recombinational

technology based on guide RNAs (gRNAs) that recognizes DNA sequences and a Cas nuclease (22).

CRISPR-Cas9 was first discovered as a mechanism of bacterial immunity against phages (23) and in 2012 Drs. Emmanuelle Charpentier and Jennifer Doudna proposed to use this bacterial defense mechanism as a genome-editing tool (24). CRISPR-Cas systems use a Cas enzyme (commonly Cas9), a crRNA, and gRNA or spacer, which is the complementary sequence to the gene to edit (25). Following the target recognition, Cas9 cleaves the DNA sequence producing a DSB that is repaired by the cellular non-homologous end joining (NHEJ) mechanism. During the repair, insertions or deletions (INDELS) change the reading frame that will encounter stop codons and consequently the end of translation and gene inactivation (KO). Alternatively, the use of a DNA donor during the DSB leads to a homology-direct repair (HDR) that brings a specific sequence to insert into the genome (22). The only limitation of this technology is the use of proto-spacer adjacent motifs (PAMs), a complementary sequence to the genome made of an NGG sequence. However, when NGGs are not present, new Cas enzymes are being investigated as alternatives and as a new technology to target RNA, for gene activation or repression and for epigenetic modulation (25, 26).

Here, we used CRISPR-Cas9 to produce TRBP KO HEK 293T cells. The creation of these mutant cells will allow analyzing the importance of TRBP within different contexts, especially in the analysis of RNAi with various viruses such as HIV-1, ZIKV, Ebola and others.

6.7 RESULTS

6.7.1 TRBP gRNA in silico and SURVEYOR assay

The critical step to KO a gene using CRISPR-Cas9, is the *in silico* design of gRNAs. Therefore, gRNAs for TRBP were made using tool editing program designed by Feng Zhang (27) and compared with gRNA made using gRNA design tool from Dharmacon (28). Among the options, we chose one of the best-ranked gRNAs in both programs that revealed only five possible off-target genes. We cloned the gRNA for TRBP KO using GeneArt CRISPR Nuclease vector kit (Life Technologies) and transfected HEK 293T cells. After the cell sorting for orange fluorescence protein expression, we amplified 37 of 192 clones that were generated. Next, we tested 12 clones in a SURVEYOR assay using GeneArt Genomic Cleavage Detection Kit (Life Technologies) to detect INDELs. We found that only the 5M and 15L clones were positive to the assay, which generate 13 and 17% of INDELS accordingly (Fig 6.3).

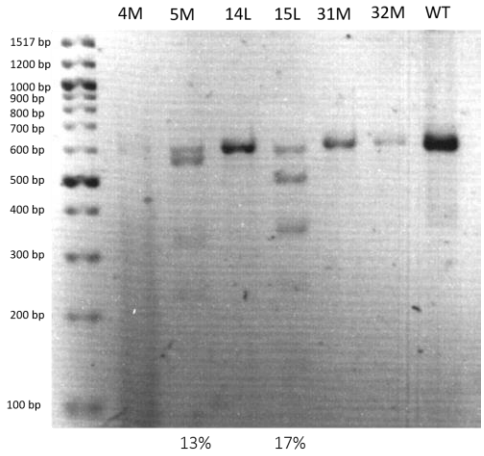

Figure 6. 3 INDELs detection in TRBP KO.

The percentage of insertions and deletions were confirmed by SURVEYOR assay in clones 5M (13%) and 15L (17%). INDELs percentage was calculated according to (27). Bands at 350 and 500 bp represent PCR products that were re-annealed and detected by the Detection Enzyme (Life Technologies) that cleaved and generated products of different sizes.

6.7.2 TRBP KO confirmation of 5M and 15L clones.

We confirmed the TRBP KO cells by Western blot using the clones that were positive for the SURVEYOR assay. We also tested two other clones that had a good intensity during the sorting. TRBP has two isoforms, TRBP1 and TRBP2. TRBP2 is 21 amino acids longer than TRBP1 in the N-terminal end (29). To confirm the KO in the two isoforms, we compared our results with the overexpressed TRBP1 and TRBP2. In our four tested clones, we could not detect any TRBP signal (Fig 6.4).

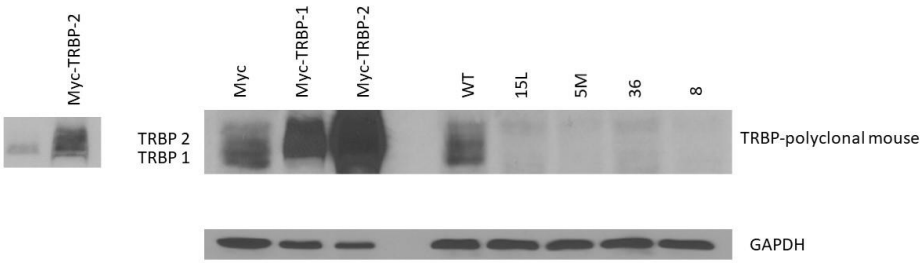

Figure 6. 4 TRBP KO confirmation by Western blot.

From left to right, the first three lanes correspond to transfected cells with Myc or Myc-TRBP1 or Myc-TRBP2. The fourth lane is an empty well followed by HEK 293T TRBP wild type (WT), TRBP KO clones 15L, 5M, 36 and 8. On the left side, a lower exposure of overexpressing TRBP1 and TRBP2 is shown. GAPDH was used as housekeeping control.

6.7.3. Sequencing and confirmation of INDELS in TRBP alleles.

We continued our confirmation of TRBP KO clones using capillary electrophoresis sequencing. We designed and used primers that flanked the cleavage produced by Cas9 in the mutants 5M and 15L. KO genes by CRISPR-Cas9 technology produce a DSB that is repaired by NHEJ, which introduces random nucleotides or deletes part of the original sequence (22). Our results showed that CRISPR Cas9 produced deletion for clones 5M and 15L in *tarbp2* compared to the WT (Fig 6.5). The translation of these products showed stop codons and, therefore, the complete inhibition of TRBP.

Figure 6. 5 Interruption of *tarbp2* in HEK 293T.

TRBP KO clones 5M and 15L were sequenced in proximity to DSB produced by Cas9. From top to bottom, translation comparison between TRBP WT, TRBP 5M and TRBP 15L mutant. Red stars represent the stop codons.

6.8 DISCUSSION

CRISPR-Cas9 is a state of the art technology for gene editing that has constantly improved in recent years (25). Here, we showed that using this technology, we successfully created a HEK 293T cell line that lost *tarbp2* and TRBP protein expression (Fig 6.4). TRBP is an essential protein for the correct processing of pre-miRNAs. Its absence or lack of interaction with Dicer has severe consequences in RNAi, PKR activation, cancer, and spermatogenesis (8, 17-19). Nonetheless, the lack of TRBP in cells has been poorly described, especially in the context of virology. TRBP KO murine models (19, 30) are not suitable to study most human viruses and *tarbp2*$^{-/-}$ HeLa cells (17) have not been distributed to virologists. The main goal of KO TRBP was to explore different effects with various viruses like HIV-1, ZIKV, Ebola and influenza. We partially know TRBP's behavior in the context of HIV-1 (9, 10, 31). However, research in the RNAi context has not been completely analyzed. Therefore, TRBP KO cells will be used to elucidate miRNA changes in the presence of HIV-1 and whether these changes could impair or not the HIV-1 replication. Furthermore, evidence suggests that ZIKV replication might be affected by the RNAi pathway (32, 33). TRBP KO cells might add interesting insights to determine TRBP importance during ZIKV infection. The modulation of isomiRNAs likely plays roles that establish mechanisms of dysregulation of ZIKV. In conclusion, we have provided a new model to study the various implications of TRBP in cell biology. We especially suggest using this KO cell line to study viruses and their implications on RNAi.

6.9 MATERIALS AND METHODS

6.9.1. Guide strand analysis for TRBP KO

We first designed gRNAs *in silico* via the CRISPR design tool suggested in (27) and we compared them to guides produced in (28). gRNA must be chosen based on PAMs for Cas9 and must contain minimal off-targets.

6.9.2. GeneArt CRISPR for TRBP KO cells.

GeneArt CRISPR Nuclease vector kit (Life Technologies) was used according to the manufacturer protocol and cloned in HEK 293T. Sorting was carried out in a FACSAria Fusion (Beckman-Dickinson). Clones that produced Cas9-orange fluorescent protein at 560 nm were classified in low, medium and high intensity. Cell sorting was performed in the flow cytometry and cell imaging core facility at the Lady Davis Institute. After two weeks of incubation, the surviving clones were expanded in 6 well plates.

6.9.3. Detection of INDELs by Surveyor nuclease assay.

GeneArt Genomic Cleavage Detection Kit (Life Technologies) was used for the detection of INDELS, according to the manufacturer. The products were run on a 2% agarose gel stained with redsafe (Froggabio). INDEL percentage was calculated according to the next formula:

$$\text{INDEL\%} = 100 \times (1 - \sqrt{(1 - fcut)})$$

Fcut= PCR product cleaved (27).

6.9.4. Immunobloting

HEK 293T cells WT and TRBP KO were plated in 6-well plates or plated and transfected using PEI transfection reagent at a 1:3 DNA/TransIT ratio with 2µg of Myc-TRBP1 or Myc-TRBP2 (18) for 24 h. Protein inputs were extracted and run according to (34). WT and KO out cells were washed twice with phosphate-buffered saline (PBS) (Wisent) and lysed in cold lysis buffer (50mM Tris-HCl pH7.4, 150mM NaCl, 5mM EDTA pH8.0, 10% Glycerol, 1% Nonidet (N) P-40) with protease inhibitor cocktail (Roche). The lysates were sunk in liquid nitrogen for 15-sec and centrifuged for 15 min at 13,000 rpm. The supernatant was quantified by Bradford assay (Bio-Rad) and 40 µg of protein mixed with Laemmli sample buffer were incubated for 5 min at 95°C. Protein samples were separated by sodium dodecyl sulfate polyacrylamide gel electrophoresis (SDS-PAGE) and wet-transferred overnight at 150 mA to Hybond nitrocellulose membranes (Bio-Rad) as described (35, 36). Membranes were blocked for 1 h with 5% milk in 0.1% Tris-buffered saline tween 20 (TBS-T) followed by three washes with TBS-T. The membranes were incubated overnight at 4°C with anti-TRBP (Médimabs, polyclonal mouse made in house) antibody at 1/1000 dilution and anti-GAPDH antibody (Clontech) at 1/2500 dilution. Next, three washes with TBS-T to the membranes were applied, followed by incubation with horseradish peroxidase-conjugated secondary antibodies (Amersham or Rockland Immunochemicals) at a 1:5000 dilution. After three washes with TBS-T, TRBP or GAPDH were visualized with Western Lightning Plus-ECL reagent (Perkin-Elmer).

6.9.5. DNA extraction, purification and sequencing

Nuclei lysis buffer (0.01M Tris-HCL, pH 8.2, 0.4M NaCl, 0.002M Na2EDTA), 500 µl of SDS (20%), Protein-K buffer (1% SDS, 0.002M Na_2EDTA) and 250 µl of proteinase K were mix to make a DNA extraction buffer mix. Then, HEK 293T cells WT and TRBP KO were plated in 6-

well plates. After 24 h incubation, mutant or TRBP KO were washed once with PBS and 1 ml of DNA extraction buffer was added to each well. Cell lysates were mixed and transferred to Eppendorf tubes and incubated overnight at 37℃. 200 µl pf NaCl (6M) are added and mixed vigorously for 15 sec followed by centrifugation at 13,000 RPM for 10 min. Supernatants were transferred to 15 ml tubes and 2 volumes of ethanol anhydrous must be added. The supernatant was gently mixed and precipitated at 4500 RPM for 30 min. The precipitated DNA was washed once with 70% ethanol and centrifuged at 4500 RPM for 20 min. The pelleted was dried and dissolved in water (molecular grade).

500 ng of DNA were used to produce TRBP amplicons with primers described in section 6.9.3. with the following conditions: 1 cycle of 95℃, 40 cycles of 95℃/30sec, 55℃/30 sec, 72℃/30sec and one final extension of 72 ℃/ 7 min. The products were run in a 3.5 % agarose gel and bands were extracted and purified using QIAquik Gel extraction kit 250 (QIAGEN). Purified bands were sequenced at Genome Quebec. The sequence was analyzed using CLUSTALW.

6.10 REFERENCES

1. Wang HW, Noland C, Siridechadilok B, Taylor DW, Ma E, Felderer K, Doudna JA, Nogales E. 2009. Structural insights into RNA processing by the human RISC-loading complex. Nat Struct Mol Biol 16:1148-53.
2. Lund E, Dahlberg JE. 2006. Substrate selectivity of exportin 5 and Dicer in the biogenesis of microRNAs. Cold Spring Harb Symp Quant Biol 71:59-66.
3. Filipowicz W, Bhattacharyya SN, Sonenberg N. 2008. Mechanisms of post-transcriptional regulation by microRNAs: are the answers in sight? Nat Rev Genet 9:102-14.
4. Meijer HA, Smith EM, Bushell M. 2014. Regulation of miRNA strand selection: follow the leader? Biochem Soc Trans 42:1135-40.
5. Hu HY, Yan Z, Xu Y, Hu H, Menzel C, Zhou YH, Chen W, Khaitovich P. 2009. Sequence features associated with microRNA strand selection in humans and flies. BMC Genomics 10:413.
6. Grimson A, Farh KK, Johnston WK, Garrett-Engele P, Lim LP, Bartel DP. 2007. MicroRNA targeting specificity in mammals: determinants beyond seed pairing. Mol Cell 27:91-105.
7. Golden RJ, Chen B, Li T, Braun J, Manjunath H, Chen X, Wu J, Schmid V, Chang TC, Kopp F, Ramirez-Martinez A, Tagliabracci VS, Chen ZJ, Xie Y, Mendell JT. 2017. An Argonaute phosphorylation cycle promotes microRNA-mediated silencing. Nature 542:197-202.
8. Daniels SM, Gatignol A. 2012. The multiple functions of TRBP, at the hub of cell responses to viruses, stress, and cancer. Microbiol Mol Biol Rev 76:652-66.
9. Gatignol A, Buckler-White A, Berkhout B, Jeang KT. 1991. Characterization of a human TAR RNA-binding protein that activates the HIV-1 LTR. Science 251:1597-600.
10. Gatignol A, Duarte M, Daviet L, Chang YN, Jeang KT. 1996. Sequential steps in Tat trans-activation of HIV-1 mediated through cellular DNA, RNA, and protein binding factors. Gene Expr 5:217-28.
11. Park H, Davies MV, Langland JO, Chang HW, Nam YS, Tartaglia J, Paoletti E, Jacobs BL, Kaufman RJ, Venkatesan S. 1994. TAR RNA-binding protein is an inhibitor of the interferon-induced protein kinase PKR. Proc Natl Acad Sci U S A 91:4713-7.
12. Ma E, MacRae IJ, Kirsch JF, Doudna JA. 2008. Autoinhibition of human dicer by its internal helicase domain. J Mol Biol 380:237-43.
13. Chakravarthy S, Sternberg SH, Kellenberger CA, Doudna JA. 2010. Substrate-specific kinetics of Dicer-catalyzed RNA processing. J Mol Biol 404:392-402.
14. Liu Z, Wang J, Cheng H, Ke X, Sun L, Zhang QC, Wang HW. 2018. Cryo-EM Structure of Human Dicer and Its Complexes with a Pre-miRNA Substrate. Cell 173:1549-1550.
15. Masliah G, Maris C, Konig SL, Yulikov M, Aeschimann F, Malinowska AL, Mabille J, Weiler J, Holla A, Hunziker J, Meisner-Kober N, Schuler B, Jeschke G, Allain FH. 2018. Structural basis of siRNA recognition by TRBP double-stranded RNA binding domains. Embo j 37.
16. Lee HY, Doudna JA. 2012. TRBP alters human precursor microRNA processing in vitro. Rna 18:2012-9.
17. Kim Y, Yeo J, Lee JH, Cho J, Seo D, Kim JS, Kim VN. 2014. Deletion of human tarbp2 reveals cellular microRNA targets and cell-cycle function of TRBP. Cell Rep 9:1061-74.

18. Daniels SM, Melendez-Pena CE, Scarborough RJ, Daher A, Christensen HS, El Far M, Purcell DF, Laine S, Gatignol A. 2009. Characterization of the TRBP domain required for dicer interaction and function in RNA interference. BMC Mol Biol 10:38.
19. Zhong J, Peters AH, Lee K, Braun RE. 1999. A double-stranded RNA binding protein required for activation of repressed messages in mammalian germ cells. Nat Genet 22:171-4.
20. Danna K, Nathans D. 1971. Specific cleavage of simian virus 40 DNA by restriction endonuclease of Hemophilus influenzae. Proc Natl Acad Sci U S A 68:2913-7.
21. Olorunniji FJ, Rosser SJ, Stark WM. 2016. Site-specific recombinases: molecular machines for the Genetic Revolution. Biochem J 473:673-84.
22. Chandrasegaran S, Carroll D. 2016. Origins of Programmable Nucleases for Genome Engineering. J Mol Biol 428:963-89.
23. Barrangou R, Fremaux C, Deveau H, Richards M, Boyaval P, Moineau S, Romero DA, Horvath P. 2007. CRISPR provides acquired resistance against viruses in prokaryotes. Science 315:1709-12.
24. Jinek M, Chylinski K, Fonfara I, Hauer M, Doudna JA, Charpentier E. 2012. A programmable dual-RNA-guided DNA endonuclease in adaptive bacterial immunity. Science 337:816-21.
25. Pickar-Oliver A, Gersbach CA. 2019. The next generation of CRISPR-Cas technologies and applications. Nat Rev Mol Cell Biol 20:490-507.
26. Li Y, Li S, Wang J, Liu G. 2019. CRISPR/Cas Systems towards Next-Generation Biosensing. Trends Biotechnol 37:730-743.
27. Ran FA, Hsu PD, Wright J, Agarwala V, Scott DA, Zhang F. 2013. Genome engineering using the CRISPR-Cas9 system. Nat Protoc 8:2281-2308.
28. Dharmacon. 2019. CRISPR Design Tool. https://dharmacon.horizondiscovery.com/gene-editing/crispr-cas9/crispr-design-tool/. Accessed
29. Bannwarth S, Talakoub L, Letourneur F, Duarte M, Purcell DF, Hiscott J, Gatignol A. 2001. Organization of the human tarbp2 gene reveals two promoters that are repressed in an astrocytic cell line. J Biol Chem 276:48803-13.
30. Ding J, Nie M, Liu J, Hu X, Ma L, Deng ZL, Wang DZ. 2016. Trbp Is Required for Differentiation of Myoblasts and Normal Regeneration of Skeletal Muscle. PLoS One 11:e0155349.
31. Gatignol A, Buckler C, Jeang KT. 1993. Relatedness of an RNA-binding motif in human immunodeficiency virus type 1 TAR RNA-binding protein TRBP to human P1/dsI kinase and Drosophila staufen. Mol Cell Biol 13:2193-202.
32. Xie X, Shi PY. 2019. Anti-Zika virus RNAi in neural progenitor cells. Cell Res 29:261-262.
33. Xu YP, Qiu Y, Zhang B, Chen G, Chen Q, Wang M, Mo F, Xu J, Wu J, Zhang RR, Cheng ML, Zhang NN, Lyu B, Zhu WL, Wu MH, Ye Q, Zhang D, Man JH, Li XF, Cui J, Xu Z, Hu B, Zhou X, Qin CF. 2019. Zika virus infection induces RNAi-mediated antiviral immunity in human neural progenitors and brain organoids. Cell Res 29:265-273.
34. Alpuche-Lazcano SP, Scarborough RJ, Daniels SM, Rance E, Mouland AJ, Gatignol A. 2020. HIV-1 Gag interacts with Dicer and increases its binding to specific microRNAs. submitted.

35. Daniels SM, Sinck L, Ward NJ, Melendez-Pena CE, Scarborough RJ, Azar I, Rance E, Daher A, Pang KM, Rossi JJ, Gatignol A. 2015. HIV-1 RRE RNA acts as an RNA silencing suppressor by competing with TRBP-bound siRNAs. RNA Biol 12:123-35.
36. Battisti PL, Daher A, Bannwarth S, Voortman J, Peden KW, Hiscott J, Mouland AJ, Benarous R, Gatignol A. 2003. Additive activity between the trans-activation response RNA-binding protein, TRBP2, and cyclin T1 on HIV type 1 expression and viral production in murine cells. AIDS Res Hum Retroviruses 19:767-78.